THE PHYSICAL REVIEW

A JOURNAL OF EXPERIMENTAL AND THEORETICAL PHYSICS

CONDUCTED BY

THE

AMERICAN PHYSICAL SOCIETY

BOARD OF EDITORS

Managing Editor JOHN T. TATE, University of Minnesota, Minneapolis

G. BEMT, P. W. BRIDGMAN, L. W. MCKEEHAN; I. S. BOWEN, R. S. MULLIKEN, H. D. SMYTH; E. U. CONDON, C. J. DAVISSON, F. K. RICHTMYER

OCTOBER 15, 1929

Transmission of β-Rays Through Magnetized Iron Foil: An Attempt to Polarize a Beam of Electrons — FRANK E. MYERS AND R. T. COX 1065

Test for Polarization in a Beam of Electrons by Scattering — CARL T. CHASE 1069

Experimental Demonstration of the Equivalence of a Mechanically Oscillated Electrostatic Charge to an Alternating Current — RICHARD C. TOLMAN AND DANIEL B. MCRAE 1076

M-Series Absorption Spectra of Metallic Platinum and Gold — ARTHUR J. M. JOHNSON 1103

Intensity of Reflection of X-Rays from Diamond — ALICE H. ARMSTRONG 1113

Extension of the Spark Spectrum of Cu II — GERALD KRUGER 1123

Excitation of the Mg II Spectrum by Impacts of the Second Kind with Metastable Atoms and Ions of the Rare Gases — O. S. DUFFENDACK, CLEMENT L. HEMINGWAY AND MARIE GOTHER 1130

Influence of Argon and of Hydrogen on the Spectra of Zinc Vapor — J. G. BLACK, W. G. MAHE AND C. A. PULLE 1135

Spectrum of the Neutral Hg Atom in the Wave-length Range from 1 to 2μ — E. D. MCALISTER 1140

Experimental Study of Certain Electronic Bands of CO_2 — JAMES F. DUNCAN 1148

High Intensity Non-Reversed Na Arc — CARL J. CHRISTENSEN AND G. K. ROLLEFSON 1154

Influence of the Method of Excitation on Transition Probabilities in Na Vapor — CARL J. CHRISTENSEN AND G. K. ROLLEFSON 1157

Ions and Electrical Currents in the Upper Atmosphere of the Earth — E. O. HULBURT 1167

Pierce Acoustic Interferometer as an Instrument for the Determination of Velocity and Absorption — W. H. PIELEMEIER 1184

Generalized Forms of the New Statistics — S. CHANDRASEKHAR 1204

Note Concerning the Emission of β-Rays in Radioactive Change — LEONARD B. LOEB 1213

Magnetic Properties of Isolated Paramagnetic Atoms — F. WOODRIDGE CONSTANT 1217

Letters to the Editor — 1225

Book Reviews — 1230

PUBLISHED BY THE AMERICAN PHYSICAL SOCIETY

PUBLICATION OFFICE: [illegible]

THE AMERICAN PHYSICAL SOCIETY

OFFICERS OF THE SOCIETY

[illegible]	HENRY G. GALE	University of Chicago, Chicago, Ill.
[illegible] President	W. F. G. SWANN	Bartol Research Foundation, Philadelphia, Pa.
[illegible]y	W. L. SEVERINGHAUS	Columbia University, New York City
[illegible]	G. B. PEGRAM	Columbia University, New York City
[illegible]	JOHN T. TATE	University of Minnesota, Minneapolis, Minn.
[illegible] Secretary for the Pacific Coast	L. B. LOEB	University of California, Berkeley, Calif.

THE PHYSICAL REVIEW

Published by the American Physical Society at 450 Ahnaip St., Menasha, Wis. Executive office: University of Minnesota, Minneapolis, Minn. Two volumes annually, twelve issues per volume.

First series. From July 1, 1893, to January 1, 1913, the REVIEW was conducted by Edward L. Nichols, Ernest Merritt and Frederick Bedell, with the financial support of Cornell University. The first four volumes were issued annually; subsequent volumes, semi-annually; thirty-five volumes in all.

Second series. On January 1, 1913, the REVIEW was transferred to the American Physical Society as announced on the first page of the new series which was then begun. Since then it has been conducted by a Board of Editors elected by the Society. Semi-annual volumes begin in January and July. Since July 1, 1929, the REVIEW has been issued once a month.

Contributors are referred to page 2 of the advertisements for further information.

Annual Subscription, throughout the Postal Union, $10.00 in advance.

Single copies of current volume, $1.00.

General Index, 1893-1920, $4.00, in advance.

Back Volumes, $6.00 per volume; Back Numbers, $1.00 per copy for issues prior to July 1, 1929 (Vols. 1-33), $.60 per copy for issues subsequent thereto. Postage is free when remittance accompanies order; otherwise postage is extra. No bound volumes can be supplied. The REVIEW offers to purchase a limited number of First Series, Vol. 1, No. 1 ($2.00 each); Second Series, Vol. 7, No. 1, January 1916; Vol. 7, No. 2, February 1916; Vol. 7, No. 4, April 1916; and Vol. 7, No. 5, May 1916 (at $2.00 each).

Advertisements. Rates will be supplied by the Editor on request. Copy for each number must be received at Minneapolis two weeks prior to the dates of issue; old copy is repeated until new copy is received. Send electrotypes direct to the printers, George Banta Publishing Co., Menasha, Wis.

A discount of ten percent is allowed subscription agencies and members of the American Physical Society.

Changes of address and Complaints of failure to receive the REVIEW, in the case of members of the Physical Society, should be addressed to the Treasurer; in the case of other subscribers to 450 Ahnaip St., Menasha, Wis.; or to the Editor. New copies can be sent free in response to complaint of non-delivery only if notice of non-delivery is received within three months of date of issue.

Editorial Correspondence should be addressed to the PHYSICAL REVIEW, University of Minnesota, Minneapolis, Minn.

Entered at the postoffice at Menasha, Wis., as second class matter.
Acceptance for mailing at special rate of postage provided for in section 1103, Act of October 3, 1917, authorized September 6, 1918.

Second Series *October 15, 1929* *Vol. 34, No. 8*

THE

PHYSICAL REVIEW

TRANSMISSION OF β-RAYS THROUGH MAGNETIZED IRON FOIL: AN ATTEMPT TO POLARIZE A BEAM OF ELECTRONS

By Frank E. Myers and R. T. Cox
New York University, University Heights

(Received September 13, 1929)

Abstract

This paper describes an attempt to polarize a beam of β-rays by transmission through two magnetized iron foils, the first being regarded as the polarizer and the second as the analyzer. Radium was used as the source of electrons and a Geiger counter to give the number penetrating both foils with varying angles between their directions of magnetization. The data, representing the transmission of some quarter of a million electrons, give no evidence of such polarization.

IN LOOKING for evidence of polarization in a beam of β-rays, Cox, McIlwraith, and Kurrelmeyer[1] observed the transmission of such a beam through two mica sheets, with the crystal axes of the two sheets at various angles with each other, to see if an effect was to be observed analogous to the optical effect obtained with tourmaline crystals. They obtained a negative result. It was suggested by Dr. McIlwraith that it might be worth while to try a similar experiment with two iron foils, the foils being magnetized transversely to the beam, and with varying angles between the lines of force in the two foils.

The foils used in the experiment were a mil in thickness. They were sealed on the ends of a brass tube, which was kept evacuated by continuous pumping.

They were separately magnetized by electromagnets capable of rotation about the axis of the tube, so that the direction of the lines of force in either could be varied at will. A milligram of radium, used as the source of β-rays, was placed at one end of the tube close against the foil at that end. A Geiger counter was placed about one centimeter from the foil at the other end. The foils were magnetized to the maximum intensity which would not deflect the electrons out of the range of the counter. It was reckoned from measurements of flux that this was about one-half the saturation value.

The Geiger counter was made with a large bakelite chamber, closed at one end by a thin aluminum window. Discharges due to the ejection of

[1] Cox, McIlwraith and Kurrelmeyer, Proc. Nat. Acad. Sci. **14**, No. 7 (July, 1928).

photoelectrons from the walls were thus reduced to less than two a minute, even in the presence of the γ-rays from the radium. Points for the counter were made by fusing a small knob on the end of a two-mil platinum wire in an oxygen-gas flame. With the voltage between the point and the aluminum foil maintained constant by trickle-charging the high voltage battery during operation, self-consistent results could be obtained for more than twenty consecutive hours, with the count of some two hundred thousand electrons.

The counter was connected in the conventional way to a three stage, shielded, resistance-coupled amplifier and grid-bias detector. The detector output operated a high speed relay, connected to an automatic recorder. At the suggestion of Mr. Norman Hilberry of the Department of Physics of New York University, the recorder was made from an ordinary clock by removing the balance wheel and providing the escapement with a magnetic release. Two counts about one fiftieth of a second apart could be resolved.

A series of preliminary observations showed that the apparatus was very nearly symmetrical, and that the field of the earth had no measurable effect. Counts of the electrons transmitted through the two foils were taken with the lines of force parallel, anti-parallel, and at right angles. The counts were made and compared in the manner described by Cox, McIlwraith, and Kurrelmeyer, a count at one setting of the lines of force being bracketed by counts at the setting compared with it. The transmission of about a quarter of a million electrons gave for the ratio of counts with the lines of force parallel to those with the lines at right angles a value of 0.996, and for parallel to anti-parallel a value of 1.007. The probable error is of the same order as the deviations of these ratios from unity. There is thus no evidence of the effect that was looked for.

A TEST FOR POLARIZATION IN A BEAM OF ELECTRONS BY SCATTERING

By Carl T. Chase
New York University, University Heights

(Received September 13, 1929)

Abstract

This paper contains a final report on the researches commenced by Cox, McIlwraith, and Kurrelmeyer, and reported by them in preliminary fashion. High speed beta-particles from radium impinge on lead targets and are twice scattered at right angles. The doubly scattered electrons are counted by a point-discharge counter, the number counted at various azimuthal angles being studied, as the radium and upper target are rotated as a unit with respect to the counter and lower target. Experimental refinements have increased the total number of countable electrons and have eliminated the counts due to gamma-rays, which were very troublesome in the earlier experiments. Counts taken at four azimuthal angles separated by ninety degrees show no effect of the kind suspected by Cox, McIlwraith, and Kurrelmeyer, nor any effect of the kind which occurs when x-rays are twice scattered at right angles. More than forty-five thousand electrons were counted. The experimental error is less than one percent. It is concluded that high speed beta-rays are not polarized by scattering.

Introduction

BY MEANS of an experiment analogous to that in which Barkla showed that x-rays could be polarized by scattering at right angles, Cox, McIlwraith, and Kurrelmeyer[1] have looked for evidence of polarization in a beam of beta-rays from radium which had been scattered at right angles from a gold target, a second similar target serving as an analyzer. The electrons were detected by a point-discharge counter. In their report, which is of a preliminary nature, these authors call attention to an apparent positive effect, which is not, however, of the kind that occurs when a beam of x-rays is doubly scattered at right angles. In the case of x-rays, the intensity of the beam scattered from the second target is greatest when this beam is parallel to the beam incident on the first target, and least when the two beams are at right angles to one another. In the experiments referred to, the gamma-ray counts formed such a large part of the total count that counts were not taken in all positions of the second scattered beam with respect to the incident beam; in any one run counts were taken at two positions only, alternating between these two positions every five or ten minutes as long as the counter gave consistent results, a matter of a few hours. The counts due to gamma-rays differed widely in the different positions because of difference in path from radium to counter and difference in the amount of absorbing material in the path. This factor caused the data to show evidence of a polarization effect of the kind that x-rays would show. This was not men-

[1] Cox, McIlwraith, and Kurrelmeyer, Proc. Nat. Acad. Sci. **14**, 544 (1928).

tioned by the authors, but was spoken of by Davisson and Germer.[2] It is due entirely to the gamma-ray effect as just described, which was superposed on the electron count.

Because of this difficulty with gamma-rays, most of the data were taken in the two transverse positions, where the gamma-ray effect should be equal if the apparatus were as symmetrical as care could make it. This was done also to test an earlier observation that more scattered electrons were counted in one of the transverse directions than in the other. The results were not consistent, but most of the runs showed an effect of this nature. The present work aimed to check these observations under more controllable conditions, and was not deterred by the negative results of similar experiments,[2,3] more recently published, in which slow speed electrons from filaments were used. It was felt that the scattering of high speed electrons from radium should still be carefully investigated, especially in view of the observations of Cox, McIlwraith, and Kurrelmeyer.

Apparatus

The apparatus used is shown in section in Fig. 1, which is drawn to scale. Its main part is a brass cylinder, standing vertically in the figure. Brass

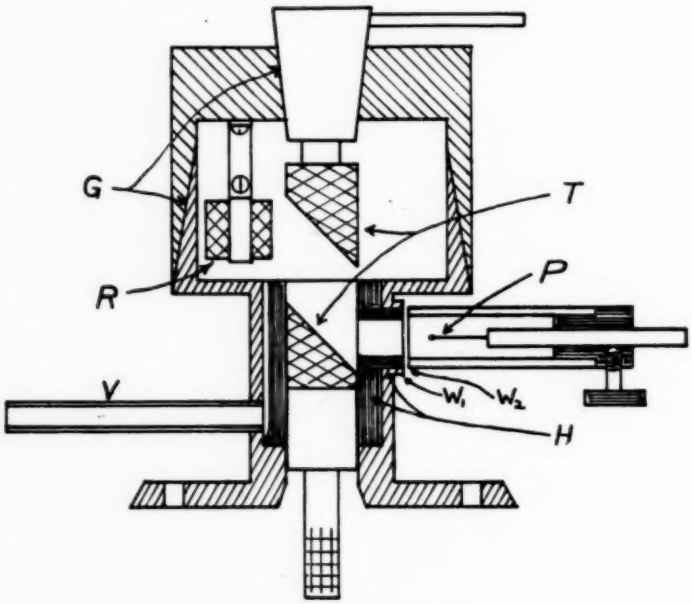

Fig. 1. Diagram of apparatus.

was used to prevent any effect of permanent magnetism. The two scattering targets T are made from lead cylinders, 1 cm in diameter, and cut at

[2] Davisson and Germer, Phys. Rev. **33**, 760 (1929).
[3] Wolf, Zeits. f. Physik **52**, 314 (1928);
Joffé and Arsenieva, Comptes rendus **188**, 152 (1929).

45° to their axis. The radium is at R, and the counter at P. The window W_1 is of mica, 0.03 mm thick, while W_2 is of aluminum foil, 0.01 mm thick. The apparatus is evacuated by means of the tube V.

Two adjustments can be made, provided for by the two ground joints G. The upper target can be rotated with respect to everything else by the plug and attached handle at the top. Or the whole upper part of the apparatus can be turned with respect to the lower part, carrying the radium and upper target together as a unit. The second adjustment allows the configuration of the path of the scattered electrons to be varied, while the first adjustment, that of the upper target alone, allows this target to be turned through 180° so that no electrons can be scattered to the lower target, a convenient method of determining how many of the counts recorded are due to gamma-rays.

H designates two tubes of hard rubber which form a lining to the lower part of the apparatus. These are to absorb the photoelectrons ejected from the brass walls by gamma-rays, and will be discussed more fully later.

Two radium sources were used. The first was a milligram of radium which had been used before by Cox, McIlwraith and Kurrelmeyer.[1] The second, to be discussed more fully, consisted of old radium emanation tubes containing radium D, E, etc., cut in half to avoid the absorption of the glass walls, and collected to form a sort of battery; seventy-five half-tubes were set into cylinders made from lead foil in order to define the electron beam, and bound in a bundle.

Continuous pumping kept the pressure in the apparatus below 10^{-4} cm of mercury, so that the mean free path of the electrons was long compared to the length of their actual path through the apparatus.

Procedure

Before giving the actual procedure, it may be well to state why the form of apparatus described above was used, and what its advantages are. When starting the present research, the writer used an apparatus similar to that used by Cox, *et al*, except that it was made of brass instead of steel, which had been used formerly, and the upper target could be turned out of the incident beam of electrons, allowing a count of the gamma-ray effect alone to be made. The dimensions were about the same as in the earlier outfit, but the targets were of lead instead of gold. A few runs showed, in the total count, an asymmetry of the same nature as had been observed by the earlier three, the effect being in the same direction and on the average of the same magnitude. To make things more certain, runs were then taken in which the gamma-ray effect was measured each time an electron count was made, in order to find what effect was due to the "net electrons." It was found immediately that the gamma-ray count was always of the order of magnitude of the total count, sometimes even more. In an attempt to get more electron counts per gamma-ray count, the present form of apparatus was developed. It has less material in the form of windows in the path of the electrons than did the earlier apparatus. By using the battery

of radium tubes, as described, the high speed electrons from radium E, which product in the milligram of radium gives more of the faster electrons than any other, were kept, while the powerful gamma-rays of the earlier radium products were absent. What gamma-ray counts remained, from one-fourth to one-third of the net electron counts, were eliminated by the hard rubber lining to the lower part of the apparatus, absorbing the photo-electrons produced there by the gamma-rays. No photoelectrons could be produced in the glass wall of the counter. The total count was thus reduced to scattered electrons; when the upper target is turned through 180° so that no electrons can be scattered to the lower target, all counts disappear, and reappear immediately the target is returned to its usual position.

Another advantage of the present apparatus is the following. By increasing the number of countable electrons, the high potential applied between the foil and point of the counter could be kept at such a value that the counter would operate consistently for twelve hours or more, whereas in the previous work it had been necessary to raise this potential so high that the counter point was strained nearly to the breakdown state, causing a complete failure of the point in a short time. The writer found that, with the copious supply of electrons now available, with counter points made of platinum wire 2 mils in diameter ending in a fused ball some 4 to 6 mils in diameter and four or five mm from the foil, counters could be worked at such a voltage that a large electron count could be obtained without shortening the life of the counter below the time chosen for the length of one run, six hours of actual counting.

The procedure then was as follows. Counts were taken for five minutes at each of the four positions mentioned earlier, separated in azimuth by ninety degrees. (The azimuthal angle is that between the plane of incidence of the upper target and the plane of incidence of the second, or lower, target). The counting continued round and round until the run was over. The average count in each position was then found.

Runs were taken with the complete apparatus in several positions relative to the earth's magnetic field. The radium gun was removed and inverted. The milligram of radium was tried instead of the radium gun. A new counter point was used for each run. The whole counter was moved and rotated about its own axis. Every experimental variation that could be thought of was tried, and over 45,000 electrons were counted.

Results

The relative counts, in the series using the radium gun (no different results were obtained when using the milligram of radium) were as follows:

Azimuthal angle	Relative count
0°	1.000
90°	0.977
180°	0.958
270°	0.969

The azimuthal angle 0° corresponds to the configuration in which the electrons leaving the second target travel parallel to the beam incident on the first target, and in the same direction. The experimental error was less than one percent.

It will be seen that there is no indication of any effect of polarization either of the kind suspected by Cox, McIlwraith, and Kurrelmeyer, or of the kind occurring in Barkla's x-ray experiment. In looking for the latter effect, the counts at 0° and 180° must be averaged and compared with the average count at the two transverse positions. Further, none of the experimental variations produced any noticeable effect on the relative counts in the four positions studied.

Critique of the Result

One must conclude then that a beam of electrons is not polarized by scattering, even when the electrons have the high speeds of the beta-rays from radium E. It is hard to see how an asymmetry in the apparatus of Cox, McIlwraith, and Kurrelmeyer, or in the earliest apparatus of the present writer, could have produced the observed effect in such a large fraction of the number of runs, because of the care used in making the apparatus symmetrical, and in inverting the radium, etc. In the writer's case, this effect must have been entirely due to gamma-rays in which case the asymmetry must have been due to some asymmetry in the apparatus. Some data of Cox and his coworkers[4] seems to show that in their case more electrons were counted per gamma-ray than in the case of the author's earliest work. If any change had taken place in the relative proportions of the various radioactive products in the milligram of radium during the year that elapsed between the two sets of observations, this change could not account for an observed asymmetry in one case and not in the other, except that perhaps more electrons per gamma-ray were counted in one case. But in the final work herein discussed, electrons alone are counted and there is no effect. It may be remarked that the apparatus of Cox *et al* and that first used by the present writer, which gave similar results, were both made on the same lathe.

In the present work it was impossible to limit the beams to strictly parallel beams without seriously decreasing the number of countable electrons. The effect of the divergence of the beams has been investigated and appears to be too small to influence the nature of the result, as far as any asymmetry of either of the two kinds mentioned above is concerned.

A theory of the experiment has just been published by Mott,[5] who considers the double scattering of Dirac electrons by atomic nuclei. This theory, while not as yet entirely complete, predicts a difference between the counts at 0° and 180°. The data just given show that more electrons were counted at 0° than at 180°, but this has been ascribed to the somewhat freer path through the apparatus which the electrons have in the 0° position.

[4] Cox, McIlwraith, and Kurrelmeyer, unpublished, privately communicated.
[5] Mott, Roy. Soc. Proc. **A124,** 425 (1929).

Beam divergence might conceivably influence the result when comparing the counts at 0° and at 180°, due to the different configurations of path and the resulting differences in the various angles of incidence and of scattering. But it is improbable that a true polarization effect could have been masked in such a way, in as much as two radium sources, giving initial beams of different degrees of divergence were used, and the result was the same with each. Further experiments are now in progress, using a stronger source and parallel beams.

The author wishes to express his most sincere thanks to Professor Richard T. Cox of this laboratory for his interest and help in pushing this work to a successful conclusion, and to Mr. Frank E. Myers for constructing and maintaining in operation the vacuum tube amplifier necessary in the operation of the couter. He is also most grateful to Mrs. Edith H. Quimby of the New York Memorial Hospital for furnishing the radium tubes without which the success of the experiment would have been impossible.

EXPERIMENTAL DEMONSTRATION OF THE EQUIVALENCE OF A MECHANICALLY OSCILLATED ELECTROSTATIC CHARGE TO AN ALTERNATING CURRENT

By Richard C. Tolman and Daniel B. McRae
California Institute of Technology, Pasadena

(Received July 30, 1929)

Abstract

Method of testing equivalence of a mechanically oscillated charge to an alternating current.—The apparatus consisted of a cylinder approximately 4 inches in diameter by 9 inches long, constructed of insulating material, but coated on the outside with a thin sheet of copper foil which could be charged to potentials which varied from 1400 to 2600 volts. The cylinder was arranged to oscillate around its axis at frequencies in the neighborhood of 20 cycles per second through an amplitude of something over 180°. It was surrounded by an "effect coil," having 260,772 turns of fine wire, which was connected through a three-stage amplifier with a tuned vibration galvanometer for detecting the electromotive force which would presumably be induced by the oscillation of the charged cylinder. The "effect coil" was shielded by a grounded covering of sheet copper, the inner portion of this covering and the coating of copper foil on the cylinder thus forming the two plates of an electrostatic condenser. Connected in series with the "effect coil" was a similar "compensating coil" having the same number of turns but connected in opposition so as to neutralize the effect of external magnetic disturbances. The electromotive force induced in the "effect coil" was measured by balancing out with the help of an auxiliary current flowing in a current sheet in such a way as to induce an opposing electromotive force in the "compensating coil," this auxiliary current having the same frequency as the electromotive force to be balanced and being adjustable as to phase and amplitude. The apparatus was calibrated by replacing the charged oscillating cylinder by a current sheet of known dimensions and carrying a known current. Accidental effects coming from a number of sources were studied and as far as possible reduced or eliminated.

Results of the test and conclusions.—A total of 64 effect runs were made, together with the necessary blank runs for correcting for the small residual effect. The runs were made in 16 different groups of 4 runs each under a given set of conditions. The changes in conditions consisted in changes in the sign and magnitude of the potential applied to the cylinder, changes in the method of connecting the "effect coil" and "compensating coil" to the grid and filament of the amplifier, changes in the neutral position around which the cylinder was oscillated, and change to a different frequency of oscillation. The phase of the effect obtained depended on the conditions of operation in the way predicted by theory. It was changed through 180° by a reversal of the sign of the applied potential, depended on the connections used and on the frequency of oscillation in the manner predicted from the calibration runs, and was independent of the neutral position around which the cylinder was oscillated. The magnitude of the effect obtained was also in agreement with theory. It was closely proportional to the potential applied to the cylinder and to the velocity of motion of the cylinder, and had very approximately the absolute value predicted from the measured capacity of the cylinder, the applied potential and the velocity of motion.

The result of the experiment is to show that a mechanically oscillated electrostatic charge of electricity surrounds itself with an alternating magnetic field, accompanied at right angles by an alternating electric field capable of producing an alter-

nating electromotive force in a suitably placed secondary. It further shows that at right angles to both the magnetic and electric fields there must be a Poynting-vector field corresponding to the observed transmission of energy to the secondary, and that these quantities all have the magnitude and time dependence predicted by electromagnetic theory. The present experiment must be regarded as testing a more extended portion of the fundamental basis of electromagnetic theory than the original Rowland experiment, and as giving a more clear-cut demonstration of the equivalence of a mechanically oscillated charge of electricity to an ordinary alternating current than have previous experiments.

I. Introduction

NATURE of the problem. It was shown over fifty years ago by the Rowland experiment that an electrostatic charge of electricity maintained in uniform mechanical motion produces in its surroundings a steady magnetic field of the strength that is calculated on the assumption that what we ordinarily call a direct current of electricity really does consist of electric charges in uniform motion, and that the velocity of light gives the ratio of the electromagnetic unit to the electrostatic unit of electricity. The result may be taken as evidence for the correctness of the usual assumptions as to the nature of a direct current of electricity, and hence as a partial confirmation of the fundamental notions upon which electromagnetic theory is based.

It was the purpose of the experimental work to be described in this article to investigate the fundamental notions of electromagnetic theory somewhat further, by testing for the equivalence which we should also expect between an ordinary alternating current and an electrostatic charge of electricity maintained in a state of mechanical oscillation, by determining if the latter will produce by induction the expected effects in a suitably placed secondary coil. As will be shown in the sequel the predicted equivalence has been satisfactorily demonstrated.

The present experiment must be regarded as providing a test for a somewhat more extended portion of the fundamental basis of electromagnetic theory than does the Rowland experiment in its original simple form. The result of the Rowland experiment is to show that a charge of electricity maintained in uniform motion surrounds itself with a steady magnetic field of the expected intensity. Using the language of ordinary electromagnetic theory, the result of the present experiment is to show that a mechanically oscillated charge of electricity surrounds itself with an alternating magnetic field accompanied at right angles by an alternating electric field, which produces an alternating electromotive force in the secondary coil, while at right angles to both the magnetic and electric fields there must be a Poynting-vector field which corresponds to the observed transmission of energy to the secondary, and these quantities must all have the magnitude and time-dependence predicted by electromagnetic theory.

It is felt that the more extended justification for the usual basis of electromagnetic theory, provided by the present experiment, should be of interest at a time when the facts that have led to the quantum theory have made

it evident that the older formulation of electromagnetic theory has to be seriously modified, if we desire to apply it to behaviour within the atom. Thus, for example, we may contrast the expected transmission of energy from an oscillating electric charge to a secondary coil demonstrated by the present experiment, with the originally unexpected lack of emission of energy from accelerated electrons which had to be assumed in the original Bohr atom. It is, however, in agreement with our modern trend of physical thought to expect no necessity for modifying the basis of electromagnetic theory when applied to *macroscopic* phenomena such as those of the present experiment, and to believe that the necessary modifications of electromagnetic theory concern themselves primarily with *microscopic* phenomena, such for example as those of the electrons within the atom.

2. Previous work on the Rowland experiment. Before proceeding, a brief statement must be made as to previous work on the Rowland experiment and its modifications, since one of the latter had certain features in common with the present experiment.[1]

In the original Rowland[2] experiment, a circular ebonite disk, which was covered with gold foil and formed one of the plates of a condenser, was charged to a high potential relative to the other plates and rotated around its axis. The magnetic field produced by the motion of this charged disk was then measured by a magnetometer placed near the periphery of the disk. Essentially this same experiment, without modifications in principle, was also later performed by Röntgen[3], Lecher,[4] Rowland and Hutchinson,[5] Himstedt,[6] and Eichenwald,[7] and incidentally to other work by Pender and by Crémieu and Pender, while E. P. Adams[8] carried out a somewhat similar experiment rotating a series of charged balls instead of a charged plate. All of these experimenters, with the exception of Lecher, observed magnetic fields of at least approximately the expected magnitude.

A quite different method of attack, however, was employed by Crémieu,[9] by Pender,[10] by Crémieu and Pender[11] together in a combined investigation and later by Karpen.[12] The method used was to rotate uniformly in a given direction one or more disks, which were alternately charged and discharged, thus presumably leading to the production of an alternating current. The effects of this alternating current, in inducing an alternating current in a

[1] For an excellent summary of work on electric convection up to the end of 1913 see the report by Eichenwald in the second volume of Graetz, "Handbuch der Elektrizität und des Magnetismus," Leipzig 1921.

[2] Rowland, Amer. Jour. of Science **15**, 30 (1878).

[3] Röntgen, Berl. Ber. 198 (1885); Wied. Ann. **35**, 264 (1888); **40**, 93 (1890).

[4] Lecher, Repert. d. Phys. **20**, 151 (1884).

[5] Rowland and Hutchinson, Phil. Mag. **27**, 445 (1889).

[6] Himstedt, Wied. Ann. **38**, 560 (1889); **40**, 720 (1890).

[7] Eichenwald, Phys. Zeits. **2**, 703 (1901); **4**, 308 (1903); Ann. d. Phys. **11**, 1 (1903).

[8] Adams, Amer. Jour. of Science **11**, 155 (1901).

[9] Crémieu, Ann. d. chim. phys. **24**, 85, 145, 299 (1901).

[10] Pender, Phil. Mag. **2**, 179 (1901); **5**, 34 (1903).

[11] Crémieu and Pender, J. d. physique **2**, 641 (1903).

[12] Karpen, J. d. physique **2**, 667 (1903); Ann. chim. phys. **2**, 465 (1904).

suitably placed secondary, were then looked for by connecting the secondary through a commutator with a sensitive direct current galvanometer. Crémieu failed to obtain the expected effect, but Pender and Karpen both obtained effects of approximately the predicted magnitude.

In the combined work of Crémieu and Pender, carried out at the suggestion of Poincare, the attempt was made to discover the cause of the above mentioned discrepancy in their results It was first satisfactorily demonstrated that the effect did not occur when the original Crémieu apparatus was operated, but did occur with the original Pender apparatus. It was then found that the physical difference which accounted for Crémieu's negative result was the presence of a thin layer of insulating material with which he had covered his disks, and it was actually demonstrated that the galvanometer deflection obtained from the Pender apparatus was reduced from 140 to 15 scale divisions by covering his rotating and stationary plates by a thin layer of mica, while the expected magnetic effect appeared when the insulation was removed from the Crémieu apparatus. The theoretical reason for this, however, is not clear and later tests made by Karpen and Eichenwald showed no such shielding effect from insulating materials. It is evident that the combined work of Crémieu and Pender still left something to be explained, and their article closes with the equivocal statement: *Il ne nous appartient pas de dire si ces effets magnétiques sont bien réellement ceux prévus pour une convection d'électricité dans le sens où Faraday et Maxwell entendaient cette expression, ni de décider s'ils sont d'accord avec les hypothèses fondamentales des théories actuelles,"*

3. Relation of present experiment to those of Crémieu, Pender and Karpen. There is a certain similarity between the present experiment and those just described above. There are also, however, important theoretical and experimental differences.

From a theoretical point of view, the foregoing experiments consisted in an attempt to demonstrate the equivalence between an ordinary alternating current and a body in uniform motion but subjected to an alternating change in the charge of electricity which it carries. Our experiments on the other hand are an attempt to demonstrate the equivalence between an ordinary alternating current and a body carrying a steady charge of electricity, but maintained in an oscillatory motion. Our experiments would thus seem to give a clearer answer to the particular question as to whether an ordinary alternating current really consists in the oscillatory motion of electricity, since the process of charging and discharging in the other method might introduce unsuspected factors.

On the experimental side also, it should be noted that the use of a charging current which has the same period as that which is to be detected is a danger which is avoided in our method. Experimentally, our work also differs from the foregoing in using an amplifier and vibration galvanometer for determining the effect in the secondary. This has the advantage of doing away with the use of commutators, which do not always operate satisfactorily. Our set

up also differed from previous ones in using a cylinder instead of a disk for the charged body, which is in some ways a more efficient shape.

4. Relation of present experiment to those of Tolman, Karrer and Guernsey, and of Tolman and Mott-Smith. The present experiment also has a certain similarity to previous experiments of Tolman, Karrer and Guernsey[13] and of Tolman and Mott-Smith,[14] in which an uncharged thick-walled copper cylinder was oscillated around its axis and a determination made of the alternating current which was presumably produced by the lag of the conduction electrons behind the motion of the cylinder. These experiments may also be regarded as giving evidence for the belief that an ordinary alternating current of electricity really does consist of charges of electricity in oscillatory motion. They do not, however, give a clear cut demonstration of this fact, since their theoretical interpretation involves hypotheses as to the nature of the conduction process in metals, and assumptions as to the mass and charge of the conducting particles, and since they do not exclude the possibility that an ordinary alternating current requires the relative motion of positive and negative charges within the material of a conducting substance. Furthermore, the results obtained from them did not precisely agree with the predictions of the elementary theory which was available for their interpretation.

II. Description of the Apparatus.

In order to permit an intelligent criticism of the measure of success that we have had in eliminating accidental effects and measuring solely the effect of interest, we shall describe the apparatus and experimental work in considerable detail. The apparatus will first be described in its final form, and in later sections a discussion will be given of successive changes that were made in order to eliminate various accidental effects which were encountered.

5. The location. Work of the kind to be described cannot be carried out in an ordinary laboratory because of unsteadiness in electromagnetic conditions, and hence the oscillating apparatus was located in a small wooden building (on the Campus of the California Institute of Technology), which had been built for the work of Tolman and Mott-Smith on the inertia of the electric carrier in copper.

The building had a floor space of 16 by 12 feet with its axis pointing toward the magnetic north, and was provided with a cement pier and cement lined pit, arranged so that the oscillating apparatus could be mounted, to reduce accidental effects, with its axis approximately parallel to the earth's magnetic field as shown in Fig. 1. The pier and pit were constructed of neat cement which was only very slightly paramagnetic, but the pier rested on an ordinary concrete foundation. The pier was 9 feet 4 inches tall measured from the floor level and the pit 4 feet 6 inches deep as described more in detail in the article of Tolman and Mott-Smith.

The horizontal component, declination and dip of the earth's magnetic field at the site of the building was determined previous to construction by

[13] Tolman, Karrer and Guernsey, Phys. Rev. **21**, 525 (1923).
[14] Tolman and Mott-Smith, Phys. Rev. **28**, 794 (1926).

Mr. Wallace M. Hill of the U. S. Coast and Geodetic Survey in the spring of 1923. The strength of the horizontal component at that time was 0.26753 gauss and the dip 59° 25′ giving us for the total intensity of the earth's magnetic field H = 0.52581 gauss which is the figure that we use in computing the results of our calibrations made against a rotating earth inductor. Since the above date, a not very distant car line has been discontinued and a new building has been built nearby on the campus, but it is not believed

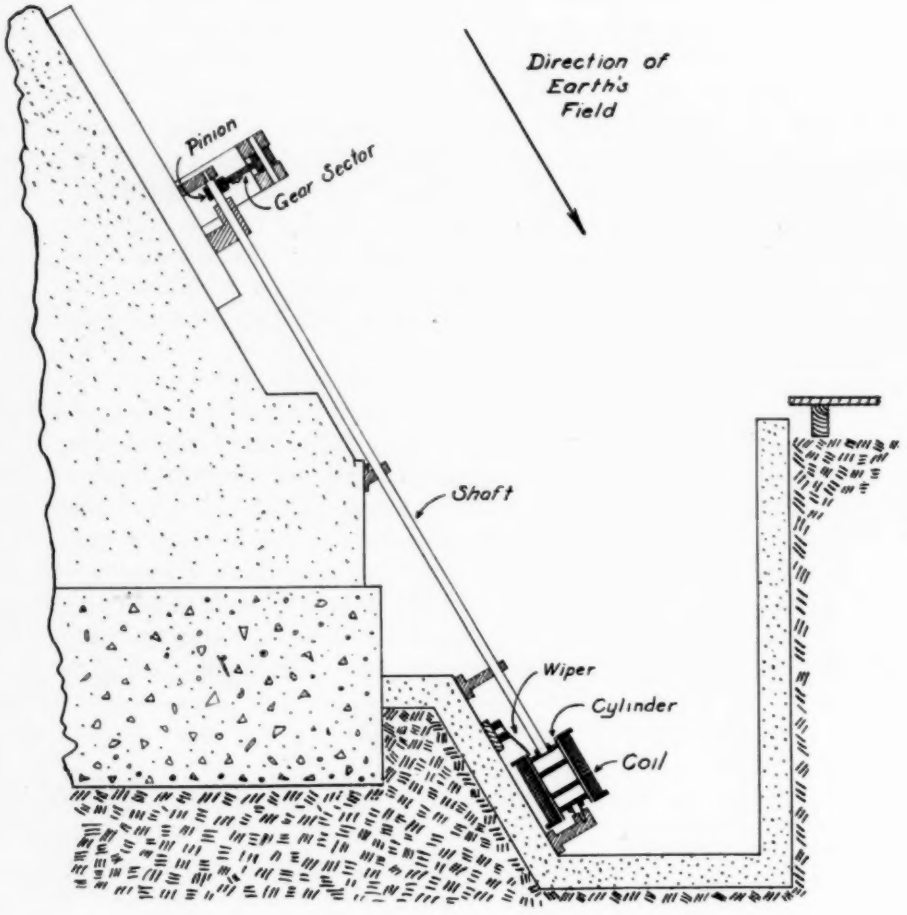

FIG. 1

that these changes have seriously affected the steady part of the earth's magnetic field.

6. The motor drive. The oscillating apparatus was driven by a five horse power direct current motor, which was mounted west of our building at a distance of approximately 42 feet from the axis of the oscillating apparatus. The motor was enclosed in a series of four magnetic shields made from sheet iron having a thickness of 1/16 inch.

The direct current for operating the motor came from a motor-generator set, located in a neighboring building, and was carried out to the motor in a duplex cable which passed at a considerable height above the small building containing the apparatus.

The main switch and starting rheostat for the motor were located on a pole near the motor and were controlled from inside the building by cords passing over pulleys. It was found possible, however, to have the rheostat for the field control of the motor inside the building containing the apparatus.

The power necessary to operate the apparatus at the speed where most of the final runs were made was about 2 kilowatts measured at the switch board.

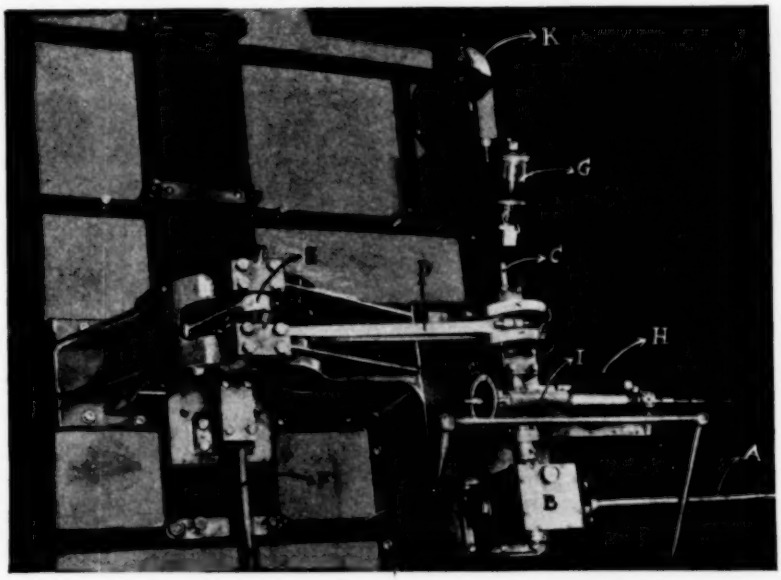

FIG. 2

7. The oscillating apparatus. The main features of the oscillating apparatus are shown in the drawing, Fig. 1, and in the retouched photographs, Fig. 2 and Fig. 3.

The power from the motor was brought to the apparatus by a one-inch Tobin bronze shaft connected directly to the shaft of the motor, and supported by eight iron hangers spaced at intervals between the motor and the building containing the apparatus. The end of this shaft is seen at *A* at the right of Fig. 2.

The power was transmitted to the Tobin bronze crank shaft *C* through a pair of 45° bronze spiral gears running in oil in the gear box shown at *B*. These gears had a reducing ratio of 16 to 13. The crank shaft *C* was supported by brass pillow blocks mounted on a heavy brass casting which was itself bolted and grouted in position on the sloping northern face of the

cement pier. The shaft carried a small Tobin bronze 45° spiral gear for operating an earth inductor, as will be described later, and a pair of brass flywheels, one on each side of the crank pin, to improve the steadiness of running.

The Tobin bronze crank pin was 1.25 inches long, 0.972 inches in diameter and was offset from the center by 1.133 inches. At first the crank pin gave considerable trouble by excessive heating, but finally, using continuous lubrication from the oil reservoir *G* seen in Fig. 2 above the end of the crank shaft, and using a connecting rod with a loose fitting fiber lined bearing, the difficulty was overcome.

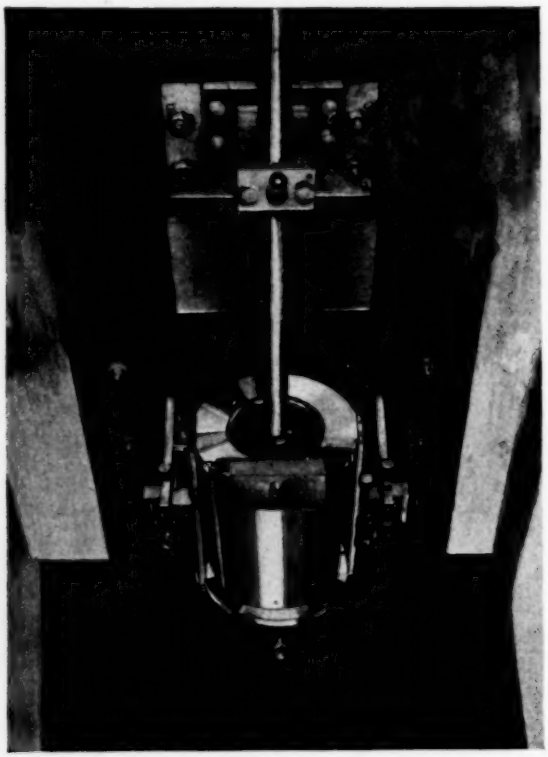

FIG. 3

The connecting rod *D* was made from a heat treated aluminum alloy (Dural) casting and transmitted the power to a wrist pin on the gear sector shown in section in Fig. 1 and at *E* in Fig. 2. The length between the centers of the connecting rod bearings was 20.147 inches.

The gear sector was made from a casting of the same aluminum alloy, and was mounted on a 7/8 inch Tobin bronze shaft, running in brass bearings which were supported by the heavy yoke which formed part of the main casting. The Tobin bronze wrist pin had a diameter of 0.747 inches, a bearing length of 11/16 inches, and was offset from the center by 4.156 inches. The distance between the centers of the crank shaft and the gear sector shaft was 20.174 inches, which, combined with the dimensions stated

above, gave the gear sector a motion through an angle of a little more than 30°.

The gear sector engaged with a fiber pinion on the upper end of the shaft that drove the cylinder. The length of face of the gear sector and pinion was 2 inches. The pitch diameters of gear sector and pinion were 12.187 and 2 inches respectively, with 16 pitch involute teeth, giving an angular motion of somewhat over 180° to the cylinder.

The shaft that drove the cylinder was made of brass tubing 1 inch outside diameter with a 1/32 inch wall, and was 6 feet 8 inches long from pinion to cylinder. It was supported by four brass bearings as shown in Fig. 1, and in addition there was a step bearing 3/8 inch in diameter at the lower end of the cylinder. The shaft was purposely made light for obvious reasons, and actually turned out to be so light that the "dynamic amplitude" of oscillation of the cylinder obtained under running conditions was appreciably larger than the "static amplitude" obtained when the apparatus was turned over slowly by hand.

8. The cylinder. The cylinder was located in the pit as seen in Figs. 1 and 3. It was constructed to be as light as possible out of a tube of pressed insulating material known in the trade as bakelite tubing. The tubing used had an outside diameter of 4 inches and a wall thickness of 1/16 inch, a light cut being taken off the outside after assembly. It was reinforced inside with four bakelite disks as shown in section in Fig. 1, the top disk being permanently connected with the driving shaft and the bottom disk carrying a short spindle which fitted into the step bearing.

The cylinder was coated on the outside with a layer of copper foil approximately 0.001 inch thick to carry the charge of electricity. The foil was soldered at the two ends to light copper rings, which were fastened to the bakelite cylinder, and was cemented on the cylinder with a mixture of 5 parts rosin to 1 of beeswax using a hot roller. The copper rings on the ends of the cylinder were cut and a very narrow longitudinal slit was left in the copper coating in such a way that electricity could not flow circumferentially around the cylinder. The total length of the finished cylinder was 23.42 cm and the average outside diameter 10.141 cm.

9. Arrangement for charging the cylinder. The direct current high voltage necessary for charging the cylinder was generated in a small building 100 feet away from the apparatus, from 110 volt 50 cycle alternating current, by transforming up to the desired potential and rectifying with a hot filament vacuum tube rectifier. The pulsating rectified potential thus obtained was used to maintain a steady charge in a condenser (Westinghouse, Style 376093) having a capacity of 0.97 microfarads.

The potential from this condenser was connected, for protection through a high resistance, to an overhead cable leading to the building containing the apparatus. Here connection was made with a Kelvin electrostatic voltmeter (Kelvin and James White, Ltd.) for measuring the applied potential, and with a double throw switch arranged so that the cylinder could be grounded or charged at will. The potential for charging the cylinder was

lead in through a light spring-brass wiper which made rubbing contact with the inside face of the copper ring at the upper end of the cylinder, as shown in Fig. 1.

10. The layout of the electrical measuring circuits. The general layout of the electrical measuring circuits is shown diagrammatically in Fig. 4, in the form which it took for calibrating the apparatus. For making the effect runs, the calibration current sheet was replaced by the oscillating charged cylinder. The layout can be regarded as composed of four individual circuits.

Circuit No. 1 contains the calibration earth inductor, the calibration current sheet which is arranged to induce electromotive forces in the effect

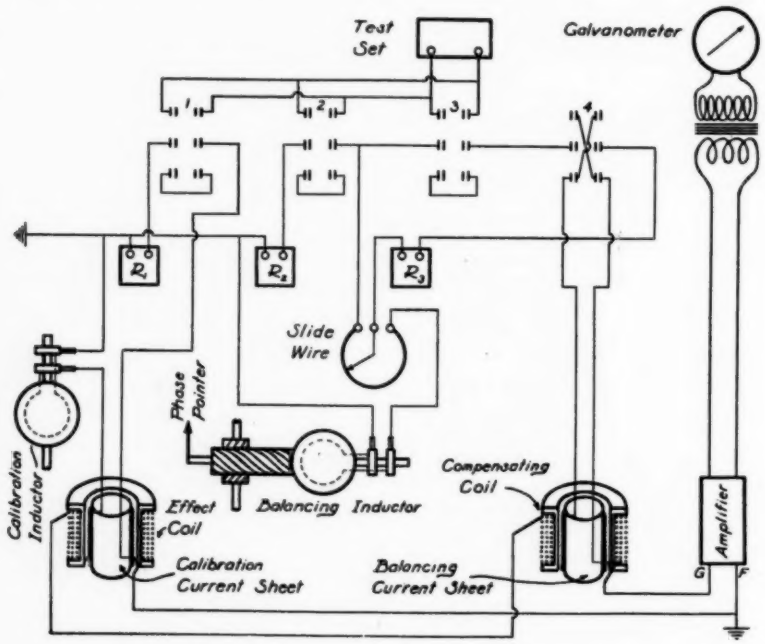

FIG. 4

coil, and the resistance boxes R_1 for regulating the current through the current sheet. The circuit is thrown into action by putting switch No. 1 in the down position, while its resistance can be measured with the help of the Leeds and Northrup test set by putting switch No. 1 in the up position.

Circuit No. 2 contains the balancing earth inductor, the slide wire and the resistance box R_2. The circuit is thrown into action by putting switch No. 2 in the down position, while the resistance can be measured with switch No. 2 in the up position.

Circuit No. 3 contains that portion of the slide wire which it is desired to tap off, the balancing current sheet which is arranged to induce electromotive forces in the compensating coil, and the resistance box R_3. The circuit is thrown into action by putting switch No. 3 in the down position,

while its resistance can be measured with switch No. 3 in the up position. An auxiliary reversing switch, No. 4, is provided for changing by 180° the phase of the current going to the balancing current sheet, while smaller changes in phase can be made by adjusting the longitudinal position of the balancing inductor as will be described more in detail later.

Circuit No. 4 contains the effect coil and compensating coil connected in series, and then connected to the grid and filament of the vacuum tube amplifier, which in turn was connected through a transformer with the vibration galvanometer. The effect coil and compensating coil were made as nearly alike as possible and were connected in opposition in order to reduce the effect of accidental magnetic disturbances coming in from outside.

The circuits were grounded as indicated in Fig. 4. The ground consisted of a pair of iron pipes driven into the earth just outside our building to a distance of several feet. Water was poured around the pipes and salt water poured into them at the time of installation. When first set up there was a resistance of a few hundred ohms between this ground and the pipes of the city water system, and after the end of our runs this had sunk to less than a hundred ohms.

It will be noted that the method of balancing the electromotive force in the effect coil by an induced electromotive force in the compensating coil, as adopted for these experiments, is different from the method of Tolman and Mott-Smith in which an electromotive force, tapped off from the slide wire, was directly opposed to that generated in the effect coil. The present method has the advantage of not introducing possible spurious effects from the balancing inductor and slide wire directly into the circuit that contains such a sensitive element as the amplifier grid, and also has the possible advantage of providing a certain measure of symmetry in the way in which the effect and balancing electromotive forces enter the detecting circuit. It has the disadvantage, however, of using the tapped off portion of the slide wire to furnish current instead of merely potential through the sliding contacts.

Certain parts of the apparatus connected with the electrical measuring circuits will now be described in more detail.

11. The earth inductors and the phase and speed measuring devices. The calibration earth inductor, which is shown diagrammatically in Fig. 4, will be seen in its actual position near *K* in Fig. 2. When the calibration runs were made, the connecting rod *D* and the oil reservoir *G* were removed and a direct connection was made between the end of the crank shaft *C* and the shaft which operated the calibration inductor through a pair of 45° brass spiral gears.

The axis of the calibration inductor was adjusted with great care so as to be perpendicular to the total earth's field, determined by Mr. Hill as already described. The wooden spool for the inductor was wound with 12 layers of 11 turns each of No. 20 enamel covered copper wire, having a diameter of 0.85 mm. The inside diameter of the coil was 9.000 cm, the outside diameter 10.740 cm, and the width of space filled by the winding 1 cm. The average radius of the coil for purposes of calculation was taken as the

square root of the mean square radius of the turns and had the value 4.963 cm.

The two ends of the coil were brought out to brass slip rings on the axis of the coil, where contact was made with brushes. These brushes consisted of strips of spring brass sheet, which were slit into three longitudinal fingers which pressed against the rings. This arrangement proved to be very satisfactory provided it was frequently cleaned with kerosene while running.

The balancing earth inductor, which is shown diagrammatically in Fig. 4 will be seen in its actual location at *H* in Fig. 2. It was of similar construction to the calibration inductor, but its exact dimensions are not necessary since it functions in the same manner both in the calibration and the effect runs. It was provided with slip rings and brushes similar to those for the calibration inductor.

This balancing inductor was driven by a 45° brass spiral gear shown in Fig. 2 at *I*, which meshed with a similar shorter gear on the crank shaft. This made it possible to vary the phase of the balancing inductor by varying its longitudinal position, and this could be done, while the apparatus was running, with the help of a lead screw which moved the entire mounting of the inductor in ways which were provided for the purpose. One end of the shaft of the inductor was provided with a phase pointer and protractor scale, as will also be seen in Fig. 2, which were used in measuring the phase settings which had been found necessary to secure electrical balance.

To obtain the phase readings in the case of the calibration runs, the apparatus was first turned over by hand until the coil of the calibration inductor was parallel to the earth's field, as shown by a suitably adjusted auxiliary pointer and reference marks which will be seen at *K* in Fig. 2, and the position of the phase pointer on the shaft of the balancing inductor was then read. The readings were always taken in pairs corresponding to the "up" and "down" positions of the auxiliary pointer, the two readings when one of them was corrected by 180° usually agreeing within a degree.

To obtain the phase readings in the case of the effect runs, the apparatus was turned over until the gear sector was in the center of its stroke as shown by suitably placed reference marks on the top face of the upper fly wheel, and the position of the phase pointer was then read. These readings were also taken in pairs, corresponding to the center of the stroke moving both east and west. Owing to the geometry of the driving mechanism the two readings when one of them was corrected by 180° differed by about 6°.

At the opposite end of the shaft of the balancing inductor from that carrying the phase pointer, a light extension will be seen in Fig. 2, which operated a centrifugal tachometer as well as a vibrating reed tachometer, the latter proving to be the more satisfactory.

12. The slide wire and resistances. The slide wire from which the current was tapped off to operate the balancing current sheet was a Leeds and Northrup Kohlrausch bridge, Type 4258, No. 82123, with a total resistance of about 32 ohms. Such an instrument is of course not specially adapted for the purpose to which we put it, since the moving contacts are not designed for the

transmission of current. Nevertheless, since the instrument was kept well cleaned with kerosene, and the resistance in circuit No. 3 which contained the balancing current sheet was made rather high, it is believed that the set-up was satisfactory for our purposes.

The resistances R_1, R_2 and R_3 for the three circuits Nos. 1, 2 and 3 were provided by Leeds and Northrup non-inductive resistance boxes, and should have the same impedance for direct current and for the low frequency currents (17 to 23 cycles) which we employed.

The total resistance in the calibration circuit No. 1 was made 10,000, 5000, 2500 or 1000 ohms according to the strength of the calibration current desired. The total resistance in the slide wire supply circuit No. 2 was always made 250 ohms, and that in the balancing circuit No. 3 was made 100 ohms with the slide wire set at zero. The resistances in circuits 1 and 2 were thus high enough to make small variations in the contact resistances at the brushes of the inductors negligible, and the resistance in circuit No. 3 high compared with small variations in the slide wire contact resistances.

13. The current sheets. The calibration current sheet was designed of course to have nearly the same dimensions as the cylinder. It consisted of 73 complete turns of No. 18 double-cotton-covered wire wound on the outside of an orangewood cylindrical block in a groove having a pitch of 1/8 inch, the total length of coil from the center of the wire at the beginning of the first turn to the center of the wire at the end of the last turn was 9.125 inches or 23.18 cm, this being the same length as the spool of the coil and a trifle shorter than the cylinder. The diameter of the coil measured to the center of the wire was 10.120 cm. A correction was made for the slight difference between the area of the coil and that of the cylinder.

The balancing current sheet was made from 605 turns of No. 28 single-silk-covered wire wound on a 4 inch bakelite tube. Its exact dimensions are not necessary since it functions in the same way in the calibration and effect runs.

14. The effect and compensating coils and their connections. The effect coil was the same one used in the work of Tolman and Mott-Smith. The spool for the coil was constructed of "micarta." It had an overall length of 9.125 inches, the end disks being 3/8 inch thick. The outside diameter was 7 inches, the inside diameter 4.125 inches, and the wall thickness of the central tube 1/16 inch. It was carefully wound in one length with soldered joints, with 18 lbs. of No. 38 enamel-coated wire, with a total of 260,772 turns, giving a resistance of 207,300 ohms and an approximate length of 67 miles. The compensating coil was made with a spool of the same dimensions and exactly the same number of turns of similar wire, and had approximately the same resistance and length.

The effect coil was located in the pit surrounding the cylinder as shown in Fig. 3. It was mounted in a cradle with adjusting screws for tipping its axis in any desired direction and for aligning it lengthwise and sidewise. It was adjusted parallel to the axis of the cylinder with the help of removable centering plates, which brought the upper end of the coil central with the

cylinder shaft and the lower end central with the step bearing. The plates were removed when the apparatus was running.

The balancing coil was placed on the floor of the building at a distance of about 6 feet from the effect coil and set in a wooden cradle which held it approximately parallel to the effect coil, in order to balance out external magnetic disturbances.

Boths coils were electrostatically shielded by enclosing them in grounded coverings of sheet copper which fitted closely to the coil and end plates and to the inside of the spool. The copper covering on the inside of the spool of the effect coil and the coating of copper foil on the outside of the cylinder thus formed the two plates of a cylindrical condenser whose capacity determined the charge carried by the cylinder.

Further electrostatic shielding was provided by enclosing the binding posts for the coils in brass boxes as seen at the front upper end of the coil in Fig. 3, and connections with the coils were made with wires enclosed in a grounded lead sheath.

The lead-covered wires from the two coils and from the amplifier input were brought together to binding posts inside a grounded brass receptacle to permit the connection of the coils and amplifier in the different ways used. Four different methods of connection, keeping the two coils connected in opposition, were possible. These different connections were called A, B, C and D and are described in Table I. The different terminals are denoted by the following symbols:—G and F are the grid and filament of the amplifier input, E_i and E_o the inner and outer terminals for the effect coil and C_i and C_o those for the compensating coil. The symbols enclosed in brackets indicate the terminals connected together.

TABLE I. *Description of connections.*

Connection	Terminals connected together		
A	$(G\,E_o)$	(E_iC_i)	(C_oF)
B	$(G\,E_i)$	(E_oC_o)	(C_iF)
C	$(G\,C_o)$	(C_iE_i)	(E_oF)
D	$(G\,C_i)$	(C_oE_o)	(E_iF)

15. The amplifier. The amplifier was a three-stage resistance coupled amplifier of standard design. It was operated with a plate voltage of 135 volts obtained from a battery of dry cells, and used a filament heating current for all three stages of a little less than one ampere, obtained from an Edison storage battery. The whole amplifier including both batteries, was electrostatically shielded by completely enclosing it in a grounded brass box. The filament of the first tube was also grounded, and the input wires from the coils as well as the output wires to the transformer were enclosed in a grounded lead sheath. The first two stages of the amplifier were operated by high μ tubes while the third stage had a lower μ tube in order to provide the power output to operate the transformer and galvanometer.

The transformer was a 284-D General Radio Company transformer. It was placed near the galvanometer at a considerable distance from the

amplifier and other apparatus. The electrostatic shielding of the connecting wires in grounded lead sheath was continued as far as this transformer.

16. The galvanometer. The galvanometer was a Leeds and Northrup vibration galvanometer with a flexible enough suspension so that it could be tuned to the low frequencies in the neighborhood of 20 cycles which were used. This possibility of using a tuned detecting instrument is of the greatest importance, since the accidental external disturbances which enter the coils are apparently many times greater than the effect of interest, but do not have the right frequency to correspond to the tuning. The direct current resistance of the galvanometer was 765 ohms. It was provided with a concave mirror which was illuminated with a single filament lamp, the distance from mirror to ground glass scale being about 14 feet.

III. Elimination of Accidental Effects

The foregoing description applies to the final form in which the apparatus was used for making the experimental runs which are to be reported. This final form, however, was partly the result of a series of changes which were made to eliminate various accidental effects and we must next describe the nature of these accidental effects and the methods by which they were reduced.

17. External electromagnetic disturbances. In work of this kind, with a powerful coil connected to a three stage amplifier, effects due to external electromagnetic disturbances are hard to eliminate, and, with the amplifier on, our galvanometer was always moving to some extent even though the apparatus itself was not operating. This residual motion of the vibration galvanometer produced a somewhat steady widening of the band of light from the galvanometer with occasional superimposed sudden "kicks." The steady widening appeared to be due at least partly to 50 cycle commercial circuits, but the cause of the sudden kicks is unknown.

The residual motion of the galvanometer was appreciably reduced by using a compensating coil in series with the effect coil as described above. This device for the elimination of external disturbances, by the connection of two similar coils in such a manner as to "buck" each other, had earlier been used by Tolman and Stewart[15] in somewhat similar work, but had not been used in the immediately preceding work of Tolman and Mott-Smith. The introduction of the device made the conditions of measurement appreciably better in the present work than in that of Tolman and Mott-Smith, even though the location of the apparatus is no longer as favorable as at that time.

The magnitude of the residual motion of the galvanometer varied somewhat from time to time, but was never large enough so that there was the slightest doubt as to the increased effect obtained from putting the charge on to the oscillating cylinder. The accuracy of the measurements was doubtless somewhat reduced by the presence of the residual motion of the galvanometer. There was, however, no reason to believe that this re-

[15] Tolman and Stewart, Phys. Rev. **8**, 97 (1916); **9**, 164 (1917).

sidual motion had any systematic effect on the results since a null method was used in which the effect of interest was balanced out, presumably without affecting the residual motion of the galvanometer. And as a matter of fact the appearance of the minimum deflection when balance was obtained was quite similar to the residual deflection when the apparatus was not running.

18. Location of high voltage generator. As already stated in Section 9, the direct current high voltage for charging the cylinder was generated in a separate building 100 feet away from that in which the experiments were performed. This was done since in earlier experiments it was found that the operation of a high voltage transformer near the apparatus produced extremely large galvanometer deflections. At a distance of 100 feet, however, there was no appreciable effect from the apparatus which produced the high voltage.

19. Location and shielding of motor. In undertaking the present experiments, the attempt was first made to adapt the apparatus of Tolman and Mott-Smith to the new purpose, by merely replacing the oscillating conducting cylinder, which they used to detect the inertial lag of the conduction electrons, by a charged cylinder of similar moment of inertia but made nonconducting by the presence of a longitudinal slit. A long series of measurements was made with this set up, but the calculated magnitude of the expected effect, which could be obtained in this way, proved to be considerably smaller than the accidental effects which were actually found to be produced by the oscillation of the uncharged cylinder. For this reason it became necessary to give up the previous method of maintaining at its natural period of oscillation a system consisting of a heavy cylinder restrained by torsion rods, and replace it by a very light cylinder driven through as large an angle as possible by a forced mechanical action. It was soon found, however, that this change involved the use of considerably more power than could be provided by the non-magnetic water motor previously used and it appeared desirable to experiment with electric motors as a source of power.

Direct current motors were chosen, since our apparatus is particularly sensitive to alternating current disturbances. A two horse power motor was first tried and found not to produce much magnetic disturbance when operating just outside the east wall of our building. It was found, however, that more power was necessary and a five horse power motor was next installed.

Unfortunately the larger motor produced a very much greater magnetic disturbance and at a distance of about 12 feet from the axis of our apparatus it produced very serious trouble when running This was much reduced but not entirely eliminated by enclosing the motor in four magnetic shields made of sheet iron 1/16 inch in thickness. Finally, as already stated, the motor was permanently installed at a distance of about 42 feet. In this latter position it still produced a slight but noticeable disturbance without the magnetic shields, but even this disappeared with the shields on. The motor was purposely arranged to run at a different speed from the apparatus

(ratio 16 to 13), so as not to have the same period as the tuned galvanometer.

Since the motor was driven by direct current, it was at first hoped that the main switch and starting rheostat could be located for convenience inside the building containing the apparatus. It was found, nevertheless,that the direct current leads apparently carried a slight superimposed alternating or pulsating component which produced a small but definite disturbance as shown by the galvanometer. For this reason the main switch and starting rheostat were finally removed from the building as already described. It was possible, however, to retain the field control rheostat for the motor inside the building and thus maintain a continuous adjustment of the speed.

20. Location of the oscillating cylinder. The attempt was first made in this work to place the cylinder directly above the fiber pinion which was driven by the gear sector. With the cylinder and surrounding coil in this position, however, accidental effects were found when the apparatus was running which appeared to come from periodic currents flowing in the heavy brass yoke which supported the bearings for the shaft of the gear sector. These currents seemed to arise from the slight vibration of this yoke in the earth's magnetic field, since the effects were modified in very systematic ways by holding a bar of iron, while the apparatus was running, with its end near different portions of the yoke.

To avoid these accidental effects, the cylinder was finally mounted, as already described, in the pit at a considerable distance below the yoke, even though this involved the use of a long shaft which proved flexible enough so that the dynamic amplitude of oscillation of the cylinder was greater than the amplitude when the apparatus was turned over by hand.

21. Leakage current from the cylinder. The cylinder was specially designed, as will be noticed from the cross section in Fig. 1, so as to give a long leakage path from the charged coating to the central shaft. It is of course desirable to keep the leakage current as small as possible, since it is conceivable that when the apparatus is rotating, the leakage current might acquire a pulsating component which would have the frequency of rotation and affect the results.

The actual resistance from the cylinder to ground was approximately measured, with the apparatus rotating, by noting the time taken for the cylinder to discharge our high voltage condenser. The leakage current from cylinder to ground could then be calculated and was found to be about 1×10^{-5} amperes at 2000 volts. As this is only about one half the expected alternating current produced by the oscillating cylinder, it is believed that the effect of possible pulsations in the leakage current can be neglected.

22. Electrostatic shielding of the amplifier and connections. During a considerable part of the preliminary work, the amplifier and connecting wires were not electrostatically shielded although the effect and compensating coils were covered with sheet copper. With such an arrangement, however, conditions were not as good as with the more complete electrostatic shielding finally used as described above.

In the first place in the absence of the more complete shielding, it appeared to be undesirable to try to ground the filament of the first stage of the amplifier, since the grid then apparently responded more markedly to electrostatic disturbances and it was better to leave both grid and filament "floating". This, however, is not as satisfactory as to have proper electrostatic shielding with the potential of the filament definitely fixed.

In the second place even with grid and filament both "floating" the set up was still very sensitive to some electrostatic disturbances. Thus the mere rubbing of one's hair in the neighborhood of the apparatus would produce violent galvanometer motions; and with the high voltage merely coming into the building to the switch for throwing it on to the cylinder, a violent galvanometer kick would often be produced when the long wooden handle leading to the switch was merely touched with the hand or even when the wall of the building several feet away from the switch was touched. With the more complete shielding these annoying effects disappeared.

23. Elimination of a special electrostatic effect from the charged cylinder. We must finally turn our attention to the elimination of a particularly serious electrostatic effect coming from the charged cylinder itself, the cause of which was not discovered until after a long period of preliminary experimentation.

In originally constructing the copper electrostatic shields for the effect and compensating coils, the inside of the spools for these coils were lined with a sheet of copper which was rolled into a cylindrical form in such a way that the opposite edges came nearly but not quite together, leaving a very narrow longitudinal slit in the shielding. This was done partly because it was thought that this slit would be an advantage in breaking what would otherwise act as a very low resistance short-circuited turn in the transformer, and partly for reasons of ease of construction since it was felt that the shielding would not be seriously affected by such a narrow slit.

Nevertheless, the preliminary effect runs, made with this narrow slit in the shielding, lead to quite erroneous results. Although a reasonably definite and reproducible effect was obtained when the oscillating cylinder was charged, the magnitude and phase of the effect were found to be different for the different methods of connection A, B, C and D described in Section 14, and to be different when the neutral position around which the cylinder was oscillated was changed, thus changing the relative positions of the longitudinal slit in the shielding of the coil and the longitudinal slit in the copper foil coating of the cylinder. Furthermore, the magnitude of this effect was in general considerably greater than that which was predicted for the effect of interest, although with connections D, in which the inside of the effect coil was connected directly to the grounded filament, the results obtained were not far from the predicted ones.

These findings suggested the possibility that a periodic electric field from the charged oscillating cylinder was passing through the narrow slit in the shielding of the effect coil and affecting the grid of the amplifier by direct electrostatic induction. This conclusion was made more certain, however, by some special experiments which were carried out as follows.

A small rotating electrostatic inductor was constructed from a cylinder of fiber $1\frac{1}{2}$ inches long and $2\frac{1}{2}$ inches in diameter. This cylinder was provided with a cylindrical brass sheath, one quarter segment of which was kept charged to a high direct current potential by a brush which was connected to our high potential supply.. Arrangements were also made so that the cylinder could be rotated, at the frequency to which our galvanometer was tuned, through a flexible shaft which made it possible to hold the cylinder so as to produce a periodic electric disturbance at any point desired. With connections *A*, in which the inside of the effect coil did not go directly to the grounded filament, there was a very large effect (galvanometer off-scale) when this electrostatic inductor was rotated in a position near the slit in the shielding of the effect coil. There was, however, no effect when the conductor was held just as near to the continuous portion of the shielding. Furthermore there was no effect or only a very small one when the rotating inductor was held near the slit, provided connections *D* were used, in which the inside of the effect coil was connected directly to the grounded filament.

As a result of the conclusions made obvious by these experiments, a new inside shield for the effect coil was constructed out of copper tubing turned down so as just to fit the inside of the coil and have a wall thickness of about 0.01 inches, and this was soldered to the copper end coverings of the coil. With this new arrangement our electrostatic shielding appeared to be entirely satisfactory as will be evident in what follows.

It is of course a matter of vital importance in this work to have proper shielding from electrostatic effects, since from an experimental point of view the amplifier is very sensitive to electrostatic disturbances, and from a theoretical point of view we are only interested in the electromagnetic action of our primary current on the secondary effect coil.

IV. The Calibration of the Apparatus

We are now ready to consider the calibration of the apparatus in its final form. We must first state the results obtained in calibrating certain separate parts of the apparatus and then present the results of the calibration runs themselves.

24. *The electrostatic voltmeter.* To calibrate the electrostatic voltmeter (see Section 9) used for measuring the high voltage on the cylinder, we employed a Weston voltmeter, Type 45, No. 33873, together with the Weston Voltage Multiplier No. 33873 (ratio 20 to 1) which went with it. Corrections to the readings of the voltmeter No. 33873 itself were first obtained by comparing it with a Laboratory Standard Weston Voltmeter, No. 822 belonging to the Electrical Engineering Department of this Institute, and the readings of our electrostatic voltmeter were then compared with those of voltmeter No. 33873 in series with the multiplier, using high potential from the source described in Section 9.

Calibrations of the electrostatic voltmeter were thus made both before and after our series of runs, without any marked difference in the results. In our range of use, 1400 to 2600 volts, it was only possible at the utmost

to estimate the readings of the electrostatic voltmeter to the nearest 5 to 10 volts and our final corrected readings are probably affected with about that amount of uncertainty.

In connection with our method of calibrating it should be noted that our source of potential was not strictly steady, since it came from a condenser kept charged by a rectified 50 cycle alternating potential. This gave a slight pulsation to the actual potential, since an appreciable current had to be supplied to operate the Weston voltmeter. It was shown by calculation, nevertheless, allowing for the fact that one voltmeter measures the mean voltage and the other the square root of the mean square voltage, that these pulsations would not have an appreciable effect on the results of the calibration.

25. The capacity of the cylinder. In order to calculate the charge carried by the cylinder, it was necessary to know the capacity of the condenser formed by the cylinder and its surroundings. To measure this, a 50 cycle electrically driven tuning fork was arranged to connect the cylinder alternately to the charged side of a half microfarad supply condenser and to ground, the voltage of the supply condenser being followed by a Cambridge and Paul string electrometer, and the time of discharge over a given range being taken with a stop watch. This time was then compared with that necessary to discharge the supply condenser over the same voltage range into a General Radio Company precision condenser, Type 222, Serial No. 482, set at 527 micro-microfarads (claimed accuracy 0.1%), which was nearly the same capacity as that to be measured.

Before making the measurements, the coil and cylinder were carefully lined up and measurements were taken with the cylinder turned to different positions, and with different adjustments of the tuning fork without any marked change in the results. In all 37 pairs of time readings on the two condensers were taken, and the final value for the capacity of the cylinder came out 538.5 micro-microfarads with a probable error[16] of 0.8.

26. The slide wire. The slide wire was calibrated over the range employed, and it was found that the resistance of the wire was indeed quite closely proportional to the readings of the instrument.

27. The tachometer. The speed of the apparatus was controlled with the help of a vibration reed tachometer. This was calibrated from time to time at the two speeds (23 cycles and 17 cycles per second) chosen for operation and was found to be approximately correct. A high order of accuracy in the control of the speed is not essential since the currents in the calibration current sheet, in the balancing current sheet, and that produced by the oscillating cylinder should all of them be closely proportional to the speed.

28. Method of making the calibration runs. We must now turn our attention to the actual calibration runs made, on the apparatus as a whole, to determine the slide wire readings and phase settings which corresponded to

[16] For the purposes of this article we are taking the "probable error" as the mean deviation divided by the square root of the number of observations. We give its values merely as a rough indication of the reproducibility of certain measurements.

a given flow of alternating current through the calibration current sheet. In making these runs, one operator controlled the speed of rotation of the apparatus and the other adjusted the phase and slide wire so as to secure the best balance. At the end of each run the apparatus was stopped, the slide wire was read, and the phase readings taken with the calibration inductor parallel to the earth's field in both the "up" and "down" positions.

The runs were taken in sets of five each. At the beginning of each set the slip rings for the earth inductors were cleaned with kerosene and the resistances R_1, R_2, and R_3 were adjusted so as to give the desired value to the total resistance in circuit No. 1, and so as to make the resistances in circuits No. 2 and No. 3, 250.0 and 100.0 ohms respectively. During the course of the set, the slip rings were again cleaned with kerosene, in general before the 3rd and 5th runs, and at the end of the set the three resistances were again measured. Usually the resistances at the end of the run agreed with those at the beginning within the accuracy of measurement and in only one case was there a difference as great as 0.2%. The resistances of circuits Nos. 1 and 2 were always measured with the apparatus running, so as to make sure that the brushes and slip rings were functioning properly, and the resistance in circuit No. 3 was always measured with a slide wire reading of zero.

29. Data obtained in the calibration runs. Calibration runs were made with the four different possible methods of connecting the coils and amplifier and with different resistances in circuit No. 1 containing the calibration current sheet. The average results, together with the probable errors[16] of those averages which are later used, are given below in Table II.

TABLE II. *Results of the calibration runs.*

Connection	Resistance in circuit 1 (ohms)	Number of runs made	Average phase (degrees)	P.E.	Average slide wire	P.E.	Current × 10^7 ÷ Slide wire (amperes)
	At 23 cycles per second						
A	10,000	20	201.6	0.5	83.3	0.8	4.313
A	5,000	5	201.3		172.0		
A	2,500	5	201.6		349.8		
A	1,000	5	201.6		878.6		
B	10,000	20	213.2	0.7	90.2	1.3	3.983
B	1,000	5	213.6		935.0		
C	10,000	20	156.9	0.5	142.2	2.3	2.526
C	1,000	5	156.1		1538.8		
D	10,000	20	150.3	0.2	135.7	0.6	2.647
D	1,000	5	149.9		1429.4		
	At 17 cycles per second						
D	10,000	20	164.1	0.4	118.8	0.6	2.235

The phase readings were taken to the nearest degree when 10,000 ohms was in circuit No. 1, and to the nearest half-degree when the smaller resistances

were in circuit No. 1, since the larger calibration currents then permitted a more precise setting of the balance. The value of the phase reading assigned to a given individual run was obtained by averaging the readings for the "up" and "down" positions of the calibration inductor after correcting the latter by 180°. The slide wire readings were made to the nearest 0.0001 part of the total length of wire, and the average results in Table II are given to one more figure than read.

Before discussing the use of the calibration runs in interpreting the effect runs, it will be desirable to show that the nature of the results obtained in the calibration runs is what would be expected from the nature of the set up, since this will increase our confidence in the method of measurement adopted.

In the first place, it will be noted from the table that, with a given method of connection, the slide wire readings for balance are not quite inversely proportional to the resistances in circuit No. 1, and hence not quite proportional to the currents in the calibration current sheet. This arises from the fact that the balancing current which flows through the balancing current sheet is itself not quite proportional to the slide wire setting, owing to the unavoidable nature of the design of circuits Nos. 2 and 3. By calculating from the various resistances involved, the currents which actually corresponded to the different slide wire settings, it was found for each method of connection that the balancing currents were themselves actually closely proportional to the calibrating currents as would be expected.

In the second place, it will be noted that the phase settings and the ratios between the balancing and calibration currents necessary to obtain balance vary as we go from one method of connection to another. This presumably arises from a lack of symmetry in the detecting circuit, and as a matter of fact calculations were made which indicated that the presence of a reasonable amount of capacity from the coils to ground, combined with the fact that the filament of the amplifier was itself grounded, would lead to results of the kind actually obtained. Furthermore, as a test of this explanation, it was found that the actual introduction of additional capacity between the ground and the wire connecting the two coils, led approximately to the expected change in the conditions of balance.

Finally, it will be noted that a change in frequency from 23 to 17 cycles had the effect of lowering the slide wire setting and retarding the phase setting necessary for balance. Calculation also showed, however, that behaviour of this kind could be expected from the lack of symmetry mentioned above. Hence in general the method of measurement appears to have behaved in a reliable manner.

30. Calculation of results of the calibration runs. We must now consider the use of the calibration runs in interpreting the effect runs. Since, as mentioned above, the slide wire settings were necessarily not quite proportional to the calibration currents the main calibration runs, upon which subsequent calculations are based, were carried out with a resistance of 10,000 ohms in

circuit No. 1 which gave slide wire readings near enough to those obtained in the effect runs so that the lack of strict proportionality could be neglected.[17]

With 10,000 ohms in the circuit and a speed of revolution of 23 cycles per second, the *average* current flowing in the calibration circuit will evidently have the value

$$I=\frac{4\times 23\times\pi(4.963)^2\times 132\times 0.5258\times 10^{-8}}{10{,}000}=4.941\times 10^{-7}\text{ amperes}$$

and at 17 cycles, the value

$$I=(17/23)\times 4.941\times 10^{-7}=3.652\times 10^{-7}\text{ amperes}$$

where 4.963 cm is the average radius and 132 the number of turns of the calibration inductor as given in Section 11, 0.5258 is the strength of the earth's field in gauss as given in Section 5, and the total impedance is taken equal to the resistance since it was shown by calculation that the self inductances of the calibration inductor and current sheet, and the mutual inductances of the current sheet with the effect coil and its copper shielding produced a negligible effect on the primary current.[18]

The currents thus calculated are those which passed through the 73 turns of the calibration current sheet when the calibration runs were made, and we must now calculate the currents which would give the same effect when passed through one turn having the dimensions of our cylinder. These equivalent currents will evidently have at 23 cycles the value

$$I=73\times 4.941\times 10^{-7}\times(10.120)^2/(10.141)^2=3.592\times 10^{-5}\text{ amperes}$$

and at 17 cycles the value

$$I=73\times 3.652\times 10^{-7}\times(10.120)^2/(10.141)^2=2.656\times 10^{-5}\text{ amperes}$$

where 10.120 is the diameter of the calibration current sheet and 10.141 the diameter of the cylinder, as given in sections 8 and 13, and the slight difference in the lengths of the current sheet and cylinder can evidently be neglected.[19]

[17] If correction were made for the lack of strict proportionality between slide wire setting and the current in the balancing current sheet, it would affect the lowest slide wire reading obtained in the effect runs by less than 0.2 percent, and would affect the other slide wire readings by an even smaller amount.

[18] Calculation showed in the case of the effect coil that the resistance was too high to get any back action of secondary current on the primary, and in the case of the copper shielding that the mutual inductance was too low to get back action. This latter was roughly checked experimentally, since it was found that the sensitivity of the apparatus was not decreased when the original inner shield of the coil, which did not permit the circumferential flow of electricity, was replaced by a continuous tube.

[19] The two lengths were 23.18 cm and 23.42 cm respectively, and the coupling between primary and secondary is not sensitive to a small motion of the primary along its axis. In addition no allowance has in any case been made for the lack of uniformity in the surface density of the charge on the cylinder.

The ratios between these values of the current and the slide wire readings obtained at balance may now be used to interpret the effect runs. These ratios have been calculated and are given in the last column of Table II.

V. The Effect Runs

31. Method of making the effect runs. The effect runs were made in sets of five runs each, the slip rings being cleaned and the resistances in circuits Nos. 2 and 3 being adjusted and measured as described in the case of the calibration runs. Usually the resistances at the end of the set agreed with those at the beginning within the accuracy of measurement and in only two cases was there a difference as great as 0.2 percent.

In order to correct for a small residual effect which was present when the cylinder was oscillating without charge, the first, third and fifth runs of each set were blank runs made with the cylinder uncharged by connection to ground, while the second and fourth runs were made with the cylinder charged to the desired potential by connection with our source of high potential as described in Section 9. In making the second and fourth runs, the apparatus was first started up without any charge on the cylinder and without making any change in the previous slide wire or phase setting, in order to see if the residual effect had remained constant. This was always found to be approximately the case, and the potential was then thrown on the cylinder with the apparatus rotating and the new balance obtained. Thus the first and second runs, and the third and fourth runs of the set each formed a pair from which a corrected value of the slide wire and phase corresponding to the effect of putting on the charge could be obtained. The fifth run of the set was considered merely as an extra blank which showed that no sudden change in the residual effect had occurred.

At the end of each run before stopping the apparatus, the potential, if any, on the cylinder was read on the electrostatic voltmeter, and the apparatus was then stopped, the slide wire was read, and the phase readings taken corresponding to the center of the stroke moving both east and west. Two sets of runs were made without changing the potential, thus giving four values of the effect corresponding to each set of conditions.

For the complete interpretation of the results obtained in the effect runs it was also necessary to measure the amplitude of the motion of the cylinder in order to calculate the current which should have been produced by the motion of the charge which it carried, and since the galvanometer was tuned to the frequency of rotation, what is really wanted is the amplitude of the first harmonic in the Fourier analysis of its motion. On account of the flexibility of the shaft which drove the cylinder and probably also to some extent on account of play in the bearings and backlash in the gears, the total dynamic amplitude of motion obtained when the apparatus was actually running was greater than the static amplitude obtained by turning the apparatus over by hand. Since a graphical analysis of the slow motion of the cylinder when turned over by hand showed that the amplitude of its first harmonic was only very slightly less than the total static amplitude, it seems reasonable to

expect that the actually desired amplitude of the first harmonic of the running motion will be somewhere in between what we have called the static and the dynamic amplitudes.

The static amplitude was carefully measured near the beginning of the effect runs and found to have the value 192.8°. The dynamic amplitude was measured by observing the extreme positions, while running, of a small white pointer which was temporarily attached to the upper end of the cylinder in such a way as to move back and forth over a protractor scale on the top of the coil. At 23 cycles, eight readings of the dynamic amplitude were taken during the course of the runs and eight more at the close of these runs, the final average being 234.0° with a probable error of 0.1°. At 17 cycles, eight readings were taken at the close of the runs with an average of 216.7° and a probable error of 0.1°.

32. Method of treating the data from the effect runs. The method of treating the data from the effect runs is shown by Tables III and IV, which contain

TABLE III. *Effect Runs Nos. 1–10.*

Run	Potential on cylinder (volts)	Dev.	Phase (degrees) E	Phase (degrees) W	Phase (aver.)	Phase (corr.)	Dev.	Slide wire	Slide wire (corr.)	Dev.
1	0		99	93	96			25		
2	−2110	8	344	338	341	330.8	0.5	113	126	0.5
3	0		97	90	93.5			26		
4	−2130	12	346	340	343	331.0	0.3	106	118	7.5
5	0		113	108	110.5			20		
6	0		113	107	110			14		
7	−2110	8	340	334	337	332.2	0.9	117	127	1.5
8	0		88	82	85			23		
9	−2120	2	344	338	341	331.0	0.3	123	131	5.5
10	0		108	102	105			12		
Aver.	−2118	8				331.3	0.5		125.5	3.8
Corr.	−2154									

TABLE IV. *Effect Runs Nos. 11–20.*

Run	Potential on cylinder (volts)	Dev.	Phase (degrees) E	Phase (degrees) W	Phase (aver.)	Phase (corr.)	Dev.	Slide wire	Slide wire (corr.)	Dev.
11	0		87	81	84			20		
12	+2290	6	147	141	144	152.5	1.6	126	117	7.5
13	0		77	71	74			24		
14	+2285	1	143	137	140	150.3	0.6	131	123	1.5
15	0		47	41	44			18		
16	0		53	48	50.5			20		
17	+2285	1	144	138	141	150.0	0.9	126	127	2.5
18	0		69	62	65.5			23		
19	+2275	9	144	138	141	151.0	0.1	135	131	6.5
20	0		57	51	54			13		
Aver.	+2284	4				150.9	0.8		124.5	4.5
Corr.	+2319									

the results from our first twenty runs made with approximately equal negative and positive potentials on the cylinder, and by Figs. 5 and 6 which illustrate the method of correcting for the residual effect.

The potential on the cylinder with a given adjustment of our high potential apparatus remained nearly enough constant so that the average value could be taken as applying to all the runs involved. The potentials as read are given in the second column of the tables, the average value, together with the corrected value obtained by applying the results of the calibration of the voltmeter, being given at the bottom of the column, and the deviations from the mean being given in the next column.

The fourth and fifth columns of the tables give the phase reading at the center of the stroke moving east and that at the center of the stroke moving west corrected by 180°. As already mentioned in Section 11, these two figures differed by an approximately constant amount of about 6°, owing

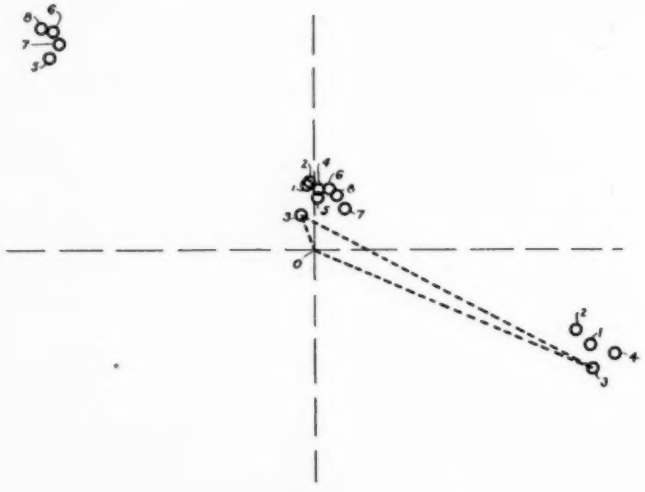

FIG. 5

to the geometry of the driving mechanism. Their average value is given in the sixth column of the table. The slide wire readings were read to the nearest 0.0001 part of the total length and are given to the number of figures read in the next but one to the last column of the tables.

The corrected values for the phase and slide wire readings, corresponding solely to the added effect produced by the charge on the cylinder, were obtained by subtracting the vectors which represented the phase and slide wire readings for the blank runs, from those which represented the results in the corresponding runs with the cylinder charged. This was done graphically as shown in Fig. 5, where the data have been plotted for the runs given in Tables III and IV.

The individual points in this plot are the termini of vectors plotted from the origin with a length equal to the slide wire reading and at an angle which equals that of the phase reading. The group of points just above the origin

represent the readings obtained in the blank runs, those in the upper left hand quadrant represent the readings obtained with the positive voltage on the cylinder, and those in the lower right hand quadrant with the negative voltage.

The points in the plot are numbered in the order in which the runs were made, the pair of points, belonging to an individual blank run and the associated following run in which the cylinder was charged, being given the same number. The vectors which connect the two points of these pairs then represent the corrected slide wire readings and phase angles which correspond to the effect of putting the charge on the cylinder. Thus the shorter vector 03 in Fig. 5 represents the result obtained in the blank run No. 5 in Table III, the longer vector 03 represents run No. 6, and the vector 33 the corrected result.

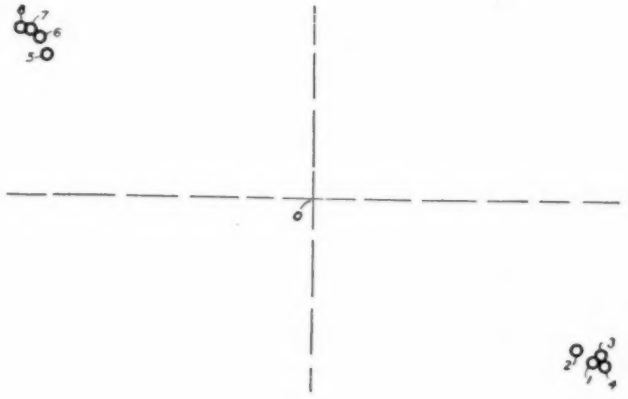

FIG. 6

The corrected results obtained in this way are shown in Fig. 6. plotted directly from the origin, the points being numbered as before. The method of correcting assumes that the residual effect given by the uncharged cylinder remains present in the same amount after the potential is applied. This is, of course, a reasonable assumption to make, especially as it seems plausible to suppose that the residual effect was due to small currents induced in the apparatus by motion through the earth's magnetic field. It will be seen by comparing Fig. 6 with Fig. 5, that the application of the correction gives a considerable improvement in the appearance of the results.

33. The results of the effect runs. With the methods described above, we made a total of 64 successful effect runs together with the blank runs which went with them. In addition three runs were tried at a potential so high that successful balance could not be made because of too frequent sparking, and two runs were tried at a moderate potential at a time, however, when the cylinder had recently been replaced in position, which appeared to produce unsteady conditions until the air gap between cylinder and coil had been "cleaned up" by treatment with higher potential.

The 64 runs consisted of 16 groups of 4 runs each, made under different sets of conditions. The average results for the 16 different sets of conditions are given in Table V in the order in which they were actually obtained. The first column gives the method of connecting the coils and amplifier as described in Section 14. The second column specifies the neutral position around which the cylinder was oscillated, by giving the direction of the longitudinal slit in the copper foil which coated the cylinder. The third and fourth columns give the average potential on the cylinder together with its average deviation. The next three columns give the average value of the phase setting corresponding to balance, together with its average deviation and the "expected" value of the phase based on the results of the calibration runs. The last columns give the average slide wire corresponding to balance, its average deviation, the calculated equivalent current flowing in a sheet having the dimensions of the cylinder which would produce this slide wire reading, and the ratio of this equivalent current to the potential of the cylinder.

34. Discussion of results obtained in the effect runs. The different conditions under which the foregoing effect runs were carried out were designed for the purpose of testing the results produced: *a*, by changing the potential on the cylinder; *b*, by changing the method of connecting the coils and amplifier; *c*, by changing the neutral position around which the cylinder was oscillated; and *d*, by changing the speed of oscillation of the apparatus. The first runs were made at the highest speed at which the apparatus would run with reasonable smoothness, using a moderate potential on the cylinder, and using connections *D*, which had given approximately the expected results in the preliminary runs without the final unjointed shield inside the coil and which had happened to give the most concordant results in the calibration runs. The potentials were then varied to as high values as could be used without too much sparking over between cylinder and shield and to as low values as would still give reasonable accuracy. This was followed by changes in the method of connection, by changes in the neutral position of the cylinder, and finally by change to an appreciably lower speed of oscillation which, however, was still high enough to give reasonable accuracy.

We must now examine the results thus obtained, as given in Table V, to see if they agree with what would be theoretically predicted. If so, the phase settings obtained at balance should agree with what would be predicted on the basis of the calibration runs; the effective current produced by the moving cylinder should be proportional to the potential of the cylinder, and to the speed of the peripheral motion; and the absolute magnitude of this effective current should agree with that calculated from the motion of the cylinder and the charge on it.

In order to compare the phase readings obtained in the effect and calibration runs, it was noted on the one hand that the average phase readings obtained in the effect runs corresponded to a position in which the cylinder was at the center of its motion moving clockwise viewed from above, and it was noted on the other hand, from a check made on the direction of motion of the calibration inductor through the earth's field, that the average phase

readings obtained in the calibration runs corresponded to a position in which the current in the calibration current sheet was at a maximum and flowing clockwise viewed from above. Hence the average phase readings obtained in the effect runs with a positive charge on the cylinder are to be compared directly with those obtained in the corresponding calibration runs, and the readings obtained with a negative charge are to be compared with those obtained in the calibration runs after correcting the latter by 180°.

TABLE V. *Results of the effect runs.*

Connection	Orientation of cylinder	Potential of cylinder (volts)	A.D.	Average phase (degrees)	A.D.	Phase obtained in calibration (degrees)	Average slide wire	A.D.	Equivalent Current $\times 10^9$ (amperes)	Current ÷ Potential $\times 10^{10}$
				At 23 cycles per second						
D	North	−2154	8	331.3	0.5	330.3	125.5	3.8	3.322	154
D	North	+2319	4	150.9	0.8	150.3	124.5	4.5	3.296	142
D	North	+1474	2	148.0	2.8	150.3	82.8	5.8	2.192	149
D	North	−1533	2	335.1	2.2	330.3	81.8	6.3	2.166	141
D	North	−2639	10	337.1	0.7	330.3	145.5	2.0	3.852	146
D	North	+2665	19	156.1	2.5	150.3	156.0	2.0	4.130	155
D	North	+1886	6	154.6	2.8	150.3	111.5	8.8	2.951	156
D	North	−1781	4	334.6	2.4	330.3	98.0	2.5	2.594	146
A	North	−2224	2	30.8	2.4	21.6	77.8	2.2	3.356	151
B	North	−2234	2	32.8	1.5	33.2	81.8	0.9	3.258	146
C	North	−2219	2	341.2	0.9	336.9	130.0	6.5	3.284	148
D	East	−2220	15	334.4	1.8	330.3	121.3	4.3	3.210	145
D	South	−2218	9	333.8	1.8	330.3	123.3	5.3	3.263	147
D	West	−2214	2	333.2	1.3	330.3	118.5	3.0	3.138	142
				At 17 cycles per second						
D	North	−2204	4	341.5	2.5	344.1	103.3	7.3	(3.371)	(153)
D	North	+2266	4	164.6	2.8	164.1	107.0	2.5	(3.493)	(154)
									Average	148.4

To facilitate the comparison, the figures thus obtained from the calibration runs have been entered in the seventh column of Table V, and their approximate agreement with those obtained in the effect runs will be noted. Attention is particularly called to the expected change in phase by 180° produced by a reversal in the sign of the charge on the cylinder, to the expected change in phase which accompanied a change in connections, to the expected lack of any change from a mere change in the neutral position around which the cylinder was oscillated, and to the expected change in phase which accompanied the change in frequency.

To test the expected proportionality between the effective current produced by the moving cylinder and the potential on the cylinder, we have used the figures in the last column of Table II, to calculate the equivalent currents flowing in a sheet having the dimensions of the cylinder which would have produced the same slide wire readings as were obtained in the effect runs, and have entered these values of equivalent current in the next to the last column of Table V. These values have then been plotted against the potentials in Fig. 7, where they will be seen to fall as well as could be expected on a straight line. In addition the ratios of equivalent current to potential have been calculated and entered in the last column of Table V, and will also be seen to be as constant as could be expected.

In order to compare the two results obtained at 17 cycles with those obtained at 23 cycles, we have multiplied the values which they gave for

equivalent current by the ratio of the two frequencies 23/17 and by the ratio of the two dynamic amplitudes[20] 234.0/216.7. The corrected values of equivalent current thus obtained have been inserted in brackets in the next to the last column of Table V, and are included in the plot in Fig. 7, and have also been used for calculating the ratios of equivalent current to potential which are given in brackets in the last column of Table V. The agreement thus shown between the values of equivalent current obtained at 17 to 23 cycles furnishes a satisfactory check of the theoretical dependence of the current on the velocity of the cylinder.

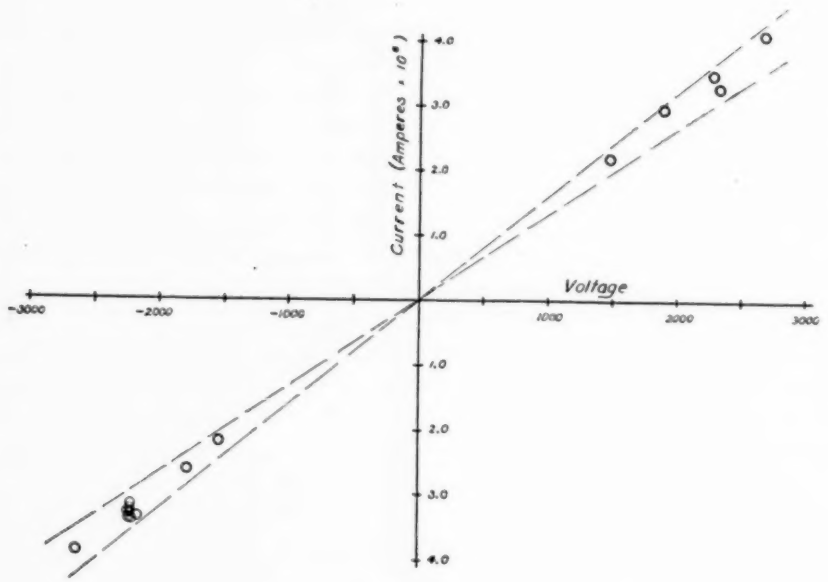

FIG. 7

Finally to test the absolute magnitudes of the equivalent currents we must calculate the theoretical current which would be produced by the motion of the charged cylinder, and in doing this shall use both the static and dynamic amplitudes, since, as stated in Section 31, it seems reasonable to expect that the first harmonic of the actual running motion of the cylinder would have an amplitude lying between these two. For the *average* value[21] of the theoretical current which would be produced by the moving cylinder when charged to a potential of one volt, we may evidently write for the two cases in question,

$$I = 2\times 23\times\frac{192.8}{360.0}\times 5.385\times 10^{-10} = 132.6\times 10^{-10} \text{ amperes}$$

[20] This assumes that the ratio of the total amplitudes of the two motions is the same as he ratio of the amplitudes of their first harmonics, which may not be exactly true.

[21] Note that the calibration runs were also calculated for the *average* value of the current

and

$$I = 2 \times 23 \times \frac{234.0}{360.0} \times 5.385 \times 10^{-10} = 161.0 \times 10^{-10} \text{ amperes}$$

where the values of the static and dynamic amplitudes 192.8 and 234.0 degrees are those given in Section 31, and 5.385×10^{-10} is the capacity of the cylinder in farads as given in Section 25.

Comparing now with the values in the last column of Table V, it will be at once seen that the experimental values of the equivalent currents do fall as expected between the two theoretical values, calculated using the static and dynamic amplitudes for the motion of the cylinder. This is also shown in the plot in Fig. 7, where the two diagonal lines through the origin have been drawn so as to give the two calculated relations between current and potential.

35. Conclusion. In view of all the foregoing correspondences, the conclusion can now be drawn that the experiments described above do give a very satisfactory demonstration of the equivalence of a mechanically oscillated electrostatic charge to an ordinary alternating current. Attention is specially called to the consistency of the effects obtained with different methods of connecting the coils and with different neutral positions for the cylinder, since this furnishes evidence for the elimination of accidental effects which were present before the apparatus was put into its final form. In summary, it can be said, that qualitatively the effects obtained from the oscillatory motion of our charged cylinder were in entire agreement with theory, and that quantitatively the correspondence between experimental and theoretical values was good and as close as could be expected.[22]

We desire to express our appreciation to the California Institute for the support which it gave to this expensive investigation, and to give our thanks to Mr. Julius Pearson and his assistants for their skill in the construction of apparatus.

[22] Using the language in which the results of the original Rowland experiment were expressed, this quantitative check would have been expressed as furnishing evidence that the ratio of the electromagnetic unit of current to the electrostatic unit of current is equal to the velocity of light. This method of expressing the quantitative check has, however, not occurred in the present article since we have from the start given the capacity and potential of the cylinder in farads and volts instead of in electrostatic units.

THE M-SERIES ABSORPTION SPECTRA OF METALLIC PLATINUM AND GOLD

By Arthur J. M. Johnson
Hall of Physics, State University of Iowa

(Received July 27, 1929)

Abstract

The M-absorption spectra of metallic platinum (78) and gold (79) have been investigated by the use of a vacuum spectrograph. Five discontinuities were found for platinum at 5.711A (M_1), 5.506A (M_2), 4.677A (M_3), 4.085A (M_4), and 3.742A (M_5). For gold four were found at 5.506A (M_1), 5.315A (M_2), 4.501A (M_3) and 3.603A (M_5). No M_4 discontinuity was found for gold and the M_4 for platinum was very faint. The $(\nu/R)^{1/2}$ values for the experimentally determined edges compare very favorably with the values predicted by the use of absorption and emission data from the L-series except in the case of M_1 and M_2 where an unmistakable deviation, previously reported by other investigators on other elements, appears to be confirmed. No measurable shift in the position of any of the discontinuities due to a change in valence of four, in the case of the platinum atom, was observed. No "white line" absorption was observed at any of the discontinuities.

Introduction

THE work of Rogers[1] on the x-ray M-absorption spectra of osmium (76), iridium (77), and platinum (78) revealed a systematic discrepancy between the actual positions of the M_1 and M_2 discontinuities and those predicted by Bohr and Coster[2] and by Sommerfeld[3] by the use of emission and absorption data from the L-series.

Rogers' results were in agreement with those previously reported by Zumstein[4] in his work on tungsten. Rogers and Zumstein found that the M_1 and M_2 absorption discontinuities occurred at frequencies greater than those predicted, indicating a somewhat tighter binding of the electrons in these levels than was to be expected from the application of the combination principle to the L-emission and absorption data as mentioned above.

The existence of a chemical influence upon the positions of the M discontinuities, due to the state of combination of the atoms composing the absorbing screen, has been suggested[1] as a possible partial explanation of the results observed. The work of a number of authors[5] has definitely established

[1] R. A. Rogers, Phys. Rev. **30**, 747 (1927).
[2] Siegbahn "Spectroscopy of X-Rays" Eng. pp. 184–5.
[3] Sommerfeld "Atombau—" 4th Ger. ed. pp. 304–5.
[4] R. V. Zumstein, Phys. Rev. **25**, 747 (1925).
[5] J. Bergengren, Zeits. f. Physik **3**, 247 (1920); Comptes rendus **171**, 624 (1920).
A. Lindh. Comptes rendus **172**, 1175 (1921); Zeits. f. Physik **6**, 303 (1921); Comptes rendus **175**, 25 (1922); Ark. f. Mat., Astr. och Fys. **18**, Nr. **14**, (1924); Zeits. f. Physik **31**, 210 (1925).
K. Chamberlain, Nature **114**, 500 (1924); Phys. Rev. **26**, 525 (1925).
D. Coster, Zeits. f. Physik **25**, 83 (1924).

the existence of such an effect in the *K*-absorption of lighter atoms. The effect has not been reported for the absorption discontinuities of heavier atoms.

Since the investigations of Rogers and Zumstein were made with a compound of the element in question as the absorbing material, it seemed that the "chemical effect" explanation was at least possible. The work here reported was undertaken for the purpose of testing this point by the use of absorption screens made of the pure element.

Platinum was chosen from the elements investigated by Rogers because it seemed to be better suited to the proposed production of absorption screens of the pure element. The method proposed was the evaporation of the metal in a vacuum and its condensation upon a base that would be transparent to the comparatively long and easily absorbed x-radiation to be used in this work.

The investigation of gold was undertaken for the reason that it lies next to platinum in the periodic classification and can be obtained in sheets thin enough for use in the absorption screens. Edges obtained by the use of such screens would certainly be free from effects due to chemical combination. For this reason results in comparative agreement with those found for platinum by the use of the evaporated metal screens should tend to confirm belief in the reliability of such results. The *M*-absorption spectrum of gold has never been investigated to the knowledge of the author.*

Experimental

The vacuum spectrograph used has been described by both Zumstein[4] and Rogers.[1] Its operation in this work differed in minor details only. The slit-window separating the metal x-ray tube from the spectrometer chamber was made of goldbeaters skin rendered opaque to ordinary light by a thin coating of lamp black. This type of window, though somewhat less transparent to the x-radiation than the collodion windows used previously, was much stronger. The increased absorbing power of the slit-window was more than offset by the marked increase in intensity of the x-radiation from the metal tube due to the removal of all mercury vapor by the use of a liquid-air trap.

The crystals used were very fine specimens of gypsum ($Ca\,SO_4 \cdot 2\,H_2O$). Note has been made of their peculiar behavior in an appendix.

The production of uniform platinum absorption screens of the required thickness was the most difficult part of the present problem. The method of finely ground metal suspended in collodion having failed[1] the only other methods that seemed to promise success were the use of very thin foils or the deposition of the metal upon an appropriate base by cathodic sputtering or by evaporation. After unsuccessful attempts to secure platinum foil of

---

Franck u. Kuhn, Ziets. f. Physik **43**, 3/4 May (1927)

O. Stelling, Zeits. f. Anorg. Chem. **131**, 48 (1923); Zeits. f. Phys. Chen. 117, 161 (1925).

S. Aoyama K. Kimura. Y. Nishina. Zeits. f. Physik **44**, 810 (1927).

* See note appended.

the desired thickness, the method of evaporation was chosen. The problem of obtaining a suitable base upon which such deposition could be made was finally solved by the use of very thin glass. These bases were prepared by blowing large thin bubbles of soft sodium glass. It was easily possible to find pieces of these bubbles sufficiently flat and of thicknesses of the order of 10^{-4} cm. Such sheets were quite transparent to the rays, were not very seriously affected by proximity to a white-hot platinum filament in vacuum, and with care could be mounted upon pasteboard frames for use in the spectrometer.

The evaporation chamber was very simple in construction. It consisted of a three-litre bell-jar mounted on a brass base. The junction of the jar and base was ground to fit and made vacuum-tight by the use of beeswax melted around the outside of the joint by gently heating the parts with a flame. The use of a harder wax was prohibited by the impossibility of heating the heavy bell-jar sufficiently to melt the wax without cracking the jar.

The filament was made by coiling a platinum wire 0.010 in. in diameter about the shank of a number 60 twist drill. The filament was then suspended horizontally about five or six millimeters above a water-cooled copper table upon which the deposit base was held by two small drops of collodion-amyl-acetate solution.

The evaporation chamber was evacuated by means of a Cenco Hyvac oil pump and a diffusion pump operating through a liquid-air trap.

With the platinum filament operating at temperatures only slightly below the melting point visible deposits could be obtained in from eight to ten minutes. Satisfactory screens for the production of the desired absorption edges were obtained by evaporation of from three to twenty hours depending of course upon the depositing conditions and the discontinuity for which the screen was to be used. The deposits thus obtained were very smooth and had a metallic lustre. In order to try to test the films thus deposited for purity an especially heavy deposit was made on a portion of a microscope slide from which it was dissolved with aqua regia for chemical analysis. Due to the small weight of the sample (less than 0.01 gram) only slightly more than 80 percent of the weight was recovered as platinum. It is felt that the films were much more pure than this single attempt at analysis indicated.

The wave-lengths of the discontinuities here reported are regarded as accurate to within ± 0.005A excepting the wave-length of the M_2 absorptions. On account of their diffuse character these edges are harder to measure with accuracy. They are regarded as accurate to at least ± 0.008A or slightly more than one-tenth of one percent.

Results

The following tables include the average wave-length results of the plate measurements with the corresponding (ν/R) and $(\nu/R)^{1/2}$ values together with the corresponding data taken from Bohr and Coster's revised tabulations (see Siegbahn "Spectroscopy of X-rays") of the computed values

of the M-absorptions for both gold and platinum. In the table of the results on platinum there have been included the values previously reported by R. A. Rogers in his article to which frequent reference has been made.[1]

TABLE I. *Platinum M-series absorption. Wave-lengths of all emission lines used as reference are taken directly from Siegbahn's "Spectroscopy of X-rays."*

Edge	Wave-length	(ν/R)	$(\nu/R)^{1/2}$	Reference lines	Author*
M_1	5.711A	159.6	12.63	Au $M\alpha$; Au $M\beta$; Pb $M\alpha$.	J.
	5.736	158.9	12.60		R.
	5.826	156.4	12.51		B&C.
M_2	5.506	165.5	12.86	Au $M\alpha$; Au $M\beta$; Pb $M\alpha$.	J.
	5.541	164.5	12.83		R.
	5.615	162.3	12.74		B&C.
M_3	4.677	194.8	13.96	Bi $M\alpha$; Bi $M\beta$; Pb $M\alpha$; Pb $M\beta$; Cl $K\alpha$.	J.
	4.674	195.0	13.96		R.
	4.671	195.1	13.97		B&C.
M_4	4.085	223.1	14.94	Th $M\alpha$; Th $M\beta$; K $K\alpha$.	J.
					R.
	4.063	224.3	14.98		B&C.
M_5	3.742	243.5	15.61	Th $M\alpha$; Th $M\beta$; K $K\alpha$.	J.
	3.738	243.8	15.61		R.
	3.744	243.4	15.60		B&C.

* J. = Johnson; R. = Rogers: experimental values.
B&C. = Bohr and Coster: calculated values.

TABLE II. *Gold M-series absorption.*

Edge	Wave-length	(ν/R)	$(\nu/R)^{1/2}$	Reference lines	Author
M_1	5.506A	165.5	12.86	Au $M\alpha$; Au $M\beta$; Mo $L\alpha$; Mo $L\beta$; Bi $M\alpha$; Pb $M\alpha$.	J.
	5.594	163.0	12.77		B&C.
M_2	5.315	171.5	13.09	Same as for M_1	J.
	5.383	169.3	13.01		B&C.
M_3	4.501	202.5	14.23	Bi $M\alpha$; Bi $M\beta$; Pb $M\alpha$; Pb $M\beta$; Cl $K\alpha$; Pb $M\gamma$; Bi $M\gamma$; Th $M\alpha$.	J.
	4.494	202.8	14.25		B&C.
M_4					J.
	3.876	235.1	15.33		B&C.
M_5	3.603	252.9	15.90	K $K\alpha$; Th $M\beta$; Th $M\alpha$.	J.
	3.604	252.9	15.90		B&C.

DISCUSSION

The values of the M_1 and M_2 absorption wave-lengths of platinum as measured by the author appear to be such as to indicate a somewhat *tighter* binding of the electrons of these two levels than found by Rogers, being shorter in wave-length than the values reported by him by 0.025A and 0.035A respectively. This apparent difference has no significance for at least two rea-

sons. Rogers used the mercury M_α and M_β lines for reference in making his measurements on these edges. The wave-lengths of these lines as given in Siegbahn are taken from Karcher's measurements,[6] which are found to be on the average about 20XU too high in value by the method of measurement by interpolation using strong neighboring emission lines whose wave-lengths have been measured more accurately by Stenstrom. (Siegbahn "Spectroscopy of X-rays" page 125.) Karcher's M lines, α and β in particular of the elements lead, thallium, gold and platinum also show a corresponding variation of from 0.013A to 0.031A above the values reported by Stenstrom. Thus it would seem that the use of these lines as reference would introduce an error of at least 0.020A in the proper direction to explain the above disagreement. Reduction of the values reported by Rogers by this amount brings the value of the M_1 edge to agreement with the values here

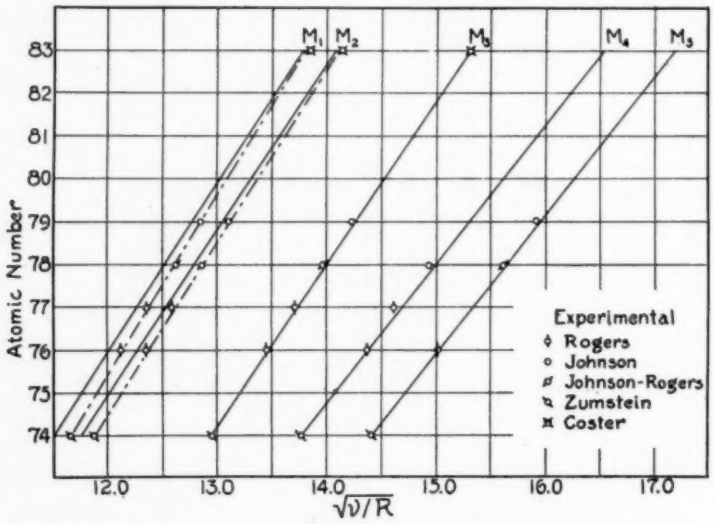

Fig. 1. Values of $(\nu/R)^{1/2}$ plotted against atomic number. Full lines represent the average computed values of both Bohr and Coster and of Sommerfeld.

reported within the experimental accuracy claimed for these results. The discrepancy of 0.015A remaining between the result here reported for M_2 and that of Rogers can certainly be partly due to the very diffuse character of this edge. Rogers' three reported measurements on this edge differ among themselves by 0.011A.[1] The author's remeasurements of Rogers' original plates have given an average value somewhat shorter than the average reported by him. Careful comparison of the two sets of plates has shown no observable difference in the positions of the M_2 edges.

Such small discrepancies observed between the wave-lengths reported for Pt M_1 and Pt M_2 by Rogers and the author in no way approximate the value of the displacement of the values of $(\nu/R)^{1/2}$ for these two edges toward higher values than those predicted by computation from L-series data.

[6] J. C. Karcher, Phys. Rev. 15, 288 (1920).

The positions of the measured values of $(\nu/R)^{1/2}$ plotted against the atomic number for the elements W (74) to Bi (83) are shown in the figure. The solid lines represent the average computed values of both Bohr and Coster[2] and of Sommerfeld.[3] The displacements of the absorption edges on the photographic plates corresponding to the displacements in $(\nu/R)^{1/2}$ values from the average predicted values as shown in the figures are from about 0.18 cm to 0.30 cm. The accuracy of measurement of the positions of these discontinuities as determined by repeated measurements was at least to ± 0.015 cm in the case of the M_2 edge, which is the most diffuse, and at least to ± 0.01 cm for the other edges. The accuracy of such measurements over this region of wave-lengths has been discussed elsewhere[1] and will not be further treated here.

That the predicted positions are subject to the errors of measurement of the L-series phenomena necessary for such computations is recognized. Supposing the errors inherent in such L-series measurements to be as great as the errors admitted for these measurements it can be shown by a simple computation that at most the effect upon the position of an M-discontinuity will not be greater than five times the error of measurement of the edge by the present method. Such an error is apparently out of the question but if it were not it would be insufficient to account for the variation observed.

The variation seems to increase with decreasing atomic number (See Tables I and II) the experimental points falling upon the broken lines, (Fig. 1) which are displaced toward higher frequency values. The calculated and observed values for the elements Bi (83), Th (90), and U (92), the only other elements upon which measurements have been made,[7] agree well within the limits of experimental error.

Certainly the present investigation shows no shift in the positions of the M_1 and M_2 edges of pure platinum from the positions observed by Rogers using chloroplatinic acid as absorbing material. That the state of chemical combination of the absorption screen exerts no observable effect upon the positions of these edges is further borne out by the observed positions of the corresponding edges for gold. Here there is certainly no valence effect, yet the edges show relatively the same displacements from their predicted positions as do those of the elements observed in which compounds were used as absorbing screens.

A word must be said concerning the nature of the edges observed. With no exception they were of the " edge" type. The "white line" type of absorption reported by Rogers for the M_3 and M_5 discontinuities of platinum was not observed. (He did not observe M_4.) In this research both M_4 and M_5 of platinum were very faint and it cannot be definitely stated that they did not exhibit white lines. M_5 of gold however was very strong and certainly showed no such fine structure. The M_3-absorptions of both platinum and gold were strong and sharp and were certainly of the true edge type. No explanation can be offered at this time for the two different types of edges observed in

[7] D. Coster, Phys. Rev. **19**, 20 (1922).

the two investigations. It might be suggested, however, that the explanation put forward by Miss Chamberlain[8] have some confirmation here. She has attempted to explain the appearance of white-line phenomena as being due in some manner to the reduction of the chemical compound in the absorption screen by the action of the rays themselves.

Though the errors inherent in the prediction of the M-levels from L-series data are from four to five times greater than the error of actual measurement of these same edges, granting the same accuracy of determination of the L-absorptions as has been claimed for the M-absorption measurements, it seems that the comparatively greater accuracy of measurement possible in the case of the L-series wave-lengths makes the predicted and the measured values of almost exactly equal reliability. We have therefore great confidence in the reality of the displacement of the edges from the positions at which we should expect to find them.

These marked systematic discrepancies apparently cannot be explained upon the basis of errors either of prediction or of measurement, and since the use of the carefully measured L_1-absorption with the appropriate emission line of the L-series results in the prediction of the M_4 and M_5 levels with satisfactory accuracy, while the use of this same edge with the strong sharp lines, which have their origins on the M_1 and M_2 levels, does not result in values sufficiently close to the measured values, it seems possible that the simple application of the combination principle is insufficient in this case. This principle has received such general confirmation from spectroscopic and other sources that we cannot well question its general applicability. We may suggest however that the general truth of the principle as applied to the radiation of characteristic spectral lines involves energy levels whose frequencies *may* not be exactly identical with the frequencies associated with these same "levels" when the atom is being excited by the absorption of incident x-radiation. The usual conceptions of the changes that take place in the absorption and emission of x-radiation leave no room for such possibilities, and yet we have evidence here of a phenomenon that at present is unexplained. We can only say that we regard the measured values as accurate, within the limits assigned to them, and *apparently* the experimental measurements upon which the predictions of these levels have been based are of sufficient accuracy to permit of their use with confidence in the order of accuracy of the results.

The writer wishes to thank the members of the staff of the Department of Physics of the State University of Iowa for their interest and assistance. Thanks are especially due to Dr. G. W. Stewart who suggested and directed this investigation.

Note added August 3, 1929

After the preparation of this article for publication, an article appeared by Ernst Lindberg[9] in which some of the absorption discontinuities here re-

[8] K. Chamberlain. Phys. Rev. **26**, 525 (1925).
[9] E. Lindberg, Zeits. f. Physik **54**, 632 (1929).

ported have been measured. His values of the M_1 and M_2 absorption wave-lengths for platinum and gold are longer than those reported here by amounts seemingly greater than is permitted by the errors of measurement. His wave-length values nevertheless show the same tendency as those here reported, being unmistakably shorter than those predicted. The following tables show how these new values compare with those reported here and with the computed values.

TABLE III. *Comparison of the results of Lindberg and of Johnson on the absorption-edge wave-lengths.*

Edge	Calc.	Johnson	Lindberg	Δ_1*	Δ_2*	Δ_3*
Pt M_1	5.826A	5.711A	5.746A	0.115A	0.080A	0.035A
Pt M_2	5.615	5.506	5.544	.109	.071	.038
Pt M_3	4.671	4.677	4.676	−.006	−.005	−.001
Au M_1	5.594	5.506	5.529	.088	.065	.023
Au M_2	5.383	5.315	5.330	.078	.053	.015
Au M_3	4.494	4.501	4.508	−.007	−.014	.007

TABLE IV. *Comparison of* (ν/R) *values.*

Edge	Calc.	Johnson	Lindberg	Δ_1*	Δ_2*	Δ_3*
Pt M_1	156.4	159.6	158.6	3.2	2.2	1.0
Pt M_2	162.3	165.5	164.4	3.2	2.1	1.1
Pt M_3	195.1	194.8	194.9	−.3	−.2	−.1
Au M_1	163.0	165.5	164.8	2.5	1.8	.7
Au M_2	169.3	171.5	171.0	2.2	1.7	.5
Au M_3	202.8	202.5	202.2	−.3	−.6	.3

TABLE V. *Comparison of* $(\nu/R)^{1/2}$ *values.*

Edge	Calc.	Johnson	Lindberg	Δ_1*	Δ_2*	Δ_3*
Pt M_1	12.51	12.63	12.59	.12	.08	.04
Pt M_2	12.74	12.86	12.82	.12	.08	.04
Pt M_3	13.97	13:96	13.96	−.01	−.01	.00
Au M_1	12.77	12.86	12.84	.09	.07	.02
Au M_2	13.01	13.09	13.08	.08	.07	.01
Au M_3	14.25	14.23	14.22	−.02	−.03	.01

* Δ_1 = Difference between Johnson and calculated values.
Δ_2 = Difference between Lindberg and calculated values.
Δ_3 = Difference between Johnson and Lindberg values.

The maximum variation between the values given by Lindberg and those of the author above corresponds to a distance on the photographic plate of approximately one-half millimeter. The obvious explanation would seem to be that the gold emission lines, which form part of our reference system for the measurement of Pt M_1 and M_2, are in error. Lindberg has measured these lines[10] and though his reported values are longer by 0.008A for Au M_α and by 0.010A for Au M_β this will only account for one-third of this discrepancy. With the data at hand the reasons for the too large difference between our values is not apparent.

[10] E. Lindberg, Zeits. f. Physik **50**, 91 (1928).

Appendix

Very marked deterioration of the gypsum crystals used in this investigation with respect to their reflecting power for x-rays was noticed after use for certain lengths of time. This deterioration occurred four times during the progress of this work at intervals of several months. The only crystal upon which any data were taken exhibited this peculiarity after having been in vacuum for about eighteen hundred hours during which time it was exposed to x-radiation from a tungsten coated cathode excited by potentials of from four to ten kilovolts for approximately nine hundred hours.

It is suggested that the effect may be due to dehydration of the crystal, possibly due to the exposure of the crystal to the radiation in a partial vacuum; which would be destructive of the crystal arrangement. No visible deterioration of the crystal was observed. It remained clear with no traces of the white powdry appearance usually associated with the dehydration effect caused by heat.

The effect is not confined to the reflecting "surface", for the reflecting power of the face approximately one sixteenth of an inch below the original surface is also very poor, although slightly better than that of the original outside surface. This was tested by simply splitting thin layers from the reflecting surface of the bad crystal and taking photographs with the newly exposed surfaces. No appreciable recovery of reflecting power after several months "rest" under atmospheric conditions was observable. In the article "The Dehydration of Barium Platino-cyanide Crystals under the Action of X-Rays" reported by Trapesnikow[11] it was found that the crystals recovered the lost water of hydration when air was admitted to the vacuum system. No further suggestions can be offered at this time to explain the phenomenon observed. That it occurs there can be no doubt.

[11] A. Trapesnikow, Zeits. f. Physik **47**, 732–4 (1928).

THE INTENSITY OF REFLECTION OF X-RAYS FROM DIAMOND

By Alice H. Armstrong
The Rockefeller Institute for Medical Research

(Received August 22, 1929)

Abstract

Ionization spectrometer measurements of the intensity of reflection of the $K\alpha$ doublet of molybdenum by fine diamond powder were made by the transmission method. The diameter o the individual particles was 10^{-4} cm or less, whereas 3×10^{-5} cm is the length of the cube edge of a block small enough so that primary extinction, calculated from Darwin's formula, be less than 1 percent. Secondary extinction was probably negligible. The relative intensities of the radiation reflected from the different planes of the diamond were obtained by comparisons of the areas under the peaks. From these relative intensities the relative F values were obtained by use of a formula derived by Compton and modified to fit the conditions of this experiment. These relative values were placed on an absolute scale by comparison of the intensity of the (220) reflection of diamond with that of the (220) reflection of NaCl, for which the absolute value has been determined. The (222) reflection, previously observed by W. H. Bragg and by Ehrenberg, Ewald, and Mark in studies of single crystals, was also observed here. It might occur if the carbon atoms are of two kinds with different scattering powers, or if adjacent carbon atoms shared electrons between them in such a way as to provide scattering centers upon the line joining them. Neither explanation, however, is entirely compatible with the experimental data. A Fourier analysis was applied to the data and the resulting distribution curves compared with those calculated by Havighurst from Hull's and Bragg's data.

SPECTROMETER measurements of the intensity of reflection from different planes of diamond have been made only by W. H. Bragg[1] on a single crystal and by Ponte[2] on rather coarse diamond powder. As primary extinction may have been operative to an appreciable extent in both cases, it has seemed worthwhile to repeat the experiment with finer powder,[3] in order that more accurate determinations of the scattering power be obtained.

Experimental Procedure

The diamond powder was molded into a flat plate. On account of the small amount of powder available and the consequent small size of the briquet, the transmission method described by Compton[4] was used. The ionization currents were measured by means of a Curie quadrant electrometer and scale system with a sensitivity of about 3 meters per volt.

[1] W. H. Bragg, Proc. Phys. Soc. London **33**, 304 (1921).

[2] M. Ponte, Phil. Mag. **3**, 195 (1927).

[3] The author is greatly indebted to Mr. B. W. St. Clair and the General Electric Company of Lynn, Massachusetts, who lent the diamond powder used in these investigations.

[4] A. H. Compton, X-rays and Electrons, p. 131 (Van Nostrand, 1926).

In order that the focussing condition be fulfilled, the focal spot on the target of the x-ray tube and the slit of the ionization chamber were equidistant from the axis of the spectrometer.

The $K\alpha$ doublet of the molybdenum spectrum was used in these measurements and was obtained by filtration of the molybdenum radiation through a screen of zirconium oxide of appropriate thickness. For most of the observations the x-ray tube was operated at 25 milliamperes and a constant potential of about 33,000 volts furnished by a storage battery.

Discussion of Extinction

The greatest source of uncertainty is extinction. Havighurst[5] has shown that when the individual particles of various kinds of crystals become as small as 10^{-3} cm in size, secondary extinction is negligible. He found, however, that primary extinction might in some cases remain effective until the size of the crystal blocks was 10^{-5} cm or less. These figures were obtained for powders known to approach the ideally imperfect type. For diamond, which has been found to be more nearly perfect, it is possible that the size of the individual fragments should be still smaller in order that extinction become negligible. Estimates of the size of the powder particles used in this investigation were obtained by reflecting onto a distant screen by means of a prism the image given by a high-power microscope. The diameter of most of the particles was about 10^{-4} cm. A few larger images may have been due to larger individual crystals scattered through the mass, or merely to clusters of smaller crystals. The latter was more probably the case, as the method used by the General Electric Company in obtaining the powder was one which should give uniformity of size. The dust was that which had remained suspended in thin oil for thirty days.

A rough estimate of the amount of primary extinction entering in was obtained by calculation. By means of a formula given by Darwin[6] the correction for extinction was evaluated for the reflection from the (111) planes of a crystal block of edge 10^{-4} cm, the approximate size of the powder particles used here. As the (111) reflection is the strongest and occurs at the smallest angle, the effect of extinction would be most marked. It was found that the intensity of the (111) reflection may have been reduced 10 percent by primary extinction. While it has been pointed out by Waller[7] that the formula used here does not hold as exactly in the case of transmission through a powder as in the case of reflection from the surface, still it serves to give an idea of the magnitude of the effect.

The length of cube edge necessary if primary extinction is to be limited to 1 percent, say, may be calculated from Darwin's formula and is found to be approximately 3×10^{-5} cm. It is probable, however, that in many cases primary extinction is negligible even for crystals of larger size than that calculated from theoretical considerations; for parts of each fragment of

[5] R. J. Havighurst, Phys. Rev. **28**, 882 (1926).
[6] C. G. Darwin, Phil. Mag. **43**, 800 (1922).
[7] cf. footnote, W. L. Bragg, C. G. Darwin, R. W. James, Phil. Mag. **1**, 897 (1926).

crystal which are perfect may be much smaller than the fragments themselves. The process of grinding would also tend to cause distortion. The fact that Mark[8] has found only very few diamond crystals which give perfect reflection would indicate that even in small fragments the degree of perfection may not be high.

Method of Calculation from Data

The peaks obtained by the ionization method were plotted on a large scale, and the relative intensities of the radiation reflected from the different planes of the crystal were obtained by comparisons of the areas under the peaks. One particular reflection was chosen as standard, and the intensities of the other reflections were expressed relative to that for the standard. A. H. Compton[4] has derived the following expression for the ratio of the power of the rays scattered to the ionization chamber to the power of the rays that have traversed the powdered crystal mass:

$$\frac{P_s}{P}=Q\frac{phl\rho'}{4\pi r\rho}\frac{1}{\sin 2\theta}. \tag{1}$$

p is the number of planes in the crystal belonging to the form which reflects the rays at angle θ; l is the height of the ionization chamber slit which is distant r from the powder; h is the thickness of the powder plate, ρ' its density, and ρ the density of the individual crystals. Q is given by the formula

$$Q=\frac{1}{2}N^2F^2\lambda^3\frac{e^4}{m^2c^4}\frac{1+\cos^2 2\theta}{\sin 2\theta}, \tag{2}$$

where N is the number of atoms per unit volume and F is the atomic scattering factor (as modified by the effects of thermal agitation).

It was necessary to modify formula (1) slightly to fit the experimental method of the determination of relative F values by direct comparison of the intensities of the diffracted beams. As P is the power transmitted through the powder plate at angle θ, it varies for each reflection. If an expression for the ratio of the power P_s transmitted to the ionization chamber to the power P_i in the incident beam is evaluated instead of the ratio of the power P_s to the power P in the transmitted beam, a form more applicable to experiment is obtained. Since

$$P=P_ie^{-\mu h\sec\theta},$$

$$\frac{P_s}{P_i}=Q\frac{plh\rho'}{4\pi r\rho}\frac{1}{\sin 2\theta}e^{-\mu h\sec\theta}. \tag{3}$$

μ is the linear coefficient of absorption of the plate of powder.

In the determination of relative F values, all quantities independent of the angle of reflection remain constant. If they are set equal to R, then

[8] H. Mark, Naturwiss. **13**, 1042 (1925).

$$F^2 = \frac{RP_a}{P_i} \frac{\sin^2 2\theta}{1+\cos^2 2\theta} e^{-\mu h \sec\theta} \tag{4}$$

An absolute value of F for one reflection will place on an absolute scale all of the relative values of F obtained from formula (4). In this investigation the intensity of the (220) reflection from diamond was compared with the intensity of the (220) reflection from powdered sodium chloride under the same experimental conditions. The value of F used for the (220) reflection from NaCl was 15.62, the figure given by James and Firth[9] in their recent study of rock-salt.

The absorption of the powder plate was obtained directly by comparison of the intensities of the direct beam and of the same beam transmitted through the powder when the normal to the briquet made angle zero with the direct beam. The effective thickness necessary in the calculation of F_{220} for diamond by comparison with NaCl was obtained from the weight and surface area of the powder briquet.

Experimental Results

In Table I are given the experimental results of this investigation, and in Fig. 1 the values of F are shown against $\sin\theta$. All but one of these values of

Table I. *Relative intensities and the resultant F-values of carbon as diamond.*

Reflection	$\sin\theta$	P_a	F
111	0.173	100	2.78
220	.282	32.5	2.15
311	.331	16.4	1.28
222	.345	1.8	.76
400	.400	4.8	1.69
331	.435	7.5	1.16
422	.489	8.8	1.43
511, 333	.518	4.8	.97
440	.564	2.9	1.32
531	.590	4.1	.82
620	.631	2.8	1.01
533	.654	1.5	.75
444	.691	1.1	1.11
711, 551	.711	2.0	.61

F fall on two curves. The unit cube of the generally accepted structure for diamond contains eight atoms in the coordinate positions 000; $\frac{1}{2}\frac{1}{2}0$; $\frac{1}{2}0\frac{1}{2}$; $0\frac{1}{2}\frac{1}{2}$; $\frac{1}{4}\frac{1}{4}\frac{1}{4}$; $\frac{3}{4}\frac{3}{4}\frac{1}{4}$; $\frac{3}{4}\frac{1}{4}\frac{3}{4}$; $\frac{1}{4}\frac{3}{4}\frac{3}{4}$. Calculation of the structure factors for this arrangement shows that the F's for appearing reflections with all odd indices are the atomic F-values of carbon. These give the points on the upper curve of Fig. 1. The F's for the all odd reflections (lower curve) are $1/2^{\frac{1}{2}}$ of the atomic F-values. The crosses of Fig. 1 represent all odd F's multiplied by $2^{\frac{1}{2}}$. For the most part they lie quite closely on the upper curve. Since F-values may be considered as the ratio of the amplitude of the wave scattered by the whole atom to the amplitude of the wave scattered by a

[9] R. W. James and E. M. Firth, Proc. Roy. Soc. **A117**, 62 (1927).

single electron, at small angles of reflection they should approach a number equal to the total number of extra-nuclear electrons in the atom. In the carbon atom there are six such electrons.

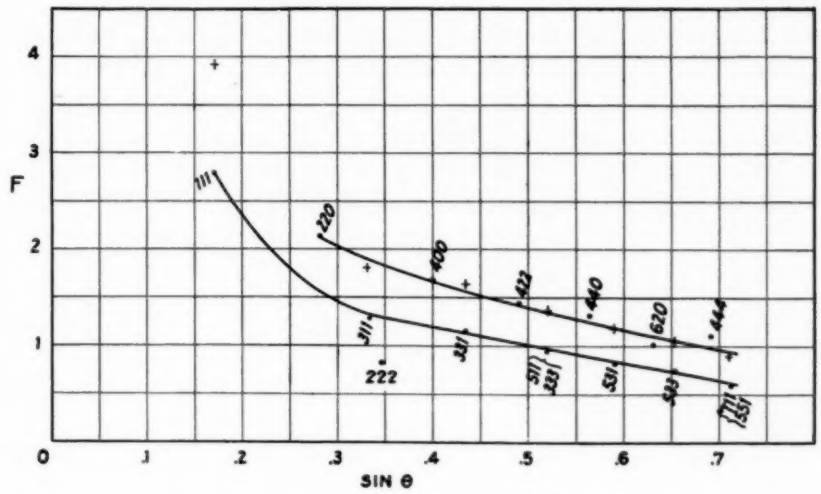

Fig. 1. The experimental *F*-values of the diamond.

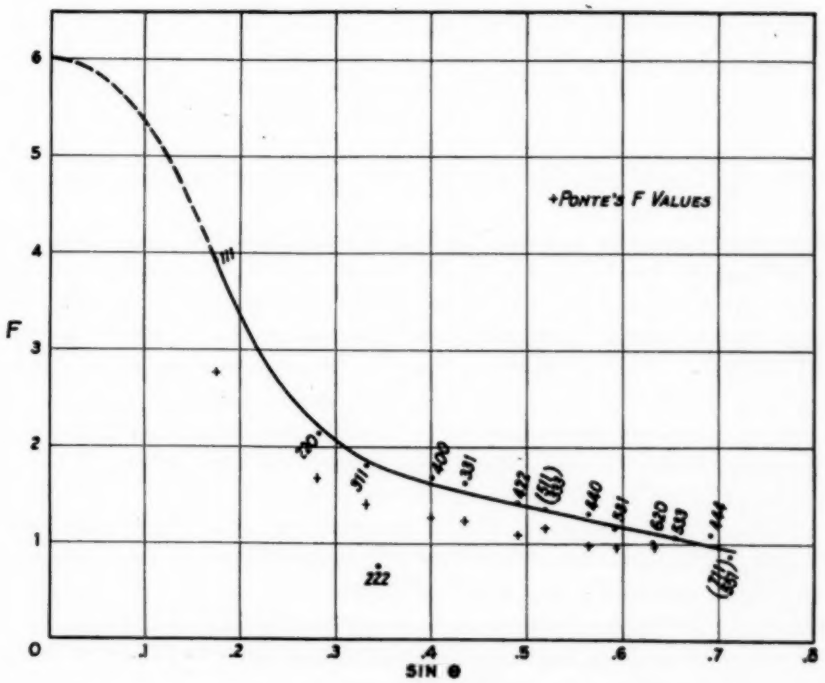

Fig. 2. A comparison between the experimental *F*-values of this paper and those found by Ponte.

Discussion of Results

The absolute values of F of Ponte are compared with those obtained in this investigation in Fig. 2. It seems possible that extinction effects in the relatively large diamond particles used by Ponte may be the cause of the very considerable discrepancy between these two F-curves.

Of special interest is the appearance of the (222) reflection. It should not appear if the diamond has exactly the structure usually assigned to it and consists of carbon atoms that are all alike. This reflection, however, has been observed by W. H. Bragg[1] and also by Ehrenberg, Ewald, and Mark[10] in studies of single diamond crystals. It might occur if the carbon atoms are of two kinds with different scattering powers. In this case a (200) reflection

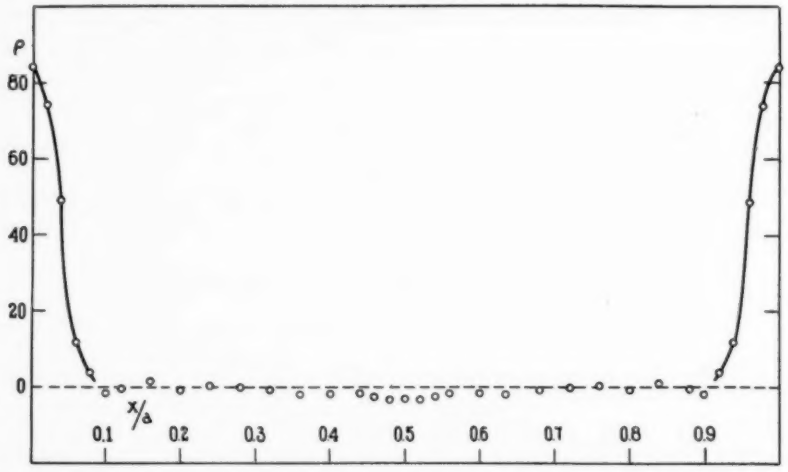

Fig. 3. The density of diffracting power along the cube edge of the diamond.

should also be found. Previous search for this reflection was unsuccessful. A (222) would also be expected if adjacent carbon atoms shared electrons between them in such a way as to provide scattering centers upon the line joining them. Such a structure would resemble the high temperature modification of cristobalite (SiO_2)[11] with carbon nuclei replacing the silicon atoms and the extra-nuclear electrons in place of oxygen atoms. An examination of the structure factors of this arrangement indicates that the F's for (113) and (115, 333) should lie beneath the lower curve of Fig. 1 and (111) and (133) above it. These results are compatible with the experimental data. F for (400), however, should be relatively less than those for (220) and (422). The fact that these three reflections lie on a smooth curve thus conflicts with such an explanation of (222).

Havighurst[12] applied a Fourier analysis to Hull's and Bragg's data, and obtained results which he suggested might indicate the presence of valence

[10] W. Ehrenberg, P. P. Ewald, and H. Mark, Zeits. f. Krist. **66**, 547 (1928).
[11] R. W. G. Wyckoff, Am. J. Sci. **9**, 448 (1925).
[12] R. J. Havighurst, Proc. Nat. Acad. Sci. **11**, 507 (1925).

electrons between the carbon atoms. A similar analysis of the data of this investigation does not give humps between the maxima which correspond to atomic positions. If the coefficients A' and A'' of the two series are adjusted according to the value of $(A'-A'')$ obtained from the (222) reflection, negative distributions are obtained at the points where Havighurst obtained small humps. A negative distribution of diffracting power is meaningless. If, however, A' and A'' are assumed equal (i.e. if the scattering power of the atoms in one group of atoms is assumed equal to that of the atoms in the other group), the abnormal inverted humps very nearly disappear. The distribution curves calculated on the basis of these latter assumptions are shown in Figs. 3 and 4.

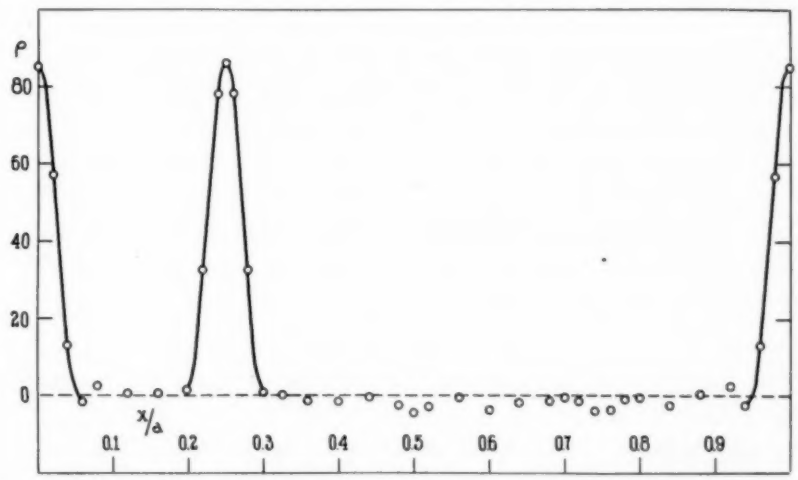

Fig. 4. The density of diffracting power along the body diagonal of the diamond.

The writer wishes to express her appreciation to Professor William Duane, of Harvard University, who suggested this problem, and who made possible the carrying out of much of the investigation in his laboratory at the Cruft High Tension Electrical Laboratory of Harvard University while she was a member of the staff of the Rockefeller Institute.

AN EXTENSION OF THE SPARK SPECTRUM OF COPPER, Cu II

By Gerald Kruger
Cornell University, Ithaca, N. Y.

(Received July 13, 1929)

Abstract

The ground term of Cu II is a $3d^{10}\ {}^1S_0$. The next higher terms are $3d^9\,4s\ {}^1D\ {}^3D$ and still higher are found the terms $3d^9 4p\ {}^1(P^\circ D^\circ F^\circ)\ {}^3(P^\circ D^\circ F^\circ)$. These facts were already known from the work of other investigators. With a Schüler lamp of the hollow cathode type as a source, the spectrum of copper was photographed by means of a vacuum spectrograph which was so designed that the region 0A—2600A could be photographed on one plate. Two higher members of the $3d^9ns\ {}^1D\ {}^3D$ series have been found, thus giving in all four members of both series, from which the limits of the series have been calculated. The calculations show that the $3d^{10}\ {}^1S_0$ level lies 163, 634.2 cm^{-1} below the $3d^9\ {}^2D_{5/2}$ of Cu III from which the ionization potential of Cu II is computed to be 20.2 volts. This places the first members of the $3d^9ns\ {}^3D_{3,2,1}$ series at 141,709.2 cm^{-1}, 140,790.7 cm^{-1} and 139,639.5 cm^{-1} respectively. Higher members of the $3d^9np\ {}^1(P^\circ D^\circ F^\circ)\ {}^3(P^\circ D^\circ F^\circ)$ series have also been identified, thus making it possible to confirm Hund's predictions concerning the limits which the various series members approach.

Introduction

THE first two terms of the $3d^9ns\ {}^1D{}^3D$ series and the first term of the $3d^9np\ {}^1(P^\circ D^\circ F^\circ){}^3(P^\circ D^\circ F^\circ)$ series of the Cu II spectrum have been reported by Shenstone.[1] From these data no accurate calculation of the series limits could be made, and therefore no absolute energy level values could be assigned.

F. Hund[2] recently predicted which levels of the terms arising from the $3d^9ns$ and the $3d^9np$ electron configurations of Cu II should approach $3d^9\ {}^2D_{2\frac{1}{2}}$ or $3d^9\ {}^2D_{1\frac{1}{2}}$ of Cu III as a limit.

Since the previous work on Cu II was also insufficient to test Hund's prediction, it was the object of the present work not only to extend the above series so that accurate limits could be established but also to determine, if possible, whether the series approached the limits predicted by Hund.

The characteristics of the Schüler Lamp[3] are such that it should produce the type of spectrum necessary for the completion of this work and it was accordingly chosen as the light source.

The Spark Spectrum of Copper (Cu II)

According to the Hund theory of the production of atomic spectra it has been shown[1] that the first spark spectrum of copper has for its ground term $3d^{10}\ {}^1S_0$. The next higher terms are $3d^9 4s\ {}^1D{}^3D$, and still higher are found the

[1] Shenstone, Phys. Rev. **29**, 380 (1927).
[2] F. Hund, Zeits. f. Physik **52**, 601 (1929).
[3] Schüler, Zeits. f. Physik **35**, 323 (1926).

terms $3d^9 4p\ {}^1(P^\circ D^\circ F^\circ)\ {}^3(P^\circ D^\circ F^\circ)$. The $3d^{10}\ {}^1S_0$ term was reported by Lang[4] to give combinations with $3d^9 4p\ {}^3P^\circ_1$, $^3d^9 4p\ {}^3D^\circ_1$ and $3d^9 4p\ {}^1P^\circ_1$. As in the case of Ni I all of the above levels are inverted except the $3d^9 np\ {}^3F^\circ$ which is partially inverted. When the levels are inverted it has been shown by Hund[2] that the $3d^9 ns\ {}^1D_2{}^3\ D_1$ series should approach $3d^9\ {}^2D_{1\frac{1}{2}}$ of Cu III as a limit. The $3d^9 ns\ {}^3D_{2,3}$ series should approach $3d^9\ {}^2D_{2\frac{1}{2}}$ of Cu III as a limit. Moreover, Hund predicts that the $3d^9 np\ {}^1P^\circ_1$, $^1D^\circ_2$, $^1F^\circ_3$, $^3P^\circ_{0,1,2}$ should all approach $3d^9\ {}^2D_{1\frac{1}{2}}$ of Cu III, while all six levels of $3d^9 np\ {}^3D^\circ$, $^3F^\circ$ should approach $3d^9\ {}^2D_{2\frac{1}{2}}$ of Cu III as a limit.

A 1500 volt d.c. potential was applied between the anode and hollow copper cathode of the Schüler lamp, and the current limited to about 300 m.a. by a suitable external resistance and the resistance of the He, (varying with pressure) in the lamp. It was found in this work that a relatively high He pressure (about 4 mm) increased the intensity of the copper lines. This is not in agreement with the phenomena observed when using certain other metals as the cathode. For in the case of Ni, Al, and Ge it has been found that a low He pressure in the lamp was most favorable for the production of the spectrum in question. It may also be remarked that successful operation of a Schüler lamp necessitates a careful cleaning of the lamp by running a discharge in oxygen so that all impurities may be oxidized and pumped out.

A vacuum spectrograph designed according to Sawyer[5] was built for use with a 1.5 meter grating which was ruled by Anderson at the Mt. Wilson Laboratory and which had approximately 15,000 lines per inch. This gave a dispersion of about 11.2A per mm which was generally adequate for the work, but was not large enough to separate all the lines. The spectrograph was about 10 inches in diameter, so that it was possible to photograph the whole region from 0A to 2600A on one plate which was bent to a radius of curvature of 75 cm.

It was found that the copper spectrum was very easy to excite. Within two hours after a copper cathode had been put into the lamp a satisfactory copper spectrum was obtained. Four exposures were taken, the time of exposure varying from 10 hr to 18 hr. During the run the He gas was constantly purified by passing it through a liquid-air-cooled carbon trap and through a hot copper oxide trap the latter to remove traces of hydrogen gas.

The notation used in this paper is in accordance with that proposed in the "Report on Spectroscopic Notation," by H. N. Russell, A. G. Shenstone Louis A. Turner.[6] For this reason it is desirable to include a short explanation of the notation. When the sum of the l values for all the electrons in a configuration is even, none of the terms is primed. Thus, terms arising from the configuration $3d^{10}$ are expressed by $3d^{10}\ {}^1S_0$ and those from $3d^9 4s$ are expressed by $3d^9 4s\ {}^1D_2$ and $3d^9 4s\ {}^3D_{3,2,1}$. When the sum of the l values for all electrons in the configuration is odd, this fact is denoted by a superscript to the right. Thus, terms arising from the configuration $3d^9 4p$ are

[4] Lang, Phys. Rev. **31**, 773 (1928).
[5] Sawyer, J.O.S.A. & R.S.I. **15**, 305 (1927).
[6] Russell, Shenstone and Turner, Phys. Rev. **33**, 900 (1929)

expressed by $3d^94p\ ^1(P^\circ_1\ D^\circ_2\ F^\circ_3)\ ^3(P^\circ_{2,1,0}\ D^\circ_{3,2,1}\ F^\circ_{4,3,2})$. In Table II, giving the term values the designation is as follows: $3d^9(^2D_{2\frac{1}{2}})\ 4s\ ^1D_2$. This means that the $^1D_2$ term arises from the $3d^94s$ configuration and approaches $^2D_{2\frac{1}{2}}$ of Cu III as a limit.

Measurements were made on all four plates. Lines of the He and H (it was not possible to remove all traces of H) arc and He spark were used as standards in the region 600A to 1600A. Above 1600A, known lines of Cu II which had been measured by Mitra were used. The final value given to a line is the average of all measurements made. Estimated relative intensities were gotten in the same way. A part of one plate (800A to 1200A) was run through a Moll microphotometer and the relative intensities of the lines in this region were compared with the estimated intensities obtained when the plates were measured. Good agreement was found in all but a few cases and these intensities were made to agree with the values given by the microphotometer.

The first part of the analysis consisted in determining the $3d^96s\ ^1D_2$, $^3D_{3,2,1}$, $3d^97s$, $^1D_2{}^3D_{3,2,1}$ levels. Since the intervals between the terms for $3d^94s\ ^1D^3D$, $3d^95s\ ^1D^3D$ and $3d^94p\ ^1(P^\circ D^\circ F^\circ)\ ^3(P^\circ D^\circ F^\circ)$ were known from Shenstone's work, it was possible to predict from the first two members of the series where the third and fourth members would be. Sixty lines were found which resulted from possible combinations between $3d^94p\ ^1(P^\circ D^\circ F^\circ)$, $^3(P^\circ D^\circ F^\circ)$ and $3d^96s\ ^1D^3D$, $3d^97s\ ^1D^3D$ terms. The $3d^96s\ ^3D_3-3d^96s\ ^3D_1$ separa- separation equals 2069.6 cm^{-1} and the $3d^97s\ ^3D_3-3d^97s\ ^3D_1$ separation is 2071.2 cm^{-1}. At the same tine the $\Delta\nu$ separations $^3D_3-{}^3D_2$ and $^3D_1-{}^1D_2$ are getting smaller for each successive term in the series. This agrees with Shenstone's[1] data and confirms Hund's[2] recent prediction that the $3d^9ns\ ^3D_{3,2}$ levels approach $3d^9\ ^2D_{2\frac{1}{2}}$ of Cu III while $3d^9ns\ ^1D_2\ ^3D_3$ approach $3d^9\ ^2D_{1\frac{1}{2}}$ of Cu III.

Some of the lines which were not found in the present set of data have been computed from the term values and are included in the parentheses in Table III. Line $3d^94p\ ^1P^\circ_1-3d^96s\ ^3D_1=62067.0$ cm^{-1} (cal) falls on a third order line $\nu=62070.9$ cm^{-1} of He I, $\lambda=537.12$A. Line $3d^94p\ ^1F^\circ_3-3d^97s\ ^1D_2$ $=75014.3$ cm^{-1} falls together with line $3d^94p\ ^3F^\circ_2-3d^97s\ ^3D_2=75013.7$ cm^{-1}. This line appears in the data with an intensity of 8 and is so recorded in the tables. However, it would be expected from our data that $3d^94p\ ^3F^\circ_2-3d^97s$ $^3D_2$ would have an intensity of about 4, so it would not be unreasonable to attribute the other 4 units of intensity to $3d^94p\ ^1F^\circ_3-3d^97s\ ^1D_2$. Line $3d^94p\ ^1D^\circ_2$ $-3d^97s\ ^1D_2=73581.3$ cm^{-1} (cal) falls within 12.5 cm^{-1} of $3d^{10}\ ^1S_0-3d^94p\ ^1P^\circ_1$ $=73593.8$ cm^{-1} (Int. 17), so it is suspected that $3d^94p\ ^1F^\circ_3-3d^94s\ ^1D_2$ is included in the line $\nu=73593.8$ cm^{-1} of the data.

Having once established the $3d^96s\ ^1D^3D$ and $3d^97s\ ^1D^3D$ terms, it was possible to compute the limits of the $3d^9ns\ ^1D^3D$ series and assign absolute term values to the levels. By carrying out the computation it was found that the best value for the $3d^94s\ ^3D_3$ term was 141709.2 cm^{-1}. This places the $3d^{10}\ ^1S_0$ at 163634.2 cm^{-1} from which the ionization potential of Cu II is computed to be equal to 20.2 volts.

The term values for all terms found are given in Table II. Table I gives the Rydberg denominators of characteristic terms of each series.

TABLE I. *Rydberg denominators.*

		$n=4$	5	6	7
	n^*	1.759980	2.809117	3.822282	4.828684
$3d^9ns$	$^3D_3$	111709.2	55625.5	30044.7	18825.9
	n^*	2.147390	3.047517	3.460066	
$3d^9np$	$^3F_3^\circ$	95190.1	47263.0	36664.4	
	n^*	2.174906	3.106328		
	$^3D_3^\circ$	92796.7	45490.3		
	n^*	1.774222	2.816254	3.828378	4.835444
$3d^9ns$	$^1D_2$	139443.2	55343.9	29949.1	18773.3
	n^*	2.102597	3.102147	3.710623	
$3d^9np$	$^3P_2^\circ$	99289.0	45613.0	31880.1	
	n^*	2.163386	3.136019	4.009437	
	$^1F_3^\circ$	93787.6	44633.0	27306.5	
	n^*	2.182977	3.130609	3.986427	
	$^1P_1^\circ$	92111.8	44787.4	27621.4	

The second step in the analysis was an attempt to classify two groups of lines which were found to lie between 90000 cm^{-1} and 115000 cm^{-1}. Many of the frequency differences between the terms $3d^94s\ ^1D^3D$ were found between these lines. From this it is concluded that the lines under consideration must come from combinations between $3d^9np\ ^{1,3}(P^\circ D^\circ F^\circ)$ and $3d^94s\ ^{1,3}D$. Combinations with the next most probable electron configuration ($3d^94d$) would lie to longer wave-lengths and would have to combine with terms arising from the $3d^94p$ configuration, which would not give all the above separations.

The line $3d^94s\ ^3D_3 - 3d^96p\ ^3F^\circ_4$, $\nu = 105411.8$ cm^{-1}, gives a $\Delta\nu$ separation for $^3F^\circ_4 - {}^3F^\circ_3$ which seems rather large, for the separation which one would expect by comparison with the two lower series members is approximately 250 cm^{-1}. In this case the line would fall on the hydrogen line $\lambda = 949.73$A and this H line in the data does not have sufficient intensity, so that one could safelysay that $3d^94s\ ^3D_3 - 3d^96p\ ^3F^\circ_4$ coincided with it. Since $\nu = 105411.8$ cm^{-1} was the only other strong line in this region, it was assigned to the above transition.

Line $\nu = 98754.7$ cm^{-1} has an intensity of 8 in the data. This line was used twice and the intensity split. Line $\nu = 122857.7$ cm^{-1} ($3d^{10}\ ^1S_0 - 3d^95p^3\ D^\circ_1$) is 12.7 cm^{-1} from the computed value but since the standards used in this part of the spectrum were poor such an error may be allowable. Line $3d^{10}\ ^1S_0 - 3d^95p\ ^1P^\circ_1$, $\nu = 138003.4$, is 79.1 cm^{-1} from its computed value and is surely a questionable classification. These last two lines are the only ones classified in this paper where the discrepancy in frequency is large enough to justify comment.

The identifications involving transitions from $3d^95$, $6p$ to $3d^94s$ and $3d^{10}$ must necessarily be regarded as somewhat tentative until they are confirmed

by the finding of predictable radiation frequencies between terms involving these higher configurations and those of $3d^9 5, 6, 7s$. Some of these predicted lines will lie in the infra-red and may be very difficult to observe. Radiations arising from transitions $3d^9 5s - 3d^9 6p$ and $3d^9 5p - 3d^9 7s$, should lie within the region $\lambda = 4400$A and $\lambda = 3000$A and should, therefore, be reasonably easy to observe.

Curves showing the variation in the Rydberg denominator with successive terms are given in Fig. 1.

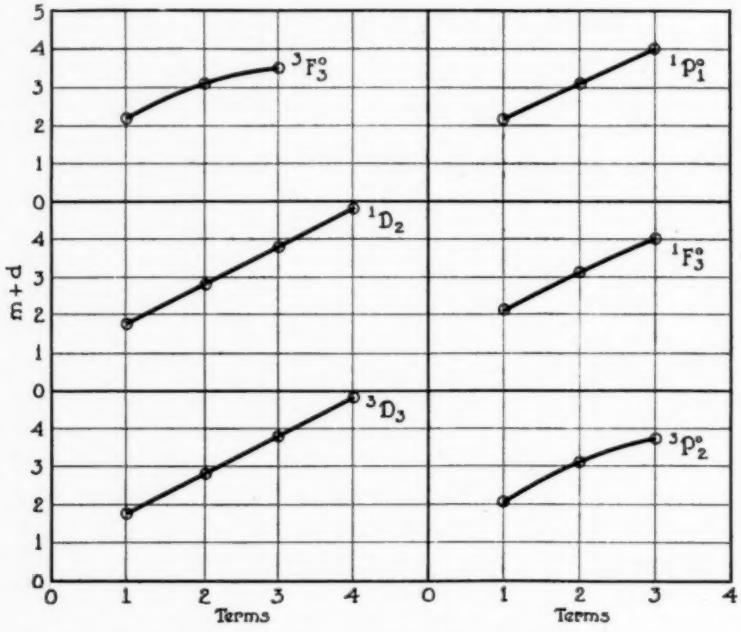

Fig. 1. Rydberg denominators for series of Cu II.

Figure 2a shows how regularly the members of the $3d^9 ns\ ^3D$ series approach their respective limits.

Figure 2c shows the corresponding change in the $3d^9 np\ ^3F^\circ$ series. In Figure 2b there is to be noted a peculiar spreading of the $3P^\circ$ terms in the second member of the series and a sharp contraction in the third member. The $3d^9 np\ ^3D^\circ$ series members show a similar spreading in the second member, but since only two members are known a curve for the $3d^9 np\ ^3D^\circ$ series was not plotted.

The $3d^9 4p\ ^3D^\circ$ terms are the lowest terms arising from this configuration. But the $3d^9 5p\ ^3D^\circ\ ^3P^\circ$ terms are interspaced and when the $3d^9 6p$ terms are reached the $3d^9 6p\ ^3P^\circ$ terms are above those of $3d^9 6p\ ^3D^\circ$.

This, together with the fact that the $3d^9 6p\ ^3P^\circ$ terms are closer together than either the $3d^9 4p\ ^3P^\circ$ or $3d^9 5p\ ^3P^\circ$ terms leads one to suspect that the $3d^9 np\ ^3P^\circ$ approaches the limits $^3d^9\ ^2D_{1\frac{1}{2}}$ of Cu III as Hund predicts.

Computations on the $3d^9 np\ ^1F^\circ_3$ and $^1P^\circ_1$ show definitely that these two series approach $3d^9\ ^2D_{1\frac{1}{2}}$ of Cu III according to the Hund prediction.

In like manner, since the $3d^9np\ ^3F^\circ$ has in the third member of the series become lowest, it might be suspected that $3d^9np\ ^3F^\circ$ approaches the $3d^9\ ^2D_{2\frac{1}{2}}$ of Cu III as a limit, which is also in accordance with Hund's prediction.

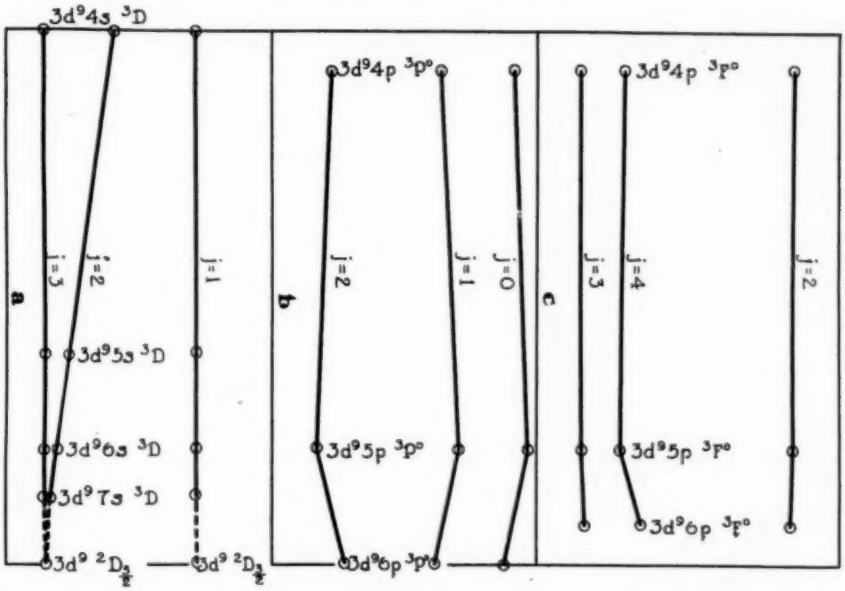

Fig. 2. Relative term separations for consecutive series members.

Table II is a complete list of all terms and term values. Column one gives the term, the electron configurations from which the term arises, and the limit which the term approaches. Column two gives the term values with respect to $3d^9\ ^2D_{2\frac{1}{2}}$ of Cu III, whether the term approaches this level as a limit or not. Column three gives only the term values with respect to $3d^9\ ^2D_{1\frac{1}{2}}$ of the term which approach $3d^9\ ^2D_{1\frac{1}{2}}$ of Cu III as a limit.

TABLE II. *Term values of singly ionized copper, Cu II.*

Term	Term values with respect to $3d^9\ ^2D_{2\frac{1}{2}}$ ν cm^{-1}	Term values with respect to their own limit $3d^9\ ^2D_{1\frac{1}{2}}$ ν cm^{-1}
$3d^{10}\ ^1S_0$	163634.2	
$3d^9(^2D_{2\frac{1}{2}})4s\ ^3D_3$	141709.2	
$3d^9(^2D_{2\frac{1}{2}})4s\ ^3D_2$	140790.7	
$3d^9(^2D_{1\frac{1}{2}})4s\ ^3D_1$	139639.5	141709.2
$3d^9(^2D_{1\frac{1}{2}})4s\ ^1D_2$	137373.5	139443.2
$3d^9(^2D_{1\frac{1}{2}})4p\ ^3P_2^\circ$	97219.3	99289.0
$3d^9(^2D_{1\frac{1}{2}})4p\ ^3P_1^\circ$	95721.4	97791.1
$3d^9(^2D_{2\frac{1}{2}})4p\ ^3F_3^\circ$	95190.1	
$3d^9(^2D_{2\frac{1}{2}})4p\ ^3F_4^\circ$	94907.1	
$3d^9(^2D_{1\frac{1}{2}})4p\ ^3P_0^\circ$	94788.0	96857.7
$3d^9(^2D_{2\frac{1}{2}})4p\ ^3F_2^\circ$	93769.9	
$3d^9(^2D_{2\frac{1}{2}})4p\ ^3D_3^\circ$	92796.7	
$3d^9(^2D_{2\frac{1}{2}})4p\ ^3D_2^\circ$	92144.3	
$3d^9(^2D_{1\frac{1}{2}})4p\ ^1F_3^\circ$	91717.9	93787.6
$3d^9(^2D_{2\frac{1}{2}})4p\ ^3D_1^\circ$	90535.9	
$3d^9(^2D_{1\frac{1}{2}})4p\ ^1D_2^\circ$	90284.9	92354.6

TABLE II (*Continued*)

Term	Term values with respect to $3d^9\,{}^2D_{2\frac{1}{2}}$ ν cm^{-1}	Term values with respect to their own limit $3d^9\,{}^2D_{1\frac{1}{2}}$ ν cm^{-1}
$3d^9({}^2D_{1\frac{1}{2}})4p\ {}^1P_1^\circ$	90042.1	92111.8
$3d^9({}^2D_{2\frac{1}{2}})5s\ {}^3D_3$	55625.5	
$3d^9({}^2D_{2\frac{1}{2}})5s\ {}^3D_2$	55304.6	
$3d^9({}^2D_{1\frac{1}{2}})5s\ {}^3D_1$	53555.9	55625.6
$3d^9({}^2D_{1\frac{1}{2}})5s\ {}^1D_1$	53274.2	55343.9
$3d^9({}^2D_{2\frac{1}{2}})5p\ {}^3F_3^\circ$	47263.0	
$3d^9({}^2D_{2\frac{1}{2}})5p\ {}^3F_4^\circ$	46995.2	
$3d^9({}^2D_{2\frac{1}{2}})5p\ {}^3F_2^\circ$	45844.1	
$3d^9({}^2D_{2\frac{1}{2}})5p\ {}^3D_3^\circ$	45490.3	
$3d^9({}^2D_{2\frac{1}{2}})5p\ {}^3D_2^\circ$	44596.8	
$3d^9({}^2D_{1\frac{1}{2}})5p\ {}^3P_2^\circ$	43543.3	45613.0
$3d^9({}^2D_{1\frac{1}{2}})5p\ {}^1P_1^\circ$	42717.7	44787.4
$3d^9)^2D_{1\frac{1}{2}})5p\ {}^1F_3^\circ$	42563.3	44633.0
$3d^9({}^2D_{1\frac{1}{2}})5p\ {}^3P_1^\circ$	41806.0	43875.7
$3d^9({}^2D_{2\frac{1}{2}})5p\ {}^3D_1^\circ$	40888.6	
$3d^9({}^2D_{1\frac{1}{2}})5p\ {}^3P_0^\circ$	40884.8	42854.5
$3d^9({}^2D_{2\frac{1}{2}})6p\ {}^3F_3^\circ$	36664.4	
$3d^9({}^2D_{2\frac{1}{2}})6p\ {}^3F_4^\circ$	36297.4	
$3d^9({}^2D_{2\frac{1}{2}})6p\ {}^3F_2^\circ$	35268.7	
$3d^9({}^2D_{2\frac{1}{2}})6s\ {}^3D_3$	30044.7	
$3d^9({}^2D_{2\frac{1}{2}})6s\ {}^3D_2$	29910.8	
$3d^9({}^2D_{1\frac{1}{2}})6p\ {}^3P_2^\circ$	29810.4	31880.1
$3d^9({}^2D_{1\frac{1}{2}})6p\ {}^3P_1^\circ$	28503.4	30573.1
$3d^9({}^2D_{1\frac{1}{2}})6s\ {}^3D_1^\circ$	27975.1	30044.8
$3d^9({}^2D_{1\frac{1}{2}})6s\ {}^1D_2$	27879.4	29949.1
$3d^9({}^2D_{1\frac{1}{2}})6p\ {}^3P_0^\circ$	27582.1	29651.8
$3d^9({}^2D_{1\frac{1}{2}})6p\ {}^1P_1^\circ$	25551.7	27621.4
$3d^9({}^2D_{1\frac{1}{2}})6p\ {}^1F_3^\circ$	25236.8	27306.5
$3d^9({}^2D_{2\frac{1}{2}})7s\ {}^3D_3$	18825.9	
$3d^9({}^2D_{2\frac{1}{2}})7s\ {}^3D_2$	18756.3	
$3d^9({}^2D_{1\frac{1}{2}})7s\ {}^3D_1$	16754.7	18824.4
$3d^9({}^2D_{1\frac{1}{2}})7s\ {}^1D_2$	16703.6	18773.3

Table III gives all classified lines in the order of increasing frequencies and the assigned term combinations from which the line arises.

TABLE III. *Classified lines of copper II.*

Int.	λ vac.	ν cm^{-1}	Combination $3d^95p-3d^96s$
10	1663.01	60131.9	${}^1P_1^\circ-{}^3D_2$
5	1660.02	60240.2	${}^1D_2^\circ-{}^3D_3$
2	1656.35	60373.7	${}^1D_2^\circ-{}^3D_2$
9	1649.44	60626.6	${}^3D_1^\circ-{}^3D_2$
10	1621.39	61675.5	${}^1F_3^\circ-{}^3D_3$
2	1617.94	61807.0	${}^1F_3^\circ-{}^3D_2$
	(1611.16)	(62067.0)	${}^1P_1^\circ-{}^3D_1$
1	1610.30	62100.2	${}^3D_2^\circ-{}^3D_3$
4	1608.66	62163.5	${}^1P_1^\circ-{}^1D_2$
9	1606.87	62232.8	${}^3D_2^\circ-{}^3D_2$
3	1604.88	62310.0	${}^1D_2^\circ-{}^3D_1$
9	1602.40	62406.4	${}^1D_2^\circ-{}^1D_2$
9	1598.41	62562.2	${}^3D_1^\circ-{}^3D_1$
	(1596.00)	(62656.5)	${}^3D_1^\circ-{}^1D_2$
13	1593.56	62752.6	${}^3D_2^\circ-{}^3D_3$
6	1590.19	62885.6	${}^3D_3^\circ-{}^3D_2$
1	1569.21	63726.3	${}^3F_2^\circ-{}^3D_3$
7	1566.45	63838.6	${}^1F_3^\circ-{}^1D_2$

TABLE III (*Continued*)

Int.	λ vac.	ν cm^{-1}	Combination
			$3d^9 4p - 3d^9 6p$
6	1565.94	63859.4	$^3F_2^\circ - {}^3D_2$
5	1558.38	64169.2	$^3D_2^\circ - {}^3D_1$
	(1556.05)	(64264.9)	$^3D_2^\circ - {}^1D_2$
15	1541.77	64860.5	$^3F_4^\circ - {}^3D_3$
5	1540.51	64913.6	$^3D_3^\circ - {}^1D_3$
8	1535.03	65145.3	$^3F_3^\circ - {}^3D_3$
15	1531.91	65278.0	$^3F_3^\circ - {}^3D_2$
6	1519.90	65793.8	$^3F_2^\circ - {}^3D_1$
6	1519.53	65809.8	$^3P_1^\circ - {}^3D_2$
1	1517.65	65891.3	$^3F_2^\circ - {}^1D_2$
6	1496.72	66812.8	$^3P_0^\circ - {}^3D_1$
12	1488.72	67171.8	$^3P_2^\circ - {}^3D_3$
1	1485.67	67309.7	$^3P_2^\circ - {}^3D_2$
1	1485.67	67309.7	$^3F_3^\circ - {}^1D_2$
2	1476.10	67746.1	$^3P_1^\circ - {}^3D_1$
2	1474.03	67841.2	$^3P_1^\circ - {}^1D_2$
	(1444.16)	(69244.2)	$^3P_2^\circ - {}^3D_1$
1	1442.11	69342.8	$^3P_2^\circ - {}^1D_2$
			$3d^9 4p - 3d^9 7s$
1	1402.80	71286.0	$^1P_1^\circ - {}^3D_2$
0	1399.41	71458.7	$^1D_2^\circ - {}^3D_3$
1	1393.13	71780.8	$^3D_1^\circ - {}^3D_2$
5	1371.88	72892.7	$^1F_3^\circ - {}^3D_3$
	(1370.58)	(72961.6)	$^1F_3^\circ - {}^3D_2$
	(1364.49)	(73287.4)	$^1P_1^\circ - {}^3D_1$
	(1363.91)	(73318.4)	$^3D_2^\circ - {}^3D_3$
2	1363.54	73338.5	$^1P_1^\circ - {}^1D_2$
5	1362.61	73388.6	$^3D_2^\circ - {}^3D_2$
2	1359.94	73532.7	$^1D_2^\circ - {}^3D_1$
			$3d^{10} - 3d^9 4p$
17	1358.81	73593.8	$^1S_0 - {}^1P_1^\circ$
			$3d^9 4p - 3d^9 7s$
	(1359.04)	(73581.3)	$^1D_2^\circ - {}^1D_2$
2	1355.35	73781.7	$^3D_1^\circ - {}^3D_1$
6	1351.88	73971.1	$^3D_3^\circ - {}^3D_3$
4	1350.61	74040.6	$^3D_2^\circ - {}^3D_2$
	(1334.33)	(74944.0)	$^3F_2^\circ - {}^3D_3$
8	1333.09	75013.7	$^3F_2^\circ - {}^3D_2$
8	1333.09	75013.7	$^1F_3^\circ - {}^1D_2$
2	1326.46	75388.6	$^3D_2^\circ - {}^3D_1$
1	1325.57	75439.2	$^3D_2^\circ - {}^1D_2$
16	1314.40	76080.3	$^3F_4^\circ - {}^3D_3$
	(1314.18)	(76093.1)	$^3D_3^\circ - {}^1D_2$
4	1309.51	76364.4	$^3F_3^\circ - {}^3D_3$
10	1308.35	76432.1	$^3F_3^\circ - {}^3D_2$
6	1299.30	76964.5	$^3P_1^\circ - {}^3D_2$
6	1298.47	77013.7	$^3F_2^\circ - {}^3D_1$
1	1297.59	77065.9	$^3F_2^\circ - {}^1D_2$
2	1281.49	78034.2	$^3P_0^\circ - {}^3D_1$
8	1275.62	78393.3	$^3P_2^\circ - {}^3D_3$
	(1274.48)	(78463.0)	$^3P_2^\circ - {}^3D_2$
0	1274.06	78489.2	$^3F_3^\circ - {}^1D_2$
2	1266.38	78965.2	$^3P_1^\circ - {}^3D_1$
3	1265.53	79018.3	$^3P_1^\circ - {}^1D_2$
	(1242.78)	(80464.6)	$^3P_2^\circ - {}^3D_1$
1	1242.01	80514.6	$^3P_2^\circ - {}^1D_2$
			$3d^9 4s - 3d^9 5p$

TABLE III (*Continued*)

Int.	λ vac.	ν cm^{-1}	Combination
			$3d^94p-3d^96p$
2	1088.39	91878.8	$^1D_2-{}^3D_3^\circ$
5	1069.18	93529.6	$^3D_3-{}^3F_3^\circ$
2	1066.15	93795.4	$^3D_1-{}^3F_2^\circ$
6	1065.74	93831.5	$^1D_2-{}^3P_2^\circ$
2	1058.82	94444.8	$^3D_3-{}^3F_3^\circ$
6	1055.81	94714.0	$^3D_3-{}^3F_4^\circ$
12	1054.67	94816.4	$^1D_2-{}^1F_3^\circ$
4	1052.16	95042.6	$^3D_1-{}^3D_2^\circ$
2	1049.28	95303.4	$^3D_2-{}^3D_3^\circ$
5	1039.56	96194.5	$^3D_2-{}^3D_2^\circ$
5	1039.28	96220.5	$^3D_3-{}^3D_3^\circ$
10	1036.45	96483.2	$^1D_2-{}^3D_1^\circ$
1	1031.76	96921.8	$^3D_1-{}^1P_1^\circ$
1	1029.74	97111.9	$^3D_3-{}^3D_2^\circ$
4	1028.31	97246.9	$^3D_2-{}^3P_2^\circ$
1	1022.11	97836.8	$^3D_1-{}^3P_1^\circ$
3	1019.65	98072.9	$^3D_2-{}^1P_1^\circ$
11	1018.69	98165.3	$^3D_3-{}^3P_2^\circ$
3	1018.04	98228.0	$^3D_2-{}^1F_3^\circ$
8	1012.61	98754.7	$^3D_1-{}^3P_0^\circ$
7	1010.29	98981.5	$^3D_2-{}^3P_1^\circ$
7	1008.62	99145.4	$^3D_3-{}^1F_3^\circ$
3	1001.00	99900.1	$^3D_2-{}^3D_1^\circ$
			$3d^94s-3d^96p$
9	992.95	100710.0	$^1D_2-{}^3F_3^\circ$
1	979.41	102102.3	$^1D_2-{}^3F_2^\circ$
8	960.38	104125.5	$^3D_2-{}^3F_3^\circ$
9	958.13	104370.0	$^3D_1-{}^3F_2^\circ$
6	948.66	105411.8	$^3D_3-{}^3F_4^\circ$
1	947.68	105520.9	$^3D_2-{}^3F_2^\circ$
3	939.47	106443.0	$^3D_3-{}^3F_2^\circ$
3	910.48	109832.2	$^3D_1-{}^3P_2^\circ$
9	901.10	110975.5	$^3D_2-{}^3P_2^\circ$
9	899.77	111139.5	$^3D_1-{}^3P_1^\circ$
2	894.26	111824.3	$^1D_2-{}^1P_1^\circ$
16	893.65	111900.6	$^3D_3-{}^3P_2^\circ$
9	892.40	112057.4	$^3D_1-{}^3P_0^\circ$
12	890.60	112283.9	$^3D_2-{}^3P_1^\circ$
2	867.78	115236.6	$^3D_3-{}^1P_1^\circ$
5	865.42	115550.8	$^3D_2-{}^1F_3^\circ$
			$3d^{10}-3d^95p$
10	827.05	120911.7	$^1S_0-{}^1P_1^\circ$
9	823.98	122857.7	$^1S_0-{}^3D_1^\circ$
			$3d^{10}-3d^96p$
2	724.62	138003.4	$^1S_0-{}^1P_1^\circ$

A line $3d^94s\ {}^3D_2-3d^94p\ {}^3D^\circ_3$, $\nu=47994.0$ cm^{-1}, which Shenstone did not find has been found in the present study with intensity 2.

Values of α and μ, constants in the Ritz term formula, have been computed so that the formula which represents the $3d^9ns\ {}^3D_3$ series becomes

$$T_n=\frac{4R}{[n+\mu+\alpha(T_n)]^2}$$

where n takes on integer values, and has the same value as n in the electron configurations

$$\mu = -2.1606515 \quad \alpha = -5.52 \times 10^{-7}.$$

The ionization potential of Cu I is known to be 7. 7 volts, and from the present data the I. P. of Cu II is found to be 20.2 volts. This means that 27.9 volts would be necessary for complete ionization of Cu II and since in the present case the energy available from the He ion is only 24.5 volts, it would be expected that complete ionization of Cu II would not occur. This is found to be true. In the present work the highest term found in Cu II is $\nu = 16703.6$ cm^{-1}. The frequency difference between this value and the value of the lowest term of Cu II is 146930.6 cm^{-1} which corresponds to 18.1 volts. This means that the light source is supplying at least 25.8 volts for use in producing the spectra, and since the He ion will supply only 24.5 volts, 1.3 volts must be accounted for in some other way.

Even though the largest potential fall occurs in the region of the dark space which surrounds the negative glow, it seems probable that the potential fall across the negative glow should be at least of the order of magnitude of several volts, (i.e. 4 or 5 volts). Under these conditions some of the kinetic energy, which the He ion acquires upon being accelerated through the potential fall of the negative glow, might be transferred to the Cu atom by collision, thus increasing the amount of energy available for exciting the Cu atom to more than the 24.5 volts which the He ion supplies upon recombining with an electron. The author believes that it is at least plausible to assume that the extra 1.3 volts mentioned above comes from the transfer of mechanical kinetic energy to atomic energy of excitation.

The limit of available energy is shown very nicely in the spectrum by the distribution of the line intensities. In most cases the intensity of the lines of the spectrum falls off rapidly, and the reason that higher members of a series are not observed is that the intensity is too small. In this case, however, the intensity did not fall off rapidly, and in the case of the $3d^9np\ ^3(P^\circ F^\circ)$ to $3d^94s\ ^3D$ combinations the lines resulting from the $3d^96p\ ^3(P^\circ F^\circ)$ to $3d^94s\ ^3D$ combinations were stronger than the lines $3d^95p\ ^3(P^\circ F^\circ)$ to $3d^94s\ ^3D$. This indicates that the failure to observe the lines was not due to the usual progressive falling off in the intensities but rather to the fact that there was not enough available energy sufficiently to excite the atom so that it would radiate these lines. A similar condition exists for the series of lines

$$3d^94p\ ^1(P^\circ D^\circ F^\circ)\,^3(P^\circ D^\circ F^\circ) - 3d^9ns\ ^1D\,^3D.$$

The author wishes to take this opportunity to express his appreciation and indebtedness to Professor R. C. Gibbs for his valuable advice and criticism during the period of this investigation.

THE EXCITATION OF THE Mg II SPECTRUM BY IMPACTS OF THE SECOND KIND WITH METASTABLE ATOMS AND IONS OF THE RARE GASES

By O. S. Duffendack, Clement L. Henshaw, and Marie Goyer
University of Michigan

(Received September 9, 1929)

Abstract

The Mg II spectrum was excited in normal low voltage arcs in mixtures of magnesium vapor with hydrogen, argon, neon, and helium respectively in a tungsten furnace apparatus. The densities of the spectral lines were measured with a Moll microphotometer. The excitation is believed to be due to impacts of the second kind between normal magnesium atoms and metastable atoms or ions of the gas used. It is shown that a small amount of kinetic energy may be added to the inner energy available in the impacts of the second kind and that a larger amount of excess inner energy may be transformed into kinetic energy in such an impact. The probability of an impact of the second kind decreases after the excess energy reaches a certain value.

Introduction

THIS report covers an investigation of the excitation of the spectrum of Mg II by impacts of the second kind between normal Mg atoms and excited atoms and ions of the rare gases. The principal purpose of the investigation was to study the excitation of those levels of Mg^+ which lie just above and just below the levels of the metastable and ionized states of the rare gases in order to determine whether the levels excited were closely selected by "resonance" and to determine to what degree non-quantized kinetic energy may be added to quantized energy in impacts of the second kind to produce "anti-Stokes" radiation. Magnesium was selected for the experiments because the Mg II spectrum has many levels lying near those of the excited and ionized states of neon and helium. The Mg II spectrum converges at a level 22.5 volts above the normal state of Mg. This is only one volt above the ionizing potential of Ne and 2.7 volts above the metastable 2^3S state of He.

Method

The experiments were carried out with the use of the tungsten furnace apparatus described by Duffendack and Black,[1] the apparatus being regulated so as to effect the simultaneous ionization and excitation of magnesium atoms by the excited atoms or ions of the gas used in accordance with the method of Duffendack and Smith.[2] Normal low voltage arcs were maintained in mixtures of magnesium vapor with hydrogen, argon, neon, and

[1] Duffendack and Black, Phys. Rev. **34**, 35 (1929).
[2] Duffendack and Smith, Phys. Rev. **34**, 68 (1929).

helium respectively. In each case the pressure of the gas was about 2 mm. The vapor pressure of the magnesium in the furnace was controlled by regulating the temperature of the furnace so that the green arc lines of Mg appeared faintly in the spectrum of the arc viewed with a small hand spectro-

TABLE I.

Wave-length	Classification	Ex. pot. (volts)	Relative Densities H_2	A	He	Ne_a	Ne_b
2802.70	$3s\ S-\ 3p\ P$	12.02	8.28	8.10	8.58	7.43	
2795.52	$3s\ S-\ 3p\ P$	12.03	8.56	8.14	8.58	7.50	
3615.64	$4s\ S-\ 5p\ P$	19.64	—	—	Obs	3.20	
13.80	$4s\ S-\ 5p\ P$	19.64	—	—	by He	2.86	
2936.50	$3p\ P-\ 4s\ S$	16.23	6.22	8.14	8.57	7.48	
28.62	$3p\ P-\ 4s\ S$	16.23	4.50	7.91	8.57	7.34	
2797.99	$3p\ P-\ 3d\ D$	16.44	7.73	7.67	8.58	7.46	
90.77	$3p\ P-\ 3d\ D$	16.44	5.02	7.02	8.58	7.46	
4433.99	$4p\ P-\ 6s\ S$	20.35	—	—	—	5.21	
28.00	$4p\ P-\ 6s\ S$	20.35	—	—	—	Combined	
3553.51	$4p\ P-\ 7s\ S$	21.04	—	—	—	671	
49.61	$4p\ P-\ 7s\ S$	21.04	—	—	—	Comb.	
3175.84	$4p\ P-\ 8s\ S$	21.46	—	—	—	6.38	
72.79	$4p\ P-\ 8s\ S$	21.46	—	—	—	6.20	
2971.70	$4p\ P-\ 9s\ S$	21.72	—	—	—	—	
69.02	$4p\ P-\ 9s\ S$	21.72	—	—	—	—	
4390.59	$4p\ P-\ 5d\ D$	20.38	—	—	—	6.41	
84.64	$4p\ P-\ 5d\ D$	20.38	—	—	—	Comb.	
3538.86	$4p\ P-\ 6d\ D$	21.05	—	—	—	7.05	
35.04	$4p\ P-\ 6d\ D$	21.05	—	—	—	7.04	
3168.98	$4p\ P-\ 7d\ D$	21.45	—	—	—	6.25	
65.94	$4p\ P-\ 7d\ D$	21.45	—	—	—	5.14	
2967.87	$4p\ P-\ 8d\ D$	21.72	—	—	—	—	
65.19	$4p\ P-\ 8d\ D$	21.72	—	—	—	—	
3850.40	$3d\ D-\ 5p\ P$	19.64	—	—	3.70	3.40	
48.24	$3d\ D-\ 5p\ P$	19.64	—	—	6.89	6.74	
4481.33	$3d\ D-\ 4f\ F$	19.19	—	—	8.01	6.43	
81.13	$3d\ D-\ 4f\ F$	19.19	—	—	Comb.	Comb.	
3104.81	$3d\ D-\ 5f\ F$	20.41	—	—	7.00	9.49	
04.71	$3d\ D-\ 5f\ F$	20.41	—	—	Comb.	Comb.	
2660.82	$3d\ D-\ 6f\ F$	21.07	—	—	—	7.60	
60.76	$3d\ D-\ 6f\ F$	21.07	—	—	—	Comb.	
2449.57	$3d\ D-\ 7f\ F$	21.47	—	—	—	7.50	6.52
2329.58	$3d\ D-\ 8f\ F$	21.73	—	—	—	0.83	4.60
2253.87	$3d\ D-\ 9f\ F$	21.91	—	—	—	—	1.45
2202.68	$3d\ D-10f\ F$	22.04	—	—	—	—	0.22

scope. Experience enabled us to determine the proper intensity of these lines so that the intensity of the Mg II spectrum would be great relative to that of Mg I in the photographed spectrum of the arc. In all cases the arc current was held between 45 and 55 milliamperes and the applied potential difference was 23 to 25 volts. The spectra were photographed with a Hilger E_2 quartz spectrograph.

The relative densities of the spectral lines on the plates were determined by means of a Moll microphotometer. The relative densities recorded in the table are those thus determined and corrected for the influence of continuous background and neighboring lines.

Results

Table I contains a list of the lines photographed and their relative densities in the spectrograms of the arcs in the various mixtures. The densities of the lines on one plate must not be compared with those on another plate, but some deductions are made as a result of comparing the relative densities of the lies of a series in the spectrum of one Mg-Ne mixture with their relative densities in the spectrum of another Mg-Ne mixture. The excitation potentials recorded in the table are computed relative to the normal state of the neutral Mg atom. The relative densities of the lines recorded in the column headed Ne_a are those for a spectrogram in which the intensity of the Mg II spectrum is great compared with that of the Mg I spectrum, while those recorded in the column headed Ne_b are for a spectrogram in which the lines of the Mg I spectrum are very strong, the ^3PS series being present to the eighth member and the ^3PD series to the ninth member. In the other spectrograms only the first one or two members of the series of arc lines were present.

Table II gives the critical potentials of the elements involved in this investigation. A consideration of these critical potentials in connection with the excitation potentials of the lines of the Mg II spectrum observed in each mixture affords the basis for the explanation of the results given in the following paragraphs.

Table II. *Critical potentials of elements.*

Element	Excited states	Ionization
Mg		7.61 volts
H_2		16.3–16.5
A	11.6 volts	15.69, 15.86
Ne	16.6	21.5
He	19.8, 20.5	24.5

Discussion

That the Mg II spectrum was excited by impacts of the second kind rather than by direct electron impacts is evidenced first of all by the great strength of the spark spectrum relative to the arc spectrum when the vapor pressure of magnesium is low. In all of the work in this laboratory and else-

where in a low voltage arc of the order of 25 volts, the arc spectrum of the gas has always been predominant. Furthermore, with the magnesium vapor constituting only a small percentage of the total gas in the region of the arc, the probability of an electron collision with a magnesium atom is small compared with the probability of an impact between a magnesium atom and metastable atom or ion of the rare gas.

Then too the distribution of intensity of the lines of a series in the spectrum of Mg II is quite different in this excitation than in a case of excitation by direct electron impacts. It will be noted from Table I that the Mg^+ ion was excited in each mixture only to a level corresponding to that of a metastable state or the ionized state of the gas molecule. It may be observed that each series is cut off suddenly. The intensity of the last line observed is much higher than one usually expects. There is no gradual diminution of intensity in the series until the lines fail except in the case of the ^2DF series in the neon mixture, Ne_b, in which the magnesium constituted a much larger percentage of the total gas, and excitation by direct electron impacts was an important factor.

The excitation can be accounted for by impacts of the second kind that may be represented by the following equations:

$$\begin{aligned}
Mg + H_2^+ &= Mg^{+\prime} + H_2 \\
Mg + A^+ &= Mg^{+\prime} + A \\
Mg + Ne' &= Mg^{+\prime} + Ne \\
Mg + Ne^+ &= Mg^{+\prime} + Ne \\
Mg + He' &= Mg^{+\prime} + He
\end{aligned}$$

These equations represent reactions in which a normal magnesium atom is simultaneously ionized and excited on contact with an excited molecule or ion of the gas with which the magnesium vapor is admixed. The inner energy of the excited molecule, or the energy of recombination of an ion with an electron as the case may be, is utilized in ionizing the magnesium atom and in simultaneously exciting the ion. In such a reaction the amount of energy available is limited to a quantity equivalent to the excitation potential or the ionization potential of the gas molecule. Thus the magnesium ion may be excited to the degree that the excitation potential, or the ionization potential, of the gas molecule exceeds the ionization potential of magnesium. Any remnant of energy remaining over must go into the kinetic energy of the reacting molecules.

The kinetic energy of the reacting particles in impacts of the second kind may serve not only as a sink but also as a source of energy. The excitation of the $8f^2F$ level in the neon mixture Ne_a must involve the addition of nonquantized kinetic energy to the energy of recombination of the neon ion and electron during the impact. The amount of kinetic energy needed in this instance is 0.23 volts, a quantity certainly available in a gas mixture at a temperature of about 1000°C. The higher F levels reached in the neon mixture Ne_b were probably reached by direct electron impact, as the percentage of magnesium vapor in this mixture was large. The variation in the

relative intensities of the ^2DF series lines in these two neon mixtures is typical of the difference between excitation by impacts of the second kind and excitation by direct electron impacts. Of course, impacts of the second kind are effective also in the case of the Ne_b mixture but are responsible for only a part of the excitation. The excitation of the $4s\ ^2S$ and $3d\ ^2D$ levels in the argon mixture would not be expected to result from impacts of the second kind of argon ions with normal magnesium atoms. The ionization potential of argon is less than the excitation potentials of these levels. The excess energy demanded (0.58 volt), furthermore, is larger than one would expect to come from the kinetic energy of the impacting particles at the temperature of the mixture, about 1000°C. These levels were probably excited by nitrogen ions for, unfortunately, the argon employed was badly contaminated with nitrogen. We regret that lack of time prevented our repeating the argon excitation with pure gas.

An interesting question that suggests itself is whether the amount of excess energy remaining over in an impact of the second kind and transformed into kinetic energy of the reacting particles is limited. Obviously the amount of energy that can be drawn from kinetic energy as a source is limited to that available and is determined almost wholly by the temperature of the gas. It is possible that there is a dissymmetry with respect to the amounts of kinetic energy that can be taken from this source and that can be put into this sink. The only level excited that required the addition of kinetic energy was the $8\ f^2F$ level in the neon mixture Ne_a when 0.23 volt energy was drawn from the kinetic energy of the gas. On the other hand the $5d\ ^2D$, $6s\ ^2S$, $5p\ ^2P$, and $4f\ ^2F$ levels in the neon mixture Ne_a must have been excited by impacts of the second kind with neon ions leaving excess energy of amounts 1.12, 1.15, 1.86, and 2.31 volts respectively to be absorbed as kinetic energy by the reacting molecules. A quantative study of the probability of such collisions of the second kind as a function of the excess energy to be disposed of would require very careful quantitative measurements on the intensities of the spectral lines. These measurements were not made, but, taking into consideration the change with the wave-length in the sensitivity of the photographic plates used as well as the transition probabilities, one can safely say that the probability of such a collision does decrease after the excess energy reaches a certain value.

One of the most striking results of this investigation is the demonstration that higher excited levels of the magnesium ion are reached in the neon mixture than in the helium mixture. This is evidently because in the neon mixture both metastable neon atoms and neon ions are effective, while only metastable helium atoms make impacts of the second kind with magnesium atoms. The ionization potential of helium is higher than the second ionization potential of magnesium. Consequently, if helium ions were to be effective, a considerable excess of energy would have to be disposed of. The highest level that did give a spectral line in our region of observation was the $10f\ ^2F$ level, and its excitation by helium ions would have required the disposal of 2.46 volts excess energy. Though this amount is not greatly in excess of

the maximum amount observed in the neon mixture, the $3d\ ^2D - 10f\ ^2F$ lines were not present in the spectrum of the helium mixture.

Excitation in Hollow Cathodes

Considerable evidence has accumulated recently to indicate that the types of impacts described above are effective in the excitation of the spark spectra of metals in hollow cathodes. Professor Sawyer and Dr. Lang[3] have used the hollow cathode method recently in this laboratory for the excitation of the spark spectra of gallium and indium. They find these spectra developed to the levels that can be reached by impacts of the second kind with metastable atoms and ions of helium which they used as the conducting gas. Very recently, too, Professor Takahashi visited this laboratory and reported that some experiments by Professor Paschen and himself revealed two maxima in the excitation of the spark spectrum of cadmium in a hollow cathode with helium. One maximum occurred at levels close to the minimum excitation potential of helium and the other close to the ionizing potential of helium. We believe this is the first instance where two maxima have been observed in a single spectrum excited in a mixture with a single gas. Other explanations[4] have been given for the excitation of spark spectra in hollow cathodes, but many of the cases on record can be accounted for solely by impacts of the second kind like those described above. The exceptions to this explanation occur in cases where the percentage of metallic vapor in the mixture is considerable, and hence excitation by direct electron impacts may be expected to be important.

[3] To be published soon.

[4] Frerichs, Ann. d. Physik **85**, 362 (1928). Paschen, Sitzungsberichten der Preuss. Akad. der Wiss. 1928.

THE INFLUENCE OF ARGON AND OF HYDROGEN ON THE SPECTRA OF ZINC VAPOR

By J. G. Black, W. G. Nash and C. A. Poole
University of Kentucky (J. G. B. and C. A. P.), Georgetown College (W. G. N.)

(Received August 15, 1929)

Abstract

An experiment to determine the influence of argon and hydrogen gases on the spectrum of zinc vapor is described. Low voltage arcs were struck in zinc, zinc-hydrogen, and zinc-argon mixtures under controllable conditions and the resulting spectra showed marked changes in the intensities of certain lines. The following lines were markedly quenched by both A and H_2: λλ6479, 6214, 5894, 5772, 5182, 4924, 4911, 4298, 4292, 4113, 3965, 2801, 2770. The following lines, λλ6362, 4810, 4722 and 4680 showed a small decrease in intensity but the quenching action on them was very small compared with that on other lines. The resonance line at 3075A, which is very intense in the pure zinc spectrum, is also very strong in the zinc-argon mixture. There is absolutely no trace of this line, however, in the zinc-hydrogen mixture. Special discussion of lines 4629, 3345, 3302 and 3282 is given. A simple explanation of the intensity changes in terms of the critical potentials of the two gases cannot be made except in the case of the 3075.8 line, since it is found that the monatomic, inert gas argon, with relatively high critical potentials produces the same type of quenching as molecular hydrogen, with this exception.

THE purpose of this work was to determine the influence of foreign gases on the spectra of metallic vapors and to try to explain the increases and decreases in line intensities in terms of energy transfers between the excited states of atoms or molecules which were being excited.

The work was prompted by a recent article by Crew[1] which described the influence of a hydrogen atomosphere on the spectra of Mg, Zn, Al, Cd, and C. Related studies have been made by Wood[2], Cario and Franck,[3] Mohler,[4] Foote,[5] Duffendack and Smith,[6] Duffendack and Black,[7] Kaplan,[8] Frayne and others.

It was thought at first that the intensity increases observed by Crew could be explained by the theory of the excitation of spectra by atomic hydrogen, while the decreases in intensity could be explained as due to impacts of the second kind between excited metal atoms and hydrogen molecules in which the atom lost its energy upon collision, dissociated the molecule, and returned to the normal state without radiating.

[1] Crew, Phil. Mag. **7**, 312 (1929).
[2] Wood, Phil. Mag. **50**, 774 (1925).
[3] Cario and Franck, Zeits. f. Physik **11**, 161 (1922).
[4] Mohler, Phys. Rev. **29**, 419 (1927).
[5] Foote, Phys. Rev. **30**, 288 (1927).
[6] Duffendack and Smith, Phys. Rev. **34**, 68 (1929).
[7] Duffendack and Black, Phys. Rev. **34**, 35 (1929).
[8] Kaplan, Phys. Rev. **31**, 997 (1928).

A reasonably complete idea of the excitation of spectra by atomic hydrogen may be obtained from the work of Mohler[4] and the discussion by Kaplan.[8] The quenching of certain spectral lines by hydrogen is discussed by Wood[2] and by Franck.[3]

The method used in this study was that of photographing the low voltage arc spectrum of zinc in pure zinc vapor, zinc vapor and hydrogen and zinc vapor and argon. The tube used is shown in Fig. 1. It was made of heavy Pyrex glass; the electrodes being tungsten. *F* is the filament; *G*, the plate; *H*, the heater, for vaporizing the zinc; *I*, an ice jacket to serve as a vapor trap to lessen the diffusion to the end of the tube; *Q*, a transparent quartz beaker, 10 cm long and 3.5 cm in diameter to permit photographing of the ultra-violet. The length of the beaker made it possible to seal to the Pyrex tube with DeKhotinsky cement which was kept cool by a cotton pad

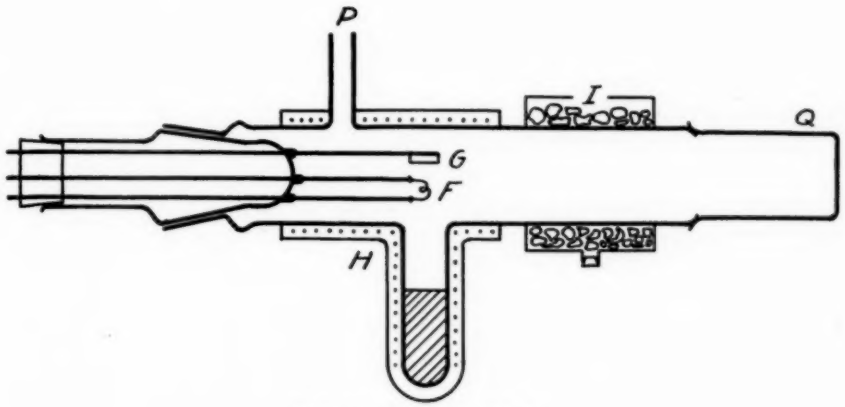

Fig. 1. Diagram of tube.

Photographs were made in the first order of a concave grating with Rowland mounting. Exposures were from forty minutes to one hour in length with arc currents of from 150 to 200 milliamperes at 40 volts. During the exposures, care was taken to keep the same portion of the arc focused on the spectrograph slit.

saturated repeatedly with ice water, while the end of the beaker could be heated to prevent the zinc from condensing upon it. This cannot be done with the usual quartz window without melting the cemented joint. The tall form of quartz beaker without lip was used. The bottom of the beaker, although not plane parallel was quite satisfactory.

P is the outlet to the pumps, which were of the usual type, a two-stage mercury vapor pump backed by a Hyvac oil pump. Liquid air was kept on the system at all times and careful precautions against impurities were taken.

Preliminary exposures at different pressures of foreign gases indicated that one millimeter pressure was very satisfactory and this pressure of both hydrogen and argon was used throughout the experiment.

The procedure was to take an exposure in pure zinc vapor, then on the same film exposures of the same length, arc current and pressure in zinc-

hydrogen and zinc-argon. The three spectra thus received very much the same treatment and conclusions are drawn from the *relative* intensities of the lines in the pure zinc as compared with the *relative* intensities of the same lines in the mixtures. No very satisfactory comparison of *absolute* intensities can be made due to the number of variables involved in the experiment.

Results

A thorough study of each line photographed, taking into consideration everything that might influence the estimated intensities leads to the following table which shows the intensity in pure zinc, then zinc-argon, then zinc-hydrogen.

Table I. *Showing effect of hydrogen and argon on the intensities of zinc lines.*

Initial state	Line	I_z	I_a	I_h	Classification
71207.0	6479.2	1	A	A	5^1S-7^1P
62458.2	6362.3	10	8	8	4^1P-4^1D
	6214.6	4	A	A	$4^3P_2-3^3D$
	5894.4	7	A	A	$4^3P_1-3^3D$
70992.6	5772.0	1	FT	A	5^3S-7^3P
66037.3	5182.0	4	FT	FT	4^1P-6^1S
	4924.0	1	A	A	$4^3D_3-4^3F$
	4911.6	0	A	A	$4^3D_2-4^3F$
53672.4	4810.5	8	7	7	$4^3P_2-5^3S$
53672.4	4722.1	10	8	8	$4^3P_1-5^3S$
53672.4	4680.2	8	7	7	$4^3P_0-5^3S$
68337.9	4629.8	8	D	D	4^1P-5^1D
70003.1	4298.4	5	FT	A	4^1P-7^1S
55788.1	4292.8	1	A	FT	$4^3P_1-5^1S$
71047.6	4113.6	1	A	A	4^1P-6^1D
71954.3	3965.7	1	A	A	4^1P-8^1S
62769.2	3345.9	10	D	D	$4^3P_2-4^3D$
62772.6	3302.9	8	D	D	$4^3P_1-4^3D$
62778.1	3282.2	1	D	D	$4^3P_0-4^3D$
32501.6	3075.8	10	8	A	$4^1S-4^3P_1$
68580.9	2801.0	1	FT	FT	$4^3P_2-5^3D$
68580.9	2770.9	0	FT	FT	$4^3P_1-5^3D$

The notations I_z, I_a, I_h, refer to the relative intensities of a line in pure zinc, zinc-argon and zinc-hydrogen, respectively. "A" means that the line is absent or has completely disappeared from the plate while "FT" denotes that the faintest trace remains. The lines marked "D" are discussed below.

Crew found that the singlet 4298.4 and the diffuse singlet 4629.8 were practically blotted out by hydrogen. The triplet of the sharp series, 4810.5, 4722.1 and 4680.2 were almost unaffected. Attention in Crew's article is also called to the diffuse triplet at 3345.9, 3302.9, and 3282.2 which appeared as an impurity in aluminum and which was brought out by hydrogen.

In our experiment it was found that 4298.4 which was very strong in the zinc spectrum, was fairly noticeable in the zinc-argon mixture. The strong singlet 4629.8 was greatly reduced in both argon and hydrogen. Little, if any, intensity changes were noticeable in the presence of either argon or hydrogen for the 4810, 4722 and 4680 lines. The work of Crew on the above lines is thus corroborated. Crew found that the lines 3345.9, 3302.9, and 3282.2

were intensified by hydrogen and we find that they are definitely intensified by both argon and hydrogen, with the exception of one plate in which the triplet is certainly quenched.

The spark doublet 4924.0 (30) and 4911.6 (25) is the strongest doublet in zinc II as classified by Salis,[9] and appears with low intensity on our plates. The 6214.6 (12) and 5894.4 (20) doublet appears with the same relative intensities on our plates but far stronger relative to the above doublet than would be expected from Salis' intensites. It should be kept in mind, however, that Salis employed the interesting method of excitation designed by Paschen[10] in which a discharge to a cylindrical cathode in helium was used. The higher members are intensified in this method. Both of the above spark doublets were absent in the mixtures.

The 3075.9 line which was very strong in the pure zinc spectrum and which was weakened slightly by the argon, is blotted out completely by the hydrogen. This is a resonance intercombination line with a wave-number of 32501.6 which is equivalent to an excitation potential of 4 volts. It is thought that this line is quenched in the same way that hydrogen quenches the 2537 line of mercury, i.e. by dissociation at impact.

Another important resonance line of zinc appears at 2138.6 and a knowledge of its action in the presence of impurities would be very desirable, but it could not be photographed satisfactorily with our spectrograph.

[9] Salis, Ann. d. Physik **76**, 145 (1925).
[10] Paschen, Ann. d. Physik **71**, 142 (1923).

THE SPECTRUM OF THE NEUTRAL MERCURY ATOM IN THE WAVE-LENGTH RANGE FROM 1 TO 2μ

By E. D. McAlister
Physics Laboratory, University of Oregon

(Received August 19, 1929)

Abstract

New information on the near infra-red spectrum of mercury has been obtained with a specially constructed thermocouple in connection with an automatic recording spectrograph. Fourteen new lines predicted by the combination principle and eight unclassified lines have been found in this region. Intensity relations for the triplet $1^3S_1-2^3P_{0,\,1,\,2}$, which extends over 2700A, have been found to follow rather closely the summation rule as refined by R. H. Fowler for wide multiplets.

VERY little has been done on the infra-red spectrum of mercury since Paschen's[1] excellent work. By taking advantage of the concentration of energy in a prismatic spectrum and using a vacuum thermocouple of minute dimensions and high sensitivity (constructed by the writer) the number of classified lines in the region from 1 to 2μ has been nearly doubled. The source used was a 300-watt quartz vacuum arc. The spectroscope is automatic recording.

I. Calibration of the Spectroscope

(1) *Wave-length.* A dispersion curve, *A* Fig. 1, (wave-length against position on the film) for the spectroscope was obtained from two sources, (a) observations on several of the more intense classified lines of the mercury spectrum whose wave-lengths have been accurately measured by Paschen[1] with a grating, and (b) observations on lines in the absorption bands of water vapor in this region—these having been accurately measured with a grating by Sleator and Phelps.[2] One of these bands extends from 1.8002 to 1.9326μ—another from 1.3480 to 1.4234μ. Sleator's wave-lengths are reduced to vacuum and by taking the vacuum wave-length for the mercury lines (i.e. reciprocals of calculated wave-numbers) the dispersion curve gives the wave-lengths of the new lines in vacuum. The lines marked with a dash (—) in Table I are those used for the dispersion curve. Sleator's wave-lengths fall very nicely upon the curve drawn through the mercury lines, the largest discrepancy being 3A. The spectrum from one to two μ covers 43 cm on the film. Reading positions on the film to 0.1 mm gives an accuracy of 2.5A. More accurate readings are not justified because of uneven shrinking of the film upon development. Most of the wave-lengths in Table I are thought to be of this accuracy, especially those near a standard line.

[1] Paschen, Ann. d. Physik **29**, 662 (1909); **30**, 750 (1909); **35**, 869 (1911).
[2] Sleator and Phelps, Astrophys. J. **62**, 28 (1925).

(2) *Intensity.* Since there is absorption and reflection over this region due mainly to the flint prisms the spectroscope was calibrated for relative intensities over the region used by observing the emission from a tungsten

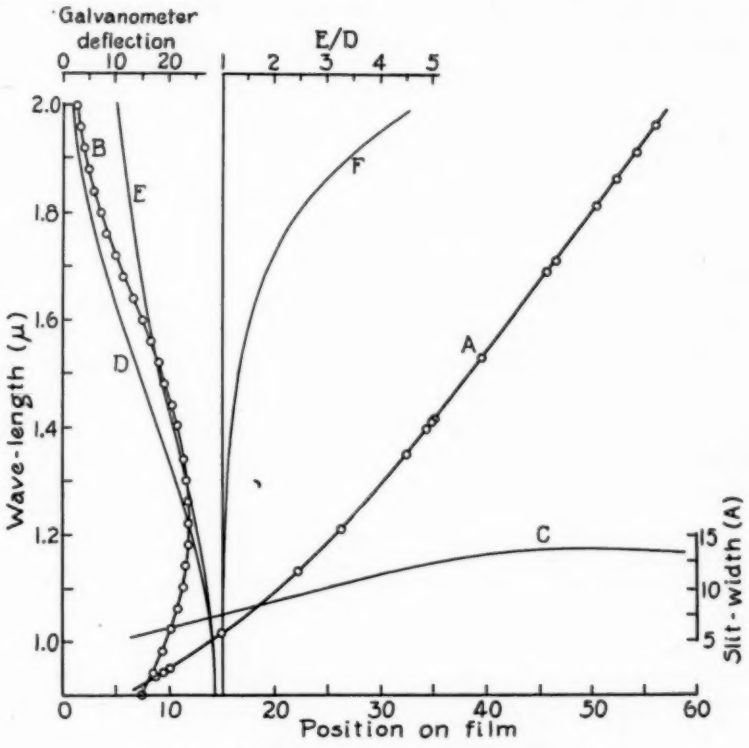

Fig. 1. Calibration curves for spectroscope.

filament at 3050°K, Fig. 2, giving curve *B* (wave-length against galvanometer deflection) on Fig. 1. To obtain the galvanometer zero the light was occulted for fifteen seconds every twenty minutes and to cover this region two revolutions of the drum are required. At this high temperature tungsten

Fig. 2. Radiation from tungsten filament, visible to 2μ.

radiates somewhat as a black body. It is observed by Coblentz[3] that as the temperature of tungsten is raised it approaches the behavior of a black body. Extrapolating his curves to 3000°K gives the constant "*a*" in

[3] Coblentz, Bull. Bur. Standards **5**, 373 (1908).

Planck's radiation formula approximately the black body value of 5. In the calibration it is assumed that tungsten radiates as a black body at the high temperature used. The temperature of the filament was observed with an "F and F" optical pyrometer and found to be 200°C below that calculated from the maximum of curve *D* by Wien's Law. The optical measurement of this temperature is not very reliable as it was obtained by a doubtful extension of the range of the instrument which is designed to operate only up to 2500°K. Curve *D* Fig. 1 (wave-length against galvanometer deflection) is curve *B* corrected for variations in the spectral range covered by the slit. Points on the slit-width curve *C*, Fig. 1 (slit-width against position on the film) are obtained by dividing the slope at a corresponding point on curve *A* by one-half of the basal width of a sharp spectral line. Curve *E* Fig. 1 (wave-length against galvanometer deflection) is the theoretical black body emission for a temperature of 3050°K calculated from Planck's radiation formula. Curve *F* Fig. 1 (intensity-correction-factor, E/D, against wave-length) which gives the intensity-correction-factor for different wave-lengths is obtained by dividing abscissae of curve *E* by the corresponding abscissae on curve *D*. The relative intensities (corrected) given in Table I are obtained by multiplying the observed intensity by an appropriate correction factor taken from curve *F*.

II. The Spectrum Obtained

Figures 3 and 4 are two automatic records of the mercury spectrum from 1 to 2μ—Fig. 3 with the arc operating at 76 volts and 3.7 amps, and Fig. 4 at 86 volts and 3.8 amps. Several of the weak lines cannot be seen on the

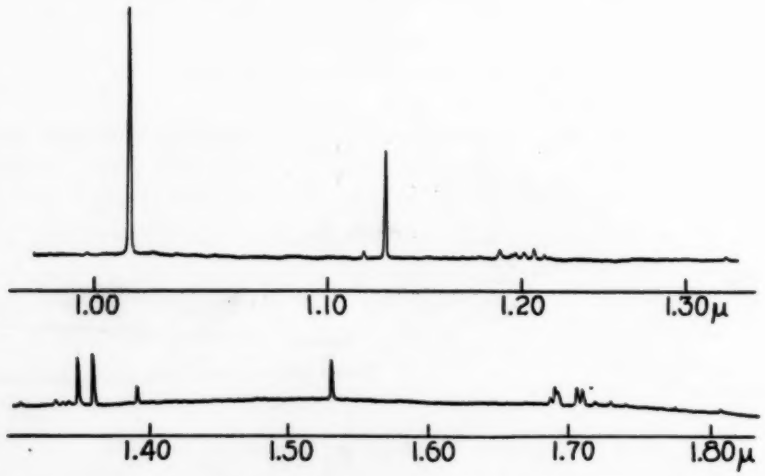

Fig. 3. Mercury spectrum in the range from 1 to 2μ. Arc operating at 76 volts.

reduced reproduction of the original record. Fig. 5 is a plot of the 86-volt record on a frequency scale, the height of a line is proportional to its corrected relative intensity. Underneath this plot the lines are grouped as

follows: 1st row, the principal triplet $1^3S_1-2^3P_{0,1,2}$; 2d row, the second sharp triplet $2^3P_{0,1,2}-3^3S_1$; 3d row, two fundamental triplets $2^3D_{1,2,3}-4^3F, -3^3F$;

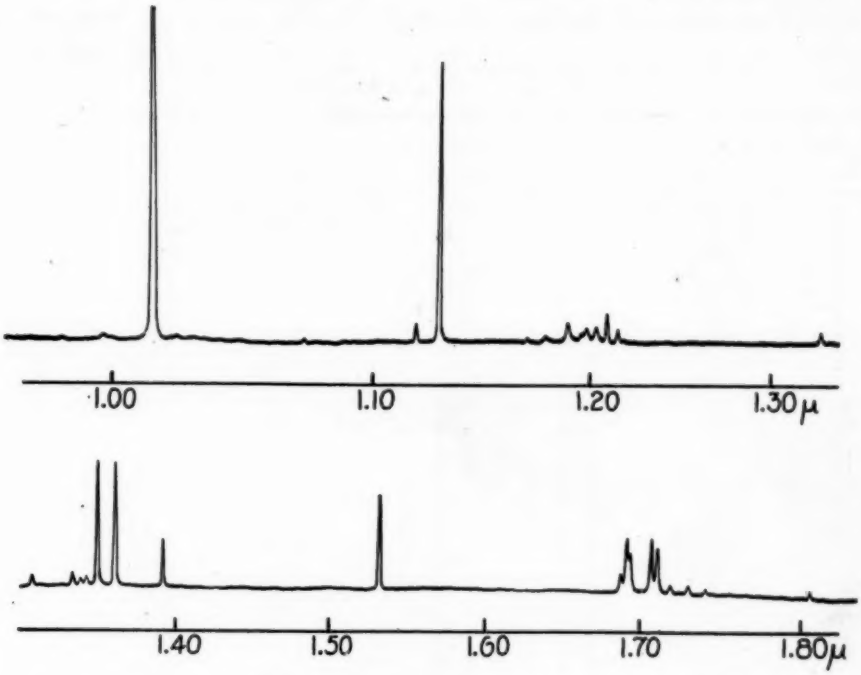

Fig. 4. Mercury spectrum in the range from 1 to 2μ. Arc operating at 86 volts.

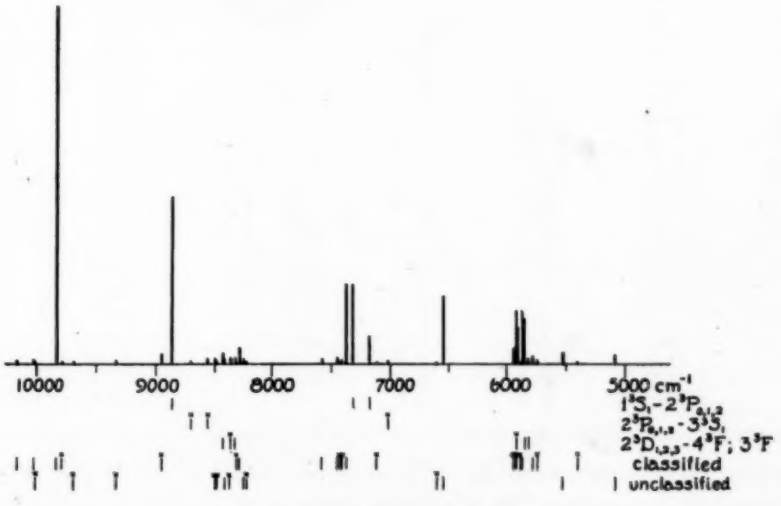

Fig. 5. Mercury spectrum in the range from 1 to 2μ plotted on a frequency scale.

4th row, classified singlets and combination lines; and 5th row, unclassified lines some of which may be mercury spark lines. Lines that have not been

reported previous to this are marked on Fig. 5 with a cross. Those marked with a circle are reclassified.

Table I gives the wave-length (in vacuum), relative intensity, classification, and frequency of the lines observed. No lines are given here that did

TABLE I. *Wave-length, relative intensity, and classification of mercury spectrum in the range from 1 to 2μ.*

Line No.	λ (vacuum) in microns	Intensity mm defl.	Intensity corrected	Classification	ν	ν (calc.)
1	0.9842	0.5	0.5	$2^3P_0-4^3D_1$	10161	10162
2	0.9975 —	1.0	1.0	$1^3P_2-1^1P_1$	10025	10025
3	0.9996	0.3	0.3		10004	
4	1.0142 —	152.2	153.0	$1^1P_1-2^1S_0$	9860	9860
5	1.0224	0.8	0.8	$2^1P_1-5^3D_1$	9781	9781
6	1.0332	0.4	0.4		9679	
7	1.0711	1.1	1.1		9336	
8	1.1187	4.2	4.3	$1^3S_1-2^1P_1$	8939	8940
9	1.1289 —	68.2	71.0	$1^3S_1-2^3P_2$	8858	8858
10	1.1497	0.3	0.3	$2^3P_0-3^3S_1$	8698	8700
11	1.1692	1.0	1.1	$2^3P_1-3^3S_1$	8553	8554
12	1.1781	1.3	1.4		8488	
13	1.1798	0.5	0.5		8476	
14	1.1889 —	4.5	4.9	$2^3D_1-4^3F$	8411	8411
15	1.1899	1.3	1.4		8404	
16	1.1957	1.4	1.5		8363	
17	1.1978	2.5	2.7	$2^3D_2-4^3F$	8349	8351
18	1.2024 —	2.5	2.7	$2^3D_3-4^3F$	8316	8316
19	1.2034	1.0	1.1	$2^3D_3-4^1F_2$	8310	8312
20	1.2075	6.8	7.4	$1^1P_1-1^3S_1$	8282	8282
21	1.2131	3.0	3.3		8243	
22	1.2159	0.3	0.3		8224	
23	1.3208	2.2	2.5	$2^3P_0-3^3D_1$	7571	7568
24	1.3434	3.0	3.5	$2^3P_1-3^3D_2$	7444	7446
25	1.3489	1.7	2.0	$2^3D_2-3^1P_1$	7414	7417
26	1.3512	2.0	2.3	$2^3P_1-3^1D_1$	7401	7402
27	1.3572	30.1	35.1	$2^1S_0-2^1P_1$	7368	7362
28	1.3676 —	29.1	33.9	$1^3S_1-2^3P_1$	7312	7312
29	1.3955 —	11.0	12.9	$1^3S_1-2^3P_0$	7166	7166
30	1.4064	0.3	0.3	$2^3S_1-5^3D_1$	7110	7110
31	1.4273	0.3	0.3	$2^3P_2-3^3S_1$	7006	7008
32	1.5186	0.4	0.5		6585	
33	1.5298 —	22.7	29.6		6537	
34	1.6878	4.7	8.2	$2^3P^2-3^3D_3$	5925	5922
35	1.6919	12.9	23.0	$2^1D_2-3^3F$	5910	5908
36	1.6935	9.0	16.2	$2^3D_1-3^3F$	5905	5905
37	1.7014	0.2	0.4	$2^3P_2-3^3D_1$	5878	5877
38	1.7073	12.9	23.8	$2^3P_2-3^1D_1$	5857	5856
39	1.7108 —	10.9	20.3	$2^3D_2-3^3F$	5845	5845
40	1.7210	1.9	3.6	$2^3D_3-3^3F$	5811	5810
41	1.7320	2.0	3.9	$2^1P_1-3^1D_1$	5774	5774
42	1.7445	1.3	2.7	$2^1D_2-3^1D_1$	5731	5731
43	1.8131	1.9	4.8		5515	
44	1.8539	0.2	0.6	$2^3D_3-3^3P_3$	5394	5392
45	1.9705	1.0	4.2		5075	

not appear on four different films. Some doubt may legitimately be expressed for classifications where the observed frequency deviates more than two units (cm^{-1}) from the calculated frequency. The calculated frequencies are obtained from Fowler's[4] term values.

[4] Fowler, "Report on Series in Line Spectra," Fleetwood Press.

III. Relative Intensities in the Principal Triplet $1^3S_1-2^3P_{0,1,2}$

The summation rule gives a theoretical relative intensity relationship of 1, 3, 5, for the members of the principal triplet $1^3S_1-2^3P_{0,1,2}$. Since this triplet extends over considerable frequency range the observed relative energies must be corrected[5] for the size of the quanta involved in each transition. Table II gives these intensities under varying conditions of excitation (E = voltage across the arc). Since these intensities rest on the assumption

Table II. *Relative intensities in the triplet* $1^3S_0-2^3P_{0,1,2}$.

Film No.	λ (microns)	Intensity observed	Intensity corrected	No. of transitions	Relative numbers
I	1.1289	15.0	15.6	176	50
$E=55.0$	1.3676	7.2	8.4	115	33
	1.3955	2.4	2.8	39	11
II	1.1289	28.9	30.1	340	50
$E=76.1$	1.3676	13.3	15.5	212	31
	1.3955	4.3	5.0	70	10
III	1.1289	53.3	55.6	628	50
$E=83.8$	1.3676	23.4	27.3	374	30
	1.3955	8.8	10.3	144	11
IV	1.1289	68.2	71.0	802	50
$E=86.3$	1.3676	29.4	34.2	468	29
	1.3955	11.0	12.9	180	11

that tungsten radiates as a black body at high temperatures—the close agreement between observed and theoretical intensities may be considered to offer information either as to the validity of this assumption or as to the applicability of Fowler's[5] refinement of the intensity rule. In this type of intensity measurement there is always the question of selective absorption by the luminous vapor. The intensity that is observed may be regarded as dependent on the algebraic sum of the energy radiating transitions plus the energy absorbing transitions.

The fundamental series of mercury lies well into the infra-red. Consequently no Zeeman pattern upon which the theoretical intensities depend has been observed. Thus no theoretical values are available to compare with experiment. The relative intensities of the lines in the two triplet members observed do not check each other because they are not resolved from lines due to transitions from other levels of $3F$ and $4F$ which are undoubtedly triple levels.

This work, was done while the writer held a fellowship in the Physics Department of the University of California at Berkeley during 1928. The writer is greatly indebted to Dr. F. S. Brackett whose spectroscope was used and whose interest and help made this work possible.

[5] Fowler, Phil. Mag. **50**, 1079 (1925).

AN EXPERIMENTAL STUDY OF CERTAIN ELECTRONIC BANDS OF CO_2

By James F. Duncan
University of Michigan

(Received September 4, 1929)

Abstract

The electronic bands of CO_2 lying near 2880A and 2895A are described and a method given for photographing them under very high dispersion. Three good plates were obtained which gave concordant results when examined with a comparator and with a Moll microphotometer. The fine structure, the probable emitter of the bands, and their relation to other bands of the spectrum are discussed.

IN A series of band-groups attributed to carbon dioxide by Duffendack and Fox[1] and later described by Fox, Duffendack and Barker[2] two bands located near 2880A and 2895A appeared to be different in structure. These bands which are of greater intensity than the others of the system, appeared under medium dispersion to be similar in form and to consist of a positive, a negative and a zero branch. The purpose of the present investigation was to examine these bands under very high dispersion with a view to resolving their fine structure.

Apparatus and Method

In order to investigate these bands it was necessary to obtain much greater dispersion than is possible with the E1 Hilger spectrograph. Preliminary tests made on a 21-foot concave grating gave a dispersion of 1.2A per millimeter in the second order which seemed sufficient for the purpose. The grating, ruled by J. A. Anderson at Johns Hopkins University, contains 14,400 lines to the inch.

The source consisted of a low-voltage arc-discharge in a continuously flowing stream of pure carbon dioxide. The discharge tube, which was made of Pyrex glass with a quartz window was connected with the gas reservoir and the pumping system in such a way that the direction of the gas stream was from the anode to the cathode (i.e. opposite the direction of the electric current). This arrangement provided that the discharge products were pumped off as soon as they were formed thus insuring pure carbon dioxide in the discharge space. The cathode consisted of three oxide-coated spirals of platinum wire connected in parallel. These were placed so as to leave a space of two or three millimeters betwen the cathode and the anode. This served to localize the discharge. The filament was heated by current supplied from storage batteries. The anode was a nickel box which surrounded the cathode except on the side next to the quartz window.

[1] O. S. Duffendack and G. W. Fox, Astrophys. J. **65**, 214 (1927).
[2] G. W. Fox, O. S. Duffendack and E. F. Barker, Proc. Nat. Acad. Sci. **13**, 302 (1927).

The carbon dioxide used in this investigation was taken from commercial tanks and, after being purified by passing through tubes of calcium chloride and phosphorus pentoxide and by freezing in a liquid-air trap, was stored in a glass reservoir. By means of a grooved stop-cock connecting the reservoir with the discharge tube it was possible to regulate the rate of passage of the gas into the tube. The pumps kept the gas flowing through the tube at a steady rate and at constant pressure, and thus fresh carbon dioxide was continually supplied at the arc.

The tube was operated at about one-tenth millimeter pressure. The filaments emitted most efficiently at currents ranging from five to ten amperes when the potential across the tube was about sixty-five volts. This gave an arc current of from six to fifteen milliamperes. It was found difficult to operate the tube with the arc current above fifteen milliamperes without producing dissociation of the carbon dioxide together with flares.

For photographic plates Cramer's Hi-speed plates were found most successful. Cramer's contrast plates were tried but were found impractical since they required a longer exposure and since the length of exposure in the case of the Hi-speed plates was already from fifty to one-hundred hours. Longer exposures than these could not be made since the temperature of the room could not be kept sufficiently constant.

The entire apparatus was set up in a room thirty feet under ground and great care was taken to house it in such a way as to shield the grating from the heat generated by the source and from all stray light. It was found that the temperature of the grating could be kept constant to within one-half degree centigrade throughout a period of one-hundred hours.

Results

Three records were obtained on which the fine structure was clearly resolved over a considerable distance. These plates were measured on a precision comparator and the frequencies of the lines were found by comparison with standard iron lines. Table I contains a composite record of the three plates together with eye estimates of intensities. A question mark follows those values for which the individual settings differed by more than 0.01 milllimeter, that is, by about 0.01A.

One of the records, taken in March, was obtained under the most favorable conditions, that is, with a temperature change of only one-tenth degree centigrade. It was, therefore, taken as standard for the absolute values of the frequencies of the lines. The other two records taken in May and July show a slight shift of all the frequencies towards the red. This shift is undoubtedly due to a temperature change of the grating caused by large temperature changes of the atmosphere outside. Therefore, certain characteristic lines of the spectra, namely, $\nu = 34{,}512.430$ and $\nu = 34{,}673.287$, were made to coincide on the three records and corrections were applied to all the other lines thus bringing the three records into good agreement.

Microphotometer records were made from these plates and the peaks on the microphotometer records of the three plates were readily identified with

TABLE I. *Composite record of wave-numbers of lines in the CO_2 bands.*

ν	I	ν	I	ν	I	ν	I
34,441.199?	00	34,498.388	2	34,561.974?	0	34,667.807	0
444.699?	00	499.543	1	580.434	6	669.309	0
447.680	0	500.746	4			673.287	10
449.957	1	501.889	3	607.482	1	678.918	4
452.463?	00	503.044	3	608.820?	2	682.203	10
454.338?	00	505.533	2	610.034	3	684.330	7
455.525?	00	507.225	5	612.409	3	685.461	3
458.126?	00	508.475	0	614.750	1	686.945	5
460.228	0	509.715?	00	616.776	2	687.869	5
463.164	0	510.977?	00	619.150	2	688.808	2
465.753	0	512.430	10	621.355	2	697.864	1
466.894	0	516.603	3	623.838	2	700.143	1
467.777?	00	518.126	6	626.080	3	702.013	1
469.627	1	520.736	10	629.522	3	704.060	1
470.994	0	525.009	7	632.978	3	705.870	2
472.000?	00	526.833	7	635.893	3	707.796	2
474.333?	00	534.901	2	638.402	3	710.254	2
476.855	2	536.498	2	641.065	3	712.508	2
479.622	4	537.836	2	643.406	3	714.639	2
482.265	4	539.199	2	646.072	2	717.185	2
484.679	4	540.522	3	648.642	2	718.980?	0
486.119	3	542.111	3	651.585	3	720.146	0
487.178	4	544.137	3	653.554	3	722.388	0
488.260	3	546.025	3	655.884	3	724.802?	00
489.331	3	547.936	3	657.781	4	727.687?	00
490.426	4	548.883	2	658.804	2	729.475?	00
491.462	3	550.012	3	659.957	4	731.381	0
492.389	3	552.019	2	661.110	3	739.960	5
493.520	4	553.688	2	663.095	3	741.392	5
494.638	3	555.388	0	664.296	3	768.742	0
495.603	3	558.073	0	665.462	2	773.313	7
496.996	2	560.142	0	666.484	1	801.210	3

each other and with the measurements of the comparator. Fig. 1 is a microphotometer record of a spectrum plate taken after the microphotometer had been carefully adjusted to render negligible the effect of plate grain. This was accomplished by lengthening the line of light on the photographic plate so that it extended over many grains of the plate. Records similar to Fig. 1

Fig. 1. Microphotographic record of band structure (retouched).

but greatly extended along the horizontal axis were used for measurements.

In order to get a clear idea of the structure of the bands it has been found convenient to represent the photographic plate by means of a graphical chart of the lines (Fig. 2) and to compare this with the microphotometer records. Some features which are not apparent on the one type of record appear prominent on the other.

In describing the general features of the bands it is possible to state immediately that the two bands with centers at $\nu = 34{,}512.430$ and $\nu = 34{,}673.287$, respectively, are similar in structure. Each has a form suggesting a positive, a negative and a zero branch. In the description which follows, these terms will be used with the understanding that these regions may not, however, be true positive, negative and zero branches.

The zero branch in each case appears as a single, very sharp and very intense line.

The negative branch is quite regular in appearance. While the lines appear to extend up to the zero branch their intensity in this region is so small that measurements on their positions can not be made with any great certainty. Extending from the zero branch through a range of about 25 wave-numbers the lines are closely spaced. While the spacing is somewhat irregular it is of the order of 1.1 wave-numbers. Extending on beyond this the spacing

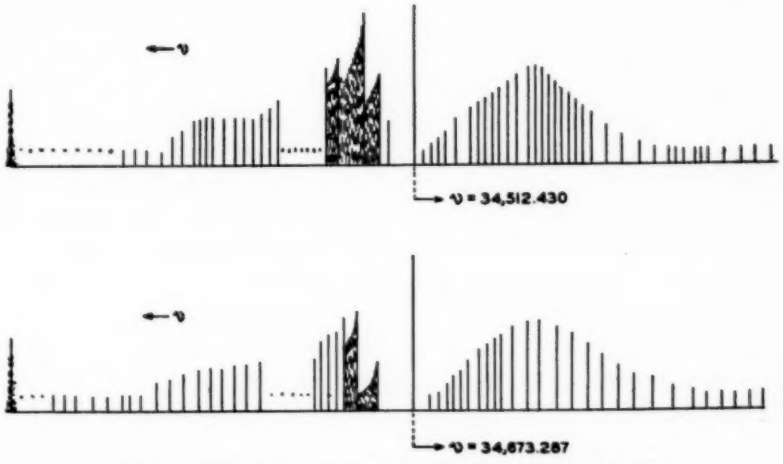

Fig. 2. Diagrammatic chart of lines of the two bands.

has a value of the order of 2.5 wave-numbers. The position of maximum intensity lies at about 14 wave-numbers from the center and lines are found as far out as 70 wave-numbers from the center of the band.

The positive branch presents an appearance very different from that of the negative branch. No fine structure is visible through a range of 5.6 wave-numbers out from the zero branch. (One plate shows a line at 4.2 wave-numbers from the center of the band.) At 5.6 wave-numbers from the center a strong edge or line is found having an intensity of about one-third that of the zero branch. At about 9 wave-numbers from the center there is a sharp edge or line of about the same intensity as that of the zero branch. In one band it appears somewhat greater than that of the zero branch, in the other somewhat less. (See Fig. 1) This difference in the two bands may be due to the fact that the resolution in the band where the intensity is greater is not as good as it is in the band where the intensity is less. Throughout this region extending out to about 10 wave-numbers from the center there

is fine structure having irregular spacing but of the order of magnitude of one wave-number. Out farther the spacing increases to about twice this amount. At about 68 wave-numbers from the center of the band the lines end in a fuzzy edge.

Beyond the end of the positive branch of the band whose center is at $\nu = 34{,}673.287$ three lines are found at $\nu = 34{,}768.742$, 34,773.313 and 34, 801.210. These do not seem to have any relation to the bands.

Discussion

None of the lines of the band systems photographed by Fox, Duffendack, and Barker[2] is absorbed in normal carbon dioxide, thus showing that the normal state of the molecule is not involved in the transitions giving rise to these spectra.

In a later paper Duffendack and Smith[3] did some work towards determining the excitation energies for these bands. They found that with mixtures of carbon monoxide, oxygen and helium, carbon dioxide was formed and the spectra were excited. In a mixture of carbon monoxide, oxygen and neon they obtained the bands but more faintly, while in a mixture of carbon monoxide, oxygen and argon they did not obtain the bands although carbon dioxide was formed as in the other cases. By means of an auxiliary filament they were able to increase greatly the electron current. This did not enhance the carbon dioxide bands. They concluded that the carbon dioxide bands are due to the ionized carbon dioxide molecule, and that there was simultaneous ionization and excitation of the carbon dioxide molecule by helium and neon ions, by excited helium and neon atoms or by both.

Their conclusions may be strengthened somewhat by the following considerations. The ionizing potential of carbon dioxide is 14.3 volts. One volt is equivalent to 8100 wave-numbers and, therefore, 34,512.430 wave-numbers (the center of one of the bands) are equivalent to about 4.3 volts. If, then, the spectra are due to ionized carbon dioxide the excitation potential must be at least 18.5 volts. This lies near an excitation potential of helium, 19.77, so that one should expect a comparatively strong excitation in the presence of excited helium. In neon the ionization potential is 21.5 volts in which case the probability of exciting the carbon dioxide ion would be less. In the case of argon, the ionization potential of which is 15.5 volts, there could not be excitation of the carbon dioxide ion. We may, therefore, conclude that the bands under consideration are due to the carbon dioxide ion.

It was intimated above that the respective regions of these bands might not be true positive, negative and zero branches. The reasons are as follows: The positive and negative branches do not show the requisite symmetry or complementary nature and the zero branch seems far too sharp to represent a region of many closely spaced lines.

[3] O. S. Duffendack and H. L. Smith, Phys. Rev. **34**, 68 (1929).

The question of what relation exists between the two bands under discussion and the groups of bands discovered by Duffendack and Fox extending from about 2800A to nearly 5000A must be left without a complete answer, at least until the groups have been photographed under greater dispersion. Very faint traces of one of the stronger groups were found on the plates obtained in this investigation but it was impossible to obtain them with sufficient intensity for measurement. A much stronger source will have to be devised before these groups can be photographed with the 21-foot grating.

The fact that both types of bands have always been found together and that no difference in excitation potential was noted by Fox, Duffendack and Barker[2] makes it probable that both types are due to a single electronic transition with the various groups due to particular vibrational transitions. Since the two bands investigated in the present work have an essentially different structure from the rest it is suggested that they may be due to a different type of vibration transition. In a linear model of the carbon dioxide molecule there are three independent frequencies of vibration and consequently the vibrational structure will be much more complex than in the case of a diatomic molecule and the different classes of vibrational transitions will give different fine structure.

Fox, Duffendack and Barker[2] fitted the leading edge of a number of the groups into a series with second differences nearly constant. However, not all the groups could be fitted into this scheme. The bands near 2880A and 2895A do not fit into this series.

Whatever may prove to be the explanation of these band groups, it seems certain that the bands near 2880A and 2895A are independent and form a system by themselves. This system may be due either to a transition from a higher electronic state containing a single vibrational level to a lower electronic state which contains two vibrational levels, or to a transition from a higher electronic state of two vibrational levels to a lower electronic state containing one vibrational level, since only the two bands appear.

In conclusion the writer wishes to express his appreciation for the kind assistance and continued interest of Professor O. S. Duffendack who directed this research and for the many helpful suggestions of Professor D. M. Dennison.

A HIGH INTENSITY NON-REVERSED SODIUM ARC

By Carl J. Christensen and G. K. Rollefson
Chemical Laboratory, University of California, Berkeley

(Received September 3, 1929)

Abstract

An improved high intensity sodium arc using the principle of the Cario, Holtgreven arc is described. This has sufficient of the second resonance radiation of sodium (3303A) so that quite brilliant fluorescence is produced in sodium vapor when this radiation is used for excitation.

AN INVESTIGATION of the fluorescence radiation of sodium vapor excited by the 3303A resonance radiation has recently been undertaken by the authors.[1] The exciting source of resonance radiation was one of the outstanding initial problems. This has been solved in a very satisfactory manner by construction of a sodium arc, the design of which can undoubtedly be employed to produce arcs of other alkali metals. The principle is that of the Cario[2] lamp; and the lamp is in some respects similar to the modifications of the original Cario lamp introduced by Holtgreven[3] and Hupfeld.[4]

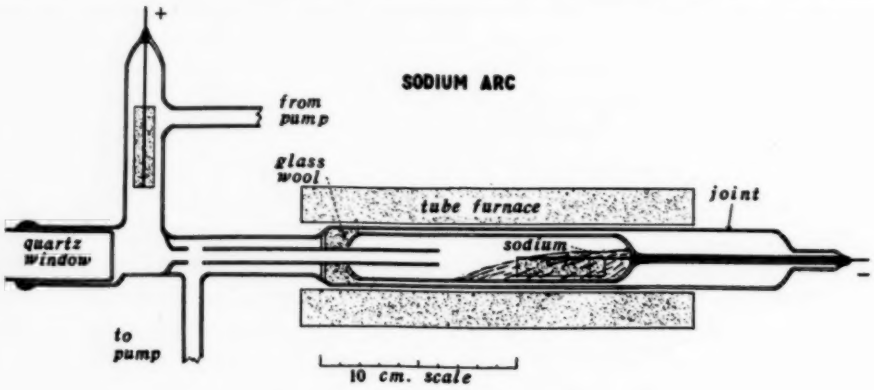

Fig. 1. Design of sodium arc lamp.

Figure 1, drawn to scale, gives the design of the lamp. The glass is of hard Pyrex throughout. The quartz window is sealed in with ordinary Dennison sealing wax. If cooling of the wax is necessary while the arc is operating at high currents this can be easily done with a wet cotton pad. The electrical leads through the glass are of tungsten and the electrodes are of sheet nickel rolled into a cylinder. The sheet from which they are rolled is wide enough so that the joint overlaps by half a turn or so. The tungsten

[1] To be published in the Physical Review.
[2] Cario and Holtgreven, Zeits. f. Physik **42**, 22 (1927).
[3] Holtgreven, Zeits. f. Physik **47**, 362 (1928).
[4] Hupfeld, Zeits. f. Physik **54**, 484 (1929).

is pushed between these overlapping layers and electrically spot-welded only at the lower end. This is an important feature, particularly for the electrode that lies in the sodium, since the action of this metal when hot is such as to cause any welded joint between the tungsten and the nickel to break. If this joint is broken the sodium quickly distills away from the tungsten lead and the arc becomes useless. In making the electrode as described, the tungsten wire always gives mechanical support to the nickel cylinder and the pressure on the tungsten due to the natural elasticity of the overlapping nickel layers is enough to give electrical contact.

The cathode is of metallic sodium. In the original Cario lamp, sodium is also the cathode; but here trouble is always encountered at high current densities (0.1 ampere) due to the fact that the arc always seems to strike just at the margin where the sodium pool is in contact with the glass. Here the sodium layer is thin and the heat conductivity from the point is poor. Hence, invariably the glass becomes heated sufficiently at these points to soften and suck through, or cause strains which very soon develop into cracks. In the Holtgreven modification a large nickel cylinder becomes the cathode, this is surrounded by sodium vapor. It is well known that the current in low voltage arcs is largely determined by the thermionic emission of the cathode. Hence the limit of the Holtgreven modification is soon reached. In the models the author constructed, a current of greater than 0.3 amperes was never attained, unless a globule of sodium of sufficient size became the cathode by making contact with the nickel cylinder, whereupon the current through the lamp immediately increased; but now the difficulty of the original Cario lamp was manifest. A particular advantage with the Holtgreven modification, however, is the ease with which a steady discharge can be obtained. When the sodium acts as cathode, there is a tendency for the intensity to fluctuate when the "active point" shifts on the cathode, although after the lamp here described has been operating for an hour or so it becomes as steady as the Holtgreven modification.

The Hupfeld modification is very similar to that of Holtgreven. It owes its advantage only to the fact that it is constructed entirely of quartz and so allows a very high operating temperature. From Hupfeld's description it would seem that a current of 1 ampere is hardly attainable.

The modification here described allows a current of 1.5 amperes without any difficulty and it seems possible to increase the current to a limit much beyond this. The lamp has been run continuously at this current for as long periods as 10 hours. The total life of any of these lamps so far constructed has been at least 50 burning hours. The advantage of this modification lies in the fact that sodium is the cathode, which gives high thermionic emission. The inner chamber holding the sodium, being evacuated on both sides, does not readily break as it would if there were a difference of pressure on the two sides. All of these inner chambers have been very badly corroded and cracked when the life of the lamp has been spent, but still they have confined the sodium.

To introduce the sodium into the lamp, the outer chamber is cut with a hot wire at the point marked "joint." The cathode and inner chamber then

easily slide away from the rest of the lamp. Purified or freshly cut sodium is introduced into the inner chamber, the lamp reassembled and the "joint" sealed. Commercial sodium contains large quantities of occluded gases. Purified sodium for the purpose of this arc is produced by heating commercial sodium in a vacuum to dispel the occluded gases, and then pouring through a capillary. If freshly cut commercial sodium is used some difficulty in starting the lamp is encountered due to the occluded gases being dispelled. If, however, the lamp is alternately struck and pumped the occluded gases are finally dispelled and the final operation is as good as the operation when the purified sodium is used. The circulating pump for argon gas is an ordinary mercury vapor pump which is operated just rapidly enough to keep the yellow beyond the break in the discharge column when the arc is operating. The gas must be sent through at least two liquid air traps filled with glass beads, or the equivalent, before it reaches the arc, otherwise a large amount of mercury is carried into the discharge. Argon is initially introduced with a pressure of 1 or 2 millimeters.

The tube furnace is brought to a temperature of from 200°C to 250°C. This has been found to be the best operating temperature. For operation of the arc, 220 volts direct current has been found adequate. A higher potential than this is advantageous however to age the arc and bring it to the stable operating condition. When "burning" at 1.5 amperes the potential across the lamp is somewhat less than 100 volts, hence a ballast resistance must be used. A choke coil in the circuit is advantageous since it has a marked stabilizing effect. The "breakdown voltage" is high, but when a high frequency spark[5] is applied anywhere the arc immediately starts. If the arc has a tendency to go out when the "active point" on the cathode surface changes position, it is found good practice to coil loosely a wire from the high frequency spark about the tube conducting the gas from the lamp to the pump.

After the arc has "burned" a short time and any residual gas in the sodium has been dispelled, by pumping if necessary, the pressure of the argon is increased to as high a value as possible, still allowing the stability of the arc to be maintained. This is important for the life of the lamp, since if the mean free path of the gas molecules is large the sodium distills away from the nickel electrode and chokes the discharge column. When this happens, the lamp must be cleaned and fresh sodium introduced. The "*D*" radiation from this lamp is very intense and causes brilliant fluorescence in sodium vapor at pressures corresponding to temperatures as low as 150°C. The 3303A fluorescence excited by radiation from this lamp is intense enough to give very black photographs through a Hilger quartz spectograph in 15 minutes when the sodium vapor is at 190° C. The "*D*" fluorescence from the 3303A excitation is intense enough to be observed easily when the fluorescing vapor is at 170°C. The authors' experience in attempting to use a number of the sodium arcs described heretofore in the literature is convincing that the arc here described is much superior to any before described.

[5] The authors use an ordinary "Eisler Vacuum Tester" which is designed for finding leaks in vacuum lines.

THE INFLUENCE OF THE METHOD OF EXCITATION ON TRANSITION PROBABILITIES IN SODIUM VAPOR

By Carl J. Christensen and G. K. Rollefson
Chemical Laboratory, University of California, Berkeley

(Received September 3, 1929)

Abstract

Fluorescence has been excited in sodium vapor at 180°C by illuminating with the second member of the principal series, $\lambda = 3303$A. Both the first and second members of the principal series appeared in the fluorescence, the first member being due to the atom returning to its normal state in steps. The ratio of the intensities of the two lines was determined by photographic photometry and the results compared with what might be expected on the basis of measurements by Weiss on the sodium arc. In the arc the atom returns to the normal state from the $3P$ by way of the $2S$ twenty-five times as often as the direct transition occurs whereas in fluorescence approximately the same number take each path. This is contrary to the usual assumption that the transition probabilities are independent of the method of excitation.

THE intensity of any spectrum line depends on the number of atoms in the state from which the line originates and a factor, called the transition probability, which determines the fraction of this number which leave the excited state by the path corresponding to the spectrum line. These transition probabilities have been assumed to be constants. For the case of lines having the same initial level this assumption requires that the ratios of the intensities shall be independent of the method of excitation used.

In this paper we wish to present evidence based on a study of the transitions from the $3P$ level of sodium that the hypothesis that transition probabilities are independent of the method of excitation is untenable.

If sodium is excited to the $3P$ state there are three paths by which it may return to the normal ($1S$) state. The following diagram shows these different paths which are labelled for convenience in discussion as (a), (b), and (c). The fine structure of the terms is not shown. Weiss* has recently published the results of an investigation showing that the ratio of the transition probabilities of $3P \rightarrow 2S$ and $3P \rightarrow 1S$ is 25 to 1 if the radiation is excited by a low voltage arc. Since the $3P \rightarrow 2S$ transition is the first step in path (b) above, the last step of which is the emission of "D" light, we should expect on the basis of Weiss' experiments that if we had a large number of sodium atoms in the $3P$ state the ratio of the number of quanta of "D" light to the number of 3303A (the $3P - 1S$ transition) should be at least 25 to 1[1]. That

* Weiss Ann. d. Physik **1**, 565 (1929).

[1] According to a theory of Einstein's, the high intensity of the $2S$–$3P$ radiation in the arc used by Weiss would cause an induced emission which would increase the observed intensity. We have estimated the amount of this induced radiation assuming that energy density in the arc corresponded to 4000°K and found that the induced emission was only 20 percent of the total. We feel that this is a maximum value.

it should exceed this somewhat may be seen from the above diagram which shows that "*D*" light is also emitted by path (c).

No direct measurements have been made on sodium which would give the relative numbers taking the paths (b) and (c) but some idea of the magnitudes may be obtained from similar situations in other spectra. Such data are tabulated qualitatively by Grotrian[2] and show that the transitions by path (c) are apt to be equal to or less than those by path (b). This would mean that in the case under consideration the ratio of the intensity of the *D* lines to λ3303 should lie somewhere between twenty-five and fifty. Qualitatively this agrees with the observation of R. I. Strutt[3] on the fluorescence of sodium vapor excited by absorption of the 3303 line. In his first experiments only "*D*" light was observed in fluorescence but the later experiments showed both lines with the "*D*" line having much the greater intensity. On the other hand, the work of Terenin[4] indicates a considerably different

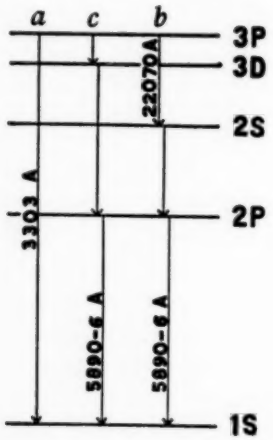

Fig. 1. Three paths by which a sodium atom in the 3*P* state may return to the normal 1*S* state.

result. He found that if sodium iodide is illuminated with light having a frequency sufficient to dissociate the salt and excite the sodium atom to the 3*P* state no fluorescence light was visible but both the *D* lines and the 3303 line could be photographed. No statement is made concerning the relative intensities of the two but from our own experience in photographing spectra we should say that the 3303 light would have to be comparable in intensity with the *D* light if it was to be observed with any reasonable photographic exposure. A comparison of the experimental conditions in Terenin's and Strutt's work indicated that there was considerable chance of collisions of the second kind transferring atoms from the 3*P* to the 2*P* state in Strutt's work. This would result in an increase in the *D* light at the expense of the 3303. It was decided, therefore, to repeat Strutt's work using pure

[2] Grotrian, Graphische Darstellung der Spektren, V. II, Springer, 1928.
[3] R. I. Strutt, Proc. Roy. Soc. (London) **A91**, 511 (1915); ibid. **A96**, 272 (1920).
[4] Terenin, Zeits. f. Physik **37**, 98 (1926).

sodium vapor at low pressures so as to eliminate the effects of collisions of the second kind.

Experimental

The fluorescence experiment was carried out with an apparatus assembly shown diagrammatically in Fig. 2. The letters in the figure indicate the following: (*s*) the source of exciting radiation, a sodium arc of the type described by the authors;[5](*l*), quartz lens; (*f*), filter to extinguish the *D* light from the exciting radiation; (*o*), opening to the furnace into which a jet of hot air was continuously blown so that sodium did not condense on the windows of the fluorescence tube; (*r*), fluorescence tube entirely of quartz; (*sp*), slit of Hilger quartz spectrograph. After testing a number of filters, the "Corex A, Red Purple" filter of Corning Glass was found the most suitable. No *D* light was registered on a panchromatic plate after 10 min-

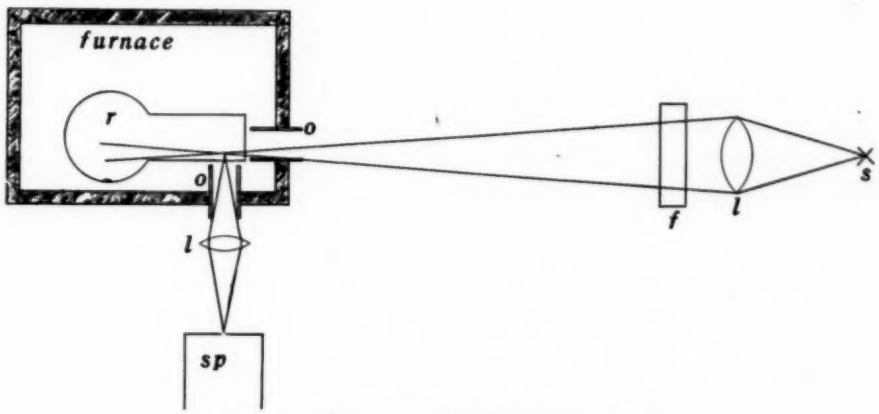

Fig. 2. Diagrammatic sketch of apparatus.

utes exposure with the full intensity of the arc. A transmission of the 2537A mercury line is allowed by this filter, hence there was no fear of a large decrease of energy of the 3303A exciting line. The cone of exciting light was brought as near as possible (1 or 2 mm) to the side of the fluorescence bulb from which the fluorescent cone was observed, so that re-absorption of the fluorescence light would be a minimum. The entire system, exclusive of the filter, was of quartz, and the number of parts through which the light must pass was reduced to a minimum so that as little energy as possible was lost by reflection. The furnace was thermostatically controlled to within 5°C of any predetermined temperature. For the investigation the temperature ranged from 170° to 220°C. A temperature lower than this gave a vapor pressure of sodium too low for photographic observation of the 3303A fluorescence, and a temperature higher than this caused the flask to be "browned" by the sodium vapor so that it became opaque to the ultraviolet. In most of the work a temperature of about 180°C was maintained. At this temperature the fluorescence energy was sufficient so that a suitable

[5] Christensen and Rollefson, Phys. Rev. **34**, 1154 (1929).

photographic blackening for photometry was obtained in three hours; the vapor pressure was also low enough so that the fluorescent cone of light extended with very little diminution throughout the length of the fluorescence bulb. If the excitation is by *D* light, at this pressure, the light cone also extends throughout the bulb and is fairly sharp, looked at from the window to the spectrograph. This gives evidence of the fact that there is little absorption of the fluorescence light before it leaves the bulb in the direction of the spectrograph.

The photographic plate chosen for the photometry was the Wratten and Wainwright Panchromatic, although photographs were also obtained on the Eastman Orthochromatic and Astronomical Green plates. The spectral photometry was accomplished by enlarging the image on the photographic plate with a well corrected lens and moving the image across a narrow slit in front of a photoelectric cell. Since only the lines 3303A and *D* appeared on the plate, the slit of the spectrograph was well opened, allowing a rather broad band to appear on the photographic plate where each line was located. These broad bands made the photometry an easy problem. The photoelectric cell was tested for energy response which was found to be linear. The light screens used in the photometry were calibrated with a thermopile and checked with a photoelectric cell. They were also tested and found to be neutral in the spectral regions of interest in this investigation.

The sodium for the fluorescence bulb was carefully purified by repeated fractional distillation in the highest attainable vacuum. When the sodium was finally introduced into the well baked-out fluorescence bulb, it was distilled from one side to the other as long as the pumping continued. The bulb was never sealed off until a vacuum of about 10^{-6}mm of mercury had been maintained for some time. By this procedure it is believed a high purity of sodium was obtained in the fluorescence bulb. The entire fluorescence bulb except the windows was well blackened with lamp black to reduce to a minimum the effect of any stray light. The inside of the whole furnace was likewise blackened. That there was no stray radiation present of appreciable amount is shown by the fact that several 3-hour exposures while the fluorescence bulb was cold failed to cause any photographic blackening, even though the full radiation of the exciting lamp was used.

Experimental Procedure and Results

A series of photographs of the fluorescence under 3303A excitation was obtained, the temperature of the fluorescence bulb ranging from 170°C to 220°C.[6] In all of the exposures made, the 3303A radiation appeared photographically much more intense than the *D* radiation.

Because of the long exposure-time necessary to obtain photographic plates usable for photographic photometry, it appeared almost a hopeless

[6] That the 3303A radiation alone was causing the excitation was clearly shown by placing in the exciting beam of light a piece of ordinary clear window glass. This transmits all the incident radiation to about 3600A. When this was done the radiation from the fluorescence bulb entirely disappeared.

task to obtain on one plate all the necessary data for an accurate measurement of the relative transition probabilities of the transitions giving rise to the two radiations. We were forced, therefore, to standardize the photographic procedure and use a number of plates from the same emulsion. Also as far as possible, plates from the same box were used for the most important exposures. A stable hydrochinon developer was made up, put in small bottles with the tops paraffined, and placed in a cool dark place until needed. A standard temperature and time were chosen for the development, fixing and washing. During development the plates were continuously brushed with a wide camel hair brush to decrease uneven development.[7] By this procedure, fogging and unevenness of development were held within a 5 percent limit. In all cases where a check was possible, the variation of the same subject photographed and photometered on different plates agreed within about 10 percent.

To obtain the standard blackening[8]-energy curve of the plates, in the two spectral regions of interest, a direct current helium discharge was used. This has strong lines at 5875A and 3187A. Harrison[9] in his work in spectral photometry finds calibration of the plates in the visible at 25A intervals and in the ultra-violet at 300A intervals sufficient for a 2 percent accuracy anywhere in the spectrum. Thus it is evident that taking these helium lines as standard our error will not be large. It was possible to control the current in the helium discharge very closely; and the intensity ratio of the two lines was checked at the beginning and end of its use.

To obtain the energy ratio of the two lines in the helium discharge a photographic method was also necessary, a thermopile of sufficient sensitivity not being available to measure directly the energy of the two lines. This procedure was as follows: A tungsten filament electric lamp in a thin soda-glass bulb will emit a rather large amount of ultra-violet radiation extending to almost 2900A. A lamp with a straight, tightly coiled filament was selected. The normal operating current of this was 7.5 amperes. To obtain a maximum of ultra-violet, it was forced to burn at from 9.5 to 10 amperes and the image of the filament focused, with a quartz lens, on the slit of a Hilger quartz monochromator. The energy from a narrow spectral region of this source was measured on a thermopile. The thermopile was then removed and the energy allowed to fall on the slit of the quartz spectrograph used throughout the entire experiment. A series of 1-second exposures was then made, the energy being successively decreased by inserting the calibrating screens in the illuminating beam of light. The spectral energy in the *D* region was suitably adjusted so that about equivalent blackening was obtained in the two spectral regions investigated, 5890A and 3303A. In this manner three different plates were exposed, each with a series of calibration exposures in the two spectral regions. The energy coming from the mono-

[7] Photographic Photometry; Dobson, Griffith, Harrison, p. 76.

[8] The blackening value as used in this work was calculated in the manner set forth by Dorgelo; Phys. Zeits. **26**, 756 (1925).

[9] Harrison, J. Optical Soc. Am. **17**, 397 (1928).

chromator was measured with the thermopile before each series of photographs. To obtain the relative energy falling on unit area of the photographic plate, the energy as given by the thermopile was corrected for the dispersions of the two instruments, though the sum of these corrections was small, it being apparent that the corrections from the two instruments would tend to cancel each other. Stray light from the monochromator was unavoidable, and correction for this was also made. The resulting blackening-energy curves were accurately parallel though they were displaced from each other somewhat.[10] It is evident that by this procedure correction for the instrument loss in the quartz spectrograph is automatic, since the energy was measured as it was thrown on the slit of the spectrograph.

Plates were now exposed for 1 second to the helium discharge operated under the selected standard conditions,[11] and the relative energies of the two lines, 3187A and 5875A, determined from the standard blackening curves, obtained in the manner just described. The following table expresses the result, giving the ratio of the energy of these two lines.

TABLE I. *Ratio of the energy of λ5875 to that of λ3187.*

Plate	Exposure	Referred to Standard Plate 1	Referred to Standard Plate 2	Referred to Standard Plate 3
1	1	12.2	9.8	10.0
1	2	11.3	8.9	9.2
1	3	12.3	9.7	9.9
1	4	11.7	9.2	9.6
1	5	12.1	9.4	9.9
1	6	11.7	9.1	9.6
2	1	13.1	9.7	11.6
2	2	13.1	9.7	11.6
2	3	13.0	10.0	11.6
2	4	13.5	10.0	11.6
2	5	13.2	10.3	11.5
		Average, $E(5875A)/E(3187A) = 10.9$		

In the table, $E(5875A)/E(3187A)$ is the ratio of the energy of the 5875A line to the 3187A line when the discharge operates under the standard conditions. The values for the ratio given in the three columns are the values as obtained from the standard blackening curves given by standard plates 1, 2, and 3. The values from all three plates are used in the determination of the final average value of the ratio, 10.9.

To obtain the standard three-hour energy-blackening curves, a small-intensity helium discharge was used.[12] The energy-blackening curves for

[10] These plates will be referred to as "standard plates" 1, 2, and 3, respectively.

[11] This discharge was operated directly from a 600-volt storage battery, suitable resistance being placed in the circuit to limit the current to 60 milliamperes. The current was not allowed to vary more than 2 percent.

[12] This was deemed necessary, since the standardized helium discharge was so intense that the screens necessary to diminish the light intensity to a suitable value for 3-hour exposures were so dense that accurate calibration of them was very difficult and subject to great error. We feel sure the error of the experiment as carried out is less than it would have been by the method of dense screens. This small helium discharge was energized by a direct current of 0.2 milliamperes. The current was controlled to 2 percent by the use of a thermionic "current limiter."

this discharge were first constructed in arbitrary units the full energy of each radiation being assigned the value 100. The units for the 3187 radiation were then evaluated in terms of the units assigned to the 5875 radiation. This was done by reducing the intensity of the standard helium discharge with screens so that three-hour exposures were practical. Since the ratio of the intensities of the radiations from this discharge has been determined the 3187 curve from the small discharge can be placed in its proper position relative to the 5875 curve.

Figure 3 gives the final blackening-energy curve for the 3-hour exposure; from this the relative energy of the 3303A and *D* light obtained from fluoresc-

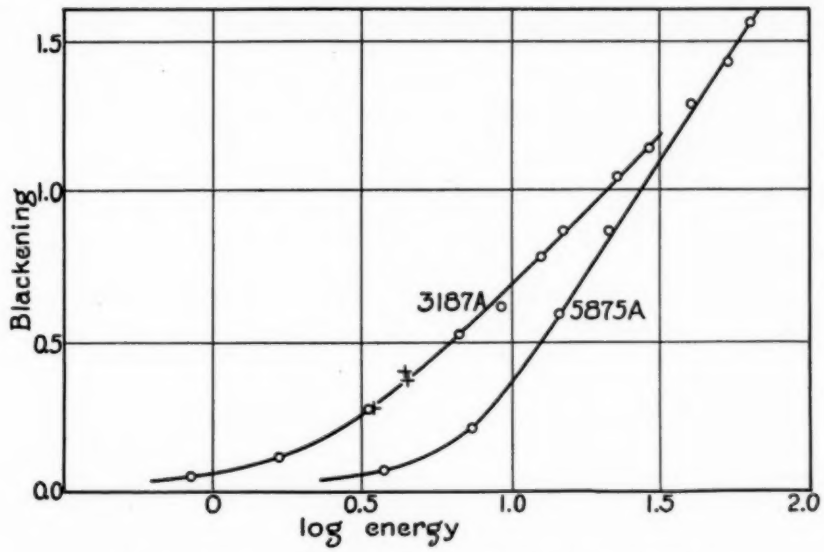

Fig. 3. Final blackening-energy curve for λ3187 and λ5875A.

ence was measured. The curves were checked from three plates. The crosses give the position of the 3187A curve relative to the 5875A curve as determined from the standard helium discharge. These points were determined from three exposures on as many different plates.

Results of Measurement of Fluorescence

From three plates the mean of the energy ratio (designated by *R*) of the two radiations from the fluorescence tube reaching the slit of the spectrograph was

$$R = \frac{E(5890-6A)}{E(3303A)} = 0.64$$

For the determination of this ratio the temperature of the fluorescent sodium was 180°C. The cone of exciting light was as close as possible to the window toward the spectrograph, the center of the cone being about 3 millimeters distant. Photographs were now obtained of the fluorescence and the energy ratio of the two radiations determined when the center of the exciting cone of light was 9 millimeters distant from the window. The temperature of the

sodium remained the same, 180°C. In this case the energy ratio was observed to be

$$R = 0.30$$

It is evident that the reabsorption must be corrected for, the D radiation being relatively more absorbed than the 3303A radiation.

If we assume, as a first approximation, the decrease of radiation energy is proportional to the average absorbing layer,[13] then we can write

$$-dE = kEdl$$

where E is the energy of a particular radiation and l is the absorbing layer. By integration this leads to the following expression,

$$E = E_0 e^{-kl}$$

Now if E, the energy of the 5890–6A radiation, is measured in terms of the energy of 3303A radiation, E', then

$$R = \frac{E}{E'} = \frac{E_0}{E_0'} e^{l(k'-k)} \tag{1}$$

We have determined this ratio R at two different values of l; comparing these two values of R, we get

$$R_1/R_2 = e^{(k'-k)(l_1-l_2)}$$

where the subscripts 1 and 2 refer respectively to the values obtained at 3 and 9 millimeters. Substituting in the last expression the appropriate experimental values,we obtain

$$(k'-k) = -0.127.$$

This value can be used now for determining the true energy ratio ($R_t = E_0/E_0'$) of the two lines. From equation (1) above, we get

$$R_t = Re^{-l(k'-k)} = Re^{0.127l}.$$

Substituting in this expression the values of R and l, we get

$$R_t = 0.94.$$

Thus we find that the relative energy of the D radiation to 3303A radiation will be 0.94, when these radiations have their origin from the $3P$ level of sodium excited by resonance radiation 3303A.

To obtain the relative transition probabilities, this ratio of energies must be changed to one of quanta. If N is the number of quanta and the other terms have their usual meaning, then

$$E = N(h\nu) = Nch/\lambda.$$

[13] This seems justified in this case since we are observing resonance radiation and since there is still considerable energy in both lines when coming from the 9 millimeter depth. While we realize this assumption cannot be strictly accurate, still we feel certain it will give a correct value of the energy ratio which will be well within our other experimental errors.

Using this expression we obtain for R

$$R=\frac{N_D ch/\lambda_D}{N_{3303} ch/\lambda_{3303}}=\frac{N_D}{N_{3303}}\ \frac{\lambda_{3303}}{\lambda_D}$$

$$\therefore \frac{N_D}{N_{3303}} = R\frac{\lambda_D}{\lambda_{3303}}$$

where N_D/N_{3303} is the relative number of quanta measured in the two radiations, which is also the ratio of the probabilities of paths (a) to $(b)+(c)$. From the value of R determined in this experiment, we find

$$N_D/N_{3303}=5890/3300\times 0.94=1.7$$

Although this value was obtained from measurements on a single fluorescence bulb, still the qualitative observations of photographs taken from other fluorescence tubes confirm this value.

Error of the Measurement

From the data (Table 1) used to determine the relative intensity of the two lines in the standard helium discharge, variations as large as 24 percent from the average occur. It is probably correct to say this ratio was determined to within 25 percent. The error in placing and determining the relative positions of the two energy-blackening curves in Fig. 3 is not more than 10 percent, assuming the ratio for the standard helium lamp as correct. The error involved in determining the correct photographic blackening caused by the fluorescence radiation is 10 percent. The method of correcting for reabsorption is certainly not more than15 percent in error. The sum of all these errors gives 60 percent. One other factor must be considered, the possibility of quenching. No method was available to measure the pressure of foreign gases in the fluorescence bulb under operating conditions. Since every precaution was taken, however, to get the sodium of great purity, it is believed the error cannot be large. However, the error would undoubtedly favor an increase in the relative energy of D light.

Taking all the errors into consideration we feel that the net error in the ratio of the intensities of the two radiations does not exceed 25 or 30 percent.

Discussion of Results

If we designate the probability of return by paths (a), (b), and (c) as P_a, P_b, P_c respectively, then the result we have obtained may be expressed as

$$\frac{P_b+P_c}{P_a}=1.7$$

From this it is apparent that P_b/P_a is less than 1.7 and probably about equal to one. This value is totally different from that obtained by Weiss in the arc. The difference is far too large to be explained as due to experimental errors, therefore we are forced to conclude that the relative probabilities of the transitions $1S$–$3P$ and $2S$–$3P$ depend upon the method of excitation of the $3P$ state.

The values for the ratio of the intensities of the two radiations calculated from theoretical considerations do not agree with either of the experimental values. Bartels,[14] using the correspondence principle, obtained a value of four for the ratio. A value based on the wave mechanics can be obtained from the work of Kupper.[15]

The approximation involved in the derivation of his equations cause considerable errors for low values of n, the principal quantum number. However, if we calculate the ratio $(2S-mP/1S-mP)$ for large values of n and observe the trend as we go to low values we find that the ratio $(2S-3P)/(1S-3P)$ must be greater than 0.05.

A comparison of Trumpy's absorption measurements on sodium vapor[16] with the theoretical values shows that for low values of n the observed intensities are higher than the calculated ones, the deviation increasing as n decreases. From this it is to be expected that the deviation for the $2S-3P$ transition would be greater than that for the $1S-3P$ and therefore the experimentally determined ratio of the two should be greater than the calculated value, as is actually the case.

Very little is to be found in the literature concerning the relative intensities of lines originating in the same energy level under different conditions of excitation. Crozier[17] has studied the intensities of some mercury lines when excited by electrons of various velocities. In the case of the transitions $2^3P_1-3^3D_1$ and $2^3P_0-3^3D_1$ he obtained quite different curves but for $2^3P_1-2^3S$ and $2^3P_2-2^3S$ the curves were practically identical. To account for his results he suggests the possibility that under different conditions different fine structure levels are excited. The work of Collins[18] on the fine structure of some mercury lines under different conditions of excitation indicates that different fine-structure levels are excited by altering the method of excitation. This might be of value in explaining differences when there is a difference in the l or j of the final level but it can scarcely account for the case we are considering in sodium where the only difference between the two final levels is one of principal quantum number. It is possible that collisions may affect the transition probabilities in an arc but would have no effect in a fluorescence experiment such as we have described in this paper since the pressure was so low that the time between collisions was much greater than the mean life of the excited atom.

Further experiments have been planned which it is hoped will cast some light on the behavior of atoms in excited states. For the present, all we can say is that the future of an atom in one of its higher quantum states depends to a very marked degree either on its past or its surroundings or possibly both. Future work in this field must separate these two factors.

[14] Bartels, Zeits. f. Physik **32**, 415 (1925).
[15] Kupper, Ann. d. Physik **86**, 511 (1928).
[16] Trumpy, Zeits. f. Physik **44**, 575 (1927).
[17] Crozier, Phys. Rev. **31**, 800 (1928).
[18] Collins, Phys. Rev. **32**, 753 (1928).

IONS AND ELECTRICAL CURRENTS IN THE UPPER ATMOSPHERE OF THE EARTH*

By E. O. Hulburt
Naval Research Laboratory

(Received September 11, 1929)

Abstract

It is assumed that the ionization in the upper atmosphere is caused by the ultra-violet light of the sun and that the ion and electron densities at noon at the equator are in keeping with the facts of wireless waves. From the laws of recombination of the ions and of diffusion and drift of the ions in the earth's magnetic, gravitational and electric fields the distribution of the ions over the earth is worked out. The distribution is found to agree with wireless data over the earth, and with Gunn's diamagnetic theory of the solar diurnal variation of the earth's magnetism, (Phys. Rev. **32,** 133 (1928). The gravitational drift currents are found to flow mainly along the parallels of latitude in the following way: (1) a current sheet in the daylight hemisphere flowing eastward in the levels above 150 km which at the sunrise and sunset longitudes divides into two sheets; (2) one of these flows westward on the day side of the earth underneath (1) in the levels below 150 km, and (3) the other sheet continues eastward around on the night side of the earth. The current is mainly (4/5) between the 40'th parallels of latitude north and south, and falls to lower values at the higher latitudes. The total currents in the three sheets are about 1.16×10^7, 8.7×10^6 and 2.9×10^6 amperes, respectively. The east and west daytime current sheets subtract from each other leaving in effect an eastward current of about 2.9×10^6 amperes flowing around the earth all the time. This causes a magnetic field agreeing in magnitude and type with that obtained by Bauer in his 1922 analysis of the magnetic field of the earth of external origin, (Terr. Mag. **28,** 1 (1923)). The current sheets are not of the type required by Chapman's drift current theory of the diurnal magnetic variation, (Proc. Roy. Soc. **A122,** 369 (1929)). As a result of the drift currents, the sunset longitude of the earth is at a potential around 2000 volts above that of the sunrise longitude. This electric field combined with the earth's magnetic field causes the ions and electrons on the night side of the earth to drift upward with velocities between 100 and 200 cm sec^{-1}. The ions and electrons move into regions of lower pressure and therefore do not recombine as fast as they otherwise would. This removes a difficulty from an earlier calculation which yielded a slightly too great rate of disappearance of the free charges at night. The upward drift of the ionization causes a rise of the Kennelly-Heaviside layer which is, partially at least, compensated for by the fall due to the cooling and contraction of the atmosphere at night, and is complicated by the diffusion of the ions. It is difficult to say how much of the nighttime rise of the layer observed in experiments with wireless rays may be a genuine rise and how much may be an apparent rise due to delayed group velocities, or to other causes.

THE development during the past five years in the physical theory of the upper atmosphere of the earth guided by the facts of wireless wave propagation phenomena has yielded information about the electrons in the upper atmosphere. The conclusion was reached[1] that the ionization was

* Published with the permission of the Navy Department.

[1] Hulbert, Phys. Rev. **31,** 1018 (1928).

caused by the ultra-violet light of the sun and that the electron density increased with the height above the earth to a maximum value of about 3×10^5 electrons cm^{-3} at about 190 km for the sun directly overhead, the sun being quiet and at an epoch midway between the periods of minimum and maximum solar activity. The wireless waves indicated that ionization of some sort existed below 190 km down to about 100 km and put an upper limit upon the amount of ionization in this region, but did not decide whether the ionization was predominately electronic or ionic. Exact theoretical calculations of the ionization below 190 km were not possible because many facts about the photo-ionization of the atmospheric gases were, and are still, unknown.

2. The facts of terrestrial magnetism and their physical interpretation offered further clues to the ionization below 190 km. Gunn[2] remarked that long free path ions in a magnetic field were diamagnetic and worked out his diamagnetic theory of the quiet day solar diurnal variations in the earth's magnetic field. He was able to account for the prominent features of the solar diurnal variation on the assumption that the diamagnetism of the atmosphere due to the ions was a maximum directly underneath the sun and fell off roughly with the cosine of the angular distance from high noon, becoming at night about 1/10 or less of its noon maximum value. At the noon maximum the theory required in a 1 cm^2 column of the atmosphere 5×10^{16} ions at a temperature of 300°K, or, since the diamagnetism of an ion depends on its kinetic energy and hence on the temperature, 3×10^{16} ions at 500°K, or 1.5×10^{16} at 1000°K. Below 150 km the free paths are so short that the ions do not contribute to the diamagnetism. Therefore the ions were taken to be mainly in the levels from 150 to 180 km, although the exact height to which they extended was not very important as long as it was not too great, below 200 km, say. Maris[3] had previously shown that the noon-day temperatures in the atmosphere above 100 km were probably 300°K or greater and Maris and Hulburt[4] that the temperatures might be as much as 1000°K. Maris' tables[3] of the molecular densities in the upper atmosphere indicated that the 150 km levels of the atmosphere, because of the expansion of the lower levels of the atmosphere due to the heat of the sun, moved upward about 20 km in the morning and descended in the afternoon. Gunn assumed that because of the lack of thermal equilibrium in the atmosphere (reference 3, page 243) the maximum height was attained about 2 P.M., local time, and thereby secured agreement with the observed occurrence at about 11 A.M., local time, of the maximum of the horizontal field variation in temperate latitudes.

3. Maris and Hulburt,[4] and simultaneously and independently Chapman,[5] recognized that an ion of mass m and charge e, c.g.s.e.m.u., in a gravita-

[2] Gunn, Phys. Rev. **32**, 133 (1928); Terr. Mag. and Atmos Elect. **34**, 17 (1929).
[3] Maris, Terr. Mag. and Atmos. Elect. **33**, 233 (1928).
[4] Maris and Hulburt, Phys. Rev. **33**, 412 (1929).
[5] Chapman, Proc. Roy. Soc. **A122**, 369 (1929).

tional field g and magnetic field H, drifts perpendicular to these two vectors with a velocity w given approximately by

$$w = mg \sin \phi / He, \tag{1}$$

the positive and negative ions going in opposite directions; ϕ is the angle between H and g. For a uniformly magnetized sphere, and the earth approximates this quite closely, H at latitude θ is given by

$$H = H_0(1+3 \sin^2 \theta)^{1/2}, \tag{2}$$

where $\cot \theta = 2 \tan \phi$, and H_0 is 0.3227 gauss the value of H at the equator at sea-level. (2) is taken to give H on the 100 to 200 km levels of the atmosphere. With these expressions (1) becomes

$$w = mgA/H_0 e, \tag{3}$$

where

$$A = (\cos \theta)/(1+3 \sin^2 \theta). \tag{4}$$

4. In the case of the earth the positive ions drift eastward and the negative ions westward; this constitutes an eastward electric current in the upper atmosphere. The drift velocity given by (3) occurs only when the free path of the ion is sufficiently long, i.e. above 150 km at summer noon. Maris and Hulburt[4] used the gravitational drift current to explain certain features of a magnetic storm, Chapman[5] suggested that the current might explain the quiet day magnetic variation. The type of atmospheric current necessary to explain the diurnal variation had already been worked out by Bartels.[6] His diagram is shown in Fig. 1, in which the abscissas are the longitudes in hours and the ordinates the latitudes; the numbers along the lines of current flow are in 10^3 amperes. Thus the figure indicates in the northern hemisphere in the day a current sheet of 62,000 amperes wheeling counter-clockwise around a center at about 40° latitude and 11 A.M., and at night a current sheet of 32,000 amperes wheeling in the opposite direction. The maximum current density occurs at 11 A.M. at the equator and has the value 3×10^{-5} c.g.s.e.m.u., excess of the day over the night value, referring to a section of the atmosphere 1 cm wide and of a thickness made up of the total number of long free path ions in a vertical 1 cm^2 column of the atmosphere. Let us call this number $2D$, so that D is the total number of ion pairs in the 1 cm^2 column; if the positive and negative ions each carry the elementary charge e and are present in equal numbers, D represents these numbers. To be specific we shall assume throughout that the ions are singly charged positive and negative nitrogen atomic ions at a temperature of 500°K at equatorial noon; other possibilities will be mentioned later. At the equator $A = 1$, $m = 2.3 \times 10^{-23}$ grams, and from (3) $w = 4.6$ cm sec^{-1}. The drift current i is $2 Dew$, and upon equating this to 3×10^{-5} we get $D = 2 \times 10^{14}$ nitrogen atomic ion pairs, or 4×10^{14} ions. This is 1/75 of the 3×10^{16} ions required

[6] Bartels, "Handbuch Exp. Physik," Vol. 25 (1928).

by the diamagnetic theory. If the temperature is 1000°K the ratio becomes 1/38, if the ions are molecular nitrogen at 300°K the ratio is 1/250. Therefore Chapman concluded that the gravitational drift action of the ions was much more effective than their diamagnetism in causing the earth's magnetic field variation.

5. The calculation, however, is not adequate to support such a conclusion; one can not say what the value of a current may be until the entire circuit is known, and the foregoing calculation considers only the current producing part of the circuit and neglects the return path. With equal propriety we may argue as follows: diamagnetism owes its effect to 2/3 of

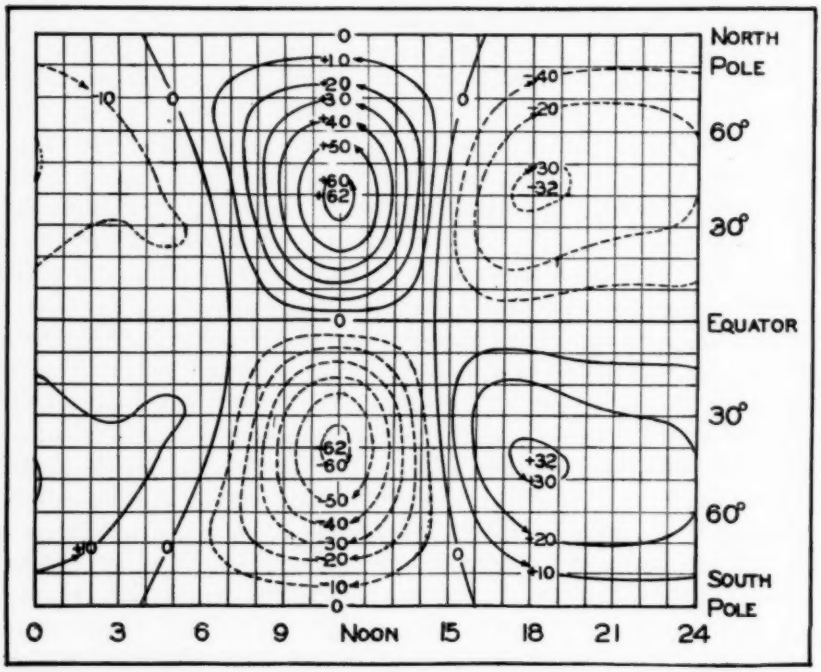

Fig. 1. The theoretical current system, due to Bartéls,[6] in the upper atmosphere necessary to produce the solar diurnal variation in the earth's magnetic field. The chart is taken from Chapman's paper.[5]

the temperature energy of the ion, or kT, where k is 1.372×10^{-16} erg deg^{-1} and T is the temperature Kelvin. The factor 2/3 enters because it is only the components of the random temperature velocities in planes normal to H which contribute to the diamagnetism. With $T=500°$, kT is 7×10^{-14} erg. The drift current derives its energy from mgh, the energy of the ion falling through a height h. With $h=30$ km mgh is 6×10^{-14}, and we might conclude that diamagnetism is equal to the drift current action. The point to be made is that neither of the arguments is sufficient. A solution of the complete problem is required before a decision is possible. This is attempted in the following pages. An ion distribution over the earth due to the ultra-

violet light of the sun is worked out. This distribution is found to be in agreement with wireless observations and with the diamagnetic theory. It possesses drift currents. The drift currents were not similar to those of Fig. 1 but were such as to explain a certain part of the permanent magnetic field of the earth.

6. Maris' tables[3] of the pressures in the upper atmosphere are used, omitting hydrogen. The summer day molecular densities are conveniently expressed by the relation

$$n = n_0 \epsilon^{-pz^2}, \tag{5}$$

where n is the number cm^{-3} of molecules of all kinds at a height z cms above the surface of the earth. $p = 0.872 \times 10^{-6}$ and for $z = 150$ km $n = 1.86 \times 10^{12}$. With these values (5) is approximately valid from 100 to 250 km, for other heights Maris' tables should be used directly. The tables are based on an upper atmospheric temperature of 300°K and in using them in calculations for 500° we are not quite consistent. We should recalculate all of the tables for the higher temperature, this would put the molecular density at about 165 km which is at 150 km on the 300° basis. The difference is not very important here, especially as the height z enters into the calculations mainly as a parameter, the molecular density being the fundamental quantity. (There is another inconsistency. I think that the arguments for noon temperatures greater than 500°, as much as 1000°, are too strong to be put aside, and yet I use temperatures of 500° and below. The same procedure occurred in the earlier paper[1] in which a temperature of 219° was used at times in spite of the fact that the 300° temperature seemed a better value. The reason was that 300° seemed then as strange and speculative as 1000° does now.)

7. The diamagnetism and the drift of the ions decrease with the free path γ according to the same ratio

$$\gamma^2/(\gamma^2+r^2), \tag{6}$$

where r is the radius of gyration of the ion in the magnetic field. r is given by

$$r = mu/He, \tag{7}$$

where u is the velocity of thermal agitation of the ion. From (2), (5), (6), and (7) it is seen that the diamagnetism and the drift are complete at 180 km and are reduced to 60% and 4% at 170 and 150 km, respectively, at noon at the equator. For simplicity we shall assume that the diamagnetism and the drift are complete above a critical level z_c and are absent below z_c; this amounts to assuming that the change from the long to the short free path region occurs abruptly. The critical level z_c is taken to be 150 km at the equator, it varies with the latitude. The assumption is made that the temperature T of the high atmosphere is 500°K at noon at the equator and that T along the noon meridian varies with cosine of the latitude θ until at the poles T is 220°K. It is assumed throughout that the geographic and magnetic poles of the earth coincide. Thus at any latitude $T = 220 + 280$

$\cos\theta$. The values of T at each latitude are given in column 2, Table I. From the values of H and T at each latitude r was determined from (7) and z_c was calculated by means of (6). The values of z_c are given in column 3, Table I.

TABLE I.

1	2	3	4	5	6	7	8	9	10
θ	T	z_c	α	$z-z_1$	σ	D	i	v	E
0°	500°K	150.0 km	0.69×10^{-25}	0.0 km	13.3×10^{-6}	1.50×10^{16}	21.9×10^{-4}	360	116
10	494	149.8	0.71	0.2	12.6	1.53	20.3	308	110
20	483	148.6	0.74	1.0	7.72	1.54	15.6	245	114
30	464	146.8	0.83	2.0	4.58	1.48	10.6	216	140
40	435	145.2	0.98	3.0	2.02	1.36	6.7	207	195
50	399	143.5	1.21	5.4	0.86	1.21	4.1	210	290
60	360	142.0	1.66	8.0	0.33	1.02	2.3	231	480
70	315	140.5	2.19	12.6	0.07	0.71	1.0	405	1380
80	268	139.0	3.32	20.5	0.00	0.32	0.2	710	5200
90	220	—	5.43	—	—	—	—	—	—

8. Denote the long and short free path regions of the atmosphere by D and S, respectively. Let y be the density of ion pairs at a height z and D be the total number of ion pairs in a 1 cm² vertical column of the D region. Then

$$D=\int_{z_c}^{\infty} y\,dz. \tag{8}$$

It is assumed that in each cm³ of the atmosphere there are approximately equal numbers of positive and negative ions. Therefore D and y are also the numbers of positive or negative ions. The general procedure is as follows: at one point on the earth, namely, the point directly underneath the sun D is assumed to be 1.5×10^{16}, as required by the diamagnetic theory of the diurnal magnetic variation, and the y,z curve is assumed to be in accord with the facts of wireless wave propagation. On the assumption that the ions are caused by the ultra-violet light of the sun, the y,z curves were then calculated for all latitudes and longitudes of the earth.

9. We shall need certain formulas which are derived in reference 1. At a height z the number of ions N which diffuse $\text{cm}^{-2}\ \text{sec}^{-1}$ vertically under gravity is $N=0.41\gamma u\ (py+dy/dz)$. Putting $\gamma=1/2^{1/2}\pi n\sigma^2$, where the molecular diameter σ is taken to be 3×10^{-8} cm, and $u=3\times10^5$ cm sec^{-1} approximately, the expression becomes

$$N=10^{19}(py+dy/dz)/n. \tag{9}$$

For equilibrium conditions in the atmosphere in each cm^{-3} the rate of production q of the ions is equal to the rate of loss, and the relation between y and z is therefore

$$q=\alpha n y^2+10^{19}(d^2y/dz^2+2p\,dy/dz+p^2y)/n, \tag{10}$$

[7] Thomson, Phil. Mag. **47**, 337 (1924); see also the discussion on page 1023, reference 1.

where $\alpha n y^2$ is the rate of loss due to recombination and the last term in (10) is the rate of loss due to gravity diffusion. We assume Sir J. J. Thomson's formula[7] for the recombination coefficient α. At low pressures α varies approximately with the $-5/2$ power of the temperature; the values of α for nitrogen atomic ions calculated from Thomson's formula are given in column 4, Table I. The formula was derived on the theory that for a positive and negative ion to combine a third body, as a neutral molecule, must be present to carry away the energy of recombination. Thus the theory considers in essence only the spatial position of the ions. It neglects at least two factors which may be of importance, namely, that recombination is probably a function of the energy states of the ions as well as of their positions in space, and that recombination may occur by a direct two body collision

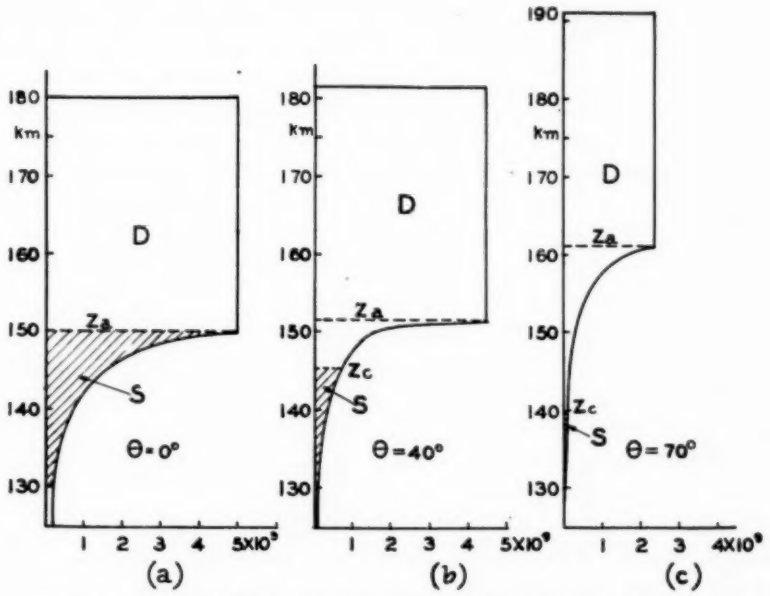

Fig. 2. Theoretical ion density curves in the upper atmosphere for latitudes 0°, 40° and 70° at noon equinox.

between the ions with a transfer of the energy into excitation or the emission of radiation or both. The one factor makes Thomson's α too high and the other too low. About all that can be concluded at the present time is that the formula is a simple one and agrees fairly well with certain laboratory experiments and that the true coefficient is probably much more complicated.

10. When the sun is directly overhead, i.e. equinoxial noon at the equator, the y,z curve is assumed to be that of Fig. 2(a), in which the abscissas are the ion densities and the ordinates the heights above the earth. $y=5\times10^9$ from $z=150$ to 180 km, hence $D=1.5\times10^{16}$. The curve below 150 km is calculated from the arbitrary formula

$$1/y-1/5\times10^9=4.54\times10^{-22}(n-1.86\times10^{12}),$$

$\cos\theta$. The values of T at each latitude are given in column 2, Table I. From the values of H and T at each latitude r was determined from (7) and z_c was calculated by means of (6). The values of z_c are given in column 3, Table I.

TABLE I.

1	2	3	4	5	6	7	8	9	10
θ	T	z_c	α	$z-z_1$	σ	D	i	v	E
0°	500°K	150.0 km	0.69×10^{-25}	0.0 km	13.3×10^{-8}	1.50×10^{16}	21.9×10^{-4}	360	116
10	494	149.8	0.71	0.2	12.6	1.53	20.3	308	110
20	483	148.6	0.74	1.0	7.72	1.54	15.6	245	114
30	464	146.8	0.83	2.0	4.58	1.48	10.6	216	140
40	435	145.2	0.98	3.0	2.02	1.36	6.7	207	195
50	399	143.5	1.21	5.4	0.86	1.21	4.1	210	290
60	360	142.0	1.66	8.0	0.33	1.02	2.3	231	480
70	315	140.5	2.19	12.6	0.07	0.71	1.0	405	1380
80	268	139.0	3.32	20.5	0.00	0.32	0.2	710	5200
90	220	—	5.43	—	—	—	—	—	—

8. Denote the long and short free path regions of the atmosphere by D and S, respectively. Let y be the density of ion pairs at a height z and D be the total number of ion pairs in a 1 cm² vertical column of the D region. Then

$$D=\int_{z_c}^{\infty} y\,dz. \tag{8}$$

It is assumed that in each cm³ of the atmosphere there are approximately equal numbers of positive and negative ions. Therefore D and y are also the numbers of positive or negative ions. The general procedure is as follows: at one point on the earth, namely, the point directly underneath the sun D is assumed to be 1.5×10^{16}, as required by the diamagnetic theory of the diurnal magnetic variation, and the y,z curve is assumed to be in accord with the facts of wireless wave propagation. On the assumption that the ions are caused by the ultra-violet light of the sun, the y,z curves were then calculated for all latitudes and longitudes of the earth.

9. We shall need certain formulas which are derived in reference 1. At a height z the number of ions N which diffuse $\text{cm}^{-2}\ \text{sec}^{-1}$ vertically under gravity is $N=0.41\gamma u\ (py+dy/dz)$. Putting $\gamma=1/2^{1/2}\pi n\sigma^2$, where the molecular diameter σ is taken to be 3×10^{-8} cm, and $u=3\times10^5$ cm sec^{-1} approximately, the expression becomes

$$N=10^{19}(py+dy/dz)/n. \tag{9}$$

For equilibrium conditions in the atmosphere in each cm^{-3} the rate of production q of the ions is equal to the rate of loss, and the relation between y and z is therefore

$$q=\alpha n y^2+10^{19}(d^2y/dz^2+2p\,dy/dz+p^2y)/n, \tag{10}$$

[7] Thomson, Phil. Mag. **47**, 337 (1924); see also the discussion on page 1023, reference 1.

where $\alpha n y^2$ is the rate of loss due to recombination and the last term in (10) is the rate of loss due to gravity diffusion. We assume Sir J. J. Thomson's formula[7] for the recombination coefficient α. At low pressures α varies approximately with the $-5/2$ power of the temperature; the values of α for nitrogen atomic ions calculated from Thomson's formula are given in column 4, Table I. The formula was derived on the theory that for a positive and negative ion to combine a third body, as a neutral molecule, must be present to carry away the energy of recombination. Thus the theory considers in essence only the spatial position of the ions. It neglects at least two factors which may be of importance, namely, that recombination is probably a function of the energy states of the ions as well as of their positions in space, and that recombination may occur by a direct two body collision

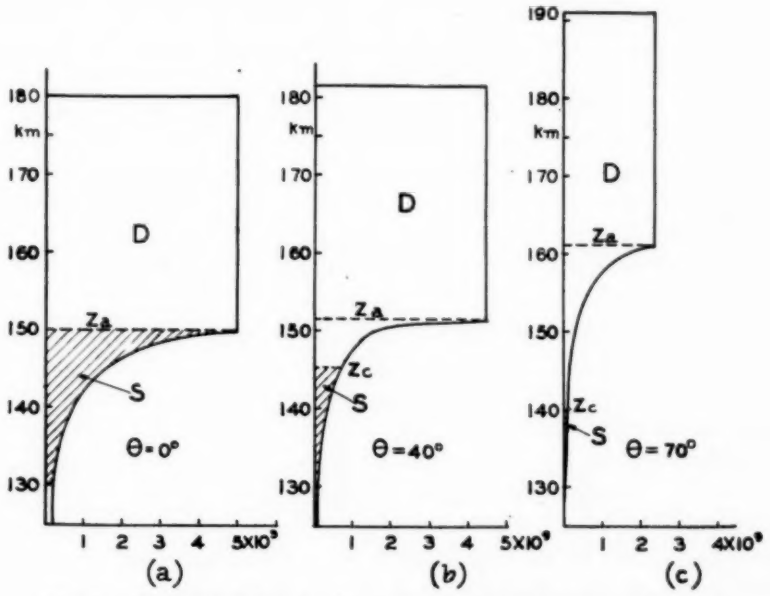

Fig. 2. Theoretical ion density curves in the upper atmosphere for latitudes 0°, 40° and 70° at noon equinox.

between the ions with a transfer of the energy into excitation or the emission of radiation or both. The one factor makes Thomson's α too high and the other too low. About all that can be concluded at the present time is that the formula is a simple one and agrees fairly well with certain laboratory experiments and that the true coefficient is probably much more complicated.

10. When the sun is directly overhead, i.e. equinoxial noon at the equator, the y,z curve is assumed to be that of Fig. 2(a), in which the abscissas are the ion densities and the ordinates the heights above the earth. $y=5\times10^9$ from $z=150$ to 180 km, hence $D=1.5\times10^{16}$. The curve below 150 km is calculated from the arbitrary formula

$$1/y-1/5\times10^9=4.54\times10^{-22}(n-1.86\times10^{12}),$$

where 1.86×10^{12} is the value of n at 150 km. With the y,z curve of Fig. 2(a) wireless rays of wave-lengths 5000, 1000, 500 and 400 meters are totally reflected (refracted) at normal incidence at heights of 68, 100, 116 and 120 km, respectively. The absorption of the ionized atmosphere from 100 to 120 km is such that the intensity of 400 meter waves is reduced $1/\epsilon$'th in about 15 km of the medium. These values are in fair accord with observation.[1] The ion curve of Fig. 2(a) gives too low an absorption of waves below 50 meters, and does not account at all for the skip distances and downward refraction of the short wireless waves. This is as it should be, for the curve comprises only a portion of the ionization of the atmosphere. It omits the electrons and to account for the behavior of the short waves the electrons must be considered; this of course has been done in earlier papers.[1]

11. The calculation of the y,z curves at various latitudes falls into two parts, first a calculation of the portion of the y,z curve in the S region and, secondly, of the portion in the D region. The second part is dependent upon the first part with additional factors. Denote the y,z curve of Fig. 2(a) by $\theta=0°$ and the quantities associated with it by the subscript 1. Referring to the portion of the curve in the S region below 150 km the gravity diffusion term in (10) is found by calculation to be less than the recombination term by an order of magnitude or more. Therefore, at each point on the curve we have approximately from (10) $q_1=\alpha_1 n_1 y_1^2$, and hence q_1 is known at each height z_1, q_1 being assumed to be due to the solar ultra-violet radiations of appropriate intensities and absorption coefficients which penetrate down to and are completely absorbed in the various levels of the atmosphere. At latitude θ $q=q_1\cos\theta$, and light, which is totally absorbed (or nearly so, see reference 1, page 1025) in reaching a level z_1 at normal incidence, reaches a corresponding level z at the angle θ, where from (5)

$$z=z_1-(\log_e\cos\theta)/p. \tag{11}$$

Thus the y,z curve at angle θ is obtained by calculating y from $y=y_1(\alpha_1/\alpha)^{1/2}$ and z from (11). This amounts to multiplying the abscissas of the curve for $\theta=0°$ in the levels below z_c by a constant factor and moving the curve upward a distance $z-z_1$. The values of $z-z_1$ are given in column 5, Table I. The y,z curves for latitudes 40° and 70° on a noon meridian are given in Figs. 2(b) and 2(c), respectively. The method just described for calculating the curves in the S region was also used to continue the curves in the D region from z_c to the level where y becomes constant. Denote this level by z_a; z_a-150 is the same as $z-z_1$ in column 5, Table I. The method, however, gives only a part of the ions in the region from z_c to z_a, namely, those produced there by the ultra-violet solar radiation. In addition there are ions which diffuse down from higher levels; these are considered in section 15.

12. The S region of a y,z curve lies below the z_c level. The electrical conductivity of a 1 cm³ of the S region is given by the usual expression for an ionized gas, $ye^2\gamma/mu$, and the electrical conductivity σ of a 1 cm² vertical column of the S region is

$$\sigma = \int_0^{z_c} (ye^2\gamma/mu)dz. \tag{12}$$

The values of σ in c.g.s.e.m.u. along a noon meridian for various latitudes were calculated from the y,z curves and are given in column 6, Table I.

13. In the D region the calculation of the y,z curve is more complex because a new factor enters, namely, an electric field. In this region the positive ions under the action of gravity and the earth's magnetic field move eastward, the negative ions westward, and build up an east-to-west potential gradient E on the day side of the earth, and hence a west-to-east gradient at night. This electric field is in such a direction that, combined with the earth's magnetic field, it causes ions in the D region of both signs to descend during the day, and to rise at night. Because of the westward electric field a current flows westward in the S region in daylight which completes the circuit of the eastward drift current i in the D region. $i=2Dew$, where w is given by (3). For equilibrium conditions a fraction f of the current in the D region flows back in the underlying S region and a fraction $1-f$ flows elsewhere, as around the night side of the earth. fi is the total current flowing across a vertical section of the S region 1 cm wide. At each latitude we may then write $fi=E\sigma$. It is shown in section 20 that f is about 3/4. Therefore

$$E=3Dew/2\sigma. \tag{13}$$

The velocity v downward in the daytime, due to the fields E and H is equal to $E \sin \phi/H$. Combining this with (2), (4) and (13) gives $v=3ADew/2\sigma H_0$. Introducing (3) and the numerical values of m, g and H_0 yields

$$v=10^{-12}A^2y/\sigma. \tag{14}$$

14. Gravity diffusion is neglected and therefore the same ultra-violet light which gave rise to the straight portion 30 km in length of the y,z curve for $\theta=0°$ causes y,z curves at other latitudes which are also straight lines above the z_a level 30 km in length. In the region above z_a we assume equilibrium and equate the rate of production of the ions to the rate of loss by recombination and to diffusion downward across the z_a level with velocity v. Therefore

$$q' \cos\theta = \int_{z_a}^{z_a+30} \alpha n y^2 dz + vy \tag{15}$$

where q' is the total rate of production of ion pairs in a 1 cm^2 column above z_a. For $\theta=0$ (13), (14) and (15) gave $q'=5.25\times10^{12}$, $v=360$ cm sec.$^{-1}$ and $E=116$ c.g.s.e.m.u. With the value of q' thus determined the y,z curves above z_c were calculated and the values of D, i, v and E were found. These are given in columns 7, 8, 9 and 10, respectively, of Table I. The neglect of the gravity diffusion term was permissible, for N from (9) came out to be less than vy at all points on the curves above z_a.

Table I gives the variation of the respective quantities with latitude along a noon meridian. The variation with longitude along the equator

is a little different because H changes with latitude but not with longitude. For θ less than 40° the difference is slight, for θ greater than 40° the difference is perceptible. For example, at 70° longitude from high noon, i.e. 4.7 P.M. on the equator, σ is about 5, D about 0.4 and E about 0.5 times the respective values at 70° latitude.

15. The portions of the y,z curves between the z_c and z_a levels were calculated in section 11 omitting the diffusion terms. The contribution to the ions in this region from those which descend across z_a with velocity v is estimated in the following way. As the ions move downward their density y decreases because of recombination. For equilibrium conditions the increase in y in an element, dz, dz being measured positive upward, is $dy=\alpha n y^2\,dz/v$, where dz/v is the length of time the ions remain in the element. Integrating and setting $y=y_a$ and $n=n_a$ at $z=z_a$ leads to

$$(1/y)-(1/y_a)=\alpha(n-n_a)/pv. \tag{16}$$

This expression gives y, z curves in the region from z_c to z_a which are approximately the same as those of Fig. 2. This means that at each point in this region the ion density y due directly to the ultra-violet light and the density due to the vy diffusion of ions from above are roughly equal, when the two effects are considered separately. When considered together the resulting ion density will be roughly $2^{1/2}y$, since the recombination loss is proportional to y^2. The gravity diffusion term in the region from z_c to z_a is complex (see equation 10) and little more can be said about it beyond the statement that in general it is smaller than the other terms which have been considered.

16. Finally, it is important to point out that although D ions diffuse by gravity across the z_c level into the S region they make only a small contribution to the number of S ions compared to the number produced directly by the sun-light. Their effect is negligible within 3 km below z_c, as calculated from (10) by the approximate method of reference 1, page 1028. There are several other approximations in the foregoing treatment which are, however, hardly worthy of discussion, for they are submerged in the greater approximation involved in the assumption, section 7, that the D region passes at the z_c level abruptly into the S region. On the whole it is concluded that the y,z curves are a fair representation of the hypotheses on which they are based and that the values in Table I are correct within 50%.

17. Calculation from the y,z curves shows that wireless rays of wavelengths, 5000, 1000, 500 and 400 meters are totally reflected (refracted) at heights of 73, 105, 121 and 125 km at latitude 30° and at heights about 12 km greater at 70°. These heights are about 5 and 17 km greater than the respective heights given by the y,z curve for $\theta=0$ (see section 10). At latitude 30° the absorption in the levels from 100 to 125 km is such as to reduce the intensity of 400 meter waves to $1/\epsilon$'th in 26 km. The values may also be taken to refer approximately to equatorial longitudes 30° and 70° measured from equatorial noon, i.e. at 2 P.M. (or 10 A.M.) and 4.6 P.M. (or 7.4 A.M.). Because the high atmosphere is cooler at $\theta=70°$ than at $\theta=0$ the 100 to 150 km levels at $\theta=0°$ correspond to levels at $\theta=70°$ about 20 km lower.

Thus it comes out that the levels where the long wireless waves are turned back to the earth do not undergo wide variations with the latitude and the hour of the day. This is in general accord with the facts for long waves as as far as they are known.

18. To determine the ionization in the night hemisphere we treat the S and D ions separately. In the case of the S ions the rate of decrease of the ion density y at a height z is given by $dy/dt = -\alpha n y^2$, neglecting gravity diffusion; this becomes $(1/y) - (1/y') = \alpha n t$, where y' is the value of y at sun-set. Taking the y, z curve for $\theta = 75°$ to refer approximately to sun-set conditions the equation gives a decrease in y of about an order of magnitude in 9 hours; because of gravity diffusion the decrease will be greater. At higher latitudes the S region is one of greater molecular density and the decrease in y during the night is greater than at the equator. The value of the conductivity σ of the night-time S region was found to be about 1/20 of that of the day S region.

19. The D ions, on the other hand, move upward at night because of the eastward electric field. They pass into regions of low molecular density and their loss from recombination is thereby reduced. Multiplying the values of E of Table I by 0.7 to obtain a rough average over the daylight longitudes gives $E = 81$ and 136 e.m.u. for latitudes 0° and 40°, respectively. Therefore at these latitudes the sun-set meridian is at a potential about 1600 and 2000 volts above that of the sun-rise meridian. The ions rise with a velocity v given approximately by 0.7 times v of Table I. From (5) the molecular density n in an element of ionic density y varies with the time t according to $n = n_0 \epsilon^{-p z + v t}$. Therefore the rate of change of y due to recombination is

$$dy/dt = -\alpha y^2 n_0 \epsilon^{-p(z+vt)}.$$

Integrating,

$$(1/y) - (1/y_2) = \alpha n_2 (1 - \epsilon^{-pvt})/pv, \tag{17}$$

where y_2 and n_2 are the values at sun-set, and the time t is measured from sun-set. We take the y, z curve for $\theta = 75°$ to refer to sun-set conditions; in this curve y has the constant value 1.7×10^7 from 165 to 195 km. Again, as in section 6, we remark that these heights are only parameters, the real heights are probably lower because of the shrinkage of the atmosphere due to cooling. The molecular density n is the important quantity, and in the present calculations whether z represents exactly the distance above the surface of the earth or not is immaterial. In calculations where geometry enters, such as those dealing with the heights reached by wireless waves, the skip distances, etc., the values of z are important.

20. With the equatorial night value $v = 250$ cm sec.$^{-1}$ and with $y_2 = 1.7 \times 10^7$ the y,z curves were determined from (17) for various values of t. The ion bank was found to decrease in density for about 3 hours and then to remain sensibly constant for the rest of the night, the y,z curve being nearly a straight line with $y = 0.54 \times 10^9$ and 1.5×10^9 at the lower and upper boundaries of the bank, respectively. Similar calculations were made for the various latitudes and the result was reached that after about 3 hours the

total number of ions in the D region at night in a north and south section from pole to pole of unit thickness was about 1/5 of the corresponding number averaged over the daylight hemisphere. This means that the night eastward drift current in the D region is about 1/5 the day eastward drift current. The night conduction current in the S region, also east because it is due to E which is eastward at night, is 1/20 the day eastward current, see section 18. Therefore the total eastward current at night is about $1/5 + 1/20 = 1/4$ the day eastward current of the D ions. This makes f of section 13 equal to 3/4.

21. In the calculations[1] of the electrons in the high atmosphere the effect of the earth's magnetic field upon the diffusion of the electrons was recognized (reference 1, page 1023), but the details brought out in the present theory were not known. The downward daytime diffusion due to the electric field E will modify the earlier electron density curves[1] below their maxima. Instead of turning in sharply to the Z-axis within about 5 km below the maximum the curve approaches the Z-axis at a point about 20 km below the maximum. This result was calculated from the equation for the case of electrons corresponding to (16). There is no need to give the details of the calculation for even when modified in this way the curves do not represent completely the electrons below their maxima; they only include those electrons which diffuse down from over-lying levels and neglect the electrons produced directly by the ultra-violet light in the levels below the maxima. In the electron density equation at night, however, the electrical diffusion term makes a needed modification, without it the equation gave too rapid a decrease in the electrons at night. Neglecting gravity diffusion the equation becomes

$$\log_\epsilon y/y_2 = bn_2'(\epsilon^{-p'vt} - 1)/p'v. \tag{18}$$

y is the density of the electrons at time t, y_2 their density at sun-set at a height where the density of oxygen molecules is n_2', b is the oxygen electron attachment coefficient,[1] and p' is connected with n' just as p is with n through (5). (18) was derived in the same manner as the ion equation (17). From (18) with equatorial values $y_2 = 1.5 \times 10^5$ and $v = 250$ cm sec.$^{-1}$ y decreases to a constant value 1.1×10^4 in about 3 hours. This is regarded as agreeing well enough with the value 5×10^4 inferred from the skip distances of wireless waves at night.[1] A more exact agreement is hardly to be expected in view of the approximate nature of the calculations. With a velocity $v = 200$ cm sec.$^{-1}$ the upward drift of the electrons and D ions at night is about 60 km in 8 hours. At the same time the ion bank spreads out in a vertical direction because of gravity diffusion, which becomes important at latitudes above 30° where the magnetic field makes an angle less than 45° with the vertical. It is difficult to say how much of the increase during the night of the apparent height of the ionization observed in certain wireless experiments[8] may be a genuine rise and how much may be an apparent rise due to delayed group velocities, or to other causes.

[8] Appleton, Nature **120**, 330 (1927); Hafstad and Tuve, Terr. Mag. and Atmos. Elec. **34**, 39 (1929).

22. The diamagnetism of the ions is proportional to TD. The values of TD along a noon meridian of longitude, taken from columns 2 and 7, Table I, and plotted as abscissas against the latitude θ as ordinates, are shown by the dots of Fig. 3; the smooth curve 1, Fig. 3, gives $\cos\theta$. The values of TD along the equator are a little less than the values of the dots for θ greater than 40°. The temperature of the high atmosphere on the night hemisphere of the earth is about 1/2 the noon day temperatures and, as shown in section 20, the average value of D at night is about 1/5 of the average value of D in the daytime. Therefore the diamagnetism of the atmosphere at night is about 1/10 of the average diamagnetism during the day and 1/15 of the noon maximum value. Thus the ionization of the atmosphere derived on the hypothesis that the ultra-violet light of the sun is the ionizing agency is found to possess the diamagnetism required by Gunn's diamagnetic theory of the solar diurnal variation of the earth's magnetic field.

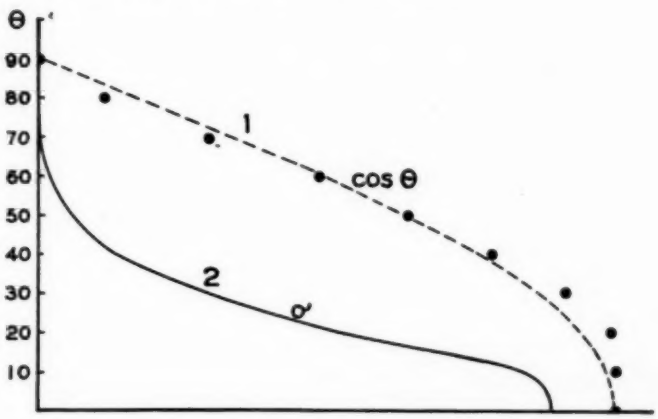

Fig. 3. Curve 1, dots and curve 2 are the values of $\cos\theta$, TD and σ, respectively.

23. The diamagnetic theory requires a maximum ionization $D=1.5\times10^{16}$ at the equator at noon. It is of interest to see what assumptions this involves as to the rate of production of the ions. As a rough beginning we will assume the mechanism of the earlier paper,[1] namely, that the solar ultra-violet radiations cause directly equal numbers of positive ions and electrons and that the electrons become attached to neutral oxygen molecules to form negative oxygen molecular ions. The theory of the skip distances of wireless waves[1] required an electron layer of maximum density 3×10^5 at 190 km. Accordingly we may assume that the electron density y_e is a constant value 2×10^5 in the region from 150 to 180 km; if it exceeded this value the calculated skip distances would be shorter than those observed. The number of oxygen molecular ions which are formed per sec. in the 150 to 180 km region is $\int_{150}^{180} bn'y_e dz=7.8\times10^9$; n' is the density of oxygen molecules, b is the attachment coefficient for a temperature of 500°K, $b=1.1\times10^{-13}$, see equation 11, reference 1. This is the rate of supply of negative ions, and since there is an equal number of positive ions, this is the rate of supply of ion

pairs. Assuming roughly that the density y of the ion pairs in the 150 to 180 km region is a constant and putting the rate of supply equal to the rate of recombination, we have $7.8\times10^9=\int_{150}^{180}\alpha n y^2 dz$. This gives $y=2.5\times10^8$ and $D=7.5\times10^{14}$, which is 20 times less than 1.5×10^{16} ion pairs. The conclusion is that the very primitive photochemical reaction which has been assumed is not entirely adequate to account for the 1.5×10^{16} ion pairs. In the reaction negative ions were regarded as being the end product of two processes, first, a splitting up of a neutral particle by light into a positive ion and an electron and, second, the attachment of the electron to an oxygen molecule. It is possible that the light may produce a positive and negative ion directly, for example, by breaking a nitrogen molecule into a positive and a negative nitrogen atom. Further, many photo-chemical effects occur in the atmosphere, such as the formation of ozone, the oxides of nitrogen, etc., which were not taken into account in the foregoing calculation. It is thought that the photo-chemical branch of atomic physics has been developed to a point where it may be used in examining the problem.

24. The eastward drift current sheet in the daylight D region flows along the parallels of latitude and divides into two sheets at roughly the sunrise and sunset longitudes, one sheet flowing westward in the underlying S region and one sheet continuing eastward on around the night side of the earth in the S and D regions. From the values of i in column 8, Table I, the total current in the daylight region from latitude 0° to 40° is 6.8×10^6 amperes. The values of i were, however, for a noon meridian, and to get a rough average over the daylight longitudes 6.8×10^6 is multiplied by 0.7 giving 4.8×10^6 amperes. Similarly the total average daylight current in the D region from latitude 40° to 90° is 1.0×10^6 amperes and from pole to pole is 11.6×10^6 amperes. Since about 1/4 of the current flows around the night hemisphere the values of the westward currents in the daylight S region are 3.6×10^6, 0.75×10^6 and 8.7×10^6 amperes, from latitudes 0° to 40°, 40° to 90° and from pole to pole, respectively. The night current from pole to pole is 2.9×10^6 amperes, of which 2.3×10^6 and 0.6×10^6 amperes are in the D and S regions, respectively. Altogether the drift currents amount to a steady eastward current of 2.9×10^6 amperes flowing along the parallels of latitude around the earth all the time. About 4/5 of this current is between the 40th parallels of latitude north and south, and the distribution of the current density with latitude is given approximately by the values of i in Table I. The value of the magnetic field at the equator due to this current is about 400γ (γ is 10^{-5} gauss). This agrees very closely with the analysis of the permanent field of the earth by Bauer.[9] He showed that a portion of the magnetic field of the earth is of external origin and is northward and upward in the northern hemisphere, nearly horizontal at the equator and northward and downward in the southern hemisphere, the value of the horizontal component at the equator being about 430γ.

[9] Bauer, Terr. Mag. and Atmos. Elec. **28**, 1 (1923).

25. The foregoing values furnish a quantitative basis for the suggestion in the ultra-violet light theory[4] of magnetic storms that the first phase of the world-wide storm was due to a pulse of current in an equatorial belt around the earth and that the current pulse in the night hemisphere flowed in the S region. According to the theory a flare of solar ultra-violet light created rather suddenly an additional 10^{16} ion pairs in a vertical column of the D region in the case of an average magnetic storm. This is about the same as the number of D ions which were used in the present paper for an average quiet day. Therefore the first effect of the storm is to double the daylight ionization and hence E, which doubles the current in the night S region making it $2\times0.6\times10^6$ amperes. No immediate change in the night D current occurs. The value of the current which girdles the earth is increased from 2.9×10^6 to $(2.9+0.6)\times10^6$ amperes. This produces a storm magnetic field of the observed order of magnitude $10^2\gamma$.

26. The drift current theory[5] of the solar diurnal magnetic variation made no quantitative suggestion as to the manner in which the gravitational drift currents would give rise to the current system of Fig. 1. According to the present calculations such a system might be produced if the westward current in the daylight S region which arises from the eastward current in the daylight D region between latitudes 0° to 40° should not flow entirely in the S region between these parallels but should spread into higher latitudes. To estimate the spreading of the S current the conductivity σ of the S region, given in column 6, Table I, is plotted in curve 2, Fig. 3. The curve shows that σ becomes small at high latitudes, the total conductivity from 60° to 90° being 0.47%, and from 70° to 90° 0.03%, of the total conductivity from 0° to 90°. The S current from $\theta=0°$ to 40° is 3.6×10^6 amperes and the spread of this current into the latitudes from 60° to 90° is $0.47\%\times3.6\times10^6=17{,}000$ amperes, whereas the chart of Fig. 1 calls for 45,000 amperes by day and $-22{,}000$ amperes by night or an excess of day over night of 67,000 amperes. Similarly from $\theta=70°$ to 90° the current spread is $0.03\%\times3.6\times10^6=1000$ amperes and the chart requires 45,000 amperes. The current sheet is therefore quite different from that required by the drift current theory of the diurnal magnetic variation.

27. The values of Table I were obtained by calculating the equilibrium conditions for each slice of the atmosphere along parallels of latitude independently of the influence of adjacent slices. Such a procedure is not entirely correct, for the separate slices influence each other because the S current of one slice spreads into the S regions of the other slices. For example, a greater E at, say 60° than at the equator will cause a current system opposite to that of Fig. 1 which will reduce the spreading of the S current into high latitudes below that which was estimated in section 26 from the σ,θ curve of Fig. 3. We may conclude that a calculation taking into account this effect would give less spreading than was found and would result in lower values of E at the higher latitudes than those of Table I.

28. The conclusion that the electric currents due to the ions in the atmosphere produced by solar ultra-violet radiations do not cause the solar

diurnal variation in the earth's magnetism remains true if the ions, instead of being nitrogen atomic ions, were ions of other types, as helium ions, molecular ions, electrons, etc. The conclusion does not depend upon the exact form of the y,z curve assumed at $\theta=0°$. For the conclusion depends essentially on the form of the σ,θ curve of Fig. 3 and in all these cases the curve would remain practically unchanged. In order for a current system similar to that of Fig. 1 to exist the conductivity of the S regions at high latitudes relative to that at low latitudes must be greater than the values of σ in Table I. To have this would conceivably require the hypothesis of another type of ionizing agency than ultra-violet light, or some other hypothesis. It does not seem probable that a rearrangement of the S ions would be brought about under normal conditions by winds blowing in the high atmosphere from warmer to colder latitudes. Winds of this kind in all probability exist, but the recombination of the ions is so rapid that no appreciable transport of the ions over distances of a thousand kilometers or more seems likely. One can not say with certainty whether high flying ions[4] have any effect or not during quiet conditions. Under unusual circumstances, during a magnetic or an ordinary storm, the ions might be blown about and give rise to electric currents and magnetic disturbances.

29. The drift current theory of the diurnal magnetic variation encounters a difficulty due to dynamo action. Maris' calculations[3] of the heating of the upper atmosphere show that a daytime expansion takes place, the atmosphere rising in the morning and descending in the afternoon. His tables show that the atmosphere at 150 km at summer noon descends to 120 km at summer midnight, a vertical movement of 30 km in 12 hours. This amounts to a rough average velocity $v'=70$ cm sec^{-1} of the S conduction region in tropical latitudes vertically upward during the morning and downward during the afternoon. The motion is a real one and not a fictitious one as would occur if the upward, or downward, displacement of the S region came about by removal of the underneath ions by recombination and a production of ions on the upper side. For at 150 km at the equator the number of recombinations cm^{-3} sec.$^{-1}$ is 3.2×10^{6} whereas the number of collisions cm^{-3} sec^{-1} is 7.3×10^{12}. There are thus many collisions which do not result in recombination and therefore the ions are forced by molecular impacts to move up or down with the atmosphere of which they form a part. On the other hand the motion of the daytime ionization around the earth with the sun is a fictitious one, the ions being formed at dawn and blotted out at evening by recombination.

30. The movement of the S region across the magnetic field $H=0.32$ gauss gives rise to an e.m.f. cm^{-1} E' which at the equator is westward in the morning and eastward in the afternoon. $E'=v'H=22$ e.m.u. cm^{-1}, a value about 1/6 of the temperate and equatorial values of E of Table I. The e.m.f. E' gives rise to a current system roughly opposite to that of Fig. 1 in the morning and in the same direction in the afternoon. Thus if the high latitude values of σ are such that E causes the current system of Fig. 1 the resultant current system will be that obtained by the superposition of

the systems due to E and E', i.e. $E-E'$ in the morning and $E+E'$ in the afternoon. This would displace the maximum of the diurnal magnetic variation an hour or two later than noon, which is contrary to the fact that the maximum occurs at 11 A.M.

31. Several small magnetic effects of the drift currents remain to be discussed. The equivalent vertical distance between the S and D current sheets in the day hemisphere is not greater than 30 km. These current sheets will cause a magnetic variation apart from, and opposed to, that due to the diamagnetism of the D ions, which, however, is found by calculation to be less than 5% of the diamagnetic effect at the equator, and of a less amount at the higher latitudes. The dynamo effect causes a 50% variation in this small magnetic effect due to the current sheets. Certain other currents not mentioned here-to-fore, such as the westward gravitational drift current in the S region, the drift currents due to temperature gradients and to magnetic gradients[10] were found to give magnetic effects negligibly small compared to those of diamagnetism. The general conclusion is that the main features of the diamagnetic theory are undisturbed by drift currents.

32. For the purposes of this paper tables of the ion distribution, i.e. the y,z curves, at all points on the earth were worked out as described in sections 10 to 16. Glimpses of the tables are given in the curves of Fig. 2 and in Table I, but the tables themselves are not printed. I think that the explicit publication of such tables would be premature. The physics of the upper atmosphere has developed so rapidly during recent years that the tables can at best be regarded as an early attempt, to be modified rather than to be used by future writers. Additional electromagnetic effects, old in the literature of physics but novel in their application to the atmosphere, continue to be recognized and new experimental discoveries, such as those dealing with wireless waves, with ozone, etc., continue to be made. One can not be sure at the present time that all the important facts have been brought to light, nor is it at all certain that the various facts have been given their proper emphasis in the theory.

[10] Gunn, Phys. Rev. **34**, 335 (1929).

THE PIERCE ACOUSTIC INTERFEROMETER AS AN INSTRUMENT FOR THE DETERMINATION OF VELOCITY AND ABSORPTION

By W. H. Pielemeier
University of Michigan, Ann Arbor

(Received May 27, 1929)

Abstract

Sputtered quartz crystals of known natural frequency were used as sources of high frequency sound in a Pierce acoustic interferometer. The interfering sound waves react on the crystal driver in such a way as to change periodically the plate current, I_p, when the mirror is displaced a half wave-length or more. The galvanometer-deflection, mirror-displacement curves show that multiple reflections take place at the movable mirror and at the crystal surface. The general agreement of these curves and those which represent the resultant pressure amplitude in the gas at the crystal surface as ordinates and the mirror displacement as abscissa shows that the changes in galvanometer deflection are a direct function of the changes in pressure amplitude. Check runs made with a torsion vane detector indicate that this function expresses a proportionality between the deflection change and the square of the change in the pressure amplitude, provided the latter change remains small.

Observed facts indicating a variation of wave velocity with intensity are: *1st*, the asymmetry of the deflection peaks; *2nd*, the change in the type of this asymmetry with increasing mirror displacement; *3rd*, non uniform spacing of deflection maxima; *4th*, sudden changes in the logarithmic decrement of the I_p-maxima. The precision in the value of the wave velocity is diminished considerably by this velocity variation.

Measurements are made on air and CO_2 at frequencies ranging from $3(10)^5$ to $14(10)^5$ cycles per sec. The apparent velocity obtained from the average spacing of I_p-maxima is slightly higher than the commonly accepted value for audible frequencies.

The absorption by air and by CO_2 increases with frequency through this range, CO_2 being nearly opaque at $14(10)^5$ vps. Lebedew's constant, A, has a value of 0.00037 for air at 20°C. The observed value obtained with the interferometer at $12(10)^5$ vps. was 0.00039 which agrees well with a torsion vane determination. At the lower frequencies the observed value is higher, partly because of the multiple reflections. The torsion vane arrangement used with CO_2 and with the highest frequency in air was not suitable for the lower frequencies in air. The observed value of A for CO_2 was 0.0073 at $12(10)^5$ and 0.012 at $3(10)^5$ vps. A careful torsion vane determination at $6.555(10)^5$ gave 0.0096. Abello's data at $6.12(10)^5$ extrapolated to 100 percent CO_2 give 0.0063. The humidity has a marked effect on the absorption in CO_2.

I. Introduction

THE absorption of audible sound in a gas medium is very small. However it has long been known that the absorption increases with increasing frequency of the sound. In 1911 Lebedew[1] published a paper in which the absorption of high frequency sound in air was treated from a theoretical point of view. This article and one by Neklapajeff[2] on an experimental de-

[1] Peter Lebedew, Ann. d. Physik **35**, 71 (1911).
[2] Neklapajeff, Ann. d. Physik **35**, 175 (1911).

termination of the absorption helped suggest that more accurate data on absorption might throw some light on molecular structure. In an unpublished investigation by G. E. Raburn it was discovered that CO_2 absorbs sound of frequency 100,000 to 300,000 per sec. to such an extent that it is almost opaque to it. This excessive absorption has since been verified by the author by two independent methods. G. W. Pierce[3] and T. P. Abello[4] refer to it also.

It is a familiar fact that the *velocity* of sound varies with the intensity. Such a change in velocity was observed and recorded by Regnault in connection with his experiments in 1863 on the velocity of sound in the newly laid Paris water pipes. Regnault states that the velocity decreases as the intensity diminishes but that a limiting velocity of 330.6 m per sec. for feeble sounds is soon reached. A. L. Foley[5] observed a similar decrease in velocity in 1920. H. O. Taylor[6] records a diminished wave-length in a highly absorbing tube. Hitchcock[7] reported that the velocity of the waves from a vibrating crystal is a function of the energy which the crystal radiates and he obtained a value in air nearly twice the velocity of ordinary sound waves. No other record of a variation in the velocity with intensity for a continuous low or high frequency sound has been found by the author. Both Regnault's and Foley's observations were on sound *pulses*.

Briefly stated, the problem is (a) that of testing the possibilities of the Pierce interferometer as an instrument for the determination of the absorption of high frequency sound in air and in CO_2 and (b) investigating the relations which the observations have to the velocity of sound at the frequencies used.

II. History of the Work on Absorption

Although considerable theoretical work had been done on the absorption of sound previous to 1911, that date may be considered as the beginning of the experimental work on the problem. In a preliminary report in 1924 on the author's[8] work, reference was made to Lebedew's theoretical value of A, the so-called absorption constant, which is defined by the equation

$$I = I_0 e^{-(A/\lambda^3)x} \tag{1}$$

where I is the sound intensity at the position x, measured from the source, I_0 is the intensity at the source and λ is the wave-length. The equation is written for plane waves. The theoretical value of A, given by

$$A = \frac{4\pi^2}{a\rho}\left[\frac{4}{3}\mu' + \left(\frac{C_p}{C_v} - 1\right)\frac{K}{C_p}\right] \tag{2}$$

[3] G. W. Pierce, Proc. Amer. Acad. Arts and Sciences **60**, 271 (1925).

[4] T. P. Abello, Proc. Nat. Acad. Sci. **13**, 699 (1927); also Phys. Rev. **31**, 1083 (1928).

[5] A. L. Foley, Phys. Rev. **16**, 449 (1920).

[6] H. O. Taylor, Phys. Rev., Vol. 2, p. 270 (1913).

[7] R. C. Hitchcock, Proc. Inst. R.E. **15**, 907 (1927).

[8] D. L. Rich, University of Michigan and W. H. Pielemeier, Pennsylvania State College, "Absorption of High Frequency Sound," Phys. Rev. **25**, 117 (1925).

is approximately 0.00037 for air at ordinary room temperature. In this equation, a is the velocity of sound, ρ, is the density of the medium, $\mu' = \mu(1+0.146)$, where μ is the coefficient viscosity of the medium, C_p and C_v are the two specific heats and K is the coefficient of thermal conductivity. The value of A should increase about 1 percent for each 5°C rise in temperature.

From Equation (1)

$$A = \left(\log \frac{I_1}{I_2}\right) \lambda^2 \Big/ (x_2 - x_1). \tag{3}$$

Neklapajeff,[2] under Lebedew's direction, attempted to check the value of A, experimentally. The mean of all his values was approximately twice the theoretical (0.00073 as against 0.00037). Considering, however, the crude apparatus used, the work was remarkably good.

Work on the problem was first taken up at the University of Michigan Physical Laboratory in 1917 by D. L. Rich and G. E. Raburn. Echelette gratings were used. The excessive absorption of CO_2 to which reference has already been made was observed with this form of apparatus. Pressure vanes were used as detectors and the source was an electric spark which was placed at the principal focus of a movable mirror. The source spark was in series with a rotary gap. The set differed from that of Neklapajeff chiefly in the type of grating and the electrical circuit containing the source spark gap. When the author began work on the problem the difficulty was that of finding a suitable source. Several types of electric spark, a Poulson arc, a direct current with superimposed a.c. of proper frequency, a Hewlett tone generator, and a glow microphone were tried and discarded. The glow microphone which was kindly loaned by the Westinghouse Electric and Manufacturing Company, had some excellent features, such as maximum frequency possibilities and convenience of adjustment in the collimating system but the intensity was too small and unsteady for absorption measurements.

The best source used previous to the present one was a piezo-electric tone generator constructed of two 6×6 inch aluminum plates which were driven by small squares of quartz cemented between the aluminum plates with molten shellac. Langevin[9] and others used similar oscillators under water for submarine detection, etc., during the recent war. The results obtained with this source were presented in a report[8] at the November meeting of the American Physical Society. This source was very limited as to the frequencies which could be obtained with it. Moreover it behaved as if certain portions of the oscillator had a slightly different resonance frequency than others. This might have been expected because each quartz square would differ

[9] The experiments along this line made by the Columbia University Group (Professors M. I. Pupin, A. P. Wills and J. H. Morecroft) in 1918, have never been published. The experiments of Langevin and Chilowsky are given in *Nature* May 9, 1925, pp. 698–90, in an article on "Echo Sounding." A more complete description of Langevin's apparatus is given in "Ultra Sonic Waves for Echo Sounding," Hydrographic Review, (Monaco) II, No. I, 1924, p. 57. A brief account of such apparatus is given by Crandall, p. 142 (See reference 11).

slightly in natural frequency from all the rest. Those portions of the entire oscillator for which the natural frequency was below that of the driver would be exactly out of phase with the parts for which the natural frequency was above that of the driver. This would result in unequal distribution of sound energy in the beam.

The determinations of A with this source lay between Lebedew's theoretical value and Neklapajeff's experimental value.

III. Experimental Arrangement

The apparatus used in obtaining the data presented in this paper is a modification of that used by Pierce.[3] It consists of a piezo-electric oscillator connected into a thermionic vacuum tube circuit. The oscillator is a quartz plate sputtered on both faces with platinum. The orientation of the axes in natural quartz crystal and the method of sectioning for an oscillator is shown by Pierce[3] and also by Cady.[10]

Most of the crystals were cut by A. Espositor, 64 W. 48th Street, New York. One was loaned by the Alfred Loomis Laboratory. They were sputtered by Dr. Shohat, Department of Physics, University of Michigan. In operation one of the prepared crystals is placed on a horizontal brass base so that it radiates a parallel beam of sound vertically upward. The brass base is attached to the lower end of the ways of a micrometer screw. It is fitted with leveling screws. A reflecting mirror is operated by the screw. The mirror can be displaced upward or downward in the direction of the sound beam. It is a piece of plate glass a trifle larger than the largest crystal used. It is fitted with three leveling screws. It is always oriented with its face parallel to that of the crystal. Its position can be read on the screw scales. The whole assembly, which Crandall[11] calls an acoustic interferometer, is mounted against the back wall of a cast iron box fitted with leveling screws and two glass windows.

The electric circuit for producing vibrations. This circuit is approximately the same as that used by Pierce.[3] It is one for which the frequency of oscillation is determined by the crystal and not by the electrical constants of the circuit. It consists of a 135-volt B-Battery (see Fig. 2) in series with a load coil of large inductance, a UX-201-A thermionic tube, a lamp and scale type galvanometer with adjustable shunts, and a group consisting of a telephone and a small fixed condenser in parallel. In most cases the crystal is connected between the plate and the grid of the tube. Usually no grid leak was used. Connected to the galvanometer and its shunts is a bias battery and a high variable resistance. This makes it possible to reduce the current through the galvanometer to approximately zero. Then the sensitivity of the galvanometer is increased to the desired value by selecting the proper shunt. By merely operating the rotating shunt switch the sensitivity can be changed by factors of ten from approximately 10^{-7} to 10^{-4} amperes per mm deflection.

[10] G. W. Cady, Proc. Inst. Radio Eng. **10**, 83 (1922).

[11] Irving B. Crandall, Theory of Vibrating Systems and Sound, p. 244.

The load coil is mounted so that it can be coupled with a wave meter. The frequency of each crystal was also accurately determined by Dr. N. H. Williams.

A final check was made on some of the absorption measurements with a very sensitive torsion vane, which was substituted for the mirror, no other change in the apparatus being involved.

Procedure. The position, x_0, of the mirror is read when in contact with a crystal. Then the mirror is raised and the contact wire is placed on the sputtered surface of the crystal. With most of the crystals I_p falls from 5 or 6 ma. to 1 or 2 ma. when the oscillations begin. The bias circuit is then closed and the galvanometer deflection is brought to nearly zero. Then the sensitivity of the galvanometer is increased and the two currents are again adjusted for

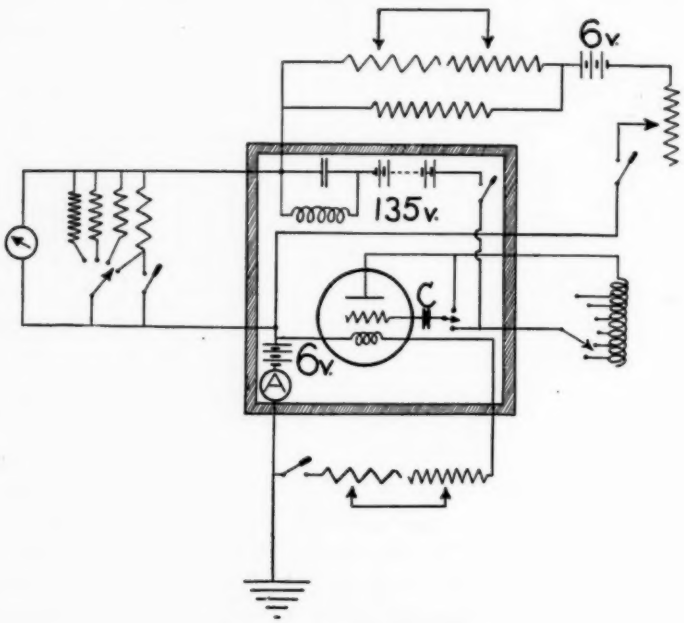

Fig. 1. Circuit diagram.

nearly zero deflection. This is repeated until the desired sensitivity is obtained. Now the mirror is displaced slowly and the deflection changes periodically. (See Figs. 2–5). At a sharp maximum the system is quite sensitive to about 1/5 of a least division on the screw head (1/200 mm). The temperature is recorded every 5 or 10 minutes. Usually the wave meter is loosely coupled to the load coil and the reading is taken so that the frequency can be computed. This reading is indispensible for those crystals which have two neighboring natural frequencies. With one of the crystals a tuned circuit had to be used in order to suppress the undesired frequency. If the galvanometer current is steady the peak and trough deflections are plotted against the number of half wave-lengths between the crystal and the mirror. A smooth curve is drawn through the peak values and another through the

trough values. A third curve is drawn of which the ordinates are the logarithms of the vertical separation of the first two curves. This separation, α, is called the I_p amplitude. If the set is not running steadily enough for this method conditions are sometimes good enough to obtain reliable I_p amplitudes in spite of an occasional shift. In such a case the I_p amplitudes are plotted as ordinates directly and the logarithms of these ordinates are plotted for a second curve. In either case the change in logarithm per half cm of mirror displacement is computed from the curve. Assuming a single round trip is made by the sound waves from crystal to mirror and back again this would be equivalent to the decrease in logarithm per centimeter of sound path, which would be equal to the factor A/λ^2 in the exponent of e in Eq.

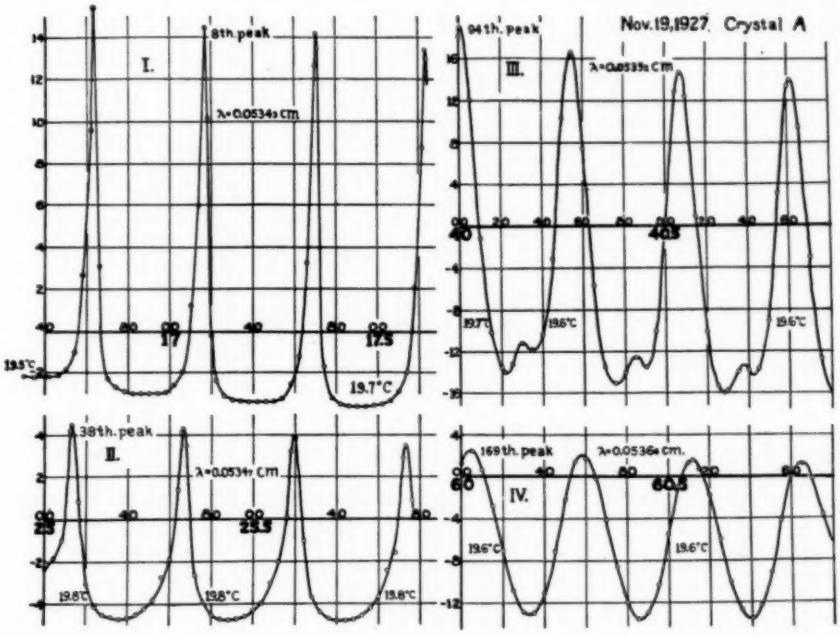

Fig. 2. Wave-form curves for crystal A in air. Galvanometer deflections in cm are plotted as a function of mirror position in mm and 200ths mm.

(1), provided the decrease in α is proportional to the absorbed sound. This method of calculating the value of A is similar to that used by Neklapajeff[2] (see Eq. 3). The value of A, found in this manner, is much larger for small mirror displacements or for the lower frequencies than the value of A found by Neklapajeff.[2] The reason for this will be discussed in Part V. However, the higher frequency crystals give approximately the theoretical value (0.00037) for all except the smaller mirror displacements.

Both with air and with CO_2 some runs were made with the gas having been dried either by P_2O_5 or by passing it through H_2SO_4. The cast iron box which had a coat of shellac on the inside was washed with commercial CO_2 for about 10 or 15 minutes before the stop-cocks were closed. Then the set was allowed to run for some time before readings were taken so that it

might become steady. A few runs were made with air which had the CO_2 removed from it. The wave-form runs were obtained in the same general manner as the absorption runs except that the deflection was read for many points in a single cycle, $(\lambda/2)$, and only a few wave-lengths were covered in this way.

IV. Data and Curves

The data herein presented consist chiefly of two general types. One type, which will be referred to as *stationary wave-form data* or merely as *wave-form data*, gives the galvanometer deflection for each setting of the reflecting mirror, the distance between settings being small fractions of a half wave-length of the reflected sound. The chief value of this type is that it throws light on the kind of vibrations which the crystal is executing and the

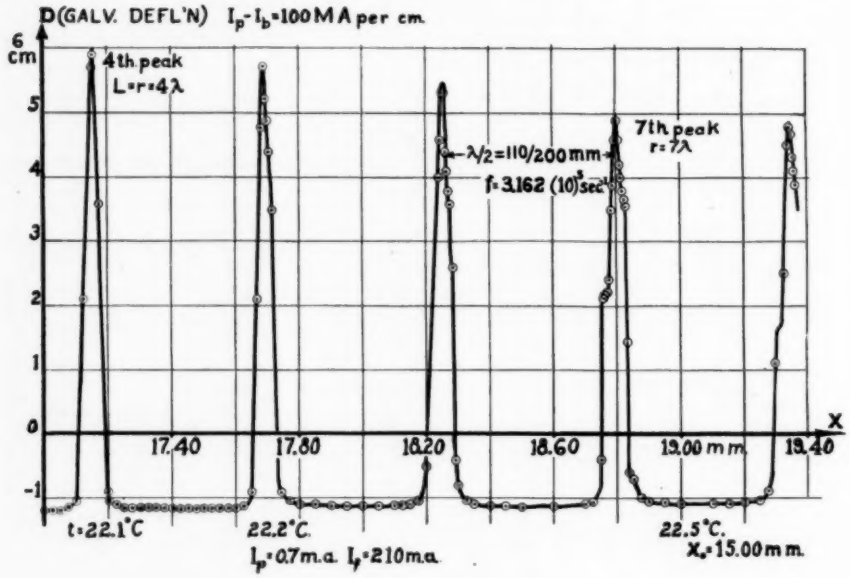

Fig. 3. Wave-form curve for crystal *D* in air.

manner in which the components of the stationary waves produce their resultant at the face of the crystal.

The other type of data which will be termed *velocity and absorption data*, or sometimes merely absorption data, gives merely the maximum and minimum galvanometer deflections and the corresponding mirror positions. This type is used in calculating the approximate velocity and absorption of the sound in the space between the crystal and the mirror. With each crystal the position of the mirror was observed when in contact with the crystal survace. Henceforth, x_0 will be used to designate this position. Great care was exercised in orienting the two so they were normal to the *path* of the mirror (or screw axis) and also parallel to each other. With every crystal it was found that a maximum galvanometer deflection fell at x_0 if the curve was extrapolated back to this point.

The torsion vane data are presented in the form of a curve. (See Fig. 9).

With the frequencies used and with the short sound paths for which observations were taken, diffraction effects[12] were negligible for one return trip from source to mirror and back. (The length of this return trip will be designated by L.) For the shorter paths the same is true for *several* return trips. In other words, the wave fronts for these cases remain confined approximately to the geometrical beam. It is evident that stationary sound waves will exist between the source and the mirror for certain mirror positions one half wave-length apart. For these positions the intervening gas acts as a resonator. Since the mirror positions corresponding to the observed galvanom-

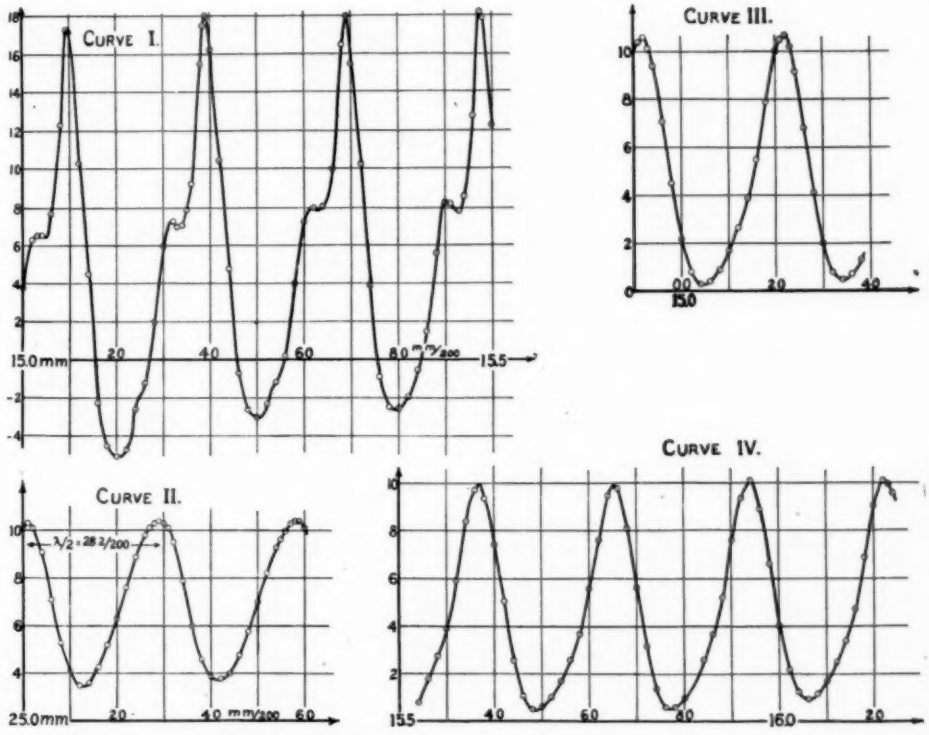

Fig. 4. Wave-form curve for crystal E in air.

eter deflection *maxima* and the mirror positions for which one would expect stationary waves are identical it is also evident that a deflection maximum occurs when a minimum displacement amplitude (a node in the stationary wave pattern) falls at the crystal surface, that is, when the gas column resonates. A maximum *pressure* amplitude corresponds to a displacement node in a stationary longitudinal wave system. Then the d.c. component of the plate current, I_p, is a maximum when a maximum pressure amplitude exists at the crystal surface. This and other considerations brought out in Part V imply that the changes in I_p are a simple direct function of the changes

[12] See p. 138 of Reference 11.

in pressure amplitude in the resultant wave at the crystal surface as the mirror takes different positions.

Observations show that the wave-meter current fluctuates also when the mirror is moved. The maxima correspond to the minima of I_p.

Table I summarizes the results from the given data and also from data not included in this article in any other form.

In Figures 2–5 galvanometer deflections are shown as functions of mirror position for the conditions indicated in the figure captions. The galvanometer deflections in Figs. 2–8 give the excess of the d.c. component of the plate current, I_p, over the bias current, I_b, namely $(I_p - I_b)$.

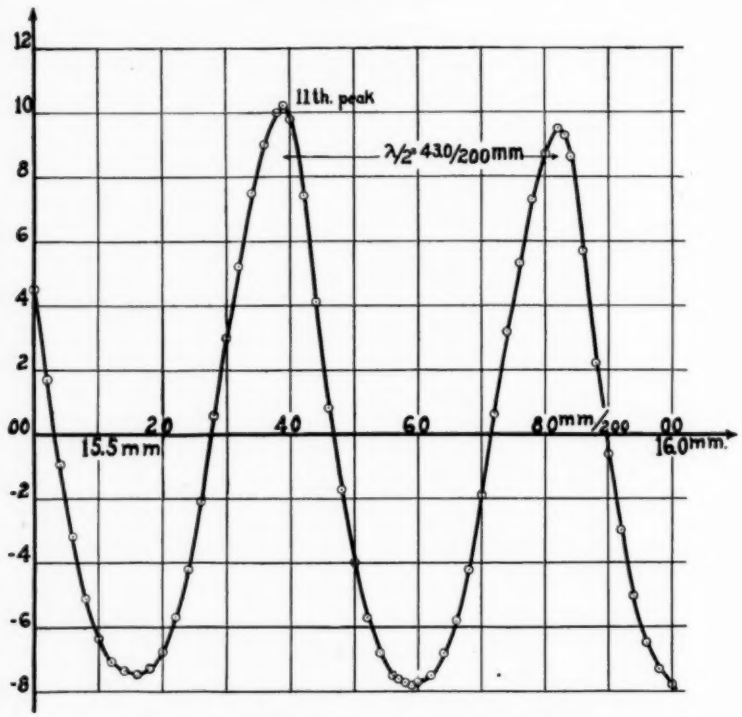

Fig. 5. Wave-form curve for crystal A in CO_2.

For Fig. 2 the crystal frequency, f, is 6.555 $(10)^5$ cycles per sec, $x_0 =$ 14.95 mm, $I_p = 2.2$ ma., $I_f = 220$ ma., $E_p = 135$V. The ordinates are in cm; the unit for the heavy numbers along the x-axis is the mm; the light numbers (screw head readings) give the number of 200th mm. $(I_p - I_b)/D = 10$ micro-amperes per cm (μA/cm) for Curves III and IV. There is a close similarity between Figs. 2–5 and Fig. 10. However the effect of the decreasing velocity is noticeable in the former. In Curve I the rise to a maximum is more gentle than the drop to a minimum. This asymmetry is much greater in the peaks of Curve II. Along the left slopes of the 2nd and 4th peaks of this curve there appears to be a slight tendency toward a hump. On account of the diminished velocity this hump lags more and more behind until it

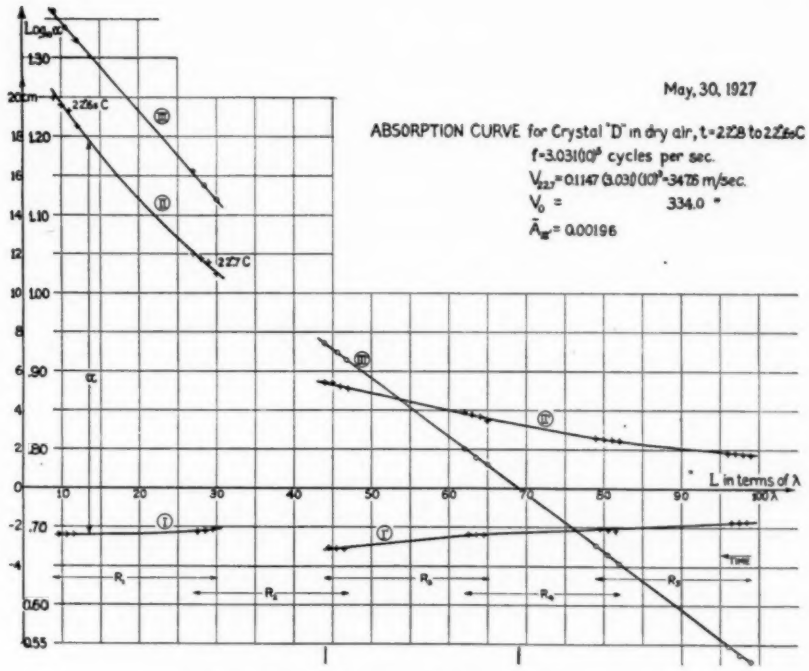
May, 30, 1927
ABSORPTION CURVE for Crystal "D" in dry air, t=22.8 to 22.6°C
f=3.031(10)⁵ cycles per sec.
V22.7=0.1147 (3.031)(10)⁵=3476 m/sec.
V0 = 334.0 "
Ā = 0.00196
L in terms of λ

Fig. 6. Absorption curve for crystal *D* in air.

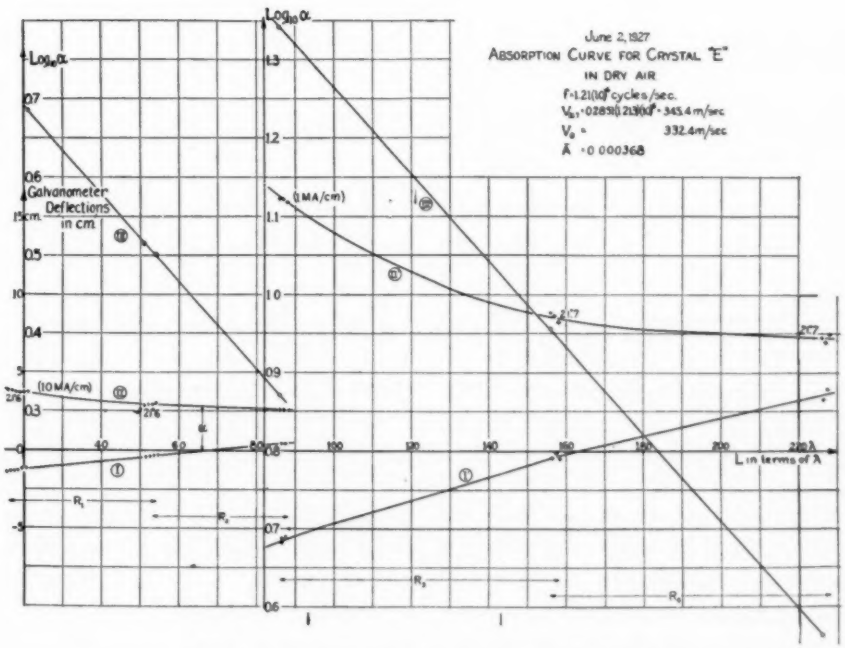

Fig. 7. Absorption curve for crystal *E* in air.

falls near the trough as shown in Curve III. In Curve IV this hump has apparently fallen behind by nearly a cycle. The data for these curves were taken as rapidly as possible and without any interruption of the oscillations. The average plate current slowly diminished during the run.

Fig. 3 resembles curve I of Fig. 10 even more than Fig. 2 does. This is due to the smaller absorption in connection with the longer waves emitted by crystal D.

For Fig. 4, $f=1.125(10)^6$; for Curves I and II $x_0=11.85$ mm and $t=21.7°C$. Approximately the same values of x_0 and t hold for Curves III and IV. In each $(I_p-I_b)/D=1\mu A/cm$. The ordinates of Curves III and IV vary approximately as the pressure amplitude varies when merely *one* reflection at the crystal takes place. With more intense oscillations, as for

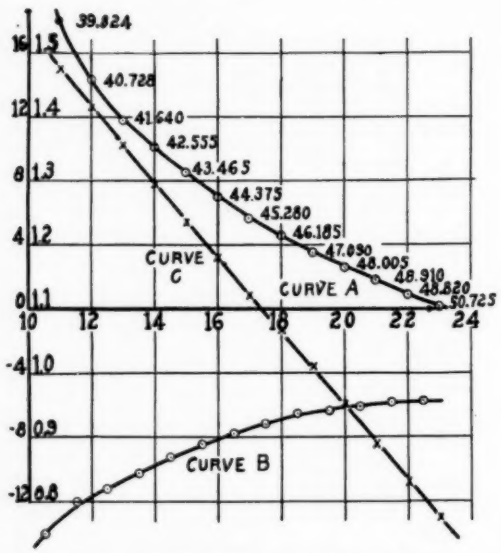

Fig. 8. Absorption curve for crystal D in CO_2 (Mirror positions are recorded along curve A).

Curves I and II, the mirror must be farther removed to obtain such results. See Part V for a discussion of the secondary peaks such as those in Curve I.

For Fig. 5, $x_0=13.34$ mm, $t=21.1°C$, $I_p-I_b/D=1\mu A/cm$. This approximates a simple harmonic curve although the mirror is less than 2.5 mm from the crystal. CO_2 absorbs the sound at $6(10)^5$ more than air does at $12(10)^5$ cps. This curve indicates that the higher order reflections are nearly negligible.

Peak and trough values of D, the galvanometer deflection, are plotted as functions of L in Figs. 6–8, where L is the path-length for the sound waves which have made one return trip, i.e. $L=2(x-x_0)$. In these figures L is given in terms of λ. The curve for $\log \alpha$ is included also. The latter is of constant slope for the entire range in Figs. 7 and 8. This indicates that the sound intensity is very much reduced in the first return trip.

In Fig. 6 the troughs are on Curves I and I′, the peaks are on II and II′ and log α points are on III and III′ where α is the vertical separation of I and II or of I′ and II′. $(I_p - I_b)/D = 10\mu A/cm$. The break between the two sets of curves is probably due to the smaller wave velocity for the higher order return trips. (See Part V) The mirror was moved toward the crystal for these data. A check run was made before the set was stopped. In this the mirror was displaced in the opposite direction. The break came at the same place in both runs. There was also a change in the *spacing* of the maxima near $L = 30\lambda$ for both runs. Since this change is small it was determined by taking averages. The ranges R_1, R_2, etc., in the figure each furnish

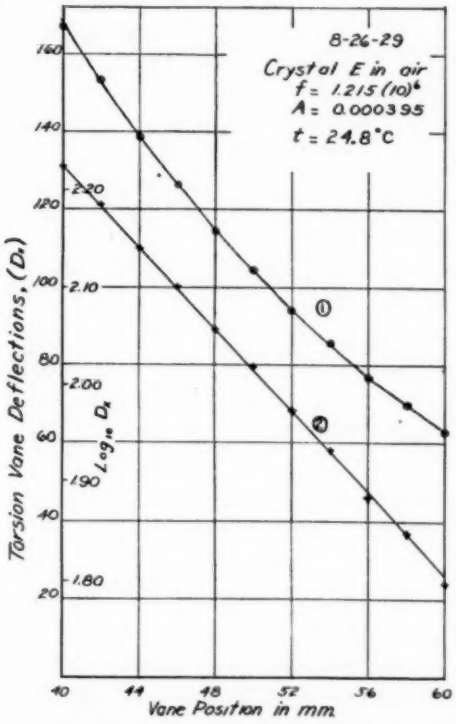

Fig. 9. Absorption curve for crystal E in air by the radiometer method. (D_x in mm) Curve 1 is a D_x curve; curve 2 is a log D_x curve.

four spaces for which the end points are determined independently of those for the other three spaces in the same range. Each of the four spaces has the same number of half wave-lengths (17 for some ranges and 18 for the others). Since the mirror position is recorded for each peak the average wave-length, $\bar{\lambda}$, can be computed for each range. For R_1 $\bar{\lambda} = 0.1142$ cm; for each of the other ranges $\bar{\lambda} = 0.1147$ cm. The only definite change is that of approximately 1/2 percent from R_1 to R_2. Curve III represents a change of 0.408 in $\log_{10}\alpha$ and a change of 6.309 cm in L whence c, the change per cm is 0.0647. This gives 0.00196 as the value of A, where $A = \lambda^2 C \log_e 10$. This is approximtely 5 times the theoretical value. Multiple reflections, even at $L = 100\lambda$ probably cause part of the large logarithmic decrement.

In Fig. 7 the break between Curves I, II, III and I′, II′, III′ is caused by a tenfold increase in galvanometer sensitivity. There is no change in the slope of the log α curves as there was in Fig. 6. Moreover the value of A from Fig. 7 agrees well with the theoretical value. (0.000368 as against 0.00037) The absence of any break in the slope is ascribed to the fact that the intensity is small and no great range of wave velocity exists. The enormous absorption makes the effect of the higher order reflections small even though there may be some phase lag. The value of $\bar{\lambda}$ for each range is as follows: For R_1, 0.02843 cm; for R_2, 0.02840 cm; for R_3, 0.02848 cm; for R_4, 0.02851 cm.

For Fig. 8 the value of A is 0.0118. This is about 42 times the value obtained from Lebedew's equation. A check run was made with a radiometer and the value of A for 93 percent CO_2, not dried, was 0.0161, therefore multiple reflections do not seem to be responsible for the excess over the theoretical value. It was found that the presence of water vapor increases the absorption, however. The wave velocity falls approximately on the extrapolation of Pierce's curve for velocity of sound in CO_2.

TABLE I. *Average values of V_0 and A.*

Crystal	Frequency	Gas	Apparent V_0	A
F	$1.408(10)^6$	air	333.3	0.00044
F	$1.408(10)^6$	CO_2		0.0014
E	$1.215(10)^6$	air	333.3	0.00039
E	$1.215(10)^6$	CO_2	265.5	0.0073
G	$1.167(10)^6$	air	332.8	0.00043
H	$1.158(10)^6$	air	334.5	0.00039
A	$6.555(10)^5$	air	333.8	0.00050
A	$6.555(10)^5$	CO_2	269.9	0.0058
C	$3.893(10)^5$	air	333.7	0.00053
C	$3.893(10)^5$	CO_2	270.	0.0064
D	$3.031(10)^5$	air	333.7	0.0014
		CO_2	265.	0.012

Table I gives the average value of V_0 and of A for each of the cases listed. Probably all these values of V_0, the velocity at 0°C, are slightly too high on account of the slightly large spacing of the I_p maxima. The velocity is a function of intensity, therefore the effect is small for CO_2. However there was probably a trace of air present with the CO_2. This would tend to make V_0 too large and A too small. The presence of water vapor with the CO_2 increases the absorption. Further data are being taken in this connection. Water vapor with *air* has little effect on the value of A. Multiple reflections, however, cause an apparently large absorption in air. With the higher frequencies this effect is slight as is indicated by the close check with the radiometer. A large number of runs were made with each crystal; for example, the tabulation for crystal E in air represents 14 independent runs in which the maximum variation from the mean V_0 was 0.3 m/sec and from the mean A it was 0.00002. The author's reliance in the values of A for air is greatest for the following crystals; E, F, G, H. The straight log α curves for CO_2 by the mirror and the radiometer methods indicate that A is exact for the partic-

ular amount of water vapor present but the uncertainty in this factor makes the CO_2 values less reliable.

V. Discussion of Results

In Part IV some evidence was given that the periodic changes in the plate current, I_p, are a simple and direct function of the changes in pressure amplitude in the gas at the surface of the crystal as the mirror is moved. This pressure amplitude and I_p reach their maximum values for the *same* position of the mirror. They are not only both periodic in space or displacement but both have the same space period, $\lambda/2$, and they are in phase. Let us now consider more in detail how the pressure amplitude should vary at the surface of the crystal as the mirror is moved. This type of variation should not be confused with the point-to-point variation along the resonating gas column between the crystal and the fixed mirror. From graphical analysis it was found that in the case of a system of undamped waves, produced by a plane source and a single reflection at a moving reflector which remains parallel to the source, the pressure amplitude at the source, resulting from the two oppositely travelling waves, goes through the same changes as those represented by the point-to-point variation along this wave system as it would exist if the reflector were to remain stationary at a resonance position. It is as if an imaginary plane, (parallel to the wave fronts) were to move through the stationary wave pattern. The same applies to displacement and velocity amplitudes. For damped waves none of these statements would hold. H. O. Taylor[6] has made excellent observations on the point-to-point variation of amplitude in *audible* stationary sound waves. The results to be expected from the theoretical considerations can then be compared with the observed details of the I_p-variation.

Let us investigate, from theoretical considerations, what the pressure amplitude at the crystal should be for several representative mirror positions. Let us assume that the emitted waves represent a *simple harmonic variation in pressure* (that p_0, the excess pressure due to the emitted wave at the crystal is a simple harmonic function of the time). For the sake of simplicity let us also assume, at first, that V, the wave velocity, is constant (independent of the sound intensity) and that the reflection is perfect at the mirror and also at the crystal. Let us first consider a *resonance* position of the mirror. For this position when an equilibrium condition has been reached the resultant pressure at the crystal at the instant when a condensation is being emitted will be the sum of a large number of condensations or pressure maxima, each of which is the result of reflection. (See Fig. 11) These components of the resultant pressure form a sequence of terms of decreasing magnitude and their sum is a series which would be infinite except for diffraction effects. Let p_R be the *resultant* instantaneous excess above normal pressure at the crystal. Let p_n be the instantaneous excess above normal pressure at the crystal, due to the nth reflection. Let P_R and P_n be the corresponding maxima or condensations, which would also equal the pressure amplitude.[13] Then $p_n = P_n \cos(\omega t - \epsilon)$ where $(\omega t - \epsilon)$ is the phase angle.

[13] K. S. Johnson and others use p to represent the r.m.s. value of the pressure variation. See K. S. Johnson, Transmission Circuits for Telephone Communication.

At a resonance position all the condensations, P_n, return to and are being reflected by the source at the instant it is emitting a condensation. For this instant

$$p_R = P_R = P_0 + P_1 + P_2 + \cdots + P_n = \sum_0^n P_n \tag{4}$$

For *any* position of the mirror Eq. (4) is of the form

$$y = \sum_{i=1}^{i=n} a_i \cos\left(\frac{2\pi}{T}t + \epsilon_i\right) = a \cos\left(\frac{2\pi}{T}t + \epsilon\right). \tag{5}$$

If $y = p_R$; $a_i = P_0 c^{nL} = p_n$, $a = P_R$, $\omega = 2\pi f$, t = time elapsed since a condensation in the n^{th} reflected wave was in phase with an emitted condensation at the crystal, $\epsilon_i = -\omega nL/V$, P_0 = the constant amplitude in the emitted wave; c = a constant, less than one, expressing the decrement; V = assumed constant wave velocity, and L = length of one return trip of the waves, then Eq. (5) is adapted to the quantities under discussion and takes the form

$$p_R = \sum_0^n P_0 c^{nL} \cos \omega(t - nL/V) = P_R \cos(\omega t + \epsilon) \tag{6}$$

where

$$P_R^2 = \left[\sum_0^n P_0 c^{nL} \cos(-\omega nL/V)\right]^2 + \left[\sum_0^n P_0 c^{nL} \sin(-\omega nL/V)\right]^2. \tag{7}$$

Since it is pressure *amplitudes* which were to be investigated Eq. (7) offers the solution. As equation (6) stands it involves four variables, i.e. $p_R = \Phi(n, Lt)$. By fixing L this may be represented graphically in three dimensions. (See Fig. 11) For $L = r$ a reasonance length, Eq. (7) becomes

$$P_R = \sum_0^n P_0 c^{nL} = P_0/(1 - c^{nL}) = P_0 (1-c)^{-nL}$$

In order to plot a $P_R^2 - L$ curve or a P_R^2-mirror position curve it will be necessary to evaluate P_R^2 in terms of P_0^2 at a number of points between two successive r-values. The values of P_R^2 and P_R for two representative values of c and several values of r are given below.

1st. $c = 0.9$; $r = 1$cm. (This value of c is approximately correct for crystal "A" provided Lebedew's theoretical value of the absorption constant holds for this frequency.)

For $L = r$	$P_R^2 = 100.\ P_0^2$;	$P_R = 10.0\ P_0$
For $L = r + \lambda/8$	$P_R^2 = 1.86\ P_0^2$;	$P_R = 1.36\ P_0$
For $L = r + \lambda/4$	$P_R^2 = 0.552\ P_0^2$;	$P_R = 0.743\ P_0$
For $L = r + \lambda/2$	$P_R^2 = 0.277\ P_0^2$;	$P_R = 0.526\ P_0$
For $L = r + 3\lambda/4$	$P_R^2 = 0.552\ P_0^2$;	$P_R = 0.743\ P_0$
For $L = r + 7\lambda/8$	$P_R^2 = 1.86 P_0^2$;	$P_R = 1.36\ P_0$
For $L = r + \lambda$	$P_R^2 = 100.\ P_0^2$;	$P_R = 10.0 P_0$

In all except the first of these values of P_R^2 and P_R the slight increase in L, the exponent of c, is neglected. The only set of values appreciably affected thereby is the last set (for $L = r + \lambda$). The value of λ for crystal

"A" in air is very nearly 1/2 mm consequently the exponent of c should be increased by 5 percent for $L=r+\lambda$. With this correction $P_R^2=91.3P_0^2$ and $P_R=9.56P_0$.

It is thus seen that, except for the damping of P_R, due to the extra distance, λ, the values of P_R are periodic in space. The values of the period is λ in terms of the length of the first return trip. In terms of mirror displacement it is $\lambda/2$, which agrees with the period of I_p. Moreover it was

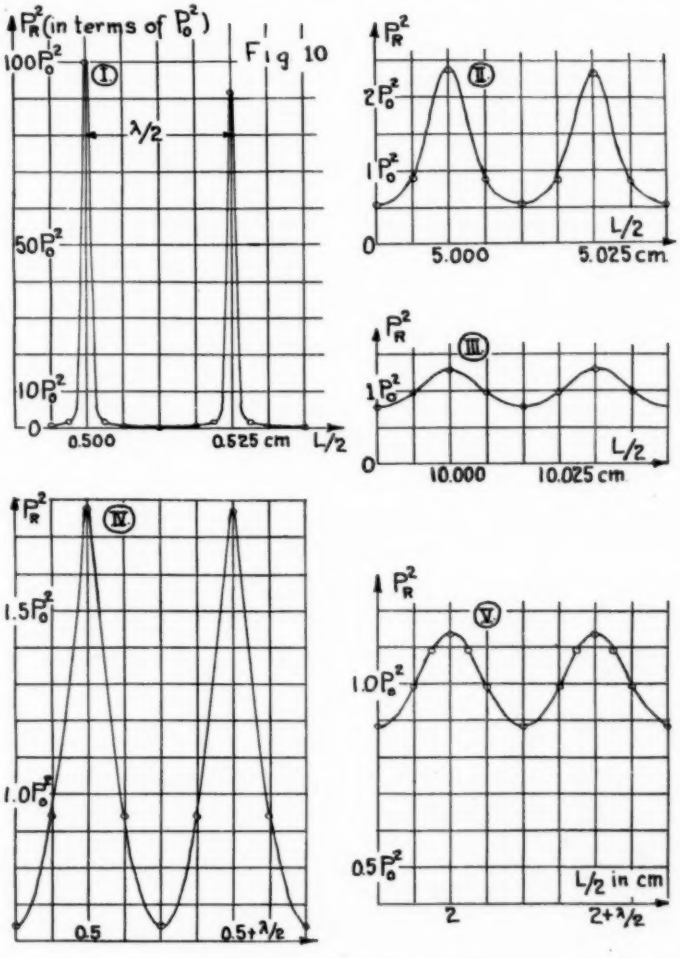

Fig. 10. Calculated pressure amplitude curves. Compare with Fig. 3–5.

found by extrapolating the very short distance back to the crystal position that, in every case, an I_p- maximum should fall at this point. The same applies to the P_R- maxima, as will be seen by setting L in equation (7) equal to zero. The variations in P_R and I_p are therefore in phase.

The above values of P_R^2 are plotted as a function of $L/2$ in Fig. 10, Curve I. For $c=0.9$ and $r=10$ cm the corresponding values of P_R^2 are plotted to a finer scale in Curve II. Curve III is for $c=0.9$ and $r=20$ cm. These

curves resemble the observed galvanometer-deflection, mirror-position curves for Crystal "*A*". (See Fig. 2). The difference between Curve I and the corresponding observed curve (Curve I) is probably largely due to the variable velocity of the sound waves.

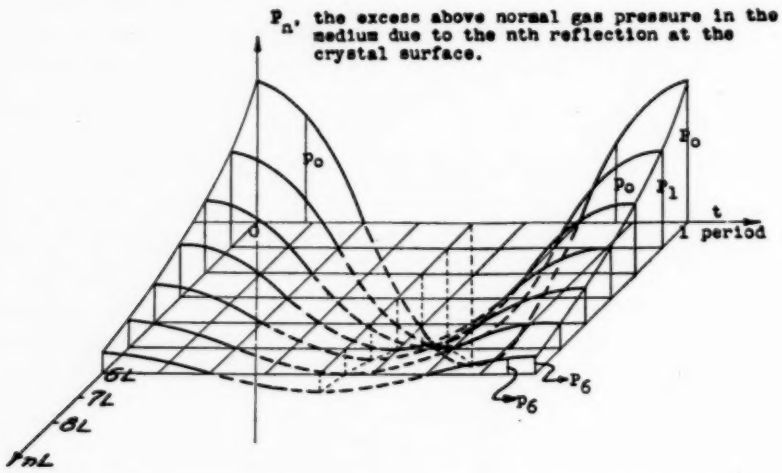

Fig. 11. Pressure time curves for successive reflections at the crystal.

If c, the fraction of P_0 which remains after 1 cm of path has been traversed, is chosen as 0.5, curves IV and V, Fig. 10, show the variation in P_R^2 near $L=1$ cm and $L=4$ cm. Compare these with the wave form curves Fig. 4.

Fig. 12 shows the positions of the maxima when projected on a plane perpendicular to the pressure axis. (See Fig. 11). The wave velocity is assumed to fall off with intensity approximately as shown by Foley's[5]

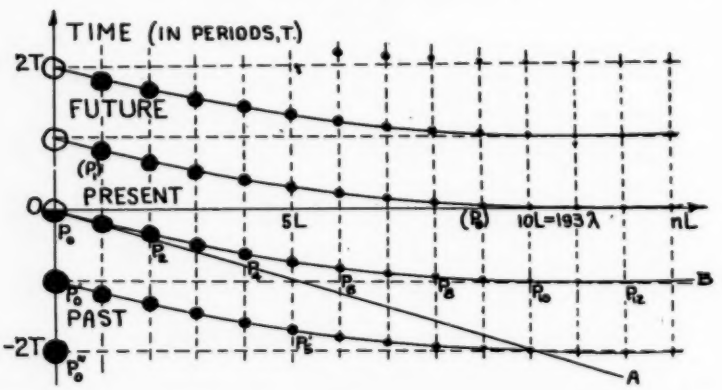

Fig. 12. Time and path length diagram for wave velocity decreasing with intensity.

curves. Such a velocity distribution places the maxima along a curved line instead of a straight one. Thus *no* position of the mirror exists for which all the maxima reach the mirror simultaneously. Consequently, the peaks corresponding to those in Fig. 10 will be somewhat lower and the entire

curve will be modified. Moreover the extent of this modification will depend partly on L. As L increases slightly the curved line joining the maxima must rotate counter clockwise about point, P_0, through a corresponding angle. For some definite angle and time the sum of the ordinates along a line parallel to the nL axis will reach a maximum which is less than the amplitude would be if the velocity had remained constant. The higher order reflections shown farther along the curved line are brought into phase with P_0 at a slightly smaller mirror displacement hence the peaks should have a more gentle slope on the right than on the left side. For certain cases even a minor peak may be developed. Fig. 12 shows such a case. In this figure 100 percent reflection is assumed. When a higher order reflection is retarded a half period the reflection is probably far from perfect but as the retardation increases reflection improves again. Thus the curved line may have nearly straight segments and the minor peaks may be magnified. However p_R will still be a simple harmonic function of the time if each of the components, p_n remains simple harmonic.

Fig. 12 shows the location of some of the pressure maxima at the crystal, in a *time* and *path length* diagram. The size of the dots is intended to represent the magnitude of the pressure maxima. P_1, P_2, P_3 etc. have already been reflected. They were emitted as P_0 's 20, 40, 60 etc. periods ago, respectively, and they would lie along the straight line P_0A if the wave velocity, V, were constant. This line would rotate counterclockwise about P_0 as shown by curved arrow if L increases. When $L=20\lambda$ it would coincide with the nL axis. The passage of *time* may be represented by moving the boundary line between past and future in the direction of the time axis (toward the future). Since $L=19.2\lambda$, P_1 was *reflected* approximately 1/5 period ago. However, P_3 was not reflected 3 times this long ago. On account of the decreasing velocity it has lagged behind so that it has been reflected merely 1/2 period ago.

The minor peak caused by (P_9) and following P's would fall approximately 1/5 space to the left of a major peak if it were represented in Fig. 10. If L were doubled this lag would become about 1/3 space. Thus the system of minor peaks moves back through the system of major peaks as L increases. This process probably helps cause the abrupt changes in the slope of the log α curves.

Possibility of other causes for such unexpected results as those shown in the wave form curves (Fig. 2–5) were investigated but no other adequate cause was found. A lowering of the crystal's frequency of oscillation due to the reaction of the resonating gas column on the crystal, does not explain the observed facts. To test whether the type of crystal mounting was responsible metal blocks of different thickness were successively placed under the same crystal. Several crystals were tested this way. It was found that the peculiarities of the wave-forms still persisted. Harmonics were also suspected. A sensitive wave meter was used to search for them but none were discovered. Finally the calibration of the screw was checked with a set of precision guages but it was found that the irregularities in the screw

were much less than those in the I_p spacing. Thus far the evidence points to a variable sound velocity as a cause for the observed peculiarities.

It is assumed that the logarithmic decrement of α may be used in computing A, in case the reflections of higher order than the first may be neglected This implies that α is proportional to that $(\Delta P_R)^2$ which corresponds to a mirror displacement of $\lambda/4$ from a resonance position. Such an assumption requires an experimental justification, hence a torsion vane determination of of A was made. Crystal E was used first because most confidence was placed in its value of A as determined with the interferometer. The data for one of the runs are given in the form of a curve (Fig. 9).

With the lower frequencies in air the deflections fall off so little with increasing mirror displacement that the results are not very decisive. With different percentages of CO_2 the logarithmic decrement was increased and it was found to be very uniform in any one run. It was found, however, that the humidity modifies the absorption enormously at these frequencies. Further measurements on this effect are being made.

Another crystal (Crystal F) was procured and tested. Its frequency is 1.408 $(10)^6$cps. The vane response was large enough to determine the value of A for air to two significant figures. (See Table I). The interferometer response was too small to obtain the same precision ($A = 0.0004$). With a mixture of 56 percent CO_2 in air, partly dried, the vane method gave $A = 0.0014$.

All the measurements on CO_2 with the interferometer and also with the pressure vane gave points falling very close to a straight log α curve but the slope of this curve was found to depend very much on the moisture content.

The wave velocity is not strictly constant as was assumed for Fig. 10. This modifies the wave form (as outlined above) and the log α curve, instead of approaching a constant slope *gradually*, may do so through comparatively straight sections, the last of which gives the correct value of A. Not much loss of energy takes place for those reflections in which the wave trains leave the crystal in phase with the emitted wave train. The higher order reflections involve considerable phase lag and loss of energy. As the phase lag approaches a complete cycle the reflection takes place with less loss of energy again. The energy losses also involve a further reduction in wave velocity. The effect of phase relationship on the reflecting power may cause the curved line in Fig. 12 to have more or less abrupt changes in direction. It may be seen from the figure that the rotation of such a broken line about the point, P_0, would result in a different wave form and a different value of P_R^2. A more or less abrupt change in the apparent value of A with increasing value of L may be expected when a minor peak is receding through a trough of the main wave-form. (See Curve III, Fig. 2).

The several runs made with the torsion vane detector of the progressive waves emitted by crystal "E" resulted in values of A that agreed well with each other and with the values found by the interferometer method. This agreement is additional evidence that the interferometer method is satisfactory for absorption measurements under certain circumstances. More-

over the latter method has the advantages of furnishing wave-length data also. Herzfeld and Rice[14] point out the need of such a method.

Conclusions

1. The galvanometer-deflection, mirror-displacement curve obtained with an acoustic interferometer is an index of the variation of the resultant pressure amplitude, P_R, with increasing mirror displacement, $(x-x_0)$.

2. For air as the transmitting medium the logarithmic decrement of the I_p—amplitude is not suitable for the determination of A, the absorption constant, at small values of L unless the frequency is of the order of 10^6 cycles per sec. or more. For a frequency of $3(10)^5$, L must be more than 10 cm.

3. The spacing of the I_p maxima indicates that the velocity of high frequency sound varies with intensity. The precision which G. W. Pierce[3] claims for the velocity has no significance for waves which suffer a decrease in velocity as their intensity diminishes. The best that can be done is to speak of the average velocity over a given path-length. Since Pierce[3] used the edges of the crystals as sound radiating surfaces in many of his tests he was probably dealing with fewer multiple reflections; nevertheless it is predicted that he would find a slight difference in the average spacing at large and at small values of L. All of the author's determinations for the velocity at 0°C are slightly greater than those found by Pierce. This is probably due to greater intensity of the emitted waves and to more reflections. Other things being equal, the spacing increases with intensity.

4. With CO_2 the reaction at the crystal is due almost entirely to the first reflection, hence the logarithmic decrement of the I_p—amplitude is much more suitable for the determination of A than is the case with air. The variation of velocity with frequency checks approximately with that found by Pierce.[3] Herzfeld and Rice[14] state the need of dispersion and absorption measurements on the same sample of gas. For cases of great absorption this method satisfies such a need.

The sonic interferometer as a research tool in acoustics is rapidly gaining in importance. This paper is being published at this time because it has a direct bearing on the work being done. There are many additional problems which suggest themselves as possibilities, problems to which the sonic interferometer appears well adapted.

Additional experimental work will probably increase the precision of the calculated quantities, V_0 and A, not because the author's direct measurements themselves lack precision but rather because these measurements are connected with the calculated quantities in such a complicated manner. Equally precise data taken under a great range of conditions should follow.

The writer wishes to express his appreciation to all who have aided him in his work; especially to Professor H. M. Randall and to Professor D. L. Rich, at whose suggestion the work was undertaken and partly carried out at the University of Michigan; also to Professor W. R. Ham, of Pennsylvania State College, where these investigations were completed. The work was directed by Professor Rich.

[14] K. F. Herzfeld and F. O. Rice, Phys. Rev. **31**, 691 (April 1928).

A GENERALIZED FORM OF THE NEW STATISTICS

By S. Chandrasekhar
Presidency College, Madras, India

(Received July 1, 1929)

Abstract

Instead of assuming the probabilities of absorption and emission of atoms in a radiation field as equal to $B_a\rho$ and $A+B_e\rho$ (the well-known Einstein equations) Strum has in a recent paper assumed them to be respectively equal to $B_a\rho+C_a\rho^2+\cdots$ and $A+B_e\rho+C_e\rho^2+\cdots$. This leads to a modification of Planck's law. It is shown in this paper that this assumption effectively amounts to replacing the new statistical law of interaction of Nordheim e.g.

$$f\left(1\pm\frac{f^*}{A}\right)f_1^*\left(1\pm\frac{f_1^*}{A_1}\right)$$

by the more general

$$(f+af^2+\cdots)\left(1\pm\frac{f^*}{A}\pm\frac{af^{*2}}{A}\pm\cdots\right)(f_1+af_1^2+\cdots)\left(1\pm\frac{f_1^*}{A_1}\pm\frac{af_1^{*2}}{A_1}\pm\cdots\right)$$

where f, f_1, f^*, f_1^* are the distribution functions for the projectiles corresponding to the numbers of each before and after collision; A, A_1 the number of cells respectively associated with them. On this basis a general H function defined by

$$H=\int(f+af^2+\cdots)\log(f+af^2+\cdots)\mp(A\pm f\pm af^2\pm\cdots)\log(A\pm f\pm af^2\pm\cdots)$$

is considered. As a consequence of this we get a generalized distribution function given by the relation

$$f+af^2+bf^3+\cdots=\frac{A}{C\exp[c|v|^2]\mp 1}$$

If we take only two terms we get approximately

$$J=\frac{A}{Ce^{c|v|^2}\mp 1}-\frac{A^2a}{(Ce^{c|v|^2}\mp 1)^2}=\frac{A}{C\exp[c|v|^2]\mp 1}-\frac{A^2a}{(C\exp[c|v|^2]\mp 1)^2}.$$

By substituting the appropriate values for A in the cases corresponding to the photons and the atoms, we get Strum's modified radiation formula, and a new distribution function for a gas. Thus as a result of a generalized analysis of the H-theorem we get a *new statistics* the successive approximations of which are a more accurate statistics which includes Strum's formula, the statistics of Bose-Einstein, Fermi-Dirac, the classical statistics of Maxwell-Boltzmann. It is suggested that this *new statistics* may be of importance in the study of dense matter at high temperature.

1. Introduction

L. Strum[1] in a recent paper has modified Planck's formula by generalizing the Einstein-Ehrenfest method of deriving it. Instead of assuming the probabilities of absorption and emission as $B_a\rho$ and $A+B_e\rho$ as Einstein did, Strum takes them as respectively equal to $B_a\rho+C_a\rho^2$ and $A+B_e\rho+C_e\rho^2$

[1] L. Strum, Zeits. f. Physik 51, 287 (1928).

where naturally C is a second order magnitude compared to the other coefficients. This assumption has been put in the most generalized form in a short note by Arthur E. Ruark[2] who takes the probabilities of absorption and emission as represented by two rapidly convergent series

$$B_a\rho+C_a\rho^2+D_a\rho^3+\cdots \tag{1}$$

$$A+B_e\rho+C_e\rho^2+D_e\rho^3+\cdots \tag{2}$$

Now the real significance of Einstein's induced emission coefficient is understood when an H-theorem in the new statistics corresponding to the old is constructed. This has been clearly pointed out by L. Nordheim[3] who has considered the kinetics of collisions from the point of view of the new statistics. Thus the probability of a collision between two projectiles in the classical statistics is given by

$$P_{v^*,v_1^*}^{v,v_1}=ff_1\phi_{v^*,v_1^*}^{v,v_1}\Delta V\Delta v\Delta v_1 \tag{3}$$

where f and f_1 denote the distribution function for the same space point for different velocities v or v_1, but on the new statistics the probability is given not by (3) but by

$$P_{v^*v_1^*}^{v,v_1}=ff_1\left(1\pm\frac{f^*}{A}\right)\left(1\pm\frac{f_1^*}{A_1}\right)\phi_{v^*,v_1^*}^{v,v_1}\Delta V\Delta v\Delta v_1. \tag{4}$$

thus making the probability depend on the nature of the products of the interaction. In the above equation the positive or the negative sign is taken according as the Bose-Einstein or Fermi-Dirac statistics is considered. The above modification in the law of interaction was first suggested by Jordan[4] and a complete analysis of it was given by Brillouin.[5]

Now the modification of Strum and Ruark in their derivation of the modified Planck's formula effectively amounts to replacing

$$f\left(1\pm\frac{f^*}{A}\right) \quad \text{by} \quad (f+af^2)\left(1\pm\frac{f^*}{A}\pm a\frac{f^{*2}}{A}\right)$$

where a is a small quantity of the second order magnitude. Thus it appears that Strum's suggestion can be generalized and a new very generalized H-theorem can be constructed giving a *new* statistics for gases and photons. The object of this paper is to consider this question in detail.

2. The Fundamental Equation of the Theory of an Ideal Gas[6]

Consider an assembly of N mass-points which may be subject to external forces but which do not exert any mutual influence except at very small

[2] A. E. Ruark, Phys. Rev. **33**, 640 (1929).
[3] L. Nordheim, Proc. Roy. Soc. (Lond) **A119**, 689 (1928).
[4] P. Jordan, Zeits. f. Physik **33**, 649 (1925).
[5] L. Brillouin, Ann. d. Physique **7**, 315 (1927).
[6] The method of procedure will be essentially that of Nordheim's generalized.

distances. Let the number of particles in the element of phase space $dxdydzd\xi d\eta d\zeta$ be given in the well-known manner by the distribution function

$$f(x,y,z,\xi,\eta,\zeta)\Delta V\Delta v \tag{5}$$

where

$$\Delta V = dxdydz\ ;\quad \Delta v = d\xi d\eta d\zeta \tag{6}$$

which is so normalized that

$$\int_0^\infty f d\Omega = N. \tag{7}$$

We shall take it in the course of the paper that in other than rectangular coordinates for position and momenta, $\Delta\Omega$ includes the transformation determinant of Jacobi, so that f is an invariant with respect to all such transformations. So that f gives simply the number of mass-points in the unit element $d\Omega$ constructed around the point.

The procedure in the classical statistics is to calculate the rate of alteration of the distribution function with time and to equate it to zero, so that we get the "stationary" or the most probable distribution. The same method can also be followed here. Thus taking an element $d\Omega$ in the phase space Boltzmann's fundamental equation becomes,

$$\frac{df}{dt}=\frac{\partial f}{\partial t}+\frac{\partial f}{\partial x}\xi+\frac{\partial f}{\partial y}\eta+\frac{\partial f}{\partial z}\zeta+\frac{\partial f}{\partial \xi}\frac{X}{m}+\frac{\partial f}{\partial \eta}\frac{Y}{m}+\frac{\partial f}{\partial \zeta}\frac{Z}{m}+a-b=0. \tag{8}$$

Here X, Y, Z are the components of the external forces in the three principal directions, a and b respectively the number of particles thrown in and out of the phase-space element $d\Omega$ by interactions (collisions) in unit time.

Now in the classical theory we assume that the probability of an interaction between two projectiles depends only on the number of each kind in the initial state. But that is not the case in the quantum theory.

Let us now consider the collision process. Consider a volume V large in comparison with the dimensions of the projectile. Through that element two properly normalized wave groups representing particles having their velocity vectors between v and $v+\Delta v$, and v_1 and $v_1+\Delta v_1$, may run. Then let $\phi_{v^*,v_1^*}^{v,v_1}$ be the probability that a scattering into the velocity v^* and v_1^* may occur. Of course v^* and v_1^* have to satisfy the conservation of momentum and energy conditions.

In the classical theory of Maxwell and Boltzmann, the probability that such a collision occurs, depends (as has been pointed out before) on the number of each in the initial states, that is it can be expressed by the well-known relation

$$P_{v^*,v_1^*}^{v,v_1}=ff_1\phi_{v^*,v_1^*}^{v,v_1}\Delta V\Delta v\Delta v_1. \tag{9}$$

But in the new statistics the probablity is, as given by Nordheim,

$$P_v^{v_1 v_1}{}_{,v_1*} = f\left(1 \pm \frac{f^*}{A}\right) f_1\left(1 \pm \frac{f_1^*}{A_1}\right) \phi_v^{v_1 v_1}{}_{,v_1}{}^* \Delta V \Delta v \Delta v_1 \tag{10}$$

where A and A_1 are the number of cells associated with each state. The above equation can be generalized to include terms proportional to f^2, f_1^2, etc. In that case the probability can be expressed by the general relation

$$P_v^{v_1 v_1}{}_{,v_1}{}^* = (f + af^2 + bf^3 + \cdots) \times \left(1 \pm \frac{f^*}{A} \pm \frac{af^{*2}}{A} \pm \cdots\right)$$

$$\times (f_1 + a_1 f_1^2 + b_1 f_1^3 + \cdots) \times \left(1 \pm \frac{f_1^*}{A_1} \pm \frac{a_1 f_1^{*2}}{A_1} \pm \cdots\right) \phi_v^{v_1 v_1}{}_{,v_1}{}^* \Delta V \Delta v \Delta v_1 . \tag{11}$$

In order not to complicate the expressions we will take only the first two terms. The further generalization will be obvious. With the above equation, the difference of the number of particles thrown out or into the phase-space-element $d\Omega$ can now be formed, and we get

$$\frac{df}{dt} + \frac{\partial f}{\partial x}\xi + \frac{\partial f}{\partial y}\eta + \frac{\partial f}{\partial z}\zeta + \frac{\partial f}{\partial \xi}\cdot\frac{X}{m} + \frac{\partial f}{\partial \eta}\cdot\frac{Y}{m} + \frac{\partial f}{\partial \zeta}\cdot\frac{Z}{m}$$

$$= -\int \Bigg[(f + af^2)\left(1 \pm \frac{f^*}{A} \pm \frac{af^{*2}}{A}\right)(f_1 + af_1^2)\left(1 \pm \frac{f_1^*}{A} \pm \frac{a_1 f_1^{*2}}{A}\right)$$

$$- (f^* + af^{*2})\left(1 \pm \frac{f}{A} \pm \frac{af^2}{A}\right)(f_1^* + af_1^{*2})\left(1 \pm \frac{f_1}{A} \pm \frac{af_1^2}{A}\right)\Bigg] \Delta v_1 \int \phi_{(\sigma)}^{v, v_1} d\sigma \tag{12}$$

It is here assumed the probability for the direct and the inverse processes are equal giving

$$\phi_v^{v_1 v_1}{}_{,v_1}{}^* = \phi_{v,v_1}^{v^*,v_1{}^*} = \phi_{(\sigma)}^{v,v_1} . \tag{13}$$

The above equation would give a statistics the successive approximations of which, are the new statistics and the classical statistics depending on the order of magnitude of f/A.

3. The Generalized Boltzmann H-Theorem

We have now to prove that the fundamental equation (7), actually allows us to build up a *very general complete theory* for an ideal gas. For that purpose we have to prove the H-theorem.
Consider the function H defined by[7]

$$H = \int (f + af^2) \log (f + af^2) \mp (A \pm f \pm af^2) \log (A \pm f \pm af^2) . \tag{14}$$

[7] The most general H-function will include terms proportional to f^3. In that case

$$H = \int (f + af^2 + bf^3 + \cdots) \log (f + af^2 + bf^3 + \cdots) \mp (A \pm f \pm af^2 \pm \cdots) \log (A \pm f \pm af^2 \pm \cdots) \tag{14a}$$

Therefore

$$\frac{dH}{dt}=\int(1+2af)\log\frac{f\pm af^2}{A\pm f\pm af^2}\cdot\frac{df}{dt}\cdot\Delta\Omega\cdot \tag{15}$$

Substituting for the value for df/dt as given by Eq. (12) we get first

$$\begin{aligned}\frac{dH}{dt}=-\iint(1+2af)\log\frac{f+af^2}{A\pm f\pm af^2}&[(f+af^2)(A\pm f^*\pm af^{*2})\\&\times(f_1+af_1^2)(A\pm f_1^*\pm af_1^{*2})-(f^*+af^{*2})(A\pm f\pm af^2)\\&\times(f_1^*+af_1^{*2})(A\pm f_1\pm af_1^2)\cdot\frac{1}{AA_1}\cdot\Delta V\Delta v\Delta v_1\int\phi(\sigma)d\sigma.\end{aligned} \tag{16}$$

This relation must be unaltered by an interchange of f and f_1, which means only a change in the notation, so that we must write

$$\frac{1}{2}\left[(1+2af_1)\log\frac{f_1+af_1^2}{A\pm f_1\pm af_1^2}+(1+2af)\log\frac{f+af^2}{A\pm f\pm af^2}\right]$$

in the place of

$$\left[(1+2af)\cdot\log\frac{f+af^2}{A\pm f\pm af^2}\right]$$

under the integral. It must also be unaltered by an interchange of the function with stars against those without stars, so that this may be replaced by

$$\begin{aligned}\frac{1}{4}\Big[&(1+2af)\log\frac{f+af^2}{A\pm f\pm af^2}+(1+2af_1)\log\frac{f_1+af_1^2}{A\pm f_1\pm af_1^2}\\&-(1+2af^*)\log\frac{f^*+af^{*2}}{A\pm f^*\pm af^{*2}}-(1+2af_1^*)\log\frac{f_1^*+af_1^{*2}}{A\pm f_1^*\pm af_1^{*2}}\Big]\\=\tfrac{1}{4}\Big[&\log(f+af^2)(A\pm f^*\pm af^{*2})(f_1+af_1^2)(A\pm f_1^*\pm af_1^{*2})\\&-\log(f^*+af^{*2})(A\pm f\pm af^2)(f_1^*+af_1^{*2})(A\pm f_1\pm af_1^2)\Big]+\Theta\end{aligned} \tag{17}$$

where Θ is a quantity of the second order and so will not affect the *sign* of the expression. One has therefore the relation

$$\begin{aligned}\frac{dH}{dt}=-\frac{1}{4}\iint\Big\{&\log\left[(f+af^2)(A\pm f^*\pm af^{*2})(f_1+af_1^2)(A\pm f_1^*\pm af_1^{*2})\right]\\&+\Theta-\log\left[(f^*+af^{*2})(A\pm f\pm af^2)(f_1^*+af_1^{*2})(A\pm f_1\pm af_1^2)\right\}\\&\times\left\{(f+af^2)(A\pm f^*\pm af^{*2})(f_1+af_1^2)(A\pm f_1^*\pm af_1^{*2})\right.\\&\left.-(f^*+af^{*2})(A\pm f\pm af^2)(f_1^*+af_1^{*2})(A\pm f_1\pm af_1^2)\right\}\times\frac{\Delta V\Delta v\Delta v_1}{AA_1}\int\phi(\alpha)d\alpha.\end{aligned} \tag{18}$$

Now the integral is always positive, since both brackets have everywhere the same sign so that dH/dt is negative, or H can only decrease. Thus expression (14a) appears as the *complete analog* of the Boltzmann H-function, and perhaps the most general manner in which the H-function, can be formulated. In the case where equilibrium conditions are considered $dH/dt=0$ which is possible only if

$$(f+af^2)\left(1\pm\frac{f^*}{A}\pm\frac{af^{*2}}{A}\right)(f_1+af_1^2)\left(1\pm\frac{f_1^*}{A}\pm\frac{af_1^{*2}}{A}\right)$$
$$=(f^*+af^{*2})\left(1\pm\frac{f}{A}\pm\frac{af^2}{A}\right)(f_1^*+af_1^{*2})\left(1\pm\frac{f_1}{A}\pm\frac{af_1^2}{A}\right) \tag{19}$$

Now we introduce a new function g instead of f which does not vitiate the generality, defined by

$$f+af^2=A/(g\mp 1) \tag{20}$$

we get at once

$$g\cdot g_1=g^*\cdot g_1^*. \tag{21}$$

It can easily be shown by an argument similar to that of Boltzmann's considering that f and therefore g also cannot depend on the direction of the velocity vectors but only on the modulus and that the energy relation

$$|v|^2+|v_1|^2=|v^*|^2+|v_1^*|^2 \tag{22}$$

holds good one can get easily that

$$g=Ce^{c|v_1|^2} \tag{23}$$

where C and c are constant, hence giving us

$$f+af^2=A/(Ce^{c|v|^2}\mp 1). \tag{24}$$

When a is zero we get the well-known Bose or Fermi formula.[8]

4. The Planck's Radiation Law

Planck's radiation-law corresponds to the Bose-Einstein's statistics and in that case we get

$$f+af^2=A/(Ce^{c|v|^2}-1) \tag{25}$$

or solving the above equation neglecting the terms of orders higher than the second we get

$$f_v=\frac{A_v}{Ce^{c|v|^2}-1}-\frac{A_v^2\cdot a}{(Ce^{c|v|^2}-1)^2}\cdot \tag{26}$$

[8] The most general form of the distribution function will be given by

$$f+af^2+bf^3+\cdots=A/(Ce^{c|v|^2}\mp 1). \tag{24a}$$

Now we know that the number of cells in the frequency range ν and $\nu+d\nu$ is given by

$$A_\nu = 8\pi\nu^2/c^3 d\nu \tag{27}$$

we get at once Strum's modified Planck's formula[9]

$$f = \frac{8\pi\nu^2}{c^3}\cdot\frac{d\nu}{e^{h\nu/kT}-1} - \frac{a\cdot(8\pi\nu^2/c^3)^2 d\nu}{(e^{h\nu/kT}-1)^2} \tag{28}$$

(assuming that at as $T\to\infty$, $f\to\infty$)

5. The Theory of an Ideal Gas

Using the thermodynamic relations

$$H = -\log P\ ;\ S = -kH \tag{29}$$

where P is the 'complexion' number and S = the entropy we can easily identify $c|v|^2$ with ϵ/kT so that our distribution function for the electrons corresponding to the Fermi-Dirac statistics is given by

$$f + af^2 = \frac{A}{e^{\alpha+\beta\epsilon}+1} \tag{29}$$

where $B = 1/kt$. From the above one can easily compute f as in the Planck's radiation law and get

$$f = \frac{A}{e^{\alpha+\beta\epsilon}+1} - \frac{A^2 a}{(e^{\alpha+\beta\epsilon}+1)^2}\cdot \tag{30}$$

In the case of particles the number of cells in the energy range ϵ and $\epsilon+d\epsilon$ is given by

$$A = 2\pi G\cdot(2m)^{3/2}\cdot\epsilon^2\cdot d\epsilon/h^3. \tag{31}$$

Substituting the above and integrating we obtain

$$N = \frac{2\pi G(2m)^{3/2}}{h^3}\int_0^\infty \frac{\epsilon^2 d\epsilon}{e^{\alpha+\beta\epsilon}+1} - \frac{4\pi^2 G^2(2m)^3 a}{h^6}\int_0^\infty \frac{\epsilon d\epsilon}{(e^{\alpha+\beta\epsilon}+1)^2}\cdot \tag{32}$$

[9] Equation (28) gives the number of quanta in the frequency range ν and $\nu+d\nu$. If we multiply throughout by $h\nu$ we get ρ_ν the density of radiation. It is given by the usual Planck formula plus an additional term which differs by a factor ν/h^3 from that given by Strum (reference 1 Eq. (6)). This arises due to the fact that in the Einstein method the number of transitions per second is taken to be proportional to the density of radiation. But really it ought to be proportional to the number of quanta in the frequency range under consideration rather than the density. However these two assumptions do not affect the final formula in the original method of Einstein and Ehrenfest. (This is clear when we note that the first term of Eq. (23) when multiplied by $h\nu$ gives the usual Planck formula.) After the work of Jordan, Brillouin and in particular that of Nordheim, there is little doubt that the proportionality depends *on the number and not the density* and the difference of our expression from that of Strum's is essentially due to the inappropriateness of Einstein's method in taking the transitions per second as proportional to the radiational density.

The above equation can be put in the more convenient manner

$$N=\frac{G}{h^3}(2\pi mkT)^{3/2}\cdot U_{1/2}-\frac{(2\pi)^2G^2(2m)^3\cdot a\cdot\log(-\alpha)}{h^6}\cdot U_0 \tag{32a}$$

where $U\rho$ is the general Sommerfeld integral[10] given by

$$U_\rho=\frac{1}{\Gamma(\rho+1)}\int\frac{u^\rho du}{\frac{1}{A}e^u+1}\cdot \tag{33}$$

Thus we see that our general analysis of Boltzmann's H-theorem brings out at the same time a modification in Planck's radiation law and in the distribution function for a gas quite naturally. This generalized statistics may be of importance in the study of dense matter at high temperatures. In particular Planck's radiation law thus modified offers an explanation for the deviation of the Stefan-Boltzmann constant calculated on Planck's formula and the observed value by Ladenburg.[11] Furthermore our generalized distribution function for the ideal gas predicts a deviation from the Maxwellian distribution even for a non-degenerate system. Whether this deviation will be observable depends on the order of magnitude of a.

[10] A. Sommerfeld, Zeits. f. Physik **47**, 1 (1928).
[11] L. Strum, Zeits. f. Physik **51**, 290 (1928).

NOTE CONCERNING THE EMISSION OF BETA-RAYS IN RADIOACTIVE CHANGE.

By Leonard B. Loeb
University of California, Berkeley

(Received September 10, 1929)

Abstract

A brief summary of the present status of the relations between β-rays and γ-rays in radioactive disintegration is given. It is shown that the escape of β-rays from the nucleus with nondescript velocities which appears to be established by the work of Ellis and his collaborators introduces a serious difficulty in that such changes of energy are sandwiched between α-ray emissions of constant energy. A possible solution is suggested by assuming that the energy of emission of succeeding β-rays in the $\alpha\beta\beta\alpha$ type of transformations supplement each other giving a constant energy between two α transformations. For the $\alpha\beta\alpha\beta\alpha$ transformations the β-ray energy differences can only be supplemented by γ-ray changes as suggested by Heisenberg. Unless a much needed investigation of relative energies of emission of succeeding β-rays and β and γ-rays upholds the above hypothesis one of the following conditions must hold, either the conclusions of Ellis in the face of his evidence are wrong, or β-ray changes occur in a part of the nucleus and in such a manner that the energy of emission of the α-rays is unaffected by differences in energy of the β-ray levels of atoms of the same species, or what is less likely, the law of conservation of energy does not apply in the usual form to nuclear disintegrations.

EVER since the work of Ellis[1] and his collaborators on the one hand and Meitner[2] on the other, dating from 1922, there has been considerable discussion concerning the nature of the relationship between β and γ-ray emission. Ellis initially contended that γ-ray emission *preceded* the emission of the primary β-ray, which ultimately escaped with a nondescript velocity giving the well-known continuous background of the β-ray spectrum. Meitner on the other hand contended that the β-rays were *initially emitted with a uniform and constant velocity* in analogy to the α-ray changes, and that the γ-rays *followed* the β-ray emission as the result of a nuclear readjustment after emission or as of *secondary origin from the extra nuclear structure.* She accounted for the continuous β-ray spectrum as due to dispersion of the initial β-ray energy by scattering, the Compton effect, and internal ionization. Time has shown that both of these views were in part right and in part wrong. It seems generally accepted today that the γ-ray emission in many cases *follows* the $\beta-$ or α-ray emission in that the *secondary* β-ray spectra show that the γ-ray has thrown these β- rays out of an atom of atomic number appropriate to the change produced by loss of an α-particle or a primary β-ray as origin-

[1] C. D. Ellis, Proc. Roy. Soc. **A99**, 261 (1921); Proc. Camb. Phil. Soc. **21**, 121 (1922).
Ellis and Skinner, Proc. Roy. Soc. **A105**, 185 (1924).
Ellis and Wooster, Proc. Camb. Phil. Soc. **22**, 844 (1925).

[2] L. Meitner, Ergebnisse der Exakten Naturwissenschaften, **3**, 160 (1924); also, Zeits. f. Physik **9**, 131 and 145 (1922); **11**, 35 (1922); **19**, 307 (1923); **26**, 169 (1924).

ally postulated by Meitner. On the other hand three excellent arguments have been advanced to indicate that the primary β-ray escapes as postulated by Ellis with a nondescript velocity from the nucleus, sometimes high and sometimes low characterized by the continuous β-ray spectrum.[3,4] These facts are, (1) if the primary β-rays have a uniform initial energy of high value (equivalent to the hardest γ-rays or fastest β-rays observed) there would be several electrons produced per primary β-ray in the process of degradation and dissipation of their energy to give a continuous spectrum. This is contrary to fact for there are less than 2 electrons per radioactive change. (2) In cases where the continuous spectrum predominates Emeleus has found closely only 1 electron per disintegrating atom. (3) Ellis and Wooster[4] have shown that the total heating effect of the β and γ-rays from RaE (where these can be measured within 10 %) is of the order of 1/3 that to be expected if all the energy for the radiations observed came from a primary β-ray per disintegrating atom with the high unitary energy of the fastest β-rays observed in the change as postulated by Meitner.

The fact that the primary β-rays actually do emerge with the nondescript velocities shown in the continuous β-ray spectrum, however, raises a very serious question. Meitner went very much further than merely stating an aesthetic idea when she assumed all primary β-rays to have the same velocity, although to the writer's knowledge she has not stated the reason for her assumption in a manner which would indicate the point as clearly as it might be made. All β-ray disintegrations are *preceded by α-ray changes* in the three well known series of disintegrations, (Ur-Ra, Act, and Th). All β-ray changes are *ultimately followed by α-ray changes*. The α-rays are emitted with energies that are constant for a given change to closely 0.1%.[5] It therefore seems hard to believe that the β-ray disintegrations in which primary β-rays are emitted with *any energy* should leave the nuclei which they depart from with unequal energies; for it is not reasonable to expect nuclei with very different energy contents following such a change to give rise to the uniform succeeding emission of α-particles.

There appeared to be some hope of avoiding the dilemma arising from the fact that the primary β-rays are emitted with all energies, though sandwiched between α-ray changes of constant energy emission, in a recent paper by Heisenberg and Pauli[6] inspired by work of Rosseland, and Condon, Gurney and Gamow.[7] Heisenberg and Pauli show that while for α-rays we should expect little* γ-ray energy to be liberated and thus quite constant initial energies for the α-rays we may expect in β-ray changes that a rela-

* This may be contrary to fact as we shall later see.

[3] K. G. Emeleus, Proc. Camb. Phil. Soc. **22,** 400 (1924).
R. W. Gurney, Proc. Roy. Soc. **A109,** 540 (1925); Proc. Roy. Soc. **A112,** 380 (1926).

[4] Ellis and Wooster, Proc. Roy. Soc. **A117** 109 (1927).

[5] Briggs, Proc. Roy. Soc. **A114,** 313 (1927).

[6] Heisenberg and Pauli, Zeits. f. Physik **56,** 1 (1929).
S. Rosseland, Zeits. f. Physik **14,** 173 (1923).

[7] Condon and Gurney, Phys. Rev. **33,** 127 (1929).
G. Gamow, Zeits. f. Physik **51,** 204 (1928) and **53,** 601 (1929).

tively large portion of the nuclear energy to be dissipated in disintegration might come out as γ-rays. Were this prediction correct the situation would be saved for a number of β-ray transformations in which primary γ-rays are emitted after β-ray emission. If we regard the table of disintegrations shown in Table I we see that only 12 out of some 20 β-ray changes have γ-rays de-

TABLE I.

α' changes
$\alpha\beta\beta\alpha$

Ur X_1	$\cdots$	Ur X_2	$\cdots$	Ur *II*
β-rays		β-rays		
no γ-rays		γ-rays		
Ra *B*	$\cdots$	Ra *C*	$\cdots$	Ra *C'*
β-rays		β-rays		
γ-rays		γ-rays		
Ra *D*	$\cdots$	Ra *E*	$\cdots$	Ra *F*
β-rays		β-rays		
γ-rays		no γ-rays		
Ac *B*	$\cdots$	Ac *C*	$\cdots$	Ac *C'*
β-rays		β-rays		
γ-rays		no γ-rays		
Mes. Th *I* — Mes. Th *II*			$\cdots$	Ra Th
β-rays		β-rays		
no γ-rays		γ-rays		
Th *B*	$\cdots$	Th *C*	$\cdots$	Th *C'*
β-rays		β-rays		
γ-rays		no γ-rays		

$\alpha\beta\alpha\beta$

Ra *B*	$\cdots$	Ra *C*	$\cdots$	Ra *C''*	$\cdots$	Ra *D*
β-rays		α-rays		β-rays		
γ-rays		Sec. β and γ-rays		γ-rays uncertain		
Ac *B*	$\cdots$	Ac *C*	$\cdots$	Ac *C''*	$\cdots$	Ac *D*
β-rays		α-rays		β-rays		
γ-rays				γ-rays		
Th *B*	$\cdots$	Th *C*	$\cdots$	Th *C''*	$\cdots$	Th *D*
β-rays		α-rays		β-rays		
γ-rays				γ-rays (soft)		
Ur *Y*	$\cdots$	Prot Ac	$\cdots$	Ac	$\cdots$	Ra Ac
β-rays		α-rays		β-rays		
γ-rays uncertain				γ-rays uncertain		

finitely associated with them while the presence of primary γ-rays in the remaining group are either very uncertain or definitely absent. When we consider furthermore that where γ-rays occur their total energy relative to the β-ray energy is quite small the suggested solution appears even less hopeful.* Obviously the theory can only be tested by actually summing up prim-

* In a recent paper Gurney[3] points out that it is probable that no γ-rays of high energy can be emitted by those radioactive bodies which expel their nuclear electrons with low energies,

ary β-ray energy in the continuous spectrum together with secondary β-rays and γ-ray quanta to see whether a constant initial β-ray energy of any sort could be derived.

It occurred to the writer that by supplementing the suggestion of Heisenberg and Pauli by the following scheme some hope of a way out of the difficulty might be found for a larger number of β-ray changes.

All β-ray changes in the series of transformations can be classed as belonging to one of two types, either those characterized by Meitner[8] as α'-transformations in which an α-ray change is followed by 2 β-ray changes, or a series of changes in which an α-ray change is followed by a β-ray and then by an α with a β-ray following immediately afterward. For the sake of discussion these changes are listed in Table I with whatever additional data is available. For the α' changes of Meitner, i.e. those first mentioned, there need be no γ-ray energy liberated for since between the α-ray changes there are *2* β-ray changes then all that is needed is that an atom nucleus which emitted a slow primary β-ray in the first step of the transformation emit the second β-ray with an energy such that the two β-ray processes together without a γ-ray can give the differences in the energies involved in the preceding and succeeding α-ray changes. β-ray changes as postulated by Heisenberg can also take place in which case the energy of the 2 β plus γ-ray energy must equal the energy difference in the α-particle changes.

For the alternating α and β-ray changes, however, Heisenberg's explanation must apply. Thus the $\alpha\beta\alpha\beta$ changes should always show an appreciable primary γ-radiation while the $\alpha\beta\beta\alpha$ changes need not do so. With the little data available it appears that in all the $\alpha\beta\alpha\beta$ changes except that of RaB-RaC-RaC''-RaD and UrY-ProtAct-Act-Ra-Act there is a γ-ray radiation observed with the β, while the data on the latter two changes are so meagre owing to the small quantities of substances involved that the failure to observe the γ-rays need not be taken as significant. In the $\alpha\beta\beta\alpha$ changes it is seen that some β-changes alone and some β-changes accompanied by γ-rays are observed.

This speculation however requires that in the $\alpha\beta\beta\alpha$ transformations the two successive continuous β-ray spectra more or less supplement each other, a point open to experimental verification. It has also been kindly pointed out to the writer by his colleague professor J. R. Oppenheimer that since in essence there is a difference in mechanism assumed in the $\alpha\beta\beta\alpha$ and $\alpha\beta\alpha\beta$ transformations there should be distinct differences in the diffuseness of the continuous β-ray spectra in the two cases detectable.

Unfortunately there is little experimental evidence of any sort bearing on these points and such evidence is sorely needed. For unless either the conclusion of Ellis as to the primary nature of the continuous β-ray spec-

---

as a result of his investigation of the continuous β-ray spectra of Thorium C and D. This experimental evidence seems to speak against the conclusions of Heisenberg as applied to this problem.

[8] L. Meitner, Zeits. f. Physik **4**, 161 (1921).

trum is wrong, or the above explanation of Heisenberg, Pauli and the writer is correct, we are inevitably forced to one of two very unsavory conclusions. These are: that either the mechanisms involving emission of α and β-rays from the nucleus are so independent and segregated as to permit constant α-ray emission independently of inequalities of energy content in the β-ray levels of the nuclei of atoms of the same species, or that which is unlikely and more unpalatable, that the law of conservation of energy needs to be modified in its application to nuclear disintegration. The importance of the conclusions to be drawn therefore seem to warrant a careful investigation along the lines indicated. In advocating such an investigation there appears still another question of similar nature to be investigated in connection with the emission of γ-rays in α-ray processes.

The Heisenberg-Pauli theory makes α-ray emission as a primary process in α-ray disintegrations rather unlikely and predicts the very constant energies of the α-rays observed. Unfortunately a number of α-ray changes are observed to emit γ-rays; these are Ra, RaD, RaAct and ActX. In part these rays are of secondary origin excited in the extranuclear structure by the α-ray emission. On the other hand as Meitner[9] has shown some of them are indubitably primary γ-rays which she attributes to a readjustment of the nucleus after the α-ray emission. Unless either the number of such primary γ-ray quanta are minute compared to the numbers of α-particles emitted and the ensuing α-rays of shorter range resulting from the γ-radiation are lost in range studies, or in case the γ-ray quanta are relatively large in number *unless they emerge in a subsequent transition in a β-ray region which does not affect later α-ray changes*, we will be forced to the task of accounting for α-ray changes of uniform energy content, with some additional energy emitted by certain of the atoms from α-ray levels in a given transformation. What is needed here is again quantitative investigation of the number of primary γ-ray quanta relative to the numbers of α-ray changes. It is accordingly the wish of the writer in thus summarizing the present status of the problem to point out the particular type of information needed before further progress can be made on the problems of β-ray emission.

[9] L. Meitner, Zeits. f. Physik **34**, 807 (1925).

THE MAGNETIC PROPERTIES OF ISOLATED FERROMAGNETIC ATOMS

By F. Woodbridge Constant*
Norman Bridge Laboratory of Physics, Pasadena, California

(Received August 12, 1929)

Abstract

In order to obtain a better knowledge of the elementary atomic magnet, its behavior when surrounded by non-magnetic atoms rather than by other magnetic ones has been studied. For this purpose alloys of 90% and 95% platinum with the remainder cobalt and nickel, respectively, have been investigated. Only the cobalt alloys were found magnetic. The magnetic moment per cobalt atom being greater than for pure cobalt, the platinum may contribute to the magnetism. Variation of magnetization with temperature and the Curie points have been measured, the latter falling rapidly as the cobalt content decreased. Various hysteresis loops, showing the relation between the magnetization and applied magnetic force have also been obtained, the hysteresis being less for the 10% Co alloy, after annealing. In the hard-drawn state, however, the hysteresis and Curie points are considerably higher. The results are shown to be in agreement with Heisenberg's theory of ferromagnetism.

Introduction

JUDGING from the varied experimental results, the subject of ferromagnetism appears to be a most complicated one, and it has been very difficult to find a theory which will explain all the phenomena satisfactorily. The actual explanation cannot be as complicated as experiments suggest, because it must be closely bound with that of atomic structure, where there is little room left for any special mechanism to account for magnetism. The work of Barnett and of Einstein and de Haas points to the spinning electron as the elementary magnet. Weiss[1] has shown that Langevin's theory of paramagnetism may be extended to account for ferromagnetism by assuming the latter to be characterised by an "internal magnetic field" of very great magnitude. The recent theory of Heisenberg,[2] based on quantum mechanical considerations, although still very rough and incomplete, appears to point the way to the most satisfactory explanation of ferromagnetism. This theory explains the inner magnetic field of Weiss as due to resonance between the spins of the valence electrons of neighboring atoms, just as Heitler and London[3] introduced the idea of resonance to explain the formation of the H_2 molecule. Ferromagnetism thus means the orientation over a crystal of the spins of the electrons, the force of orientation being really

* National Research Fellow.
[1] P. Weiss and G. Foëx "Le magnétisme" (1926).
[2] W. Heisenberg, Zeits. f. Physik **49**, 619 (1928).
[3] W. Heitler and F. London, Zeits. f. Physik **44**, 455 (1927).
W. Heitler, Zeits. f. Physik **47**, 835 (1928).
F. London, Zeits. f. Physik **46**, 455 (1928).

Pauli's exclusion principle (or symmetry considerations of the eigenfunctions). The complete success of the theory seems to be limited only by the complication of the mathematics, due to the fact that we are dealing with a problem of many particles and hence of many dimensions. But Fowler and Kapitza[4] already have succeeded in applying it in a rough way to account for the phenomena of the Curie point-change in volume, specific heat, etc.

That ferromagnetism has appeared from experiments to be such a complicated subject is due mainly to the fact that what have generally been observed are statistical phenomena from which it is naturally very difficult to arrive at a knowledge of the elementary mechanism. In the present experiment, an effort was made to simplify conditions. In a specimen of, say, cobalt, each ferromagnetic cobalt atom is immediately surrounded by others which greatly modify its behavior through interaction. But the aim of this problem was to measure the magnetic properties of alloys of cobalt with a non-ferromagnetic element, the cobalt content being so small that most of the cobalt atoms would be surrounded by non-ferromagnetic atoms. In this isolated state, it was hoped to obtain a better idea of the behavior of the cobalt atoms.

According to the theory of Heisenberg, on the other hand, ferromagnetism is not due so much to the individual atoms as to the interaction between closely neighboring atoms. A single atom may have a magnetic moment, as Gerlach and Stern have shown, but it cannot exhibit the peculiarities of ferromagnetism, such as hysteresis. In view of this, one would expect the isolation or separation of the ferromagnetic atoms to result in reduction of hysteresis or even loss of ferromagnetism. This problem was, therefore, of interest in the light of Heisenberg's theory.

The Alloys

In the choice of suitable alloys, the first consideration was that the two constituents should be mutually soluble, forming solid solutions. Consultation of the International Critical Tables[5] and other sources limited the possibilities to certain alloys of Fe, Ni, or Co with Cu, Ag, Au, Cr, Mn, Pd, or Pt. Several of these combinations have already been investigated[6, 7, 8, 9, 10] and found non-magnetic even for large proportions of the ferromagnetic element. Hadfield,[11] for example, found the Fe-Mn series non-magnetic beyond 17% Mn, due, presumably, to a chemical combination between the iron and manganese. Mn and Cr were further to be avoided because they are so closely related to Fe in their electronic configurations, and Fe, as it, with its several phases, is more complex.

[4] R. H. Fowler and P. Kapitza, Proc. Roy. Soc. **A124,** 1 (1929).
[5] International Critical Tables, Vol. II, 400–455.
[6] B. V. Hill, Verh. d. D. P. Ges. **4,** 194 (1902); Phys. Rev. **24,** 321 (1907).
[7] G. Tammann, Zeits. f. phys. Chem. **65,** 73 (1909); Z. f. anorg. Chem. **52,** 25 (1907), etc.
[8] R. Sahmen, Zeits. f. anorg. Chem. **57,** 1 (1908).
[9] K. Lewkonja, Zeits. f. anorg. Chem. **59,** 293 (1908).
[10] R. Gans and A. Fonseca, Ann. d. Physik [4] **61,** 742 (1920).
[11] R. Hadfield, Proc. Roy. Soc. **A115,** 120 (1927).

The second chief consideration was to find alloys in which the concentration of Ni or Co could be made small without disappearance of ferromagnetism. This was generally impossible, as Heisenberg's theory predicts. Fortunately, it was found that Co-Pt and Ni-Pt wires of about the desired compositions were being made by the Bell Telephone Laboratories, and that at least some of these alloys were magnetic; they very kindly supplied alloys whose compositions by weight were the following:

10% Co—90% Pt
5% Co—95% Pt
10% Ni—90% Pt
5% Ni—95% Pt

The metals used in making them had been carefully purified to 99.9+%. These alloys were analysed and found not to vary from the above proportions by more than 0.05%. The crystal structure was believed to be that of platinum, i.e. face-centered cubic, and on measurement, the densities proved to be about the same as those calculated from the relative proportions of the two constituents and their repsective densities. Platinum has been found to form solid solutions with both cobalt and nickel, and no compounds are known.

To have the alloys in the form of wires was advantageous because of the greater homogeneity produced by the cold work of drawing. The wires were 1m long and 0.003 to 0.03 inches indiameter. They were tested in both the hard-drawn state and after a heat treatment which consisted of annealing them for three hours at 1000°C and then at lower temperatures.

Experimental Method

For each alloy, two sets of measurements were made. (1) The applied magnetic force, H, was kept fixed and the intensity of magnetization, I, measured at different temperatures up to the Curie point, or temperature above which the alloy is no longer ferromagnetic. (2) At a given temperature, hysteresis loops, showing the cyclic variation of I with H, and the value of I near saturation were obtained. The results for the cobalt and nickel alloys were compared and the effect of increasing the platinum content studied.

The ballistic method was employed for measuring the magnetization. Two identical copper rings with grooves were constructed, mean diameter = 3.58 cm. In the groove of one ring was wound the alloy wire, the ends being spot-welded together. The two rings were wound identically with a primary and secondary winding of enameled copper wire, the layers being insulated with satin ribbon. The rings were connected differentially, the secondaries being in series with a ballistic galvanometer, which, on calibration, gave a sensitivity of 48 maxwells per mm. The only effect on the galvanometer was that caused by the presence of the alloy, the total flux through the circuit being:

$$F = N_s A_w (B - H) = 4\pi N_s A_w I$$

where N_s is the number of secondary turns, A_w the cross-section of the alloy, B the magnetic induction, and I the intensity of magnetization, whose change can thus be measured. The primary current was supplied by storage cells and read on an ammeter. H was then given by:

$$H=0.4N_p i/d$$

where N_p is the number of primary turns, i the current in amperes, and d the mean diameter of a ring. By means of switches and resistances any variation, ΔH, could be produced.

The two rings were placed in a Dewar flask containing a temperature-controlling bath. The temperature of the alloy was measured by copper-

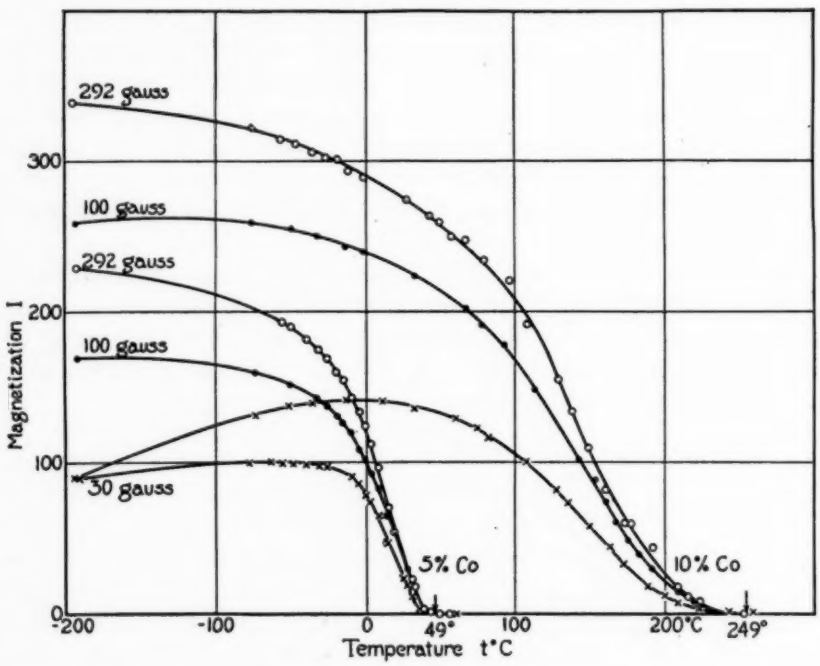

Fig. 1. Magnetization as a function of temperature.

constantan thermocouples, one set of junctions being soldered at various points around the ring of alloy and the other set kept in ice. The e.m.f.'s were measured by a potentiometer arrangement, the thermocouples being standardised at various fixed points covering the range over which they were used. For constant temperature baths, the following were used: liquid air, (about $-192°$C); a mixture of solid CO_2 and alcohol, (about $-78°$C); and boiling acetone, ($+56°$C). In measuring the variation of I with temperature, various non-conducting liquids were used for baths and the primary current allowed to warm them up at the rate of 1° per minute or less.

In order to measure the initial curve of magnetization for an alloy, the alloy was first demagnetized by heating it above its Curie point, where the

magnetization is lost; above this point, any deflection of the galvanometer on reversing H was due only to inequality in the dimensions of the two rings and in their windings, and the small correction thus obtained was applied to all the readings.

Results and Discussion

Fig. 1 gives the variation of magnetization with temperature for the two cobalt alloys in the annealed state. The values of H used were 30,

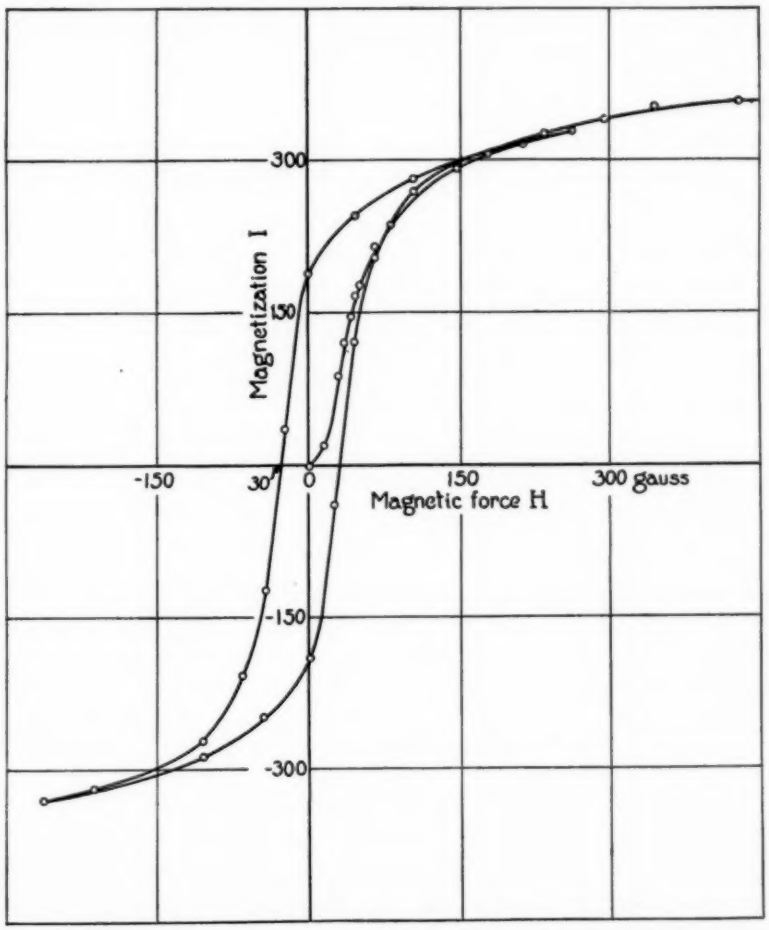

Fig. 2. Hysteresis loop for 10% Co-90% Pt alloy at −194°C.

100 and 292 gauss. As has often been observed in other cases, such as that of soft iron, with small values of H susceptibility at first increases with temperature and then rapidly falls to zero at the Curie point, while for larger values of H it decreases steadily and more gradually.

The Curie points are at 249°C (522°K) and 49°C (322°K) for the 10% Co and 5% Co alloys respectively. For pure cobalt the Curie point is 1115°C (1388°K). As the atomic percentage of platinum in the alloys was

73.1% and 85.2% respectively, the depression of the Curie point is not proportional to these percentages nor to the amount of platinum present by weight (Van't Hoff's formula), but the Curie point appears to drop more and more rapidly as the platinum content increases. This continuous depression of the Curie point has been observed for other series of alloys in which one component is ferromagnetic, e.g. the Ni-Cu series. These results agree with Heisenberg's theory of ferromagnetism, further isolation of the ferromagnetic atoms resulting in less interaction or resonance between them. This is equivalent to making the factor n of the Weiss[1] molecular field smaller and hence, the Curie point, which is proportional to n, lower.

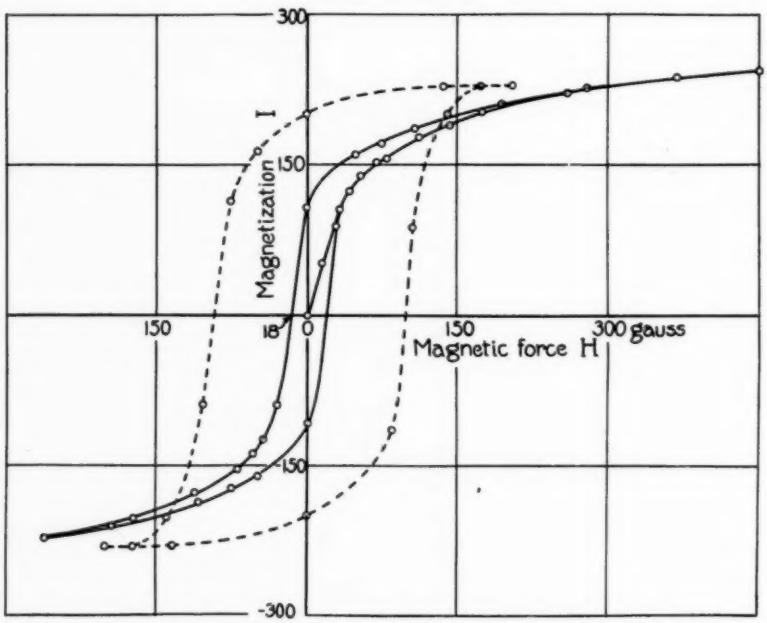

Fig. 3. Hysteresis loop for 5% Co −95% Pt alloy at −192°C.

The two nickel alloys showed no ferromagnetism, on the other hand, even down to liquid air temperatures, (80° K), although a value of I as small as 0.5 cgs units could have been measured. The question arises whether the Curie points are between 0° and 80° K, or whether the alloys are non-magnetic at all temperatures. As the Curie point for nickel is 358°C(631° K), the depression has been much more rapid and not at all proportionate to that in the cobalt series. Kamerlingh-Onnes, Hadfield and Woltjer[12] in their investigation of the Fe–Mn series found that although for all the magnetic alloys, the Curie point was at about 770°C, with 16% or more manganese, the alloys were non-magnetic even in liquid helium, due, perhaps, to the formation of a compound, Fe_5Mn. This may be the explanation in the present

[12] H. Kamerlingh Onnes, R. A. Hadfield and H. R. Woltjer, Proc. Roy. Soc. **A99**, 174 (1921).

case. However, even without compound formation sufficient separation of the ferromagnetic atoms should result in complete loss of ferromagnetism on the Heisenberg theory, so that the Curie point would probably reach absolute zero before the platinum content has become 100%.

Figs. 2 and 3 (full lines), give the curves of initial magnetization and typical hysteresis loops at liquid air temperatures for the two Co alloys after complete annealing. Although H was increased to 600 gauss a slight increase in I still continued. The maximum values attained are given in Table I.

TABLE I. *Maximum values of I and the magnetic moment per cobalt atom.*

	100% Co	10% Co	5% Co
I_{max}	1400	364	254
$\sigma_a \times 10^{20}$	1.56	1.96	2.48
		1 Bohr magneton $= 0.92 \times 10^{-20}$	

The second row of Table I gives the magnetic moment per cobalt atom, σ_a, assuming the platinum atoms do not contribute to the magnetism. But as σ_a is considerably greater as the platinum content increases it appears likely that the platinum does contribute. Consider Heisenberg's interaction integral:

$$J_0 = \tfrac{1}{2} \int\int \psi_k^{\kappa} \psi_k^{\lambda} \psi_l^{\kappa} \psi_l^{\lambda} \left\{ \frac{2e^2}{r_{kl}} + \frac{2e^2}{r_{\kappa\lambda}} - \frac{e^2}{r_{\kappa k}} - \frac{e^2}{r_{\kappa l}} - \frac{e^2}{r_{\lambda k}} - \frac{e^2}{r_{\lambda l}} \right\} d\tau_k d\tau_l$$

where k, l refer to the two electrons and κ, λ to the two neighboring nuclei, Ψ is the unperturbed wave function for the given electron near the given nucleus, and $d\tau$ is an element of the configuration space of the electron. It is essential for ferromagnetism that J_0 be positive. Now Fowler and Kapitza[4] have pointed out that it is quite likely that J_0 is positive for platinum and hence, it would not be surprising for platinum atoms to be capable of ferromagnetism.

TABLE II. *Coercive force for various loops.*

t	H_{max}	H_c(10% Co)	H_c(5% Co)
−192°	262	30	18
− 54°	262	22	12
− 69°	140	21	12
+ 56°	262	17	non-mag.

The hysteresis loops, while quite steep are otherwise normal. The hysteresis for the 5% Co alloy is, however, only about half that for the 10% Co alloy. Just as for the Curie points, this can be explained as due to the decrease in the Weiss factor, n, which Heisenberg's theory predicts. Table II gives values of the coercive force, H_c, given by various loops.

The effect of annealing was found very important. Annealing presumably produces a more uniform and regular distribution of the cobalt atoms through-

out the platinum crystal lattice, while in the hard-drawn state, groups of cobalt atoms will be bunched together. As, on Heisenberg's theory, it is only the closely neighboring atoms that contribute to the magnetism, the effect of annealing should be similar to that of further isolating the magnetic atoms. This was found to be the case. The broken curve of Fig. 3 corresponds to the hysteresis loop for the 5% cobalt wire in the hard-drawn state, and it is seen to be much larger and more rectangular; H_c is 96. The other curves for the hard-drawn state are similarly larger, though H_c is here greatest for the 5% Co alloy. Annealing at temperatures as low as 350° C produced considerable effect. The effect of annealing on the Curie point was again in agreement with theory, the hard drawn 10% Co specimen losing its magnetism at 305° C as against 249° C for the annealed state. The Curie point of the 5% Co alloy was only slightly affected.

A temperature hysteresis was noted. Although the loss of magnetism on heating and its reappearance on cooling occurred at about identical temperatures with the annealed wires, the values of I at temperatures a little below the Curie points were considerably less for the cooling measurements.

In conclusion, it may be said that while the isolation of ferromagnetic atoms attempted in these alloys has not produced any unusual changes in the magnetic properties of these atoms, except a possible increase in the average atomic magnetic moment, yet the changes that are observed are all in agreement with the Heisenberg theory of ferromagnetism.

The writer wishes to thank the National Research Council for its support and the Bell Telephone Laboratories for so kindly supplying the wires used. It also gives the writer great pleasure to acknowledge his indebtedness to Professor L. W. McKeehan for suggesting the problem, and to Professor R. A. Millikan for the facilities of the Norman Bridge Laboratory.

LETTERS TO THE EDITOR

Prompt publication of brief reports of important discoveries in physics may be secured by addressing them to this department. Closing dates for this department are, for the first issue of the month, the twenty-eighth of the preceding month; for the second issue, the thirteenth of the month. The Board of Editors does not hold itself responsible for the opinions expressed by the correspondents.

Regularities in the Ionization Potentials of Light Elements

In a recent important paper (Zeits. f. Physik **55**, 738, 1929) R. Peierls applies group theory to the approximate computation of ionization potentials of neutral atoms. Regarding the interaction of the electrons as small compared with the nuclear attraction, he obtains expressions for the energy necessary to remove all electrons from a neutral atom in terms of integrals with respect to the eigenfunctions. Subtracting from these expressions a second set of corresponding formulas for the energy of a singly ionized atom he arrives at 10 very simple equations for the first ionization potentials of the elements in the K and L shells expressed in terms of the Rydberg frequency, R, and 6 integrals. For a calculation of the absolute values of these ionization potentials it would be necessary to evaluate these integrals. Peierls eliminates them instead from his equations and thus obtains relations between the ionization potentials such as

$$V_C/6 - V_B/5 = V_N/7 - V_C/6 = V_F/9 - V_O/8$$

which indeed seem confirmed by the experimental data.

H	He	Li	Be	B	C	N	O	F	Ne
1.000	0.904	0.528	0.685	0.492	0.525	0.516	0.500	0.611	0.634
1.000	*(0.920)*	*0.811*	*0.732*	*0.703*	*0.678*	*0.657*	*0.633*	*0.594*	*0.629*
He II	Li II	Be II	B II	C II	N II	O II	F II	Ne II	Na II
2.000	1.824	1.339	1.417	1.195	1.203	1.173	1.133	1.205	1.263
1.000	*(0.983)*	*0.892*	*0.864*	*0.805*	*0.779*	*0.732*			
Li III	Be III	B III	C III	N III	O III	F III			
3.000	2.807	2.231	2.281	2.000	1.982	*1.905			
1.000	*(0.974)*	*0.931*	*0.850*	*0.844*	*0.805*				
Be IV	B IV	C IV	N IV	O IV	F IV				
4.000	3.781	3.162	3.171	2.844	*2.787				
1.000	*(0.995)*	*(0.948)*	*0.913*	*0.866*					
B V	C V	N V	O V	F V					
5.000	4.776	4.110	*4.084	*3.710					
1.000	*0.994*	*(0.962)*	*0.935*						
C VI	N VI	O VI	F VI						
6.000	*5.770	5.072	*5.019						
1.000	*0.946*	*(0.970)*							
N VII	O VII	F VII							
7.000	*6.766	6.042							
1.000	*0.998*								
O VIII	F VIII								
8.000	*7.764								
1.000									
F IX									
9.000									

While it will be interesting to see how this theory can be extended to other parts of the periodic system—a paper on this subject was announced by Peierls—we have applied the above method to higher ionizations and have arrived at similar equations for the second, third, $\cdots$, ionization potentials in terms of the *same* integrals which were mentioned above. As the formulas regard the interaction between electrons as a small perturbation, agreement with experiment should be better for higher stages of ionization. After eliminating the interaction integrals relations of the following type were found:

$V_{C\,II}/6 - V_{B\,I}/5 = V_{N\,II}/7 - V_{C\,I}/6 = V_{N\,III}/7 - V_{C\,II}/6 = \cdots = R/4$

where R is the Rydberg constant. In general if we write $V_s^{(n)+}$ for the ionization potential of an ion with nuclear charge Z and $Z-n$ electrons we obtain:

$$V_s^{(n)+}/Z - V_{s-1}^{(n-1)+}/(Z-1) = R/4 \quad (3)$$

for *any* values Z and n provided $2 < Z-n \leqq 10$. For $Z-n$ equal to one or two the above difference should be R. The following table illustrates this more closely. Under the symbol for an ion the ionization potential divided by $ZR/4$ is given. The italicized numbers are the differences between these ionization potentials divided by $ZR/4$ which according to the above equations should be equal to unity. Only for the ions with one or two electrons V/ZR is tabulated in order that the corresponding differences also approach unity.

It is interesting to note the degree of accuracy with which our relations (2) are satisfied. The experimental differences tend to unity toward the lower left-hand corner of the table. This, of course, was anticipated since in this part of the table inter-electronic interactions become relatively smaller. The original Peierls' relations (1) correspond to horizontal differences in the first row The numerical agreements found by Peierls are obviously fortuitous for we cannot expect differences between quantities of the same order of magnitude to be constant in the upper row of the table. A few differences are derived from theoretical or extrapolated ionization potentials as given by Kellner and by Millikan and Bowen. By observing the systematic progression of the italicized differences in both horizontal and vertical directions predictions of hitherto undetermined ionization potentials are possible. Values obtained by this means are included in the table and marked by an asterisk.

O. LAPORTE
L. A. YOUNG

Department of Physics,
University of Michigan
October 7, 1929.

Binding Energy of Light Atoms

In the preceding note (Laporte and Young) fundamental regularities were shown to exist among the ionization potentials of the elements from H to Ne in various stages of ionization. These regularities make it possible to predict ionization potentials not known from spectroscopic analysis with a fair degree of accuracy. Using these values it becomes possible to calculate the total energy necessary to remove all electrons from the atom since this binding energy is equal to the sum of the successive ionization potentials. This energy E_{obs} is tabulated for the elements H to F in units of the Rydberg constant:

	E_{obs}	E_{calc}
H	1.000	1.153
He	5.807	5.811
Li	14.87	14.97
Be	29.25	29.29
B	49.08	49.30
C	74.91	75.43
N	108.65	108.09
O	149.85	147.61
F	198.6	194.3

On the basis of the Thomas[1] and Fermi[2] statistical theory, in which an atom is considered as a nucleus surrounded by a degenerate electron gas, Milne[3] has shown that the total binding energy should be given by $E = aZ^{7/3}$. The above values E_{obs} were tested to ascertain whether or not they satisfied this law. When a curve was plotted with log E and log Z as ordinates and abscissas, all points with the exception of $Z=1$, (H), were found

[1] L. H. Thomas, Proc. Camb. Phil. Soc. **23**, 542 (1927).

[2] E. Fermi, Zeits. f. Physik **48**, 73 (1928).

[3] E. A. Milne, Proc. Camb. Phil. Soc. **23**, 794 (1927).

to lie on a straight line having a slope $7/3 \pm 1/1000$. The expression $E = 1.153\ Z^{7/3}$ fits the observed data quite well and it may certainly be expected to hold for higher values of Z than those considered in this note. The column E_{calc} in the above table was computed by this formula. Milne arrived (theoretically) at a value $a = 1.23$ which is about 7% higher than the one given here. It is felt that the difference may lie in the difficult numerical calculations on which Milne's result is based.

Thomas, Fermi, and Milne have supposed their theory to hold only for heavy atoms. We have shown here that it holds *exactly* for $z > 1$. Thus, when there are two or more electrons in an atom they seem to behave as a completely degenerate Fermi gas. Small deviations may arise when the outer electrons do not form spherically symmetrical closed groups.

L. A. YOUNG

Department of Physics,
University of Michigan
October 7, 1929.

Double Vibrational Isotope Effect in the Silver Chloride Band Spectrum

The emission band spectrum of AgCl already reported showed the presence of the two Cl isotopes. Photographs of the same spectrum in absorption, under higher dispersion, reveal also the two silver isotopes. The heads of the band systems due to the molecules $Ag^{107}\ Cl^{35}$, $Ag^{109}\ Cl^{35}$, $Ag^{107}\ Cl^{37}$, $Ag^{109}\ Cl^{37}$ have been measured. The measured separations of the Cl isotopes, are of the order 3 to 30 cm^{-1}; of the Ag isotopes, 1 to 4 cm^{-1}. Agreement with theoretical displacements is close.

A complete assignment of vibrational quantum numbers has been made. The (0,0) band lies at 31574.4 cm^{-1}. The heat of dissociation of AgCl in the normal state is 3.00 volts; in the excited state 0.35 volt. Complete results will be published soon.

BROOKS A. BRICE

New York University,
University Heights
October 9, 1929.

Electron Scattering in Hydrogen

In a study of electron scattering in hydrogen, Jones and Whiddington, and more recently Harnwell, have observed an energy loss that does not fit in with the current views as to the structure of the hydrogen molecule. Jones and Whiddington observed an energy loss of about 7 or 8 volts and Harnwell observed a loss of 6 or 7 volts. Harnwell also noticed that this low energy loss became less intense as the amount of atomic hydrogen in the scattering tube increased, and therefore concluded that the loss must be directly attributable to the molecule.

An attempt was made last year by the writer of this note to explain the results of Jones and Whiddington by saying that the low energy loss corresponded to a transition between the 1^3S and the 2^3S levels of the molecule. It may be recalled that the 1^3S level was theoretically predicted by Heitler and London and used by Winans and Stueckelberg to explain the continuous spectrum of the molecule. The above explanation of the low energy loss is modified now to say that it corresponds to the excitation by electron impact of molecules that are in states represented by the horizontal portions of the Franck-Condon potential energy curves associated with the 1^1S and the 1^3S levels. Molecules in these levels possess energies equal to or greater than the heat of dissociation and consequently the energy necessary to excite the low lying singlet or triplet levels is about 7 to 8 volts. This is in good agreement with the observations.

There are several ways in which a hydrogen molecule can get into the states represented by the flat parts of the potential energy curves associated with the 1^1S or the 1^3S levels. The recombination of two hydrogen atoms may result in an unstable molecule in one of these two levels. This process should of course be most probable in atomic hydrogen. The emission of the continuous spectrum should result in molecules in the 1^3S levels and these should therefore be most numerous in molecular hydrogen. Since the low energy loss is less frequent in atomic than in molecular hydrogen, it seems that on the basis of the ideas in this note, it corresponds to excitation of molecules in the 1^3S level. It may be however that the formation of quasi-molecules by recombination is very improbable.

JOSEPH KAPLAN

University of California at Los Angeles,
October 7, 1929.

A New Regularity in the List of Existing Nuclei

Beck (Zeits. f. Physik **47,** 407 (1928)) and others have listed all of the different nuclear types disclosed by Aston's work and investigated the several kinds of regularity appearing in such a list. The writer has plotted the data from Beck's table on a large scale chart and observed a regularity of occurrence not heretofore mentioned in the literature. The chart consists of points representing all the existing nuclear types, the ordinate of each point giving the number of protons or mass units and the abscissa the number of electrons in the corresponding nucleus. For example, cobalt, of atomic number $Z=27$ and atomic weight $P=59$, falls at point (59, 32) in the chart. Although the data are certainly incomplete the chart is well filled out up to $P=146$.

There appear on the chart three relatively dense groups of points, each of which groups displays a two dimensional symmetry about the group center. For example, the second group center is at point (80, 45). The existing nuclei in the neighborhood of this point are represented by the points in the following table:

80 ,45+1	80 ,45−1
80+ 1,45+1	80− 1,45−1
80+ 2,45+1	80− 2,45−1
80+ 2,45+3	80− 2,45−3
80+ 3,45+2	80− 3,45−2
80+ 4,45+3	80− 4,45−3
80+ 5,45+3	80− 5,45−3
80+ 6,45+3	80− 6,45−3
80+ 6,45+5	80− 6,45−5
80+ 7,45+5	Missing
80+ 8,45+5	80− 8,45−5
80+ 9,45+5	80− 9,45−5
80+10,45+5	80−10,45−5
Missing	80−10,45−7
80+11,45+7	80−11,45−7
80+12,45+7	80−12,45−7

The points are arranged in two columns so that symmetrical points are opposite. All of the thirty points listed represent known nuclei and no known nuclei in the region have been omitted. All but two of the thirty maintain the symmetry about the center. The pattern made by the points on the chart presents a much more graphical illustration of the symmetry than the table can, the line of points proceeding up to the right in the same manner as down to the left. The points missing may be due to lack of data. From the table, for example, we should predict the existence of nuclei (73,40) and (90,52), isotopes of arsenic and strontium respectively.

The first of the three groups mentioned is centered somewhat ambiguously at (27,14), the symmetry being of a special type such that any one of several points might be the center so long as the limits of the group cannot be fixed. It is interesting to note that the new isotopes of oxygen (17,9) and (18,10) fit nicely into this group. The third group is centered definitely at (124,72) and has a symmetry more complicated and almost as perfect as that of group II listed above. There are a number of scattered points in the less dense gaps between the groups which do not appear to have any relation to the latter.

A regularity characterized by symmetry is different in kind from the other types of regularity already discovered, the latter being concerned with the increments of constituents in passing from one nucleus to another progressively. Basis is lacking for an interpretation of such symmetrical arrangements. They may be traceable to symmetrical stability rules for the nuclei, or perhaps to some feature of the original cosmic process by which these nuclei came into existence. A suggestion in the latter direction is the following. Considering the nuclei of group II alone, suppose that they all arise from the splitting into two approximately equal parts of a single parent type of nucleus containing twice the number of protons and twice the number of electrons as the group center. Then for every nucleus $(P+x, E+y)$ formed by a split of the parent nucleus $(2P, 2E)$, there must be the remaining part $(P-x, E-y)$ also and an existence symmetry is automatically established. On the other hand, the symmetry of existence does not seem to extend itself into a symmetry of relative abundance, which would indicate that the suggestion here given is not alone sufficient to account for the facts.

A more complete and illustrative account is being prepared in which the above suggestion will be elaborated and criticized.

HENRY A. BARTON

Rockefeller Hall,
Cornell University.
October 9, 1929.

Capture of Electrons by Alpha-Particles

Elliot Q. Adams, in a letter to the Physical Review (Phys. Rev. **34,** 537 (1929)) suggests a mechanism for the capture of electrons by alpha-particles in the experiment reported by Bergen Davis and A. H. Barnes (Phys. Rev. **34,** 152 (1929)).

His suggestion necessitates the simultaneous presence of a number of alpha-particles in the electron stream. In this experiment however, the alpha-particles are passing through the electron stream at the rate of approximately 60 per minute. They traverse the entire length of the tube in 4×10^{-8} seconds. It is extremely improbable therefore that there will ever be more than one alpha-particle among the electrons at any instant. The cumulative effect proposed by Adams would therefore appear to be impossible.

ARTHUR H. BARNES

Physics Laboratories,
Columbia University,
October 9, 1929.

BOOK REVIEWS

The Principles of Thermodynamics. GEORGE BIRTWISTLE. Pp. ix+168, 24.5×13.5 cm. Cambridge University Press, and the Macmillan Company, 60 Fifth Avenue New York. 1927. Price, $2.60.

This is the second edition of the work which first appeared in 1925, and which was reviewed in this Review on page 100, vol. 27, 1926. Except for a very few minor changes, the body of the text is unchanged. It is to be noted, however, that the misspelling of Tammann's name as Jammann, in connection with the high pressure modifications of ice, has not been corrected. A chapter of five pages has been added at the end on the third law of thermodynamics in which the subject is approached from the point of view of power series expansion. The reader will doubtless want to supplement this chapter by additional reading in order to obtain an adequate physical feeling for the situation.

P. W. BRIDGMAN

Les Méthodes nouvelles en Analyse quantique. (*Mécanique quantique. Mécanique ondulatoire.*) JULIEN PACOTTE. Pp. 139. Paris, Librairie Scientifique Albert Blanchard, 1929. Price, 22 francs.

This little book presents a fairly satisfactory account of the recent developments in quantum theory. It gives a good discussion of the general principles and the general ideas leading to the basic equations, but is rather limited in the scope of the applications which are treated. Thus there is no treatment of the spectra of atoms other than hydrogen, hence no resonance or exchange phenomenon either for the helium spectrum or the hydrogen molecule. Nor is there anything on the photo-electric effect or Compton effect given. What is worse is absence of discussion of any kind of the spinning electron, although there is a chapter devoted to "La mécanique ondulatoire en relativité." The book is to be commended, however, for the final chapter on the relation of the quantum mechanics to linear transformations on Hilbert space.

E. U. CONDON

Polar Molecules. P. DEBYE. Pp. 172. Chemical Catalog Co., New York, 1929. Price $3.50.

It is seldom that a field of theoretical physics is as completely dominated by the work of one man as is the theory of dielectric constants by that of Debye. Consequently a book written by Debye on this subject carries the assurance of authenticity and accuracy. Not merely the abstract theory but also abundant and up-to-date comparisons with experiment are stressed throughout. Incidently, still more recent experimental material is covered in the subsequent german edition. The first portion of the book, devoted to the classical theory of dielectrics, inevitably parallels to a certain extent the article by Debye in Vol. VI of the Handbuch der Radiologie except that, of course, no attempt is made to include magnetic susceptibilities. It is, of course, an advantage to have now a treatment in English, although occasionally the treatment is more condensed. For instance, no discussion is given, unfortunately, of the fact that the inclusion of the kinetic energy terms, which are apparently omitted for brevity, does not impair the validity of the Debye or Langevin formulas. Many new features are found in the book, notably a chapter on solutions containing readily ionized salts. The ions, with their strong Coulomb fields, "saturate" the surrounding molecules of the solvent, and so thereby lower the latter's dielectric constant! The book closes with four chapters on dielectric constants and infra-red dispersion in the new quantum mechanics, which gives more reasonable results more nearly akin to the classical theory of dielectric constants than did the old quantum theory. As customary in Professor Debye's writings, the style is clear-cut.

J. H. VAN VLECK